8-22-2014

Transition Metal Mediated Controlled Polymerizations of 1,3-Dienes, and Main Chain Fluorinated Monomers; Towards the Synthesis of Complex Macromolecular Structures.

Christopher P. Simpson
University of Connecticut - Storrs, christopher.simpson@uconn.edu

Transition Metal Mediated Controlled Polymerizations of 1,3-Dienes, and Main Chain Fluorinated Monomers; Towards the Synthesis of Complex Macromolecular Structures.

Christopher P. Simpson, Ph.D.

University of Connecticut, 2014

Abstract

This thesis focuses on the advancement and development of new polymerization methodologies for the controlled radical polymerizations of 1,3-dienes, (2-methyl-1,3-butadiene, 1,3-butadiene, 2,3-dimethyl-1,3-butadiene) and main chain fluorinated monomers, as well as the ability to synthesize well defined block copolymers thereof.

The effect of the reaction variables in the Cp_2TiCl-Mediated controlled radical isoprene (2-methyl-1,3-butadiene) polymerizations initiated by epoxide radical ring opening (RRO), was investigated over a wide range of conditions ($[Cp_2TiCl_2]$/[epoxide] = 1/1-6/1, $[Cp_2TiCl_2]$/[Zn] = 1/0.5-1/8, [isoprene]/[epoxide] = 20/1-1000/1, T = 70-130 °C in THF and dioxane), to reveal a linear dependence of molecular weight on conversion, linear first-order kinetics and moderate polydispersities up to high conversions, with an optimum in initiator efficiency, rate and polydispersity for [epoxide]/$[Cp_2TiCl_2]$/[Zn] = 1/3/6-1/4/8 at 90 - 110 °C. NMR studies demonstrated the epoxide initiation and the stereoselectivity of a conventional radical polymerization. Furthermore, random and block copolymers with styrene could also be obtained. This methodology was then expanded, using the optimum conditions, to initiation via single electron transfer (SET) reduction of aldehydes as well as halide abstraction. Subsequently, the three initiating systems were shown to work with both 1,3-butadiene and 2,3-dimethyl-1,3-butadiene. This system was then examined with the main chain fluorinated monomer vinylidene fluoride (VDF), and a series of epoxides, aldehydes, halides and peroxides, known to initiate

both styrene and diene polymerizations in the presence of $Cp_2TiCl^{\bullet}$, were tested as potential room temperature VDF initiators. However, regardless of reaction conditions, no polymer was obtained. This is most likely due to the incompatibility of solvents appropriate for Cp_2TiCl_2 reductions with those conducive of VDF polymerizations. Thus, polar solvents appropriate for Cp_2TiCl_2 are strong chain transfer agents towards VDF (dioxane, THF, diglyme, acetone), while solvents that limit chain transfer to $PVDF^{\bullet}$, react with $Cp_2TiCl^{\bullet}$.

Finally a series of transition metal carbonyl complexes ($Re_2(CO)_{10}$, $Mn_2(CO)_{10}$, $Cp_2W_2(CO)_6$, $Cp_2Mo_2(CO)_6$, $Fe(CO)_5$, $Cp_2Fe_2(CO)_4$, $Cp^*_2Cr_2(CO)_4$, $Co_2(CO)_8$ $Mo(CO)_6$, $Cr(CO)_6$) in conjunction with alkyl or perfluoroalkyl halides ($CH_3(CH_2)_5Cl$, $CH_3(CH_2)_5Br$, $CH_3(CH_2)_5I$, CH_3I, CCl_4, CCl_3Br, $CF_3(CF_2)_3I$ $Cl(CF_2)_8Cl$, $Br(CF_2)_6Br$, and $I(CF_2)_6I$) were evaluated in the initiation and respectively control of vinylidene fluoride (VDF) polymerization. Perfluoroalkyl iodides (R_FI = $CF_3(CF_2)_3I$, $I(CF_2)_6I$) mediated the VDF controlled radical polymerization (CRP) via iodine degenerative transfer (IDT). The fastest rates were observed with R_FI used in conjunction with $Re_2(CO)_{10}$ and $Mn_2(CO)_{10}$. A selection of the metal complexes were then evaluated in the PVDF-I activation, where $Re_2(CO)_{10}$ $Mn_2(CO)_{10}$, $Cp_2W_2(CO)_6$, $Cp_2Mo_2(CO)_6$, and $Cp_2Fe_2(CO)_4$ provided complete activation of both PVDF-CH_2-CF_2-I and PVDF-CF_2-CH_2-I chain ends and were subsequently used towards the synthesis of well-defined block copolymers with vinyl acetate, t-butyl acrylate, methyl methacrylate, isoprene, styrene, and acrylonitrile, from their respective metal carbonyls.

Transition Metal Mediated Controlled Polymerizations of 1,3-Dienes, and Main Chain Fluorinated Monomers; Towards the Synthesis of Complex Macromolecular Structures.

Christopher P. Simpson

B.S., Southern Connecticut State University, 2002

A Dissertation

Submitted in Partial Fulfillment of the

Requirements for the Degree of

Doctor of Philosophy

at the

University of Connecticut

2014

APPROVAL PAGE

Doctor of Philosophy Dissertation

Transition Metal Mediated Controlled Polymerizations of 1,3-Dienes, and Main Chain Fluorinated Monomers; Towards the Synthesis of Complex Macromolecular Structures.

Presented by

Christopher P. Simpson

Major Advisor:_____

Prof. Alexandru D. Asandei, Ph.D.

Associate Advisor: _____

Prof. Douglas Adamson, Ph.D.

Associate Advisor: _____

Prof. Richard Parnas, Ph.D.

University of Connecticut

2014

ACKNOWLEDGEMENTS

If it were not for the work of my previous and current group members, support, encouragement, and understanding from my family, friends, and colleagues this research could not have been completed. I would first like to thank my advisor Dr. Alex Asandei, for his leadership, guidance, and never ending supply of advice, ideas, and his favorite question, "Any news?". His enthusiasm for our research is unmatched, and induces myself and all our group members to strive for the best and highest quality of research possible, evident in the nearly two hundred citations I have received thus far on my work over the years here.

I would also like to thank my advisory committee Dr. Douglas Adamson and Dr. Richard Parnas as well as Dr. Andrey Dobrynin, and Dr. Montgomery Shaw for their time, input, and advice.

My past and present group members, Dr. Yanhui Chen, Dr. Olumide Adebolu, Patrick Yu, and Joon-Sung Kim, your help, discussions, input, and your friendships were invaluable and I cannot thank you all enough for your support. Much thanks to the technical and administrative staff at the Institute of Materials Science, Mark, Laura, Gary, and Deb.

I would like to thank my family; my parents Jimmy and Patty, my brother Patrick and sister Mary for their support and encouragement over the years that have pushed me to succeed, and a special thanks to my girlfriend Amanda for putting up with my being in the lab so much and sticking by me all this time. A final thanks goes out to Harold, who has loomed above my desk all these years, bringing some wonderful scenery and of course oxygen to my lab.

TABLE OF CONTENTS

Chapter 1. Introduction: Transition Metal Mediated Controlled Radical Polymerizations of 1,3-Dienes, and Main Chain Fluorinated Monomers: Towards the Synthesis of Complex Macromolecular Structures.

1.1 General Background on Polymers and Polymerization.

A *polymer* can be described as "a molecule of high relative molecular mass, the structure of which comprises the multiple repetitions of units derived, actually or conceptually, from molecules of low relative molecular mass"[1] or macromolecules, with small repeat units bonded to each other with covalent bonds.[2] These smallest subunits are referred to a *monomers*. Typically, this number of repeat units range from a small number (2 = dimer, 3 = trimer, 4 = tetramer >4 = oligomer) up in to the hundred thousands, yet there seems to be no standard accepted number of units where a material crosses from a oligomer into a polymer. The reactions by which covalent bonds are formed between monomers is referred to as *polymerization*. These materials can be a product of nature (*i.e.* rubber, protein, DNA) or synthetic (polystyrene, polyurethanes, polyesters), and have been studied as early as the nineteenth century, although commercial availability did not begin until the early twentieth century.[3] It wasn't until the 1920's-30's that acceptance was garnered of what polymers in fact were, allowing for progress in their synthesis and development. During this time, development of methodologies and catalysts, which allowed for greater control of the materials generated was accomplished. As such, currently, the structure-property relationship and advances in processing and applications,[4] has led to tremendous growths in production of polymeric materials, and propelled the industry to one of the fastest growing and largest in the world.

There are two typical classification of polymers, although sometimes the terms in each are seen being used interchangeably. The first is based on the structure of the polymer while the

other, on the mechanism of polymerization.[2] Wallace Hume Carothers in 1929[5], devised the first differentiation of polymers by structure, into condensation and addition polymers, and this was based on the "compositional difference between the polymer and the monomer(s)".[2] Condensation polymers are formed from difunctional(polyfunctional) monomers (*e.g.* diol, diacid) through a condensation reaction, coupled with the elimination of a small molecule with each addition.(*e.g.* water) Prototypical examples of condensation polymers are the polyamides and polyesters, that are formed from the reactions of diamines or diols with a diacids, eliminating water (eq. 1-2).

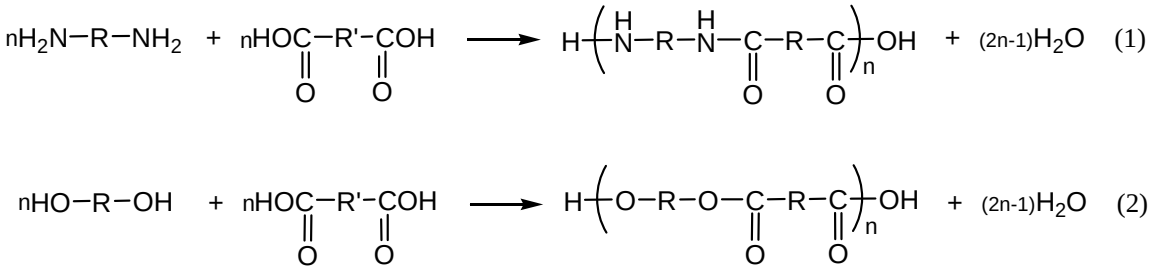

Scheme 1.1. Typical Examples of Polycondensations Reactions.

Addition polymers, are those formed without the loss of small molecule, where the repeat unit has the same composition as the monomer, generally formed by the polymerization of vinyl monomers. (*e.g.* polystyrene)

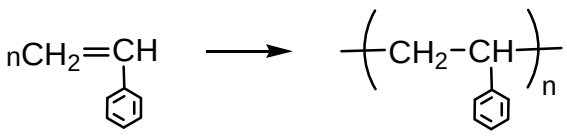

Figure 1.1. Example of Addition Polymerization with Styrene

The second classification, *via* mechanism of polymerization, can be divided in to two types; step-growth and chain polymerizations. While these two classifications are often confused with one another, (i.e. *condensation with step and addition with chain*), it should be noted that condensation-addition classification is based solely on the composition or polymer structure.[2] This more recent terminology being based on the mechanism of polymerization describes how the materials are made. The distinguishing features between these two polymerization types lies in the dependence of the polymer molecular weight with respect to conversion. (Figure 1.2) In step growth, the difunctional monomers couple with each other to form a dimer, and then with another monomer unit to form a trimer then tetramer, etc. This mechanism of polymerization yields very low molecular weight materials through the entire process until a very high conversion is reached. This relationship is governed by the equation relating the degree of polymerization (DP) to 1/(1-C), i.e. at 90% conversion there is only a DP of 10 or at 99% there is a DP of 100. For typical chain growth mechanisms where the monomer unit is added sequentially to the growing polymer chain, there is an immediate production of high molecular weight polymer, and for typical free radical polymerization this molecular weight stays constant throughout the reaction until all monomer is consumed. This is because of unavoidable chain terminating processes (mainly irreversible bimolecular coupling), occurring during the polymerization. In addition, both step-growth and chain polymerization exhibits broad polydispersity indices (PDI), (Figure 1.2) which is a measure of uniformity in the polymer chain

Although these types account for most industrially synthesized polymers, the poor control of the highly reactive species in step-growth polymerization and the irreversible bimolecular termination or chain transfer reactions in chain polymerization typically lead to uncontrolled molecular weights and broader polydispersity (PDI >2).

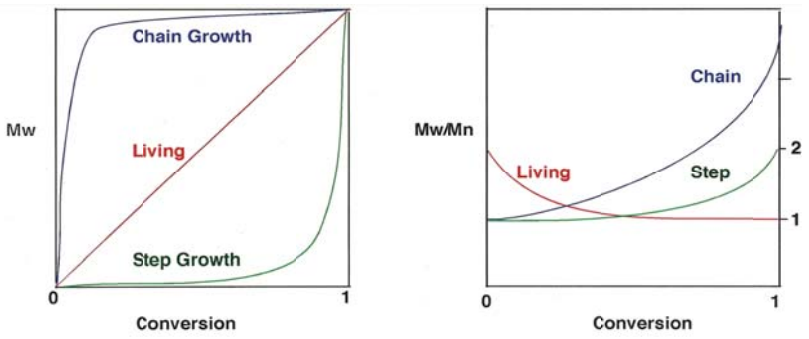

Figure 1.2 Dependence of Molecular Weight (left), and Mw/Mn (right) on conversion of step, chain and controlled polymerizations.

A unique type of chain growth polymerization was developed by Szwarc in 1956[6] known as living anionic polymerization. lengths for a given system. Living polymerizations proceed *via* fast initiation of all polymer chains followed by propagation without termination reactions. Thus the molecular weight increases linearly with conversion and polydispersity (PDI) remains low (Figure 1.2). The development of living polymerization was very desirable as the "living" nature of the growing polymer chains allows for the generation of highly functionalized materials used towards block copolymer synthesis. However, extremely stringent experimental conditions were necessary for ionic polymerizations to prevent unwanted side reactions, thus limiting its industrial applications.

1.2 Controlled Radical Polymerizations

Typically in radical polymerizations there are various reactions taking place in addition to the initiation and propagation (chain growth) of the polymer. These other irreversible reactions are bimolecular termination and chain transfer. Their effect on the polymerization is a decrease in the lifetime of the propagating radicals species and an uncontrolled system. As discussed, polymerizations without the usual termination reactions would be highly worthwhile, as they lengthen the lifetime of the propagating radicals, and allow for the synthesis of block copolymers.[2]

The contribution of Szwarc to the field of polymer chemistry with the living anionic polymerization of styrene and other vinyl monomers[6–10] provided a unique methodology for the synthesis of an array of polymers in a controlled fashion.[9] This proved effective in synthesis of star, telechelic, block and graft copolymers.[9] As such it inevitable led to a renaissance of the field of radical polymerizations,[11,12] and in 1990s new methods for controlled radical polymerizations were developed.[11-17] These techniques can be divided into a few distinct groups; atom transfer radical polymerization (ATRP), stable free-radical polymerization (SFRP) and reversible addition-fragmentation chain transfer (RAFT).[2,11] Which are based on atom transfer, dissociation-combination and respectively degenerative transfer mechanisms (scheme 1.2) and are known as reversible-deactivation radical polymerizations (RDRPs).[11,18]

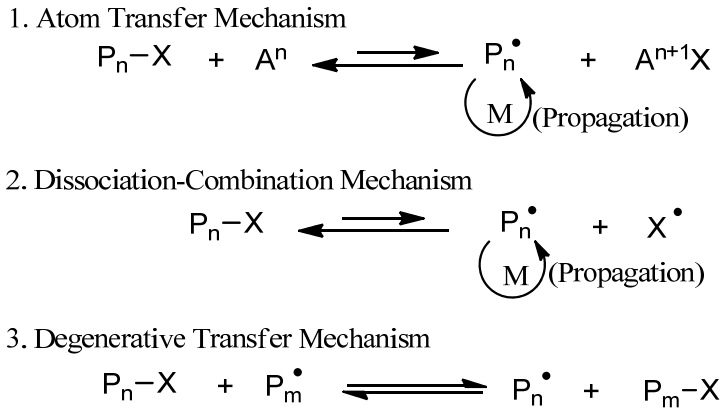

Scheme 1.2. Mechanisms of RDRPs.

ATRP typically involves the use of a metal halide catalyst in a lower oxidation state (Mt^n) in conjunction with an alkyl halide initiator to generate an initiating species and the metal halide in a higher oxidation state. The metal halide catalyst can actively undergo redox reactions with the propagating polymer chain ends thus reversibly trapping the growing chains.[13] The limitations to this technique, include toxicity of some metal catalyst, required purification, an intolerance to oxygen, have led to development of variations on the original ATRP. These include, initiator for continuous activator generation (ICAR), activators generated by electron transfer (AGET), and

activators regenerated by electron transfer (ARGET).[13] SFRP comprises the use of a stable radical, typically nitroxides such as the 2,2,6,6-tetramethyl-1-piperidinoxyl radical (TEMPO) as a deactivator.[13,19-23] One method in SFRP uses the thermal decomposition of alkoxyamine into a reactive radical and a stable radical, while the other employs a conventional radical initiator such as AIBN in conjunction with TEMPO.[2] Finally, RAFT polymerization functions *via* degenerative transfer using dithioesters (xanthates, trithiocarbonates) and other derivatives as a transfer agent in addition to conventional free radical initiators.[2,24-28] In a RAFT polymerization the polymer molecular weight is controlled by the ratio of the monomer to RAFT agent and thermal initiator used.

1.3 Cp_2TiCl mediated CRP of dienes

While the applications of early transition metals (ETM) in □-olefin coordination polymerizations[29] and organometallic reactions [30] have long been established, the unique advantages offered by the radical chemistry of Ti have only recently been recognized, [31] and this area of research has since witnessed a sustained growth,[32] currently emerging as a powerful new strategy in organic synthesis. Thus, a representative example, the soluble, lime-green paramagnetic $Cp_2Ti(III)Cl$[33] complex, inexpensively synthesized in situ by the Zn reduction of $Cp_2Ti(IV)Cl_2$[34] is a very mild one electron transfer agent and catalyzes a variety of radical reactions[35] including the radical ring opening (RRO) of epoxides.[31]

We have recently extended the use of Cp_2TiCl to polymer chemistry and introduced both epoxides[36] and aldehydes[37] as novel classes of initiators for radical polymerizations. The first examples of an ETM-catalyzed LRPs were demonstrated for styrene with initiation[38] from epoxide RRO,[36] aldehyde SET reduction,[37] redox reactions with peroxides[37b] as well as halide abstraction.[39] This methodology was also applied in the synthesis of branched and graft copolymers.[40]

While the ligand effect was thoroughly investigated in ETM-catalyzed coordination polymerizations, it is less documented for radical processes. Thus, in our efforts to optimize Ti-LRP, the effect of ligands,[36b-d] reducing agents,[36e] solvents and additives,[36f] as well as reagent ratios and temperature[36e,f] was also investigated. This study revealed the superiority of sandwich metallocenes over alkoxide and half-sandwich ligands, as well as the relatively weak influence of the substituents on the Cp ligands. Gratifyingly, the most promising catalyst (Cp_2TiCl_2) was also the least expensive one.[36g]

Polymers derived from 1,3-dienes, such as isoprene, butadiene, and chloroprene are industrially relevant.[41] However, their controlled synthesis is typically accomplished only by anionic[42] or coordination[43] methods which require stringent conditions and limit the range of initiator functionalities. While ATRP works exceptionally well with styrene and (meth)acrylates its extension to dienes,[44] VAc,[45] or VCl[46] has proven troublesome and, with the notable exception of nitroxide[47] and RAFT reagents[48], metal catalyzed LRP methods have failed to control isoprene polymerizations. Thus, as transition metal catalysts appear to be conspicuously absent from the available isoprene LRP methods, we decided to investigate the potential of the Cp_2TiCl/epoxide system in this application.[49]

1.4 Metal mediated CRP of fluorinated monomers

The typical used well established CRP methodologies were applied to the polymerization of vinylidene fluoride. However, all attempts for this CRP were unsuccessful. While CRP was claimed with boranes/oxygen initiator in the terpolymerization of VDF, TrFE and CTFE,[50] several efforts to duplicate the method for the homopolymerization of VDF have proved fruitless. Although other monomers like styrenes and (meth)acrylates containing (pendant) fluorinated groups[51-54] have been successfully polymerized using ATRP, NMP and RAFT methodologies,

extension of this to main chain fluorinated monomers such as VDF has been troublesome and futile.

Considering the Cp_2TiCl[55], a mild one electron transfer agent, is available in situ by Zn reduction of Cp_2TiCl_2[56] and catalyzes a variety of radical reactions[57], including epoxide radical ring opening RRO,[58] aldehyde SET reduction and halide abstraction, our group have perfected its use in the CRP of styrene and dienes[59,60,61,62] initiated by epoxides, aldehydes, halides , and peroxides.

We extended the same chemistry to VDF[63] with a series of epoxides, aldehydes, halides and peroxides (scheme 1.3), known to initiate both styrene and diene polymerizations in the presence of $Cp_2TiCl^{\bullet}$, as potential room temperature initiators for VDF.

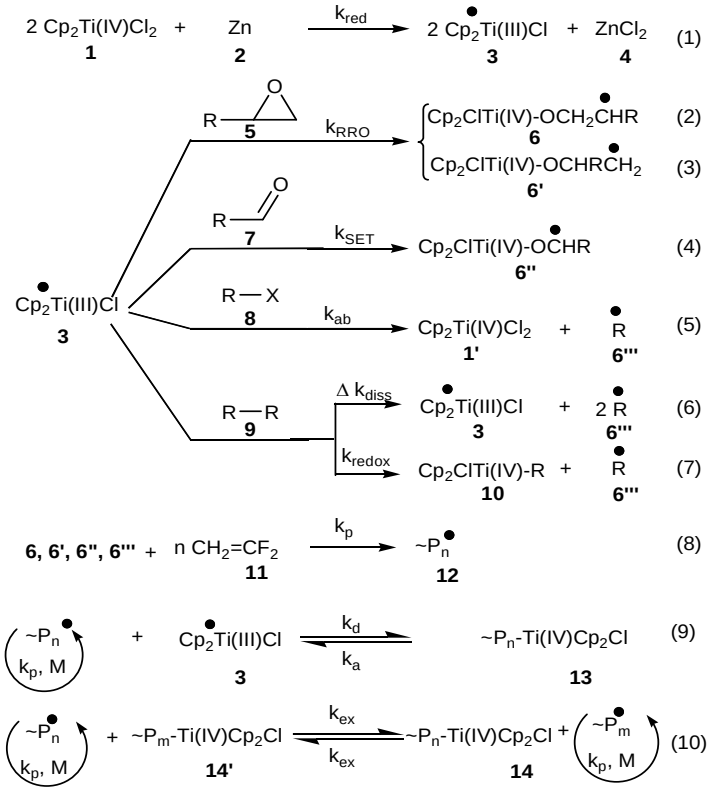

Scheme 1.3. Cp_2TiCl-mediated VDF polymerization mechanism.

As the most effective methodology to CRP of fluorinated monomers,[51] is based on iodine degenerative transfer[64,65] (IDT: $P_n^{\bullet} + P_m\text{-}I \rightleftharpoons P_n\text{-}I + P_m^{\bullet}$), on one of the oldest reported CRP methods.[66] Typically involving the use of a free radical initiator in conjunction with polyhalides especially (per)fluorinated iodine chain transfer (CT) agents at high temperatures(T = 100-250 °C).[67-71] Unfortunately this technique lacks the capability to synthesize well defined block copolymers, as it leads to ill-defined mixtures of homo and block (co)polymers upon sequential addition of other monomer(s).

Therefore the need for a more effective chemistry is necessary not only for the controlled homopolymerization of fluorinated monomers (VDF), but also one that can garner the synthesis well-defined of block copolymers. Presented is thus the recently demonstrated use of photolyzable $Mt_2(CO)_{10}/R_F\text{-}I$[72] (chapter 4) as well as copper assisted photo-iniferter (chapter 5) systems are indeed very successful for VDF-CRP and synthesis of block copolymers.

1.5 References

1 IUPAC definition of polymer.
2 Odian, G. *Principles of Polymerization*. 4th Ed. Wiley, **2004**.
3 Seymour R. B. *J Chem. Educ.* **1988**, *65(4),* 327-34.
4 Tirrel, M. *Chem. Eng. Sci.* **1995**, *50(24),* 4123-4141.
5 Carothers, W. H. *J. Am. Chem. Soc.*, **1929**, *51*, 2548.
6 Szwarc M. Living polymers. *Nature* **1956**, *178*, 1168–9.
7 Szwarc, M.; Levy, M.; Milkovich, R. *J. Am. Chem. Soc.* **1956**, *78*, 2656–7.
8 Richards, D. H.; Szwarc M. *Trans Faraday Soc* **1959**, *55*, 1644–50.
9 Yagci, Y.; Tasdelen, M. A. *Prog. Polym. Sci*. **2006**, *31,* 1133–1170.
10 Smida, J.; Van Beylen, M.; Hogen-Esch, T. E. *Prog. Polym. Sci.* **2006**, 31, 1041–1067.
11 (a) Shipp, D. A. *Polym. Rev.* **2011,** *51,* 99–103. (b) Shipp, D. *J. Macromol. Sci. Part C: Polym. Revs*. **2005**, *45*, 171–194. (c) Matyjaszewski, K. *Macromolecules.* **1993**, *26*, 1787–1788. (d) Moad, G.; Solomon, D. H. *The Chemistry of Radical Polymerization*; 2nd ed.; Elsevier: Amsterdam, **2006**.
12 Allan, L. E. N.; Perry, M. R.; Shaver, M. P. *Prog. Polym. Sci*. **2012,** *37*, 127–156.
13 Braunecker, W. A.; Matyjaszewski, K. *Prog. Polym. Sci.* **2007**, *32*, 93–146.
14 Tsarevsky, N. V.; Krzysztof Matyjaszewski, K. *Chem. Rev.* **2007,** *107*, 2270-2299.
15 Tanaka, K.; Matyjaszewski, K. *Macromol. Symp*. **2008**, *261*, 1–9.
16 Tanaka, K.; Matyjaszewski, K. *Macromolecules.* **2007**, *40,* 5255-5260.
17 Yu Wang, Y.; Soerensen, N.; Zhong, M.; Schroeder, H.; Buback, M.; Matyjaszewski, K. *Macromolecules.* **2013***, 46,* 683−691.
18 Jenkins, A. D.; Jones, R. G.; Moad, G. *Pure Appl. Chem.* **2010**, *82*, 483–491.
19 Li, J.; Zhang, Z. *J. Macromol. Sci.,Part A: Pure Appl. Chem*. **2013**, *50*, 358–363.
20 Montezuma, G. G. C.; Contant, S.; Lona, L. M. F. *Macromol. React. Eng.* **2012**, *6(12)*, 516-522.
21 Yoshida, E. *Polymers* **2012**, *4*(*2*), 1125-1156; doi:10.3390/polym4021125.
22 Ding, J.; Steven Holdcroft, S. *Aust. J. Chem*. **2012**, *65*, 1117–1123.
23 Obata, M.; Ohtake, E.; Hirohara, S.; Tanihara, M.; Yano, S. *J. Polym. Sci.: Part A: Polym. Chem.* **2012***, 50,* 3592–3597.
24 Liu, G.; Shi, H.; Cui, Y.; Tong, J.; Zhao, Y.; Wang, D.; Cai, Y. *Polym. Chem*., **2013**, *4*, 1176–1182.
25 Shanga, C.; Xu, J.; Wang, X.; Zhang, X.; Zhang, W.; Zhang, T. *Polymer*, **2013**, *54*, 614-622.
26 Niu, S.; Zhang, L.; Zhu, J.; Zhang, W.; Cheng, Z.; Zhu, X. *J. Polym. Sci.: Part A: Polym. Chem.* **2013**, *51*, 1197–1204.
27 Ramesh, K.;, Mishra, A. K.; Patel, V. K.; Vishwakarma, N. K.; Biswas, C. S.; Paira, T. K.; Mandal, T. K.; Pralay Maiti, P.; Misra, N.; Ray, B. *Polymer,* **2012**, *53*, 5743-5753.
28 Jiang, H.; Zhang, L.; Qin, J.; Zhang, W.; Cheng, Z.; Xiulin Zhu, X. *J. Polym. Sci.: Part A: Polym. Chem.* **2012**, *50*, 4103–4109.
29. Mahanthappa, M. ; Waymouth, R. M. *J. Am. Chem. Soc.* **2001**, *123*, 12093.
30. Reetz, M. T. *In Organometallics in Synthesis: A Manual.* Schlosser, M. (Ed.). John Wiley and Sons, Chichester, England, **2002**, p 817-924.
31. (a) Rajanbabu, T.; Nugent, W. *J. Am. Chem. Soc.* **1994**, *116*, 986. (b) Rajanbabu, T.; Nugent, W.; Beattie, M. *J. Am. Chem. Soc.* **1990**, *112*, 6408-6409. (c) RajanBabu, T.; Nugent, W. *J. Am. Chem. Soc* **1989**, *111*, 4525.

32. (a) Gansauer, A.; Rinker, B. *Titanium and Zirconium in Organic Synthesis*; Wiley, **2002**. (b) Cuerva, J. M.; Oller-López, J. L.; Oltra, J. E. *Top. Curr. Chem*. **2006**, *264*, 63–91. (c) Gansäuer, A.; Justicia, J.; Fan, C. A.; Worgull, D.; Piestert, F. *Top. Curr. Chem.* **2007**, 279: 25–52.
33. Spencer, R. P.; Schwartz, J. *Tetrahedron*, **2000**, *56*, 2103-2112.
34. Green, M. L.; Lucas, C. R. *J. Chem. Soc. Dalton Trans.* **1972**, *8*, 1000-1003.
35. Barden, M. C.; Schwartz, J. *J. Am. Chem. Soc.* **1996**, *118*, 5484.
36. (a) Asandei, A. D.; Moran, I. W. *J. Am. Chem. Soc.* **2004**, *126*, 15932. (b) Asandei, A. D.; Moran, I. W. *J. Polym. Sci. Part A: Polym. Chem.* **2005**, *43*, 6028. (c) Asandei, A. D.; Moran, I. W. *J. Polym. Sci. Part A: Polym. Chem.* **2005**, *43*, 6039. (d) Asandei, A. D.; Moran, I. W. *J. Polym Sci. Part A: Polym. Chem.* **2006**, *44*, 1060. (e) Asandei, A. D.; Moran, I. W.; Saha, G.; Chen, Y. *J. Polym. Sci. Part A: Polym. Chem.* **2006**, *44*, 2156. (f) Asandei, A. D.; Moran, I. W.; Saha, G.; Chen, Y. *J. Polym. Sci. Part A: Polym. Chem.* **2006**, *44*, 2015. (g) Asandei, A. D.; Moran, I. W.; Saha, G.; Chen, Y. *ACS Symp. Ser.* **2006***, 944,* 125-139.
37. (a) Asandei, A. D.; Chen, Y. *Macromolecules* **2006**, *39*, 7459. (b) Asandei, A. D.; Saha, G. *J. Polym. Sci. Part A: Polym. Chem.* **2006**, *44*, 1106.
38 (a) Asandei, A. D.; Chen, Y.; Moran, I. W.; Saha, G. *Tetrahedron*, **2008**, In press. (b) Asandei, A. D.; Chen, Y.; Moran, I. W.; Saha, G. *J. Organomet. Chem.* **2007**, 692, 3174-3182.
39. Asandei, A. D.; Chen Y.; Simpson, C.; Gilbert, M.; Moran, I. W. *Polym. Prepr.* **2008**, *49(1)*, 489-490. (b) Asandei, A. D.; Chen, Y.; Adebolu, O. *Polym. Mater.: Sci. Eng.* **2008**, *98*, 370-371. (c) Asandei, A. D.; Saha, G. *Polym. Prepr.* **2007**, *48(2)*, 272-273. (d) Asandei, A. D.; Chen, Y. *Polym. Mater.: Sci. Eng.* **2007**, *97*, 450-451.
40. (a) Asandei, A. D.; Saha, G. *Polym. Prepr.* **2004**, *45(2)*, 768. (b) Asandei; A. D; Saha, G. *Polym. Prepr.* **2004**, *45(1)*, 999. (c) Asandei, A. D.; Moran, I. W.; Saha, G; Chen, Y. *Mater. Res. Soc. Symp. Proc.* **2005,** *856E*, BB11.9. (d) Asandei, A. D.; Moran, I. W.; Saha, G.; Chen, Y. *Polym. Mater.: Sci. Eng.*, **2004**, *91*, 786.
41. (a) Schops, M.; Leist, H.; DuChesne, A.; Wiesner, U. *Macromolecules* **1999**, *32*, 2806. (b) Li, W.; Wang, H.; Yu, L.; Morkved, T.; Jaeger, H. M. *Macromolecules* **1999**, *32*, 3034. (c) Allgaier, J.; Poppe, A.; Willner, L.; Richter, D. *Macromolecules* **1997**, *30*, 1582.
42. Hirao, A.; Hayashi, M. *Acta Polym*. **1999**, *50*, 219.
43. Evans, W. J.; Giarikos, D. G.; Allen, N. T. *Macromolecules* **2003**, *36*, 4256.
44. Wootthikanokkhan, J.; Peesan, M. *Eur. Polym. J.* **2001**, *37*, 2063.
45. Xia, J.; Paik, H.; Matyjaszewski, K. *Macromolecules* **1999**, *32*, 8310-8314.
46. Percec, V.; Popov, A.; Castillo, E.; Monteiro, M.; Barboiu, B.; Asandei A. D.; Mitchell, C. *J. Am. Chem. Soc.* **2002**, *124*, 4940-4941. (b) Asandei, A. D.; Percec, V. *J. Polym. Sci.: Part A: Polym. Chem.* **2001**, *39*, 3392.
47. (a) Grubbs, R. B.; Wegrzyn, J.; Xia, Q. *Chem. Commun*. **2005**, *1*, 80. (b) Kamachi, M.; Kajiwara, A. *Macromolecules* **1996**, *29*, 2378. (c) Keosherian, B.; Georges M.; Quinlan, M.; Vergin, R.; Goodbrand, B. *Macromolecules* **1998**, *31*, 7559.(d) Benoit, D.; Harth, E.; Fox, P.; Waymouth, R. M.; Hawker, C. J. *Macromolecules* **2000**, *33*, 363. (e) Li, I.; Howell, B.; Dineen, M.; Kastl, P.; Lyons, J.; Meunier, D.; Smith, P.; Priddt, B. *Macromolecules* **1997**, *30*, 5195. (f) Gavranovic, G.; Csihony, S.; Bowden, N. B.; Hawker, C. J.; Waymouth, R. M.; Moerner, W. ; Fuller, G. *Macromolecules* **2006,** *39,* 8121.

48. (a) Germack, D. S; Wooley, K. L. *J. Polym. Sci.: Part A: Polym. Chem.* **2007**, *45*, 4100. (b) Jitchum, V.; Perrier, S. *Macromolecules* **2007**, *40,* 1408.
49. (a) Asandei, A. D.; Simpson, C. P.; Yu, H. S. *Polym. Prepr.* **2008**, *49(2)*, 73-74. (b) Asandei, A. D.; Simpson, C. P. *Polym. Prepr.* **2008**, *49(2)*, 75-76. (c) Asandei, A.D.; Simpson C. *Polym. Prepr*. **2008**, *49(1),* 452-453. (d) Asandei, A. D.; Saha, G. *Polym. Prepr.* **2005**, *46(2)*, 474-475.
50 (a) Chung, T. C.; Petchsuk, A. *Macromolecules* **2002**, *35*, 7678–7683. (b) Chung, T. C.; Petchsuk, A. US Patent 6,355,749, **2002.**
51 Ameduri, B.; Boutevin, B. *Well Architectured Fluoropolymers: Synthesis, Properties and Applications*; Elsevier: Amsterdam, **2004**.
52 Hansen, N. M. L.; Jankova, K.; Hvilsted, S. *Eur. Polym. J.* **2007**, *43*, 255–293.
53 Lacroix-Desmazes, P.; Ameduri, B.; Boutevin, B. *Collect. Czech. Chem. Commun.* **2002**, *67*, 1383–1415.
54 Ameduri, B. *Macromolecules,* **2010**, *43(24)*, 10163–10184.
55 Spencer, R. P.; Schwartz, J. *Tetrahedron*, **2000**, *56*, 2103-2112.
56 Green, M. H.; Lucas, C. R. *J. Chem. Soc. Dalton Trans.* **1972**, *8*, 1000.
57 Barden, M. C.; Schwartz, J. *J. Am. Chem. Soc.* **1996**, *118*, 5484.
58 Rajanbabu, T. V.; Nugent, W. *J. Am. Chem. Soc.* **1994**, *116*, 986.
59 (a) Asandei, A. D.; Moran, I. W.; Chen, Y.; Saha, G. *J. Organomet. Chem.* **2007**, *692*, 3174-3182. (b) Asandei, A. D.; Moran, I. W.; Saha, G.; Chen, Y. *ACS Symp. Ser.* **2006**, *944*, 125. (c) Asandei, A. D.; Moran, I. W.; Saha, G.; Chen. Y. *J. Polym. Sci.: Part A: Polym. Chem.* **2006**, *44*, 2156. (d) Asandei, A. D.; Moran, I. W.; Saha, G.; Chen. Y. *J. Polym. Sci.: Part A: Polym. Chem.* **2006**, *44*, 2015. (e) Asandei, A. D.; Moran, I. W. *J. Polym. Sci.: Part A: Polym. Chem.* **2006**, *44*, 1060. (f) Asandei, A. D.; Moran, I. W. *J. Polym. Sci.: Part A: Polym. Chem.* **2005**, *43*, 6039. (g) Asandei, A. D.; Moran, I. W. *J. Polym. Sci.: Part A: Polym. Chem.* **2005**, *43*, 6028. (h) Asandei, A. D.; Moran I. W. *J. Am. Chem. Soc.* **2004**, *126*, 15932. (i) Asandei; A.D.; Moran; I.W.; Castro, M.A. *Polym. Prepr.* **2003**, *44(1)*, 829. (j) Asandei, A. D.; Chen, Y.; Saha, G.; Moran, I. W.; *Tetrahedron*, **2008**, *64,* 11831.
60 Asandei; A. D; Chen, Y. *Macromolecules* **2006**, *39*, 7549.
61 (a) Asandei, A. D.; Chen, Y. *Polym. Mater.: Sci. Eng.* **2007**, *97*, 450. (b) Asandei, A. D.; Saha, G. *Polym. Prepr.* **2007**, *48*, 272.
62 Asandei, A. D.; Saha, G. *J. Polym. Sci.: Part A: Polym. Chem.* **2006**, *44*, 1106.
63 Asandei, A. D.; Adebolu, O. I.; Simpson, C. P. *Towards Controlled Metal Mediated VDF Polymerization. Acs. Symp. Ser. Advances in Fluorine-Containing Polymers; Smith, D. et al. Eds;* **2012**, *1106*, Chapter 4, p 47-63. http://pubs.acs.org/doi/abs/10.1021/bk-2012-1106.ch004
64 Goto, A.; Fukuda, T. *Progr. Polym. Sci*. **2004**, *29*, 329-85.
65 (a) Fukuda, T.; Goto, A.; Tsujii, Y. in *Handbook of Radical Polymerization*. Matyjaszewski, K.; Davis, T. P. Eds. Wiley, New York, **2002**, p. 407-62. *(b)* Gaynor, S. G.; Wang, J. S.; Matyjaszewski, K. *Macromolecules* **1995**, *28*, 8051-56.
66 (a) Oka, M.; Tatemoto, M.; in *Contemporary Topics in Polymer Science.* Bailey, W. J.; Tsuruta, T.; Eds. Plenun Press, New-York, **1984**, *4*, 763-81. (b) Tatemoto, M. in *Polymeric Materials Encyclopedia*, Salamone, J. C. Ed., CRC Boca Raton, FL, **1996**, *5*, 3847-62.
67 David, G.; Boyer, C.; Tonnar, J.; Ameduri, B.; Lacroix-Desmazes, P.; Boutevin, B. *Chem. Rev.* **2006**, *106*, 3936-62.

68 Ameduri, B.; Ladavière, C.; Delolme, F.; Boutevin, B.; *Macromolecules* **2004**, *37*, 7602-12.
69 Boyer, C.; Valade, D.; Sauguet, L.; Ameduri, B.; Boutevin, B. *Macromolecules* **2005**, *38*, 10353-62.
70 Boyer, C.; David, V.; Lacroix-Desmazes, P.; Ameduri, B.; Boutevin, B. *J. Polym. Sci.: Part A: Polym. Chem*. **2006**, *44*, 5763-77.
71 Valade, D.; Boyer, C.; Ameduri, B.; Boutevin, B. *Macromolecules* **2006**, *39*, 8639-8651.
72 Asandei, A. D.; Adebolu, O. I.; Simpson, C. P. *J. Am. Chem. Soc.* **2012**, *134*, 6080−6083.

Chapter 2: Cp_2TiCl-Mediated Controlled Radical Polymerization of Dienes Initiated by Epoxide Radical Ring Opening, Single Electron Transfer-Reduction of Aldehydes, and Halide Abstraction.

The effect of reaction variables in the Cp_2TiCl-Mediated controlled radical isoprene (2-methyl-1,3-butadiene) polymerizations initiated by epoxide radical ring opening (RRO), was investigated over a wide range of conditions ([Cp_2TiCl_2]/[epoxide] = 1/1 to 6/1, [Cp_2TiCl_2]/[Zn] = 1/0.5 to 1/8, [isoprene]/[epoxide] = 20/1 to 1000/1, T = 70 to 130 °C in THF and dioxane), to reveal a linear dependence of molecular weight on conversion, linear first-order kinetics and moderate polydispersities up to high conversions, with an optimum in initiator efficiency, rate and polydispersity for [epoxide]/[Cp_2TiCl_2]/[Zn] = 1/3/6 to 1/4/8 at 90 - 110 °C. NMR studies demonstrated the epoxide initiation and the stereoselectivity of a conventional radical polymerization. Furthermore, random and block copolymers with styrene could also be obtained. This methodology was then expanded, using the optimum conditions, to initiation via single electron transfer (SET) reduction of aldehydes in addition to halide abstraction. Subsequently each of the three initiating systems, RRO, SET-reduction, and halide abstraction, were shown to work with both 1,3-butadiene and 2,3-dimethyl-1,3-butadiene.

2.1. Introduction

Natural rubber has been processed and used as far back as 1600 BC by ancient Mesoamerican peoples.[1] Their source of this natural rubber was an emulsion secreted from certain plants such as the *Castilla elastica* tree. From this point in history the processing and use of natural rubber (*cis*-1,4-polyisoprene) has expanded greatly, but had limitations. In 1839 when Charles Goodyear discovered the vulcanization process, the use of natural rubber increased dramatically. Up to this point all or most the rubber used was harvested from various plants (*hevea brasiliensis*). It was not until the early to mid-20th century did the necessity for the production of synthetic rubber come into play. It was around this time that the world was engaged in the two world wars, cutting off the supply of natural rubber from many of the industrialized nations. It was here when the importance of developing synthetic means of producing polyisoprene became prevalent. Even more so was the need to develop synthetic methods for the controlled polymerization of 1,3-dienes. This came about in the 1930's in Germany with the advent of the Buna-S styrene butadiene copolymer *via* anionic methods. The research into controlled polymerization of 1,3-dienes was furthered when the Zeigler-Natta type coordination catalysts were developed in the 1950's and later by metallocene complexes[2] which provided great stereo control and living character and allowed for the synthesis of the various types of polydienes.

This polymerization of 1,3-dienes, is an important process in both academia and industrial settings[3] today. Products such as *cis*-1,4-polyisoprene, a synthetic version of natural rubber, *trans*-1,4-polyisoprene as well as styrene, isoprene, butadiene, and isobutylene copolymers are widely produced commercially. Two billion pounds of the *cis*-1,4-polyisoprene are used each year in the United States alone[4] and it is present in items such as gloves, molded objects, adhesives, rubber bands, tires, footwear, and sporting good just to name a few. *Trans*-1,4-

polyisoprene a crystalline polymer used as a thermoplastic due to its relatively high T_g, and T_m can be found in use in golf balls and orthopedic devices.[4] There are also the various copolymers specifically synthesized depending on the physical requirements of the final product, typically synthesized *via* anionic or coordination methods. However, as research into controlled radical processes has surged due to the higher flexibility and lower cost, one can see the importance of developing a catalytic system that can produce these immensely valuable polymers effectively and cost efficiently.

Polymerization of conjugated dienes such as isoprene, 1,3-butadiene, and 2,3-dimethyl-1,3-butadiene has been performed traditionally using various synthetic methods such as radical, anionic[5], and coordination[6] polymerizations. More important is the controlled polymerization of these materials. This is typically accomplished by anionic polymerizations using organolithium reagents or *via* coordination methods employing Ziegler-Natta[6] or metallocene[6] catalysts. These systems have been widely used as they can produce regioregular polymers. This is one of the great advantages of these methods as the physical properties of the material depend greatly on the microstructure. The use of $TiCl_4$, VCl_3, or titanium alkoxides, in conjunction with alkyl aluminum produce respectively *cis*-1,4-, *trans*-1,4-, and 3,4-polyisoprene[4] while organolithium reagents produce highly *cis*-1,4-polyisoprene (anionic).[4] However, there is an inherent problem with these types of reactions, as they require very stringent synthetic conditions, and on intolerant of additional functionalities on the monomers/polymer. Thus, the solvents, monomers, and other reagents must be of the highest purity, and the reactions must be performed in an inert atmosphere usually at very low temperatures to afford any control and narrow molecular weight distributions. Moreover, the transition metal catalysts used in these reactions are either specially synthesized requiring multi-step reactions or extremely expensive

when available commercially. To avoid these issues, and give a more robust means of polymerizing conjugated dienes, radical methods can be employed.

Since their inception in the mid-90s, controlled radical polymerizations (CRP) have undergone a remarkable development and have become one of the most useful and dynamic synthetic methods in modern polymer chemistry.[7] The ability of CRP to control molecular weight (M_n) and polydispersity (M_w/M_n) while requiring considerably more user-friendly reaction conditions vs. water sensitive ionic and coordination polymerizations has greatly benefited the polymer synthesis toolbox and has enabled its wide use in the synthesis of complex macromolecular structures. Accordingly, such CRP applications have motivated extensive efforts in the development of novel catalytic systems. These systems are generally more tolerant of initiator functionality, solvent polarity, temperature, and of trace impurities. The ability of CRP to control molecular weight and polydispersity *via* a reversible termination of propagating chains has enabled its wide application in the synthesis of complex macromolecular structures.[8]

It is currently accepted that the polymerization livingness/control is afforded by the reversible termination of the growing chains with persistent radicals[9] or degenerative transfer agents and that mechanistically[10], CRP occurs by atom transfer (ATRP), dissociation-combination (DC) or degenerative transfer (DT) processes. Catalyst-wise, organic derivatives such as nitroxide[11] and iodine[12] or sulfur-based transfer agents[13] mediate CRP *via* DC and respectively DT, while organometallic complexes [14] of Co[15], Te[16a], Sb[16b], Bi[16c], Mo[17a], and Cr[17b] may favor both DC and DT pathways. Finally, late transition metal halide persistent radicals[9] (Cu, Ni, Fe, Ru, etc)[7,10,18] have proven very successful in ATRP.

As such these paramagnetic metal systems utilizing the persistent radical effect have proven very successful in controlled radical polymerizations mediated by atom transfer (ATRP) or

dissociation-combination (DC). These systems typically employ only activated halides or thermal initiators. The radical methods will generally give a mixture of the various modes of addition (1,2-, 3,4-, 1,4-*cis and trans*). As the properties correlate with the microstructure, this is one drawback to this synthetic approach. While atom transfer radical polymerization works extremely well with styrene and (meth)acrylates etc., its use with dienes[19] has been problematic, yielding little to no conversion. This has been attributed to the poor solubility of the typical CuBr/amine catalyst/ligand system, low concentration of active radical species, and the chelation of the copper catalysts by the diene monomers[20]. These monomers can however be polymerized by degenerative transfer (DT) or the dissociation combination (DC) mechanisms. Thus, reversible addition fragmentation transfer (RAFT)[21] can produce relatively narrow molecular weight distributions (1.2-1.4); however they generally fail to achieve high conversions with typical values < 20% and molecular weights < 5,000[20], although there were some reports of higher conversions and molecular weights, the molecular weight distribution was considerably broader.[22] By contrast, nitroxide mediated polymerizations[23] have been shown to give conversions as high as 80% with molecular weights up to 25,000, narrow molecular weight distributions (1.1-1.3) and the ability to produce various block copolymers. However, these systems generally require multistep synthesis of the nitroxides and often times the polymerization rate slows and eventually stops.[23b] This is attributed to the persistent radical effect (PRE)[23c,d] and the irreversible generation of persistent radicals. The typical microstructure composition is generally 80-90% 1,4-polyisoprene (both *cis* and *trans*). While this does not compete with the anionic and coordinative methods in regioselectivity, this material has been show to exhibit similar physical properties20 (T_g = -61°C) with *cis*1,4-polyisoprene (T_g = -73°C). Therefore the need for a controlled radical process with which we can use inexpensive

commercially available reagents, tolerate a wide variety of functionalities and reactions conditions, and proceed with minimal irreversible termination is demonstrated.

However, current CRP systems are still somewhat limited by the restrictive choice of only activated halide or thermal initiators, which may restrict chain end functionality and by the range of monomers polymerizable by a given method. Thus, a broader initiator and catalyst selection would further enhance the usefulness of CRP in macromolecular synthesis. Epoxides and carbonyls are fundamental motifs in organic and polymer chemistry, and are commercially available with a wide structural variation. Moreover, they could provide alcohol terminal units of the polymer chains, and be very useful in block or graft copolymer synthesis. Yet, none of the current late transition metal mediated radical polymerizations has taken advantage of these possibilities.

While the applications of early transition metals (ETM) in α-olefin coordination polymerizations[24] and organometallic reactions[25] have long been established, the unique advantages offered by the radical chemistry of Ti have only recently been recognized,[26] and this area of research has since witnessed an effervescent and sustained growth,[27] currently emerging as a powerful new strategy in organic synthesis. Thus, a representative example, the soluble, lime-green paramagnetic $Cp_2Ti(III)Cl$[28] complex, inexpensively synthesized in situ by the Zn reduction of $Cp_2Ti(IV)Cl_2$[29] is a very mild one electron transfer agent and catalyzes a variety of radical reactions[30] including the radical ring opening (RRO) of epoxides.[26]

We have recently extended the use of Cp_2TiCl to polymer chemistry and introduced both epoxides[31] and aldehyde[32] as novel classes of initiators for radical polymerizations. The first examples of an ETM-catalyzed CRPs were demonstrated for styrene with initiation[33] from epoxide RRO,[31] aldehyde SET reduction,[32] redox reactions with peroxides[31b] as well as halide

abstraction. This methodology was also applied in the synthesis of branched and graft copolymers.

While the ligand effect was thoroughly investigated in ETM-catalyzed coordination polymerizations, it is less documented for radical processes. Thus, in our efforts to optimize Ti-CRP, the effects of ligands,[31b-d] reducing agents,[31e] solvents and additives,[31f] as well as reagent ratios and temperature[31e,f] were also investigated. This study revealed the superiority of sandwich metallocenes over alkoxide and half-sandwich ligands, as well as the relatively weak influence of the substituents on the Cp ligands. Gratifyingly, the most promising catalyst (Cp_2TiCl_2) was also the least expensive one.[31g]

Interestingly, the Cp_2ClTi-OR alkoxides generated in-situ by epoxide RRO[34] or aldehyde SET reduction[34b] were also found to mediate the living ring opening polymerization of cyclic esters such as caprolactone. Moreover, these novel initiating methodologies were applied in the Cp_2ClTi-mediated synthesis of graft or mixed arm brush copolymers where epoxide groups along polymer chains[35] were used as an initiating site for graft copolymerizations of both olefins and cyclic esters.

As such, diene polymers are indeed industrially relevant[36] and their controlled synthesis with a wide range of initiator functionalities is not easily accomplished via the typical anionic[37] or coordination[38] methods. Although ATRP works exceptionally well with styrene and (meth)acrylates[7], its extension to dienes,[39] VAc,[40] or VCl[41] has proven troublesome and, with the notable exception of nitroxide[42] and RAFT reagents[43], up until now metal catalyzed CRP methods have failed to control isoprene polymerizations. Thus, as transition metal catalysts appear to be conspicuously absent from the available diene CRP methods, we herein investigate the potential of the Cp_2TiCl chemistry in conjunction with epoxides, aldehydes, and halides in this application.[44]

2.2 Experimental.

2.2.1 Materials.

Activated Zn powder (Zn, 99+ %), α,α'-dibromo-*p*-xylene (DBPX, 97%) benzaldehyde (BA 99 %), benzyloxybenzaldehyde (BBA, 99 %) %), (1-bromoethyl)benzene (BEB, 97%) glycidyl 4-methoxyphenyl ether (MPEG, 99%), 2,2-bis[4-(glycidyloxy)phenyl]propane (DGEBA, 97%), and 1,3-Butadiene (BD, 99+%) all from Aldrich and bis(cyclopentadienyl)titanium dichloride (Cp_2TiCl_2, Acros, 97 %), Styrene oxide (SO, Acros, 98%) were used as received. 2,3-dimethyl-1,3-butadiene (DMBD, ChemSampCo, 99+%), was dried over CaH_2 and passed through a basic Al_2O_3 column., 1,4-dioxane (99.7 %) and tetrahydrofuran (THF, 99.9%) both from Fisher were distilled from a blue Na/benzophenone solution. Isoprene (Acros, 99%) was dried over CaH_2 and passed through a basic Al_2O_3 column.

2.2.2 Techniques.

^{1}H-NMR (500 MHz) spectra were recorded on a Bruker DRX-500 at 24 °C in $CDCl_3$ (Aldrich; 0.03% v/v TMS as internal standard). GPC analyses were performed on a Waters 150-C Plus gel permeation chromatograph equipped with a Waters 410 differential refractometer, a Waters 2487 dual wavelength absorbance UV-VIS detector set at 254 nm, a Polymer Laboratories PL-ELS 1000 evaporative light scattering (ELS) detector and with a Jordi Flash Gel ($1x10^5$ Å, 2 x 10*4* Å, $1x10^3$ Å) column setup with THF as eluent at 2 mL/min at 40 °C. Number-average (M_n) and weight-average molecular weights (M_w) were determined from polystyrene calibration plots.

2.2.3 Polymerizations.

A 35-mL Ace Glass 8648 # 15 Ace-Thread pressure tube equipped with bushing and a plunger valve and containing Cp_2TiCl_2 (49 mg, 0.20 mmol), Zn (26 mg, 0.40 mmol) CaH_2 (< 10 mg

as trace moisture scavenger) and dioxane (1.0 mL) was degassed, and the Ti reduction was carried out at rt. The tube was then cooled, opened under Ar, charged with MPEG (9 mg, 0.05 mmol) and isoprene (1 mL, 9.98 mmol), re-degassed and heated at 110 °C for 24 h. Conversion and molecular weights were determined by NMR and GPC respectively. The reported M_n and M_w/M_n values correspond to unprecipitated samples, since MeOH precipitation seemed to artificially affect the linearity of the M_n vs. conversion plots and reduce M_w/M_n, especially at low molecular weights (e.g. M_n < 5,000), *via* fractionation. Kinetic plots were constructed from one data point experiments

2.3 Results and Discussion

The proposed polymerization mechanism is outlined in Scheme 2.1. The Zn reduction of Cp_2TiCl_2 occurs readily in dioxane to generate $Cp_2Ti(III)Cl$ (eq. 1). Subsequent epoxide RRO, aldehyde SET reduction or halide abstraction (eq. 2) provides the initiating radicals for the polymerization (eq. 3), which is mediated by the reversible termination of the growing chains with a second equivalent of $Cp_2Ti(III)Cl$ *via* a combination of DC and DT mechanisms (eqs.4,5) . The initiation from epoxides, aldehydes, and halides has been evidenced *via* ^{1}H-NMR chain end analysis.

2.3.1 $Cp_2TiCl^{\bullet}$-Mediated CRP of Isoprene Initiated by Epoxide Radical Ring Opening

The mechanism of Ti-mediated isoprene CRP is presented in Scheme 2.1. Zn reduction of $Cp_2Ti(IV)Cl_2$ to the $Cp_2Ti(III)Cl$ metalloradical (eq. 1) is carried out in situ and proceeds readily in THF or dioxane at room temperature, as indicated by a typical red to green color change. While the reduction occurs even with stoichiometric Zn, a small excess was typically employed to accelerate the process. The strong affinity of the Ti radical towards epoxides is evidenced by the

rapid color change to yellow-orange upon injection of excess initiator into the green Cp_2TiCl solutions, indicating the occurrence of the corresponding SET process.

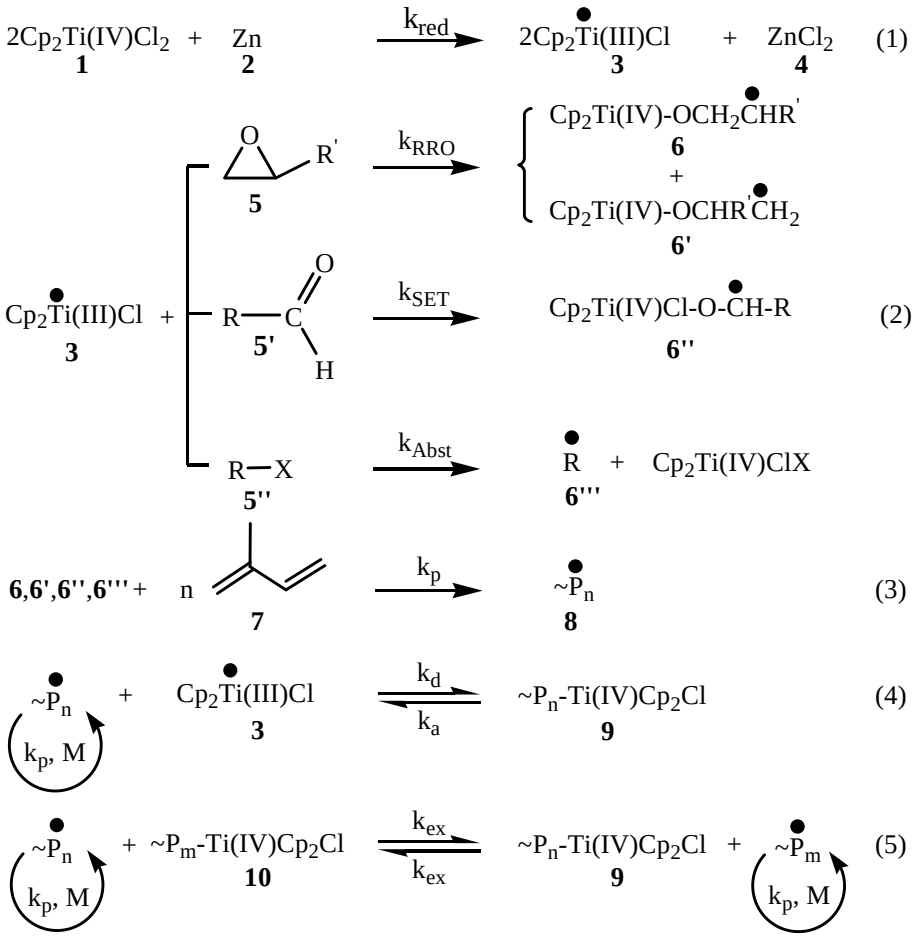

Scheme 2.1. Ti-mediated Diene CRP Initiated by Epoxide RRO, Aldehyde SET, and Halide Abstraction.

Epoxides are unique initiators as their Ti-mediated RRO[27] occurs with the formation of a pair of very reactive primary and secondary, constitutionally isomeric β-titanoxy radicals derived from RRO regioselectivity (Scheme 2.1, eq. 2), where typically the secondary radical is favored, but both have the same thermodynamic stabilization as the corresponding alkyl radicals.[27] The interaction of such radicals with double bonds is well documented,[27b] and their addition to isoprene initiates the polymerization (eq. 3) which proceeds in a controlled fashion, mediated by

the reversible end-capping of the propagating chain end with a second equivalent of Cp_2TiCl. The reversible C-Ti bond homolysis most likely occurs *via* a combination of the DC and DT mechanisms (eqs. 4, 5)[31] and is possibly catalyzed by Zn.[31] Thus, one Ti equivalent is required for epoxide RRO and a minimum of one more for polymerization control.

2.3.2 Demonstration of Initiation from Epoxides: ^{1}H-NMR Discussion.

Several aromatic epoxides (SO, MPEG, DGEBA) were selected as models. The demonstration of the epoxide initiation is available from the analysis of the spectra of the corresponding polymers in Figure 2.1 where, for simplicity, only the most preferred mode of epoxide RRO is depicted. The first observation is that the polyisoprene (PI) spectrum is comparable in terms of stereospecificity (peaks *a-f*) to that of polyisoprene synthesized by free radical as well as nitroxide or RAFT polymerizations at similar temperature[42,43] (*i.e.* ~85 % 1,4; ~8 % 1,2; ~8 % 3,4), suggesting that no special coordination mediated Ti chain end control is occurring. Moreover, specific initiator resonances such as the ones derived from the aromatic regions of SO (*g*, δ = 7.15 ppm), MPEG (*k*, δ = 6.85 ppm), and DGEBA (r_1, r_2, δ = 6.85 and 7.15 ppm) are present. In addition, -CH_x-O- alcohol or ether resonances corresponding to a combination of the primary and secondary alcohols derived from the two modes of epoxide RRO and to the original ether linkages in the initiator are observed as follows: SO (*i*, δ = 3.5-3.8 ppm), MPEG (CH_3-O-, *j*, δ~3.75 ppm; *l, n*, δ = 3.8 - 4 ppm) and DGEBA (*s, u*, δ = 3.6 - 4 ppm). Additional signals such as the small peaks at 6.3-6.6 ppm in the MPEG and DGEBA spectra correspond to a small amount of vinyl ether formed *via* alcohol dehydration during workup. In all cases, the connection of the initiator with polyisoprene is evidenced by a broad series of multiplets (*a'*, δ = ~2.3-3 ppm) corresponding to one of the diastereotopic protons of the first -CH_2- isoprene unit located next to the –CH (*h, m, t*) stereocenter derived from both modes of epoxide RRO.

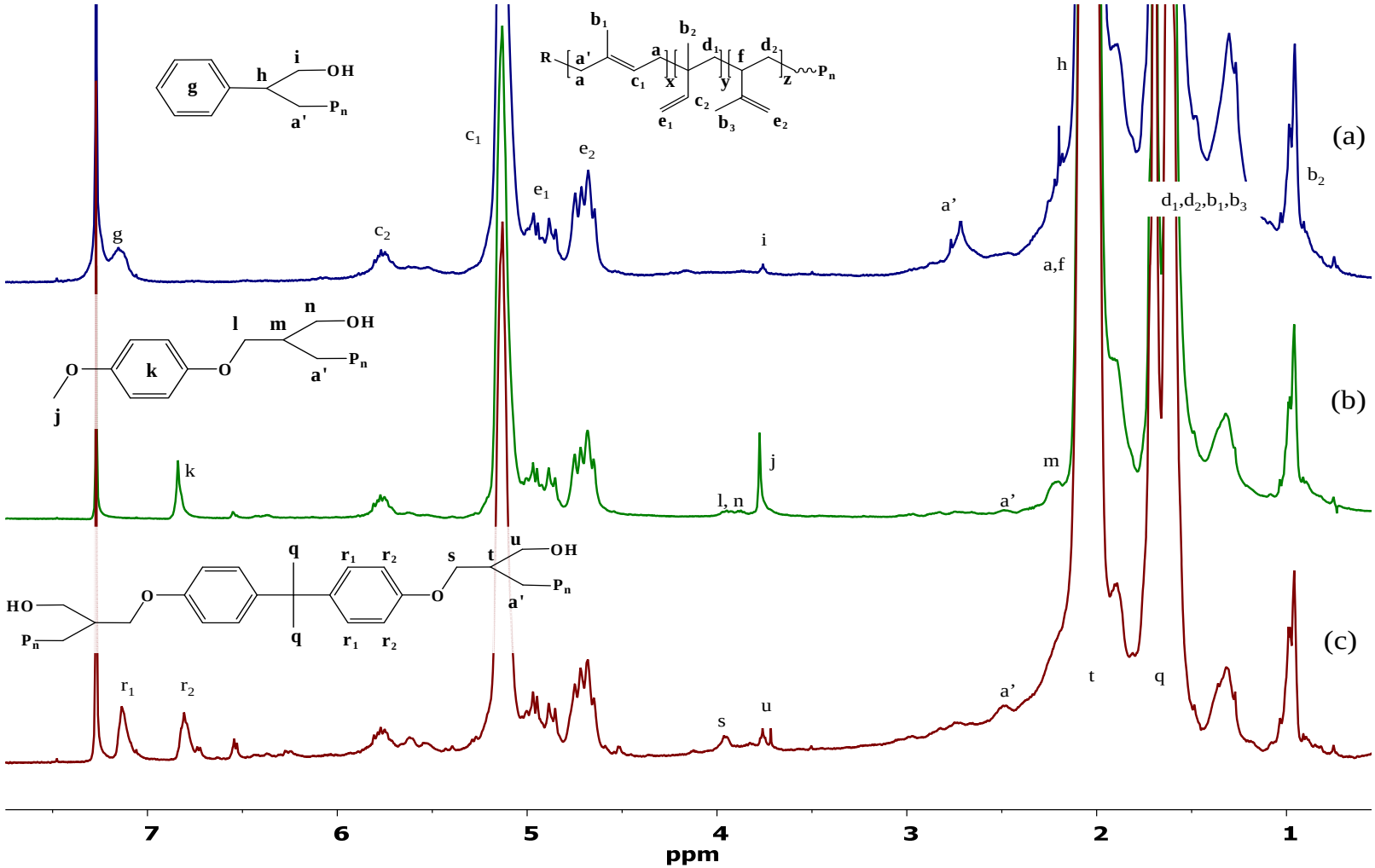

Figure 2.1. 500 MHz ^{1}H-NMR spectra of polyisoprene initiated from epoxides (Table 2.1, exp 23-25): (a) SO, M_n^{NMR} = 4,400, (b) MPEG, M_n^{NMR} = 3,800. (c) DGEBA, M_n^{NMR} = 3,200.

Finally, the integration of the initiator peaks vs. the polymer chain also enables the calculation of M_n^{NMR}, which in each case is reasonably similar to M_n^{GPC}.

2.3.3 Effect of [Isoprene]/[MPEG]/[Cp_2TiCl_2]/[Zn], Temperature, and Solvent on the Epoxide Initiated Isoprene CRP.

Several variables such as the target degree of polymerization (DP = [Iso]/[MPEG]), the [Zn]/[Cp_2TiCl_2] and [Cp_2TiCl_2]/[MPEG] ratios, as well as the solvent and temperature were tested to optimize the polymerization. The results are presented in Figures 2.2 and 2.3, and summarized in Table 2.1. In all cases, a linear dependence of M_n on conversion, moderate polydispersities and linear 1^{st} order kinetics, indicative of the controlled nature of the polymerization were observed up to high conversions. However, the reaction conditions do affect the rate, polydispersity (PDI) as well as initiator efficiency (IE).

As seen below, the effects of the [MPEG]/[Cp_2TiCl_2]/[Zn] ratios are closely intertwined and are detailed in Table 2.1, exp. 1-14 and in Figure 2.2, where progressively higher [Cp_2TiCl_2]/[MPEG] ratios were explored at various [Cp_2TiCl_2]/[Zn] levels, while maintaining [Iso]/[MPEG] = 200/1. According to the proposed mechanism, a minimum [Cp_2TiCl_2]/[MPEG] = 2/1 ratio (one Ti equiv. for radical generation, the other for control) should be enough to control the polymerization. However, excess Cp_2TiCl has a beneficial effect.

Figure 2.2a presents selected examples of the dependence of molecular weight and polydispersity on conversion for various reagent ratios and shows that controlled polymerizations are obtained in all cases. The effect of reagent stoichiometry on initiator efficiency (IE), rate (k_p^{app}) and polydispersity (PDI) are further detailed in Figure 2.2b-d.

Consistent with the proposed mechanism, a low [Cp_2TiCl_2]/[MPEG] ratio (exp 1) does not provide enough Ti for end-capping of the growing chain and the IE is very low but it increases with increasing [Cp_2TiCl_2]/[MPEG] from IE ~ 0.03 at [Cp_2TiCl_2]/[MPEG] = 1/1 to almost

quantitative at $[Cp_2TiCl_2]/[MPEG] = 6/1$. However, even larger Ti excess may contribute to side reactions such as epoxide deoxygenation. Reasonable polymerizations are already observed at $[Cp_2TiCl_2]/[MPEG] = 3/1$-$4/1$.

The trends in IE are paralleled by those in the apparent rate constant of propagation (k_p^{app}, Figure 2.2c) which is largest (~0.038 h^{-1}) at $[Cp_2TiCl_2]/[MPEG] = 4/1$ and in PDI, (Figure 2.2d) which decreases with increasing $[Cp_2TiCl_2]/[MPEG]$ and $[Zn]/[Cp_2TiCl_2]$, leveling off at about 1.4.

The overall effect of Zn on the polymerization is complex and may be explained by its involvement in the catalysis of both initiation and propagation steps. Since Zn is an insoluble reagent, a slight excess accelerates Cp_2TiCl formation, while the resulting Lewis acidic $ZnCl_2$ coordinates the epoxide and assists the Cp_2TiCl mediated RRO process.[45] In addition, organozinc species may be involved in the catalysis of the reversible termination step. Thus, Zn transmetalation/reduction of the Ti end capped dormant chains (~P_n-Cp_2TiCl) generates Cp_2TiCl and transient diallyl organozinc species, (~$P_{n2}Zn$) which thermally homolyze liberating Zn(0) and the propagating radical which adds more monomers until trapped again by Cp_2TiCl.[31,46] The effect of the amount of Zn is more significant at low $[Cp_2TiCl_2]/[MPEG]$ ratios (2/1) where Zn excess lowers IE, but it decreases in importance at higher Cp_2TiCl concentrations. Thus, polymerizations can be conducted even with stoichiometric Zn ($[Zn]/[Cp_2TiCl_2] = 0.5/1$), provided that enough $[Cp_2TiCl_2]/[MPEG]$ excess (*e. g.* 6/1) is present (Table 2.1, exp 13). Nonetheless, for large $[Cp_2TiCl_2]/[MPEG]$ values, too much Zn may increase polydispersity. Overall, an optimum in terms of IE and PDI is seen for [I]/[Ti]/[Zn] = 1/4/8 but acceptable polymerizations can also be run with [I]/[Ti]/[Zn] = 1/3/6 and even 1/2/4. Finally, extra Zn and Cp_2TiCl may also contribute to scavenging traces of oxygen from the polymerization.

By comparison with styrene, (where in fairness, optimization experiments were carried out at a lower DP of 50)[31e,f, 33] larger $[Cp_2TiCl_2]/[epoxide]$ ratios are required for isoprene, and excess

Zn does not seem to provide the same continuous decrease in PDI. Nonetheless, while polydispersities are still large by comparison, the do converge to about 1.4 at high conversions. This may also indicate that the side reactions associated with Ti-mediated isoprene polymerizations are harder to suppress than in the case of styrene. Interestingly, while the three modes of monomer enchainment (1,2, 1,4 and 3,4) lead to 3 different allyl titanium propagating chain ends, with different populations, steric effects and dissociation energy of the ~P_n-$TiCp_2Cl$ bond, the dominant 1,4-addition mode does not allow for a possible β-hydride elimination side reaction.

Table 2.1 Epoxide Initiated Isoprene Polymerizations Mediated by Cp_2TiCl

Exp.	[Iso]/[MPEG]/ $[Cp_2TiCl_2]$/[Zn]	Mn	PDI	$k_p^{app}(h^{-1})$[a]	I.E.[b]	T, °C	[Zn]/[Ti]	[Ti]/ [Epox]
1	200/1/1/2	237,000	1.77	0.005	0.03	110	2	1
2	200/1/2/4	15,000	1.4	0.013	0.45	110	2	2
3	200/1/2/6	60,300	1.9	0.011	0.11	110	3	2
4	200/1/2/8	53,500	1.65	0.016	0.13	110	4	2
5	200/1/2/16	51,200	1.86	0.009	0.12	110	8	2
6	200/1/3/6	9,300	1.52	0.019	0.74	110	2	3
7	200/1/3/9	12,400	1.39	0.017	0.53	110	3	3
8	200/1/3/12	12,700	1.4	0.013	0.53	110	4	3
9	200/1/4/4	8,500	1.35	0.02	0.84	110	1	4
10	200/1/4/8	7,300	1.41	0.038	0.93	110	2	4
11	200/1/4/12	8,900	1.4	0.035	0.9	110	3	4
12	200/1/4/16	7,300	1.6	0.018	0.94	110	4	4
13	200/1/6/3	14,500	1.45	0.023	0.46	110	0.5	6
14	200/1/6/12	6,200	1.42	0.041	1.08	110	2	6
15	50/1/3/6	3,400	1.32	0.051	0.5	110	2	3
16	100/1/3/6	8,100	1.37	0.033	0.42	110	2	3
17	400/1/3/6	24,600	1.38	0.009	0.55	110	2	3
18	1000/1/8/12	45,000	1.6	0.005	0.76	110	1.5	8
19	200/1/4/8	12,100	1.35	0.016	0.56	90	2	4
20	200/1/4/8	7,800	1.61	0.045	0.87	130	2	4
21	200/1/4/8[c]	7,400	1.3	0.011	0.93	70	2	4
22	200/1/4/8[c]	7,900	1.41	0.036	0.85	110	2	4
23	20/1/3/12	2,900	1.34	n/a	n/a	110	4	3
24	20/1/3/12[d]	3,200	1.45	n/a	n/a	110	4	3
25	20/1/5/15[e]	2,500	1.31	n/a	n/a	110	3	5
26	200/400/1/3/6[f]	17,000	1.39	n/a	n/a	110	2	3
27	75/75/1/3/6[f]	16,000	1.47	n/a	n/a	110	2	3
28	100/100/1/3/6[f]	15,000	1.46	n/a	n/a	110	2	3

[a] Calculated as the slope of the kinetic plot. [b] Calculated as M_n^{theor}/M_n^{GPC}. [c]All exp. in dioxane, except exp. 21 and 22 in THF. [d]SO, [e]DGEBA. Exp 23-28 M_n and PDI not at 50%. [f]Styrene copolymers.

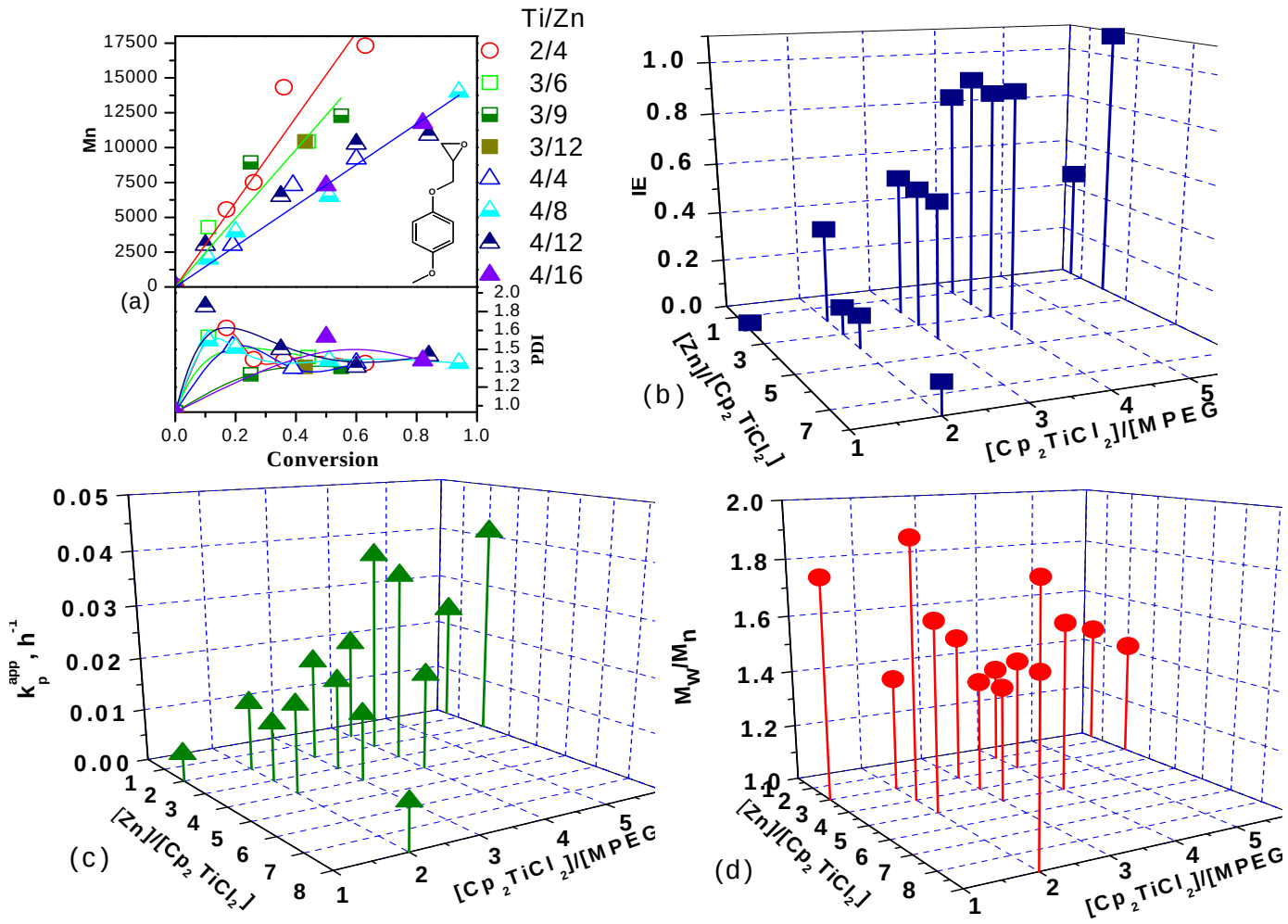

Figure 2.2 Effect of [MPEG]/[Cp_2TiCl_2]/[Zn] ratios: (a) conversion dependence of M_n and M_w/M_n. (b), (c), (d): Dependence of IE (b, ■), k_p^{app} (c, ▲) and PDI at ~50% conversion (d, ●) on [Cp_2TiCl_2][MPEG], [Zn]/[Cp_2TiCl_2]. [Iso]/[MPEG] = 200/1; T = 110 °C.

The effect of the [monomer]/[initiator] ratio is presented in Table 2.1 exp. 6, 15-18 and Figure 2.3a. A linear dependence of molecular weight on conversion and linear kinetics are observed for a wide range of DP = [Iso]/[MPEG] ratios from 50/1 to 1000/1. The polydispersity values are about 1.4 but increase at higher conversions or for larger degrees of polymerizations. The IE is about 0.4-0.5 at low DP (50, 100) but increases to about 0.75 at DP = 200. The lower IE at low DPs can be explained by the increase in the rate of possible epoxide deoxygenation[26] brought about by the high Cp_2TiCl concentrations. Conversely, IE decreases again at DP = 400 as the lower Cp_2TiCl concentration cannot suppress epoxide related side reactions such as coupling. However, this may be corrected by increasing the amount of Cp_2TiCl (*e. g.* at DP = 1,000) which brings back the IE to about 0.75. Thus, IE seems to be sensitive to the Ti concentration and it is likely that an optimization should be performed for each target DP.

The combined effect of temperature and solvent is presented in Figure 2.3b and in Table 2.1, exp. 10, 19-22. A linear dependence of M_n on conversion occurs in dioxane and THF at all temperatures in the 90-130 °C range. In both solvents, the IE is large (~0.8-0.9) and relatively independent of temperature, indicating that epoxide RRO and initiation are fast relative to initiator related side reactions. Due to the thermal suppression of termination, transfer and epoxide deoxygenation the PDIs decrease with temperature to about 1.35 at 70-90 °C. As previously described, dipolar aprotic coordinating solvents are favored in the Ti-CRP of styrene[31]. Thus, while both are reasonably good solvents for polyisoprene, the more polar THF may allow for a faster Cp_2TiCl_2 reduction and higher reactivity of Cp_2TiCl *via* a better solvation and dissociation of the $(Cp_2TiCl)_2$ dimer[27-29].

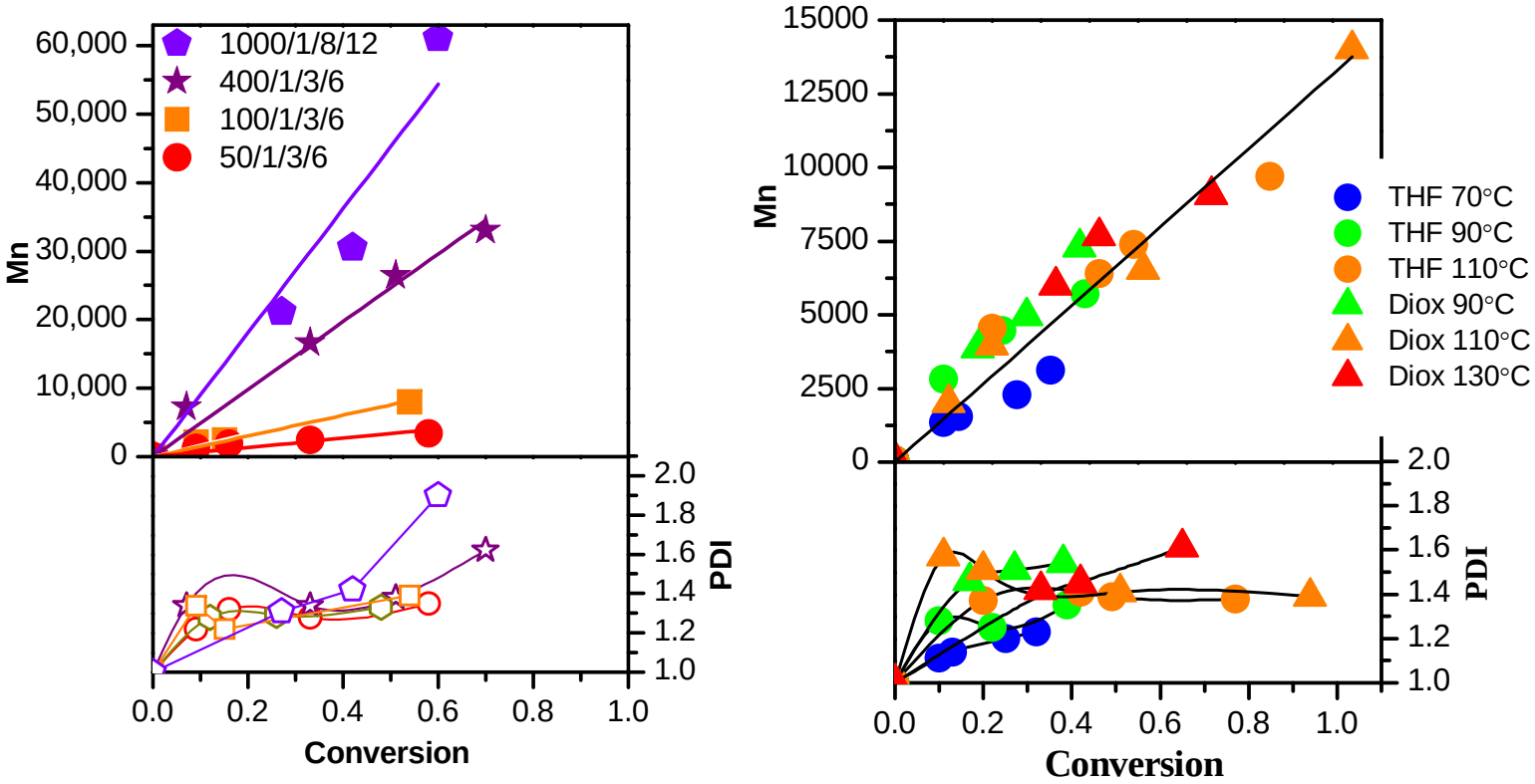

Figure 2.3. Dependence of M_n and M_w/M_n on conversion for: (a) various [Iso]/[MPEG] ratios in dioxane at 110 °C. (b) several solvent and temperature conditions ([Iso]/[MPEG]/[Cp_2TiCl_2]/[Zn] = 2001/1/4/8).

Finally, as a further demonstration of the control of the polymerization, both random and block copolymers were successfully synthesized by chain extension from polyisoprene and polystyrene which was verified by a combination of GPC and NMR (Figure 2.4) analyses. Thus, the GPC traces of the copolymers are monomodal while the resonances associated with polystyrene, polyisoprene and MPEG are clearly visible (*e.g.* aromatic, and vinyl regions as well as the methoxy at δ = 3.75 ppm). The copolymer type is identifiable by the broadness *vs*. sharpness of the corresponding signals in the random and respectively blocks copolymers.

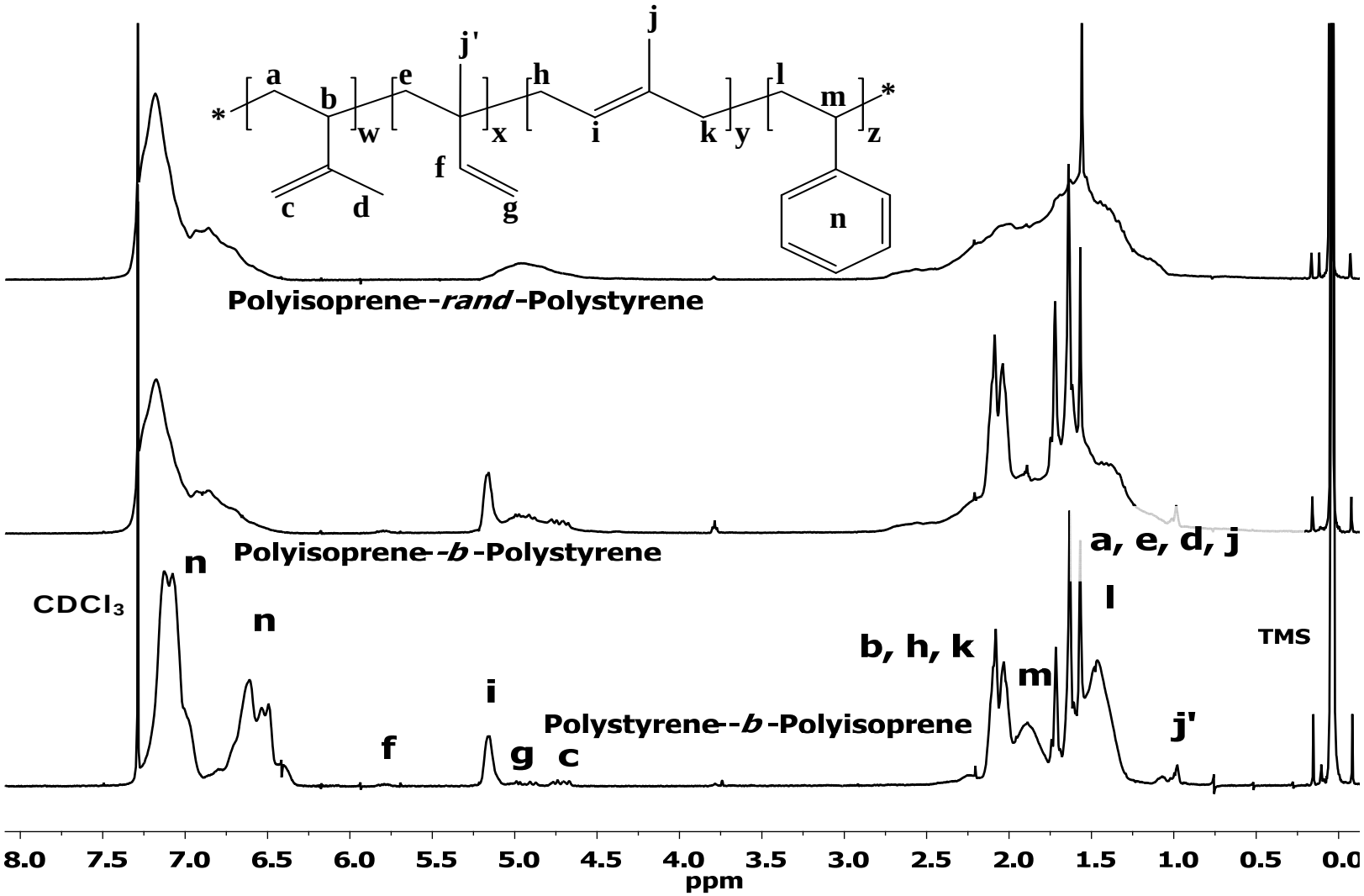

Figure 2.4. 500 MHz ^{1}H-NMR spectra of isoprene/styrene copolymers.

2.3.4 $Cp_2TiCl^{\bullet}$-Mediated CRP of Isoprene Initiated by SET-Reduction of Aldehydes.

As seen with RRO of epoxides, the aldehyde single electro transfer (SET) reduction (Scheme 2.1 eq. 2) provides the initiating radicals for the isoprene polymerization (eq. 3), which is mediated by the reversible termination of the growing chains with a second equivalent of $Cp_2Ti(III)Cl$ *via* a combination of DC and DT mechanisms (eqs. 4, 5).

The aldehyde initiation from TMBA and BBA is demonstrated by the NMR analysis of the chain termini (Figure 2.5a-b). Thus, in addition to the characteristic resonances corresponding to a typical free radical polymerization of isoprene such as the aliphatic *a, b, d, e, h k, j, j'* (0.95 - 2.00 ppm), and vinylic (*c, f, g, i*) protons (4.70, 4.91, 5.12, 5.72 ppm) specific, aldehyde derived peaks such as the aromatic *n* (6.35 ppm), benzylic *m* (5.5 ppm) and methoxy *p* (3.75 ppm) of TMBA as well as the aromatic *s, q, q'* (6.92 -7.38 ppm) and benzyloxy *f* (5.75 ppm) of BBA are present. Their integration vs. the PI main chain also allows the determination of the M_n^{NMR} which is in good agreement with M_n^{GPC}. In addition, the peak k (~2.7 ppm) corresponds to the first isoprene unit connected to the aldehyde derived benzyl alcohol.

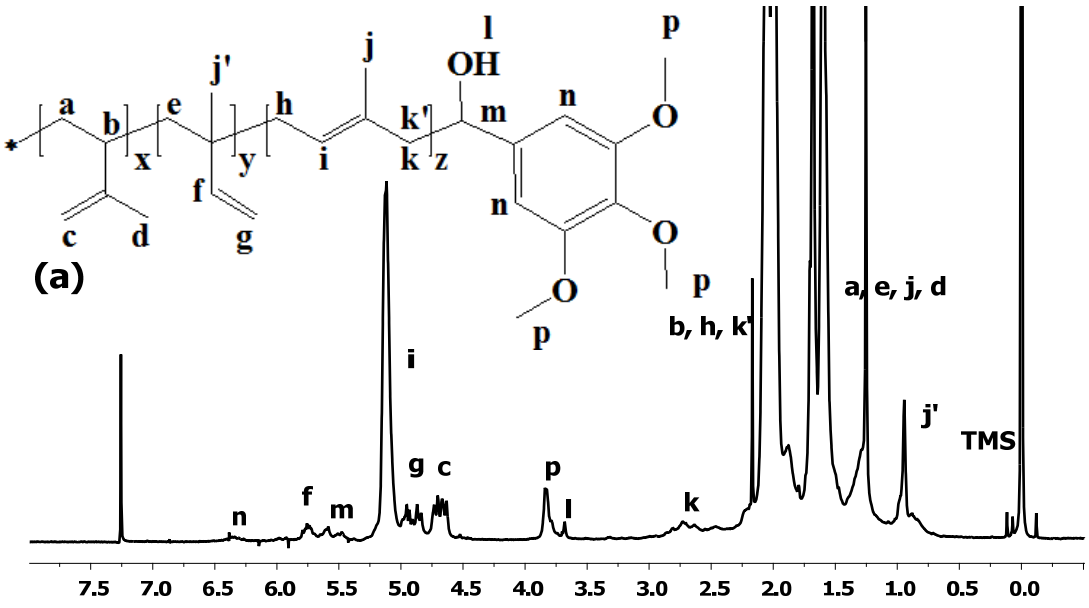

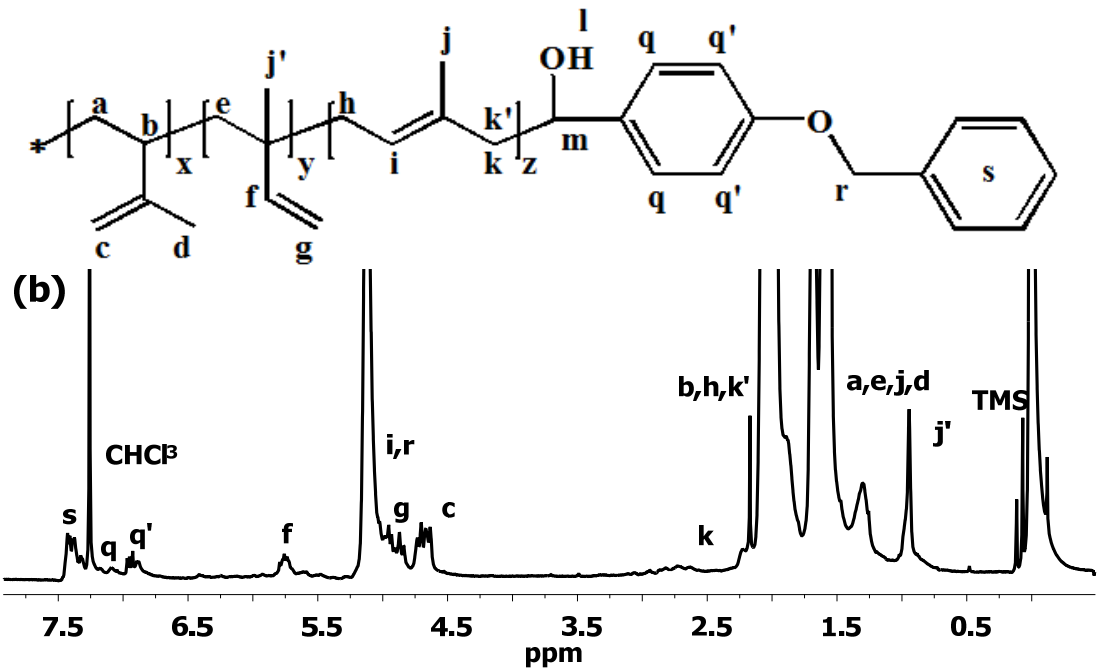

Figure 2.5. 500 MHz ^{1}H-NMR spectrum of PIP initiated by TMBA (a) and BBA (b). [IP]:[TMBA]:[Cp_2TiCl_2]:[Zn] = 15:1:2:3 at 110 °C. M_n^{NMR} = 3,900; M_n^{GPC} = 3,600; PDI = 1.5; [IP]:[BBA]:[Cp_2TiCl_2]:[Zn] = 50:1:3:6 at 110°C M_n^{NMR} = 6,800; M_n^{GPC} = 5,700; PDI = 1.4

Two examples demonstrating the controlled radical polymerization kinetics in the Cp_2TiCl-mediated isoprene polymerizations using benzaldehyde as initiator are presented below (Figure 2.6). Two different ratios and temperatures [Iso]/[BA]/[Cp_2TiCl_2]/[Zn] = 200/1/3/10 at 100 °C and respectively 100/1/4/12 at 110 °C were examined. Consistent with the proposed mechanism, a minimum initiator/ Cp_2TiCl = 1/2 ratio should be necessary to bring the polymerization under control while excess Cp_2TiCl as well as of Zn decreases PDI and increases the initiator efficiency. In both cases, a linear dependence of molecular weight on conversion indicative of a controlled process, as well as linear kinetics were observed, with a faster polymerization occurring as expected for larger M/I ratios and higher temperatures. While polydispersities converge to ~ 1.5 in both cases at larger conversions (> 70 %) lower values of the PDI are obtained at lower temperature.

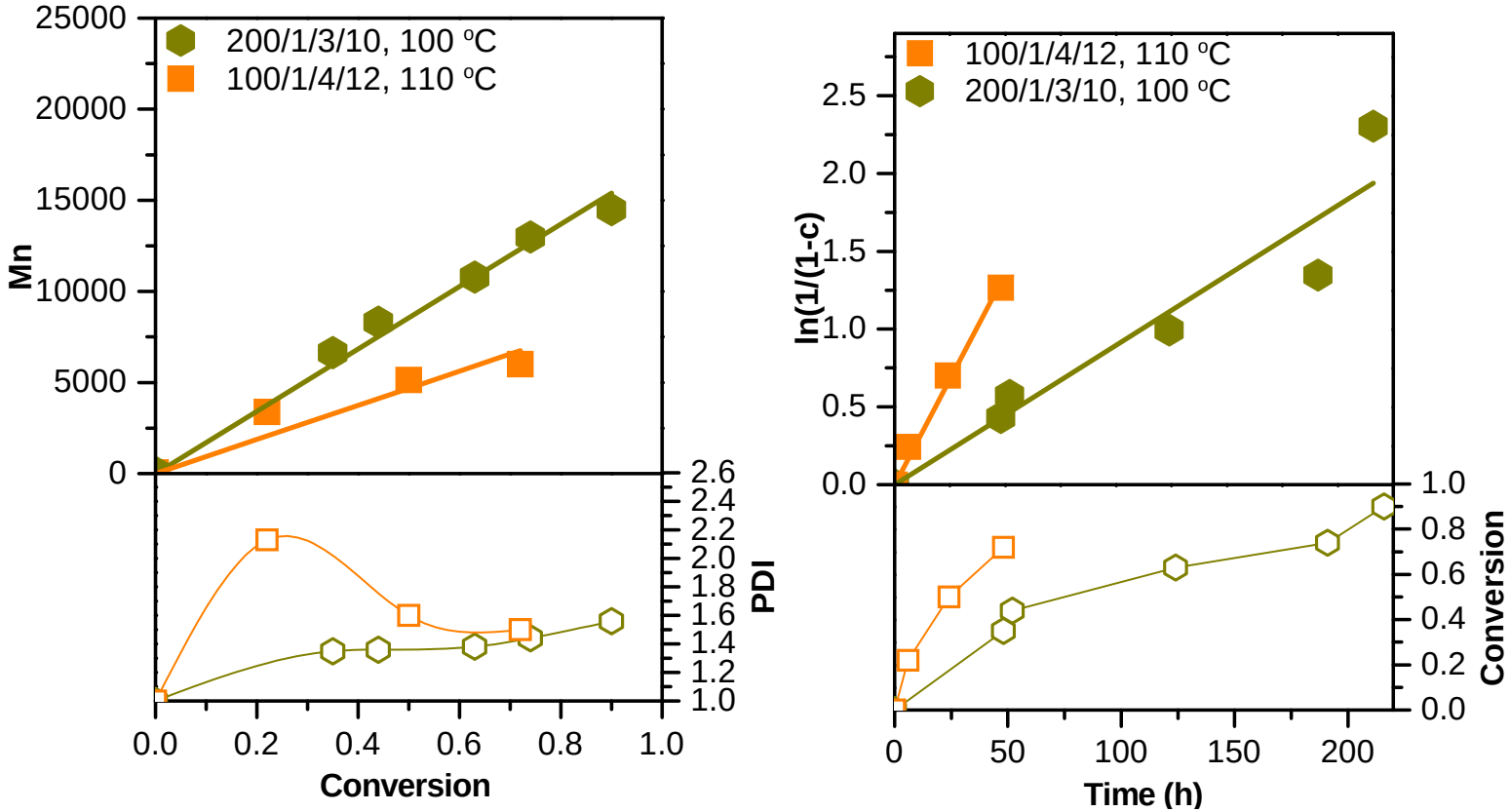

Figure 2.6 The dependence of M_n, M_w/M_n and $[M_0]/[M]$ in Cp_2TiCl Mediated Isoprene Polymerizations in Dioxane, $[Iso]/[BA]/[Cp_2TiCl_2]/[Zn]$ as Indicated in the Figure.

2.3.5 $Cp_2TiCl^{\bullet}$-Mediated CRP of Isoprene Initiated by Halide Abstraction.

The proposed polymerization mechanism is outlined in Scheme 2.1. The Zn reduction of Cp_2TiCl_2 occurs readily in dioxane to generate $Cp_2Ti(III)Cl$ (eq. 1). Subsequent halide abstraction (eq. 2) provides the initiating radicals for the isoprene polymerization (eq. 3), which is mediated by the reversible termination of the growing chains with a second equivalent of $Cp_2Ti(III)Cl$ *via* a combination of DC and DT mechanisms (eqs. 4, 5). While Zn insertion into the C-X or S-X bond of the initiator is possible, the soluble and homogenous Cp_2TiCl is probably faster in abstracting the halide *via* a radical pathway.

The polymerization from each initiator is supported by NMR investigations of the chain ends, Fig 2.7a-c. Thus, in addition to the characteristic resonances corresponding to a typical free radical polymerization of isoprene such as the aliphatic *a, b, d, e, h k, j, j'* (0.95 - 2.00 ppm), and vinylic (*c, f, g, i*) protons (4.70, 4.91, 5.12, 5.72 ppm) specific, initiator derived peaks are clearly observed. The integration of the initiator resonances vs. the PI main chain also allows the determination of the M_n^{NMR} which is in good agreement with M_n^{GPC}

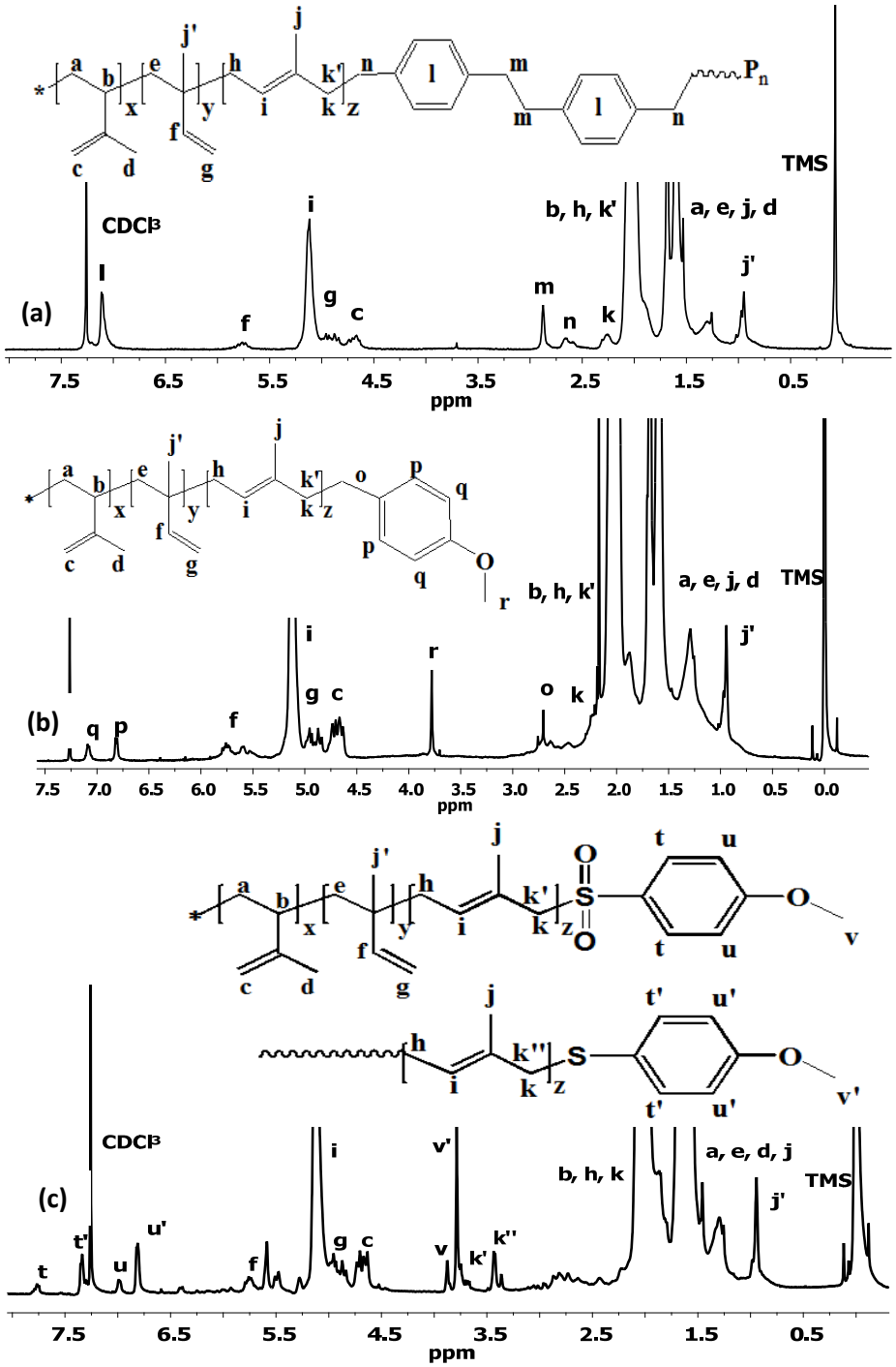

Figure 2.7. 500 MHz ^{1}H-NMR spectra of halide initiated PIP. (a) [IP]/[DBPX]/[Cp_2TiCl_2]/[Zn] = 100/1/6/20 at 70 °C. M_n^{NMR} = 2,200; M_n^{GPC} = 1,800; PDI = 1.08. (b) [IP]/[MBB]/[Cp_2TiCl_2]/[Zn] = 15/1/1/2 at 90 °C. M_n^{NMR} 4,000; M_n^{GPC} = 3,900; PDI = 1.20. (c) [IP]/[MBSC]/[Cp_2TiCl_2]/[Zn] = 10/1/1/0.6 at 90 °C. M_n^{NMR} = 4,700; M_n^{GPC} = 3,600; PDI = 1.25.

Figure 2.7a presents the initiation from DBPX which is demonstrated by the aromatic resonance at δ ~ 7.15 ppm. Interestingly, as indicated by the di-bezylic resonance *m* at δ ~ 2.9

ppm and the absence of the possible benzyl halide (Ph-CH_2-Br, ~4.5 ppm), initiator dimerization seems to occur before addition to isoprene. Similarly, for MBB (Figure 2.7b), the aromatic fragment is visible at 6.8 and 7.2 ppm with the CH_3-O group at 3.75 ppm while the benzyl initiating group is seen at ~ 2.6 ppm for both DBPX and MBB.

A more interesting case is presented by MBSC (Figure 2.7c) where the aromatic region displays two sets of resonances *t* and *u* (7.75 and 6.75 ppm) and respectively *t'* and *u'* (7.35 and 6.63 pm). This is a consequence of the partial reduction of the -SO_2- group to –SO- and ultimately to –S- by Cp_2TiCl.[47] The effect is also observed for the methoxy *v* and *v'* (3.85 ppm and 3.75 ppm) as well as for the first -CH_2- unit of the polyisoprene, *k'* and *k"* (3.5-3.6 ppm). Interestingly, this effect is observed even though a stoichiometric amount of Zn was used. Thus, while according to the proposed mechanism a typical I/Ti ratio of 1/2 or even 1/1 (due to the possible Zn re-reduction of the Cp_2TiCl_2 formed in situ after the halide abstraction from the initiator) is required, in the case of sulfonyl halides, some of the catalyst is consumed in the reduction of the SO_2 group, and consequently, larger amounts of catalyst will be required for a controlled polymerization. Moreover, resonances associated with allyl halide chain ends are absent, indicating that the polymerization does not proceed via an ATRP mechanism.

As seen in figure 2.8, a linear dependence of M_n on conversion occurs in all cases. Consistent with the proposed mechanism, a minimum initiator/ Cp_2TiCl = 1/2 ratio is necessary to bring the polymerization under control. In addition, a very interesting temperature effect is observed (Table 2.2-2.3). Thus, regardless of initiator or reagent ratios, at T $\geq$ 90 °C M_n increases with conversion but the polydispersity is relatively broad (M_w/M_n = 1.3-1.5) and the dependence has a relatively high M_n intercept at zero conversion. This indicates that the growing chain is not captured immediately after initiation, while the broad PDI may be a consequence of a weaker C-Ti bond at higher temperature and thus a larger concentration of active vs. dormant chains. By

contrast, at T < 90 °C the dependence of M_n on conversion is much weaker (lower slope) but M_w/M_n is as low as 1.1-1.2.

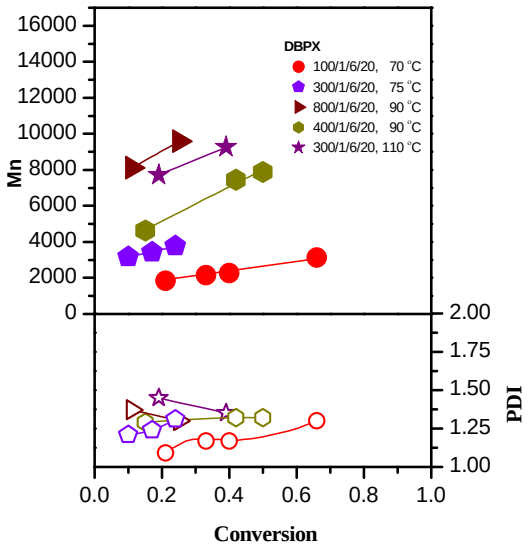

Figure 2.8 The Dependence of M_n and M_w/M_n in Cp_2TiCl-Mediated Polymerization of Isoprene Initiated from DBPX.

Table 2.2 [M]/[I] and Temperature Effects DBPX Initiated PI in Dioxane

Exp	[M]/[I]/[Ti]/[Zn]	T(°C)	M_n at 50%	PDI at 50%	k_p (h^{-1})
1	300/1/6/20	110	13,384	1.32	0.0101
2	400/1/6/20	90	7,874	1.32	0.0069
3	800/1/6/20	90	12,194	1.40	0.0039
4	300/1/6/20	75	4,883	1.40	0.0014
5	100/1/6/20	70	2,656	1.25	0.0029

Table 2.3 Temperature Effects DBPX/DCPX Initiated PI in Dioxane

Exp #	Initiator (I)	[Iso]/[I]/[Ti]/[Zn]	Temp (°C)	Time (h)	Mn	PDI	Conv	IE
1	DBPX	100/1/6/20	60	72.0	1,975	1.09	22%	0.76
2	DBPX	100/1/6/20	70	24.0	2,032	1.07	19%	0.64
3	DBPX	100/1/6/20	80	48.0	2,092	1.18	30%	0.98
4	DBPX	100/1/6/20	90	17.5	2,452	1.16	35%	0.97
5	DBPX	100/1/6/20	100	15.3	2,398	1.21	30%	0.85
6	DBPX	100/1/6/20	110	16.0	3,062	1.34	48%	1.07
7	DBPX	100/1/6/20	120	16.0	3,339	1.40	66%	1.35
8	DBPX	100/1/6/20	130	16.0	3,896	1.48	71%	1.24
9	DCPX	100/1/6/20	150	12.0	4,961	1.57	73%	1.00
10	DCPX	100/1/6/20	160	7.0	4,736	1.43	68%	0.98
11	DCPX	100/1/6/20	180	4.0	3,146	1.36	49%	1.06

These trends may be explained *via* the effect of temperature on the relative contributions of the different modes of isoprene enchainment and on the C-Ti bond dissociation energy. Thus, while the microstructure of these polymers is identical to that of polyisoprene synthesized *via* free radical polymerization, the temperature dependent propagation regioselectivity (1-4, 1-2, 3-4) may affect the C-Ti bond dissociation energy (BDE) in the chain end not only through the steric effects of each different connectivity but also *via* the different coordination modes of Cp_2TiCl with the double bond of the last repeat unit in addition to the possible coordination of Cp_2TiCl with the isoprene monomer. Hence, while the polymerization has nice controlled features at lower temperature, we speculate that the 1,2 and 3,4 modes may act as temperature-controlled "defects" with higher BDE which, similarly to chain transfer to monomer for vinyl chloride, terminate the polymerization at a predetermined M_n which is more sensitive to temperature than to reagent ratios. In addition the 1,2 and 3,4 are also more likely to support β-hydride elimination which cannot occur with 1,4. At higher temperatures the chain can propagate over these "defects" but the control is weaker. Additionally demonstrated (Table 2.4-2.6) was the ability to initiate from polyhalides, allyl halides, and sulfonyl halides with similar results as obtained from DBPX. Finally, the effect of reagent stoichiometry ([DBPX]/[Cp_2TiCl_2]/[Zn]) on initiator efficiency (IE), rate (k_p^{app}) and polydispersity (PDI) were examined and are further detailed in Figure 2.9a-c. Consistent with the proposed mechanism, a low [Cp_2TiCl_2]/[DBPX] ratio was not used as it does not provide enough Ti for end-capping of the growing chain. IE is very low but it increases with increasing [Cp_2TiCl_2]/[DBPX]. However, unlike epoxides using larger Ti excess cannot contribute to the deoxygenation side reaction. The trends in IE are paralleled by those in the apparent rate constant (k_p^{app}, Figure 2.9b) which is largest

(~0.03 h^{-1}) at $[Cp_2TiCl_2]/[DPBX]$ = 6/1 and in PDI, (Figure 2.2c) which decreases with increasing $[Cp_2TiCl_2]/[MPEG]$ and $[Zn]/[Cp_2TiCl_2]$.

Table 2.4 Isoprene Initiation from Polyhalides

Exp #	Initiator (I)	[Iso]/[I]/[Ti]/[Zn]	Temp (°C)	Time (h)	Mn	PDI	Conv	IE
1	$CHCl_3$[a]	100/1/6/20	110	24.0	4,433	1.29	37%	0.57
2	$CHBr_3$[a]	100/1/6/20	110	24.0	3,811	1.29	57%	1.02
3	CHI_3[a]	100/1/6/20	110	25.0	3,700	1.34	52%	0.96
4	CH_3I[a]	100/1/3/10	110	24.0	4,008	1.30	32%	0.54
5	CHI_3[a]	100/1/6/20	90	24.0	2,700	1.15	29%	0.73
6	CHI_3[a]	500/1/6/20	90	48.5	6,012	1.35	39%	2.21
7	CHI_3[a]	100/1/1.5/5	110	22.5	5,965	1.52	44%	0.50
8	CHI_3[b]	100/1/3/6	110	6.0	7,782	1.81	18%	0.16
9	CHI_3[b]	100/1/3/6	110	24.0	9,735	1.50	37%	0.26
10	CHI_3[a]	100/1/3/10	110	24.0	4,731	1.28	46%	0.66
11	CHI_3[b]	100/1/6/12	110	6.0	2,573	1.20	33%	0.87
12	CHI_3[b]	100/1/6/12	110	24.0	4,194	1.32	52%	0.84

a) 100 mesh Zn b) nano-Zn

Table 2.5 Isoprene Initiation from Allyl Halides

Exp	Initiator (I)	[Iso]/[I]/[Ti]/[Zn]	Temp °C	Time (h)	M_n	PDI	Conv	IE
1	Allyl bromide[a]	100/1/3/10	70	27.0	1,584	1.13	40%	1.72
2	Allyl bromide[b]	100/1/3/6	110	22.5	4,599	1.30	42%	0.62
3	Dichlorobutene[a]	100/1/6/20	90	22.0	2,530	1.20	17%	0.46
4	Dichlorobutene[a]	100/1/6/20	110	23.5	3,645	1.31	60%	1.12

Table 2.6 Isoprene Initiation from Sulfonyl Halides

Exp	Initiator (I)	[Iso]/[I]/[Ti]/[Zn]	Temp °C	Time (h)	Mn	PDI	Conv	IE
1	PTSC[a]	100/1/3/10	90	17.0	2,812	1.14	10%	0.24
2	PTSC[a]	200/1/3/10	100	48.0	8,244	1.35	46%	0.76
3	MBSC[b]	100/1/2/4	110	5.5	12,087	1.78	10%	0.06
4	MBSC[b]	100/1/2/4	110	24.0	27,395	1.89	22%	0.05

a) 100 mesh Zn b) nano-Zn

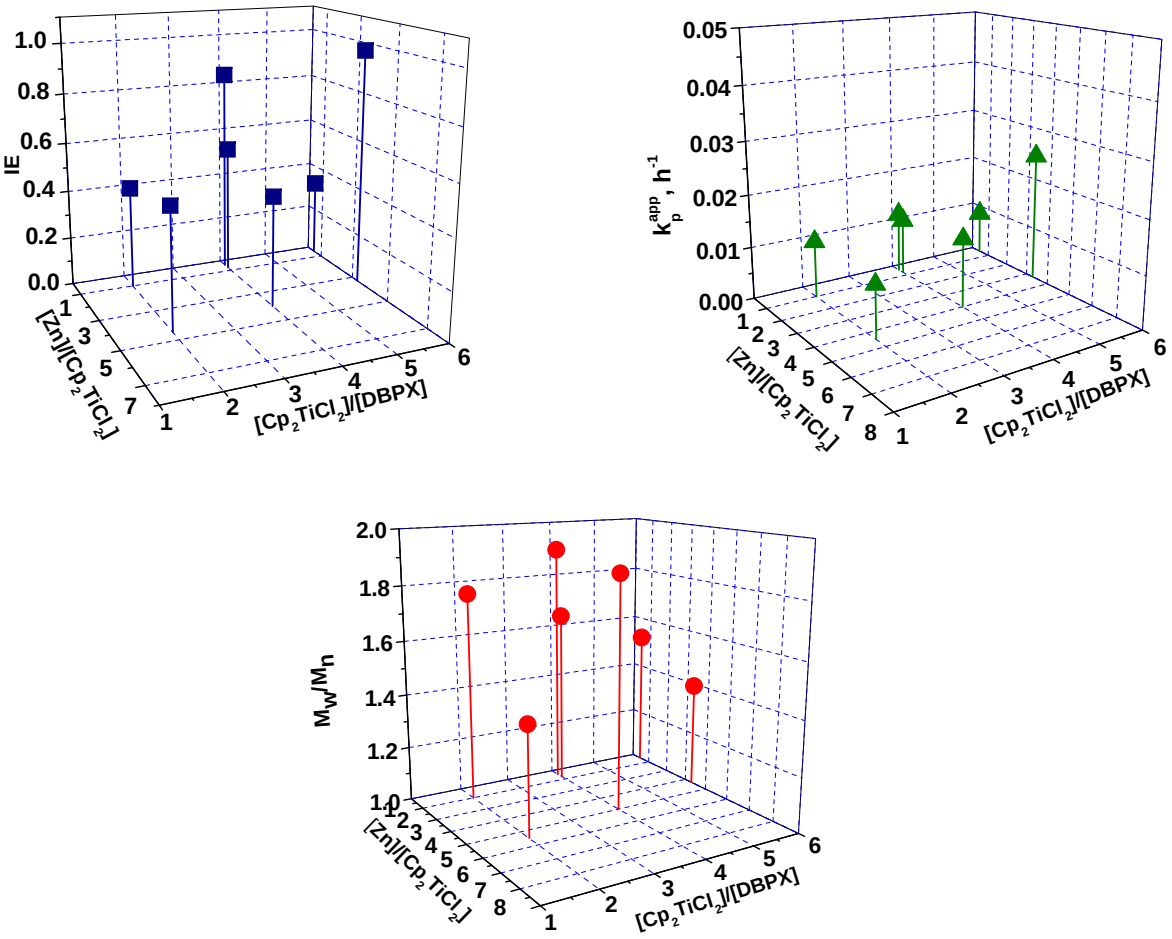

Figure 2.9 Effect of [DBPC]/[Cp_2TiCl_2]/[Zn] ratios: (a), (b), (c): Dependence of IE (a,■), k_p^{app} (b, ▲) and PDI (c, ●) on [Cp_2TiCl_2][DPBX], [Zn]/[Cp_2TiCl_2]. [Iso]/[DBPX] = 100/1; T = 90 °C in Dioxane.

Table 2.7 Effect of [DBPC]/[Cp_2TiCl_2]/[Zn] ratios on Isoprene Polymerization								
Exp #	**Initiator (I)**	**[Iso]/[I]/[Ti]/[Zn]**	**Temp °C**	**Time (h)**	**Mn**	**PDI**	**Conv**	**IE**
1	DBPX[a]	100/1/2/2	90	26.5	4,027	1.25	25%	0.42
2	DBPX[a]	100/1/2/9	90	43.0	4,870	1.32	35%	0.49
3	DBPX[a]	100/1/4/2	90	48.0	3,506	1.36	43%	0.84
4	DBPX[b]	100/1/4/3	90	18.0	3,906	1.31	20%	0.35
5	DBPX[a]	100/1/4/3	90	26.5	3,200	1.20	25%	0.53
6	DBPX[a]	100/1/4/16	90	18.0	3,200	1.18	21%	0.45
7	DBPX[a]	100/1/6/3	90	18.0	2,966	1.20	14%	0.32
8	DBPX[a]	100/1/6/20	90	17.5	2,452	1.16	35%	0.97
a) 100 mesh Zn b) nano-Zn								

Table 2.8 Effect of [DBPC]/[Cp_2TiCl_2]/[Zn] ratios on Isoprene Polymerization								
Exp	**Initiator (I)**	**[Iso]/[I]/[Ti]/[Zn]**	**Temp °C**	**Time (h)**	**Mn**	**PDI**	**Conv**	**IE**
1	DBPX[b]	100/1/0.5/0.3	70	23.0	trace	N/A	< 5%	N/A
2	DBPX[a]	100/1/0.5/2	70	23.0	trace	N/A	< 5%	N/A
3	DBPX[b]	100/1/1/0.5	70	23.0	trace	N/A	< 5%	N/A
4	DBPX[a]	100/1/1/1	70	24.0	2,828	1.30	17%	0.41
5	DBPX[a]	100/1/2/1	70	22.0	2,746	1.36	13%	0.10
6	DCPX[b]	100/1/2/4	70	23.0	2,104	1.21	26%	0.84
7	DBPX[a]	150/1/4/13	70	48.0	2,655	1.19	19%	0.73
8	DBPX[a]	100/1/6/20	70	24.0	2,032	1.07	19%	0.64

2.3.6 $Cp_2TiCl^{\bullet}$-Mediated CRP of Dimethyl Butadiene Initiated by Epoxide RRO

The MPEG epoxide initiation is demonstrated by the NMR analysis of the chain ends (Figure 2.10). First, characteristic resonances corresponding to a typical free radical DMBD polymerization,[48] such as the methylene and methyl of the 1,4-*cis* and *trans* units (-[C*H*$_2$-C(CH$_3$)=C(CH$_3$)-C*H*$_2$]-, *a, a',* δ = 2.03 ppm and -[CH$_2$-C(C*H*$_3$)=C(C*H*$_3$)-CH$_2$]-, *b, b'*, δ ~ 1.6-1.75 ppm) as well as the methylene (-[C*H*$_2$C(CH$_3$)-(C(CH$_3$)=CH$_2$)]-, *c*, δ ~ 1.6-1.75 ppm), methyls (-[CH$_2$C(C*H*$_3$)(C(C*H*$_3$)=CH$_2$)]-, *d,* δ ~ 1.0 ppm; -[CH$_2$C(CH$_3$)(C(C*H*$_3$)=CH$_2$)]-, *e,* δ ~1.25 ppm) and double bond (-[CH$_2$C(CH$_3$)-(C(CH$_3$)=C*H*$_2$)]-, *f, f'*, δ~4.6-4.8 ppm) of the 1,2-unit indicate a ratio of [*cis*-1,4]/[*trans*-1,4]/[1,2] of about 47/46/7. The smaller resonances at ~5 ppm are probably due to a combination of short 1,2-sequences and their tacticity.

Additionally, specific initiator derived peaks such as the aromatic (*j,* δ = 6.82 ppm), methoxy (*i,* δ = 3.74 ppm) as well as the benzylic ether (*h, h',* δ = 3.82-3.98 ppm) and the mixture of two alcohols derived from the two modes of epoxide RRO (*g, g'* δ ~ *3.25-3.5* ppm) are observed in the polymer spectrum. Moreover, the methylenes of the first DMBD unit (*k,* δ = 2.25- 2.75 ppm) demonstrate the polymer/initiator connectivity. The possible chain ends derived from the hydrolysis of the Ti-endcapped propagating chain (such as $-CH=CCH_3-CH_3$ or $-CH_2-CH(CH_3)(CCH_3=CH_2)$ are overlapping with the polymer resonances and could not be observed.

An example demonstrating 1st order kinetics and control of the Cp_2TiCl-mediated DMBD polymerization using MPEG as initiator are presented in Figure 2.11. According to the proposed mechanism, one Ti equivalent is required for the RRO process, whereas the second equivalent is involved in the reversible endcapping of the growing chain. Larger amounts of Ti and Zn are typically beneficial for the control of styrene and isoprene and most likely for DMBD as well. As seen from Figure 2.11, a linear dependence of molecular weight on conversion is observed up to about 80 % conversion, with initiator efficiency of about 0.3. The polydispersity is initially high but quickly decreases to below 1.5. In addition, Figure 2.11b illustrates the linearity of the polymerization kinetics ($k_p = 0.019\ s^{-1}$) indicating a constant concentration of the growing chains. Together, these data support a controlled polymerization process. Additionally, the effect of temperature on the polymerization was examined. As such, it was demonstrated that temperatures below 110°C yield better control over the polymerizations. This is likely attributed to the allylic nature of the monomer and polymer, generating considerable more irreversible chain transfer as the temperature in increased. This is very evident in the experiments performed at 130°C where no control is observed at all.

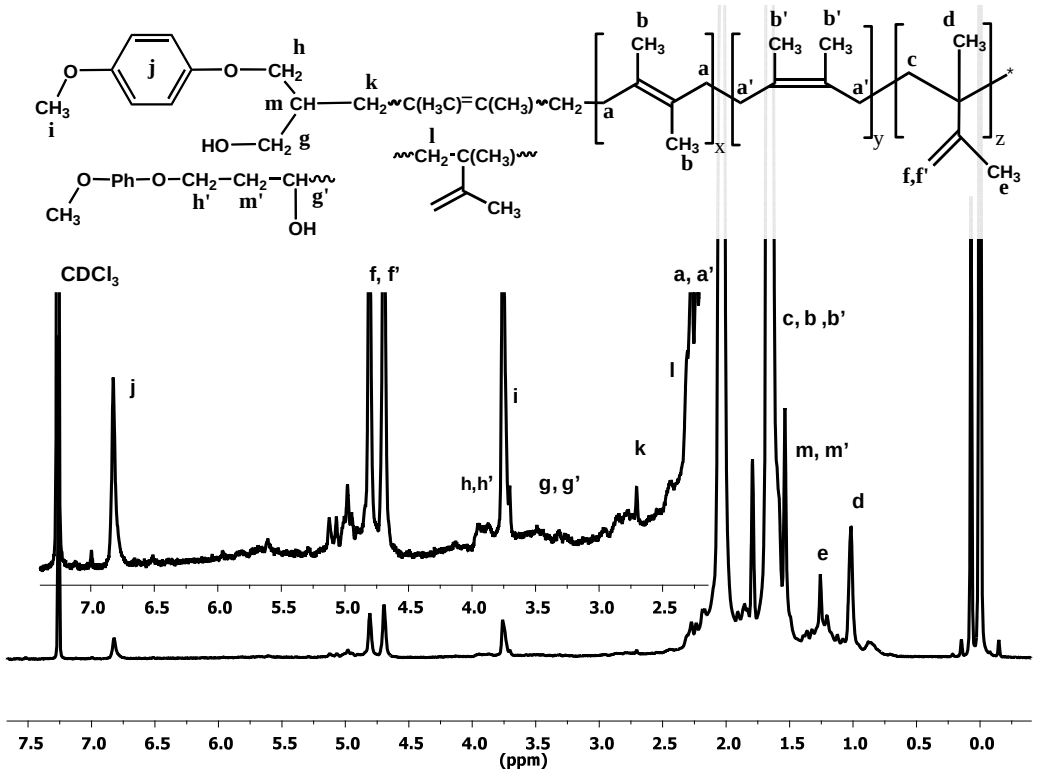

Figure 2.10 400 MHz ^{1}H-NMR spectrum of poly(DMBD) initiated from MPEG. [DMBD]/[MPEG]/[Cp_2TiCl_2]/[Zn] = 20/1/3/6, 110°C. M_n^{GPC} = 3,700; PDI =1.26. M_n^{NMR} = 5,330

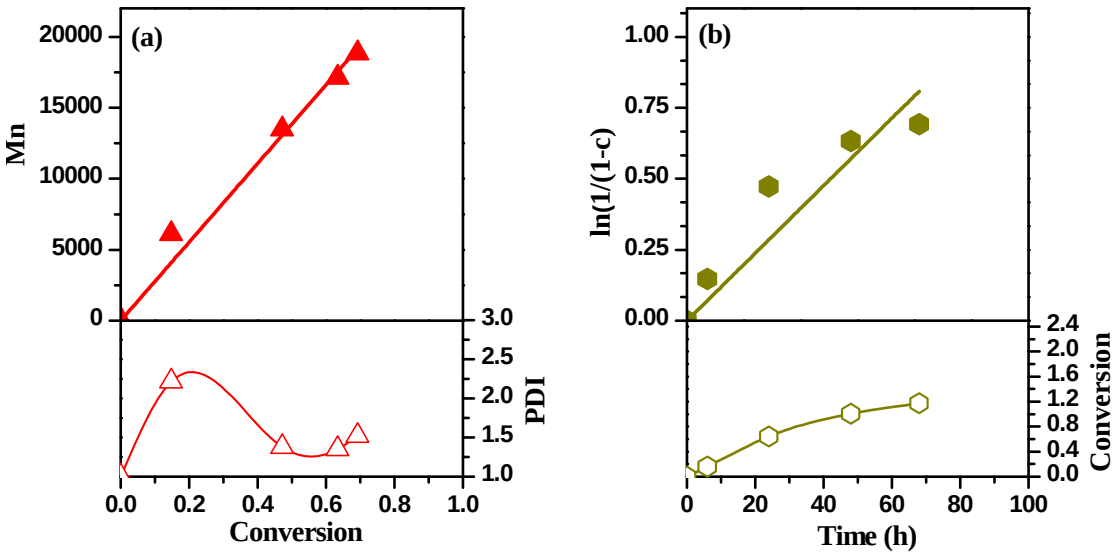

Figure 2.11 The dependence of (a) M_n, M_w/M_n and (b) ln(1/(1-c)) in the Cp_2TiCl mediated DMBD polymerizations: [DMDB]/[MPEG]/[Cp_2TiCl_2]/[Zn] = 100/1/3/6, dioxane, 110°C.

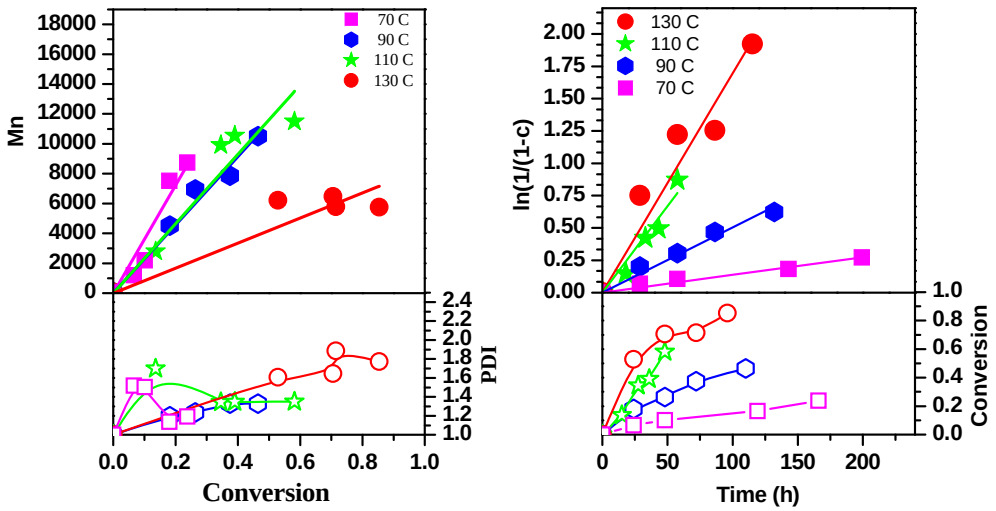

Figure 2.12 Effect of temperature on DMBD polymerization initiated from MPEG. : [DMDB]/[MPEG]/[Cp_2TiCl_2]/[Zn] = 100/1/3/6, dioxane.

2.3.7 $Cp_2TiCl^{\bullet}$-Mediated CRP of Dimethyl Butadiene via Aldehyde SET Reduction

The DMBD initiation from BBA is demonstrated by the NMR analysis of the chain ends (Figure 2.13). First, characteristic resonances corresponding to a typical free radical DMBD polymerization,[48] such as those of the methylene and methyl of the 1,4-*cis* and *trans* units (-[CH_2-C(CH_3)=C(CH_3)-CH_2]-, *a, a'* δ = 2.03 ppm, and -[CH_2-C(CH_3)=C(CH_3)-CH_2]-, *b, b'*, δ = 1.6-1.75 ppm) as well as the methylene (-[CH_2C(CH_3)-(C(CH_3)=CH_2)]-, *c*, δ~1.6-1.75 ppm), methyls (-[CH_2C(CH_3)(C(CH_3)=CH_2)]-, *d,* $\delta \sim$ 1.0 ppm, and -[CH_2C(CH_3)(C(CH_3)=CH_2)]-, *e* δ~1.25 ppm) and double bond (-[CH_2C(CH_3)-(C(CH_3)=CH_2)]-, *f, f'*, $\delta \sim$ 4.6-4.8 ppm) of the 1,2-unit indicate a ratio of [*cis*-1,4]/[*trans*-1,4]/[1,2] of about 47/46/7.

Furthermore, specific initiator derived peaks such as the aromatic (*g,* δ = 7.3-7.5 ppm, *j, i',* δ = 6.75-7.15 ppm), benzyl alcohol and ether (*h, k,* $\delta \sim$ 4.9-5.1 ppm) fragments are observed in the polymer spectrum, with the methylenes of the first DMBD unit (*m, n* δ = 2.2, 2.75 ppm) demonstrating the polymer/initiator connectivity. Moreover, the original aldehyde -C*H*O resonance ($\delta \sim$ 10 ppm) is absent, indicating complete initiator consumption.

An example of the kinetics of the Cp_2TiCl-mediated DMBD polymerization with BA as initiator is presented in Figure 2.14. According to the proposed mechanism, one Ti equivalent is required for the initiation, whereas the second equivalent is involved in the reversible endcapping of the growing chain As seen from Figure 2.14, a linear dependence of molecular weight on conversion is observed up to about 70 % conversion, with an initiator efficiency = 0.2. In addition, the polydispersity decreases with conversion towards about 1.4. Figure 2b illustrates the linearity of the polymerization kinetics (k_p = 0.016 s^{-1}) indicating a constant concentration of the growing chains. Together, these data support a controlled polymerization process.

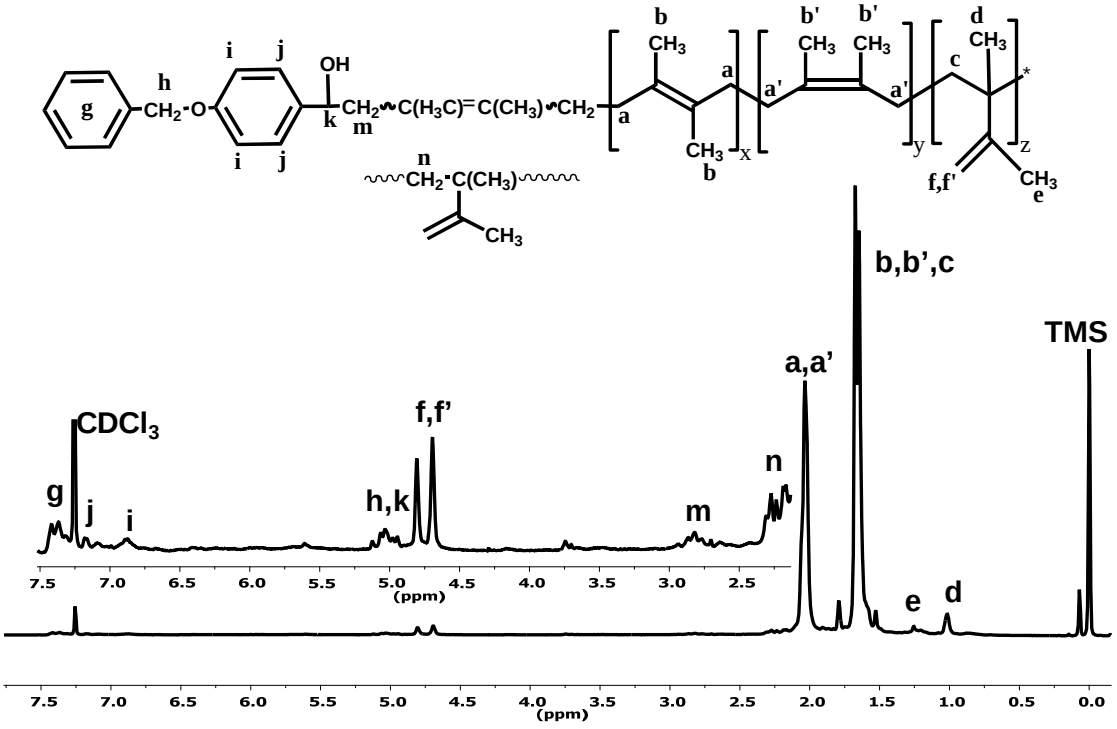

Figure 2.13 400 MHz ^{1}H-NMR spectrum of poly(DMBD) initiated from BBA. [DMBD]/[BBA]/[Cp_2TiCl_2]/[Zn] = 10/1/2/4, 110 °C. Mn^{GPC} = 3,870; PDI =1.27. M_n^{NMR} = 4,590

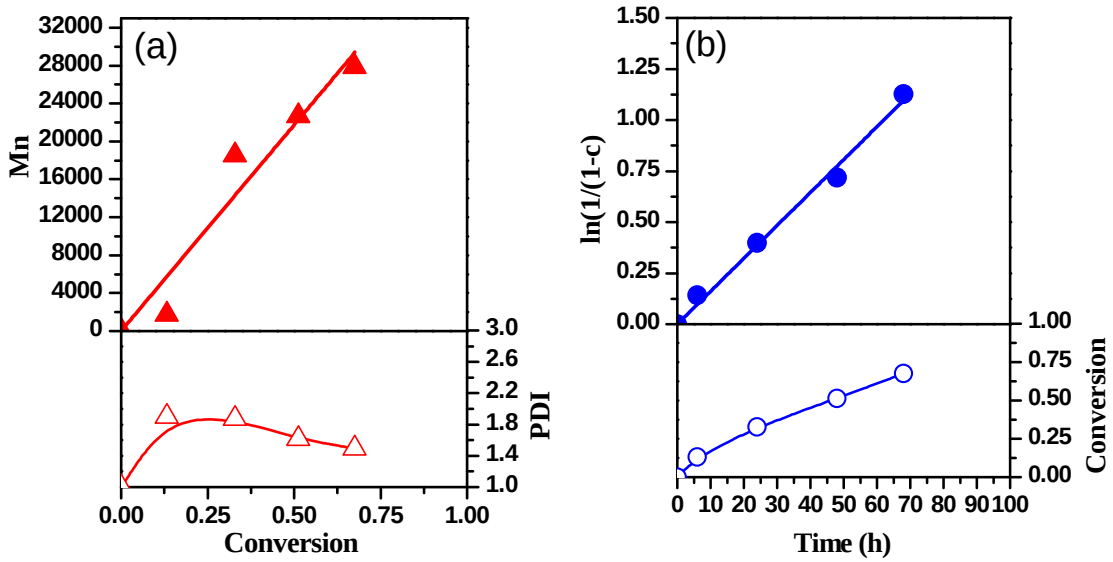

Figure 2.14 The dependence of (a) M_n, M_w/M_n and (b) ln(1/(1-c)) in the Cp_2TiCl mediated 2,3-dimethylbutadiene polymerizations: [DMDB]/ [BA]/[Cp_2TiCl_2]/[Zn] = 100/1/3/6, dioxane, 110°C.

2.3.8 $Cp_2TiCl^{\bullet}$-Mediated CRP of Dimethyl Butadiene by Halide Abstraction

The DMBD initiation from DBPX is demonstrated by the NMR analysis of the chain ends (Figure 2.15). As such, characteristic resonances corresponding to a typical free radical DMBD polymerization,[48] such as those of the methylene and methyl of the 1,4-*cis* and *trans* units (-[C*H*$_2$-C(CH$_3$)=C(CH$_3$)-C*H*$_2$]-, *a, a'* δ = 2.03 ppm, and -[CH$_2$-C(C*H*$_3$)=C(C*H*$_3$)-CH$_2$]-, *b, b'*, δ = 1.6-1.75 ppm) as well as the methylene (-[C*H*$_2$C(CH$_3$)-(C(CH$_3$)=CH$_2$)]-, *c*, δ~1.6-1.75 ppm), methyl (-[CH$_2$C(C*H*$_3$)(C(C*H*$_3$)=CH$_2$)]-, *d,* δ ~1.0 ppm, and -[CH$_2$C(CH$_3$)(C(C*H*$_3$)=CH$_2$)]-, *e* δ~1.25 ppm) and the double bond (-[CH$_2$C(CH$_3$)-(C(CH$_3$)=C*H*$_2$)]-, *f, f'*, δ~4.6-4.8 ppm) of the 1,2-unit. These resonances indicate a ratio of [*cis*-1,4]/[*trans*-1,4]/[1,2] of about 47/46/7. The smaller resonances at ~5 ppm are likely attributed to a combination of short 1,2 sequences and their tacticity. The possible chain ends derived from the hydrolysis of the Ti-endcapped propagating chain (such as –CH=CCH$_3$-C*H*$_3$ or –CH$_2$-C*H*(CH$_3$)(CCH$_3$=CH$_2$) are overlapping with the polymer resonances and could not be observed.

Moreover, specific initiator derived peaks such as the aromatic (*g*, δ = 7.1 ppm) and benzylic (*h, i* δ = 2.9 and 2.6 ppm) resonances are observed in the spectrum, as well as that of the methylene corresponding to the first DMBD unit (*j, k*, δ = 2.2 - 2.3 ppm) all assist in further demonstrating the polymer/initiator connectivity. Interestingly, as seen with isoprene and butadiene, DBPX appears to dimerize before initiating, as indicated by peak *h*.

An example showing the 1st order kinetics for the Cp_2TiCl-mediated DMBD polymerization with BEB as initiator is presented in Figure 2.15. According to the proposed mechanism, one Ti equivalent is required for the initiation, whereas the second equivalent is involved in the reversible endcapping of the growing chain. Larger amounts of Ti and Zn are typically beneficial for the control of styrene and isoprene polymerizations and most likely for DMBD as well. In addition, the $Cp_2TiClBr$ formed in the initiation step can get reduced again by Zn this generating more of the active metalloradical. As seen from Figure 2.15 a linear dependence of molecular weight on conversion is observed up to about 80 % conversion, with an initiator efficiency of about 0.3. In addition, the polydispersity decreases at higher conversions to approximately 1.3. Figure 2.15b illustrates the linear dependence of ln(1/(1-c)) on time (k_p = 0.018 s^{-1}) indicating a 1st order kinetics and constant concentration of the growing chains. Together these data support a controlled polymerization process.

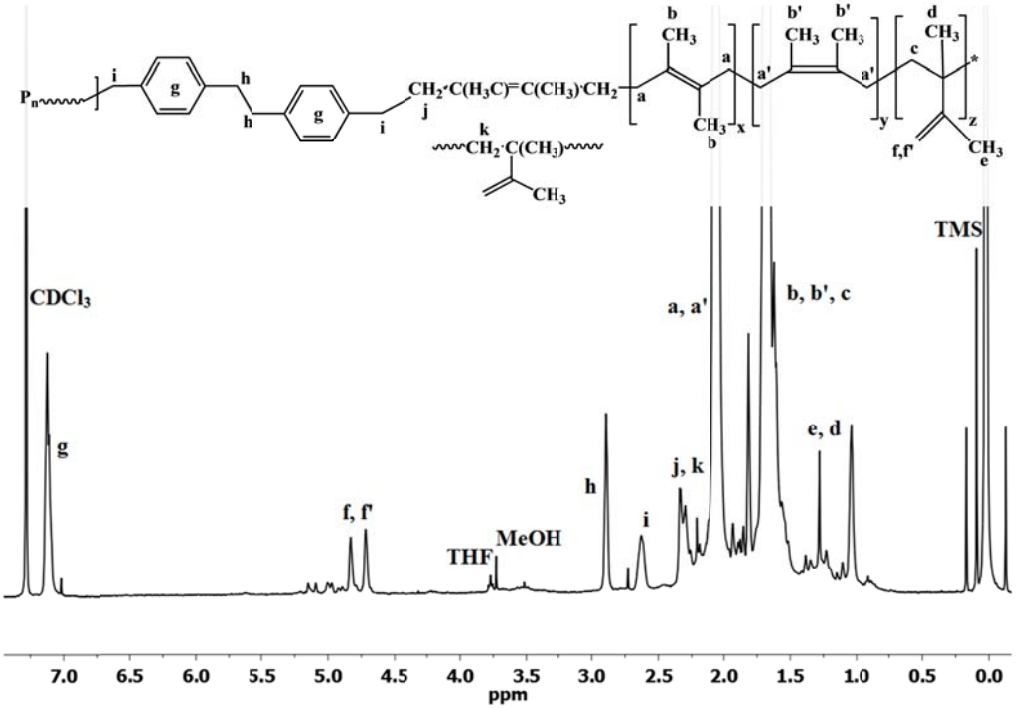

Figure 2.15 400 MHz ^{1}H-NMR spectrum of poly (dimethylbutadiene) initiated from DBPX.[DMBD]/[DBPX]/[Cp_2TiCl_2]/[Zn] = 25/1/4/8, 110 °C. Mn^{NMR} = 3,280 Mn^{GPC} = 4135; PDI =1.31.

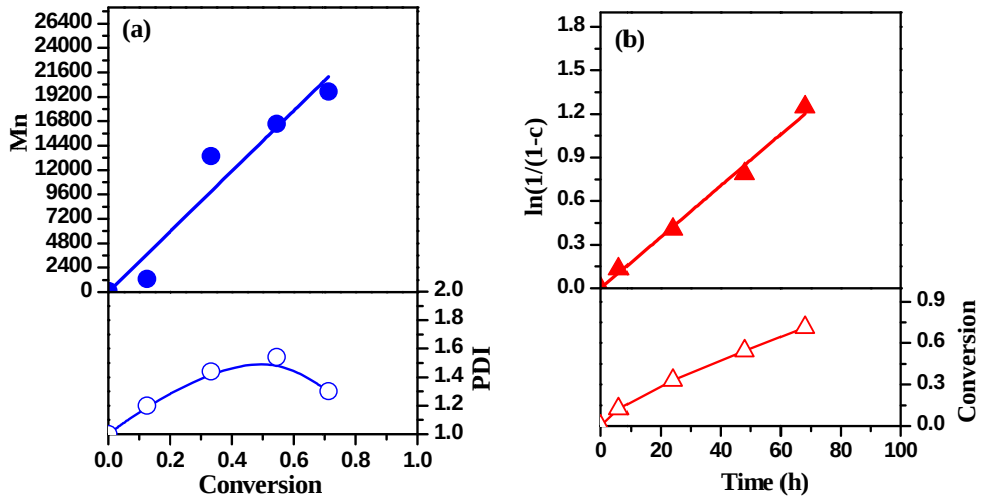

Figure 2.16 The dependence of (a) M_n, M_w/M_n and (b) ln(1/(1-c)) in the Cp_2TiCl mediated 2,3-dimethyl,1,3-butadiene polymerizations: [DMDB]/ [BEB]/[Cp_2TiCl_2]/[Zn] = 100/1/3/6, dioxane, 110°C.

2.3.9 $Cp_2TiCl^{\bullet}$-Mediated CRP of Butadiene Initiated by Epoxide RRO

The butadiene initiation from MPEG is demonstrated *via* the NMR analysis of the chain ends (Figure 2.17). Thus, in addition to the characteristic resonances corresponding to a typical free radical butadiene polymerization, such as those corresponding to the 1,2-unit (-[CH_2-C*H*]-, *a*, δ =2.03 ppm, -[CH_2-CH]-, *b,* δ = 1.25-1.45 ppm, -C*H*=CH_2, *c,* δ = 5.56 ppm, and -CH=CH_2, *d*, δ = 4.94 ppm) as well as to the *cis* and *trans* 1,4-enchainement (-[CH_2-C*H*=C*H*-CH_2]-, *f*, δ = 5.35-5.55 ppm and -[CH_2-C*H*=C*H*-CH_2]-, *e*, δ = 2.05 ppm) in an approximate 1,2/1,4 = 20/80 ratio, specific, epoxide derived peaks such as the aromatic (*i*, δ = 6.83 ppm), methoxy (Ph-O-CH_3, *j*, δ = 3.76 ppm) and methyleneoxy (Ph-O-CH_2-, *h'*, δ ~ 3.95 ppm) signals are observed in the polymer spectrum.

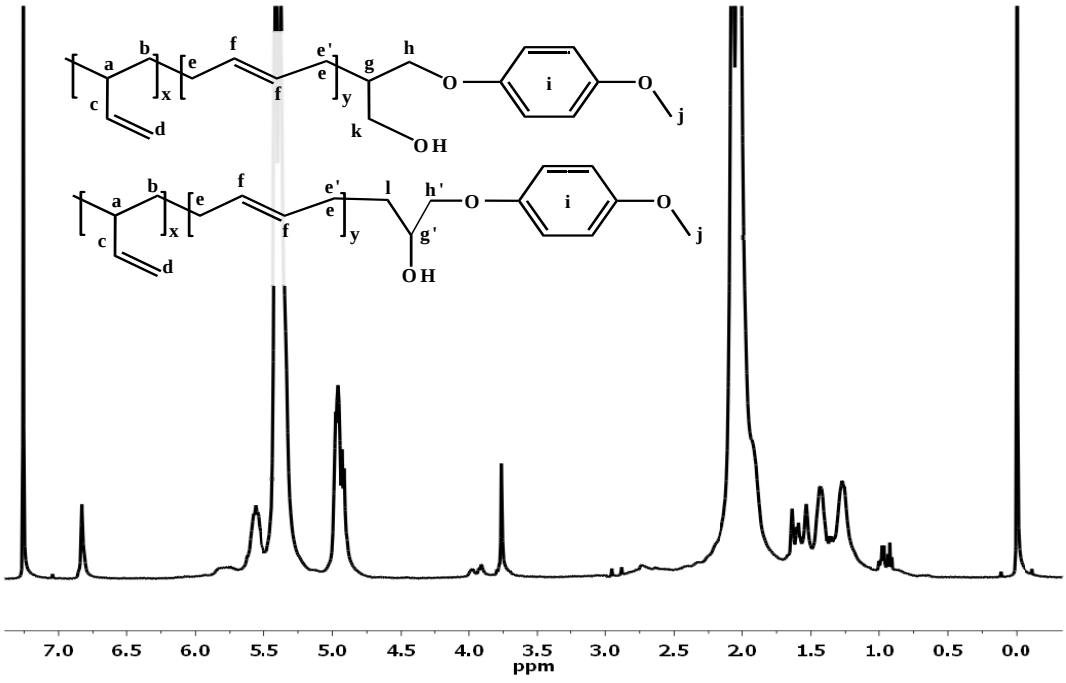

Figure 2.17 500 MHz ^{1}H-NMR spectrum of PBD initiated by MPEG. [BD]/[MPEG]/[Cp_2TiCl_2]/[Zn]=100/1/2.5/2. M_n^{GPC} = 7,700; PDI = 1.40 .

Interestingly, the absence of peaks *k* (~ 3.4-3.6 ppm) indicates that the initiation is preferentially performed by the least stable, but more sterically accessible epoxide derived radical. The possible chain ends derived from the hydrolysis of the Ti-endcapped propagating

chain (such as –CH=CH-C*H*$_2$-*H* or –CH$_2$-C*H*(CH=CH$_2$)-*H* are overlapping with the polymer resonances and could not be observed.

An example demonstrating the 1st order kinetics of the Cp$_2$TiCl-mediated butadiene polymerization using MPEG as initiator are presented in Figure 2.18 using a [BD]/[MPEG]/[Cp$_2$TiCl$_2$][Zn] = 100/1/2.5/2 ratio at 130°C. According to the proposed mechanism, one Ti equivalent is required for the RRO process, whereas the second equivalent is involved in the reversible endcapping of the growing chain, while having a larger amount of Ti and Zn are typically beneficial as seen with other monomers, and most likely for butadiene polymerization as well. As seen from Figure 2.18 a linear dependence of molecular weight on conversion is observed up to about 70 % conversion, with an initiator efficiency of about 0.5. The polydispersity increases with conversion but remains below 1.6. In addition, Figure 2.18b demonstrates the linearity dependence of ln(1/1-c) on time, indicative of 1st order kinetics.

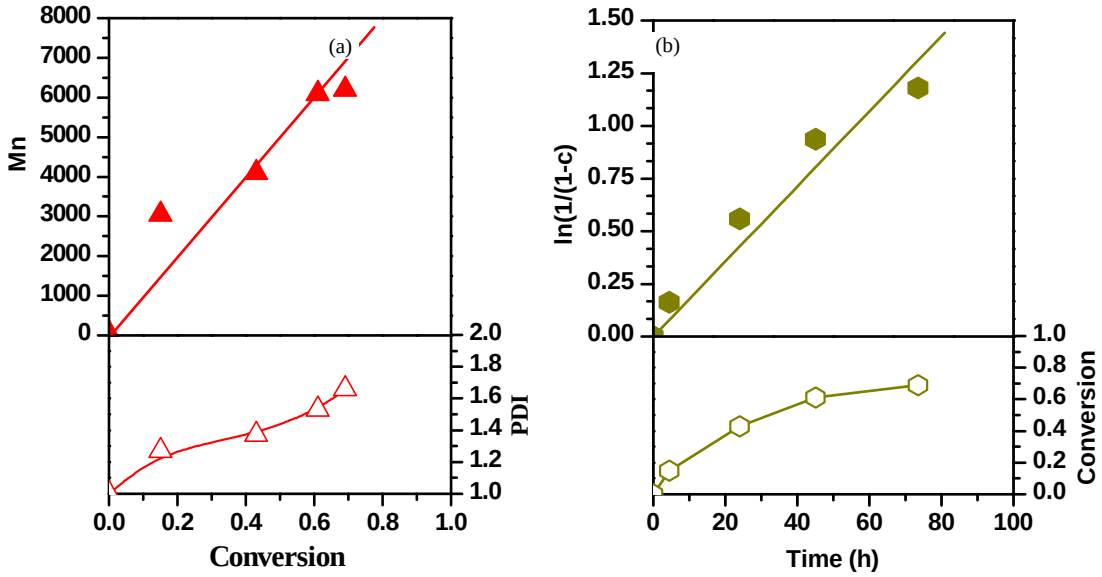

Figure 2.18 The dependence of (a) M_n, M_w/M_n and (b) ln(1/(1-c)) in Cp$_2$TiCl-mediated butadiene polymerizations: [BD]/[MPEG]/[Cp$_2$TiCl$_2$]/[Zn] = 100/1/2.5/2, dioxane, 130 °C.

2.3.10 $Cp_2TiCl^{\bullet}$-Mediated CRP of Butadiene via Aldehyde SET Reduction

The proposed polymerization mechanism is defined in Scheme 2.1. Following the Zn reduction of Cp_2TiCl_2 in dioxane the $Cp_2Ti(III)Cl$ species id generated (eq. 1). Subsequent SET reduction of the aldehyde (eq. 2) provides an α-titanoxybenzylic initiating radical for the butadiene polymerization (eq. 3), which is mediated by the reversible termination of the growing chains with a second equivalent of $Cp_2Ti(III)Cl$ *via* a combination of DC and DT mechanisms (eqs. 4, 5). The aldehyde initiation from BBA is demonstrated by the NMR analysis of the chain ends (Figure 2.19). Thus, in addition to the characteristic resonances corresponding to a typical free radical butadiene polymerization, such as those corresponding to the 1,2-unit (-[CH_2-C*H*]-, *a*, δ =2.03 ppm, -[C*H*$_2$-CH]-, *b,* δ = 1.25-1.45 ppm, -C*H*=CH_2*, c,* δ = 5.56 ppm, and –CH=C*H*$_2$, *d*, δ = 4.94 ppm) as well as to the *cis* and *trans* 1,4-enchainement (-[CH_2-C*H*=C*H*-CH_2]-, *f*, δ = 5.35-5.55 ppm and –[CH_2-C*H*=C*H*-CH_2]-, *e*, δ = 2.05 ppm) in an approximate 1,2/1,4 = 20/80 ratio. The specific initiator derived peaks such as the aromatic *k* (δ = 7.4 ppm) and *I, i'* (δ= 6.75-7.15 ppm) as well as benzylic alcohol and ether *g* and *j* (δ ~ 5.05 ppm) are observed in the polymer spectrum. Moreover, the original aldehyde –C*H*O resonance (δ ~ 10 ppm) is absent, indicating complete initiator consumption. Possible chain ends derived from the hydrolysis of the Ti-endcapped propagating species (such as –CH=CH-C*H*$_2$-*H* or –CH_2-C*H*($CH=CH_2$)-*H* are overlapping with the polymer resonances and could not be observed.

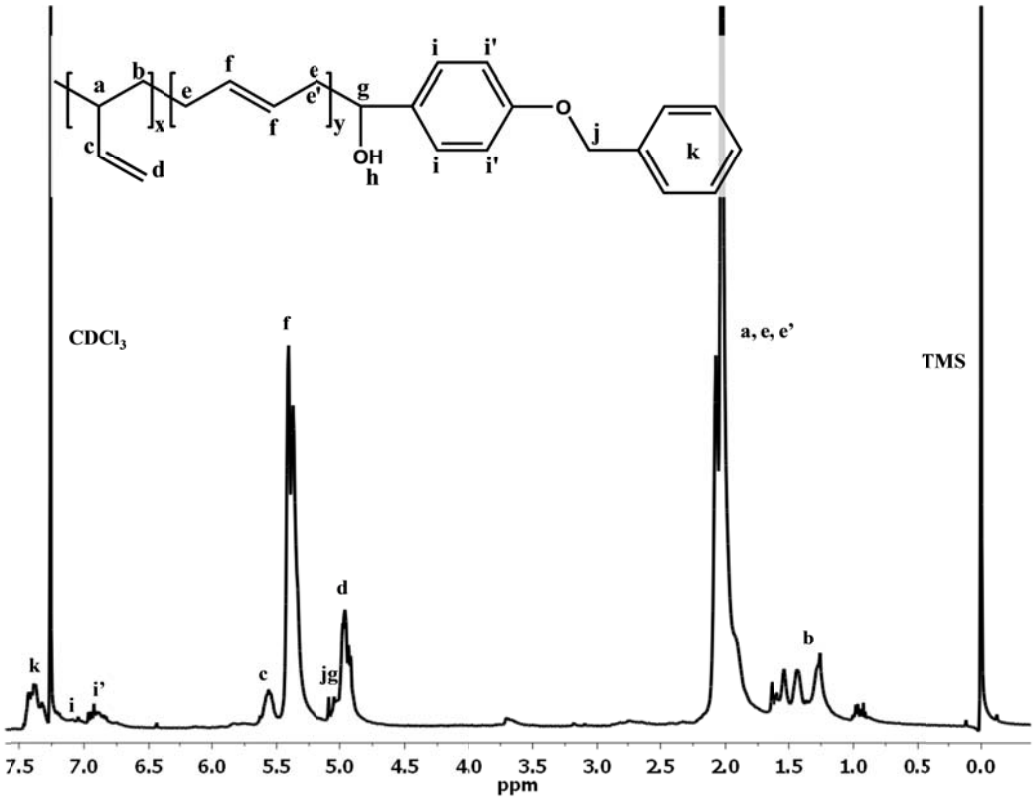

Figure 2.19 500 MHz ^{1}H-NMR spectrum of polybutadiene initiated by BBA. [BD]/[BBA]/[Cp_2TiCl_2]/[Zn] = 200/1/3/3, 130 °C. M_n^{GPC} = 6,990; PDI = 1.58.

An example demonstrating the Cp_2TiCl-mediated butadiene polymerization using BA as initiator is presented in Figure 2.20 using a [BD]/[BA]/[Cp_2TiCl_2]/[Zn] = 200/1/3/3 ratio at 130°C. In accordance with the proposed mechanism, one Ti equivalent is required for the aldehyde reduction and another one for the reversible endcapping of the growing chains. As expected based on previous results larger amounts of Ti and Zn are typically beneficial. As seen from Figure 2.20a, a linear dependence of molecular weight on conversion is observed up to about 40 % conversion, with an initiator efficiency of about 0.6. The polydispersity increases with conversion but remains below 1.8. In addition, Figure 2.20b demonstrates the linearity of the kinetics of the polymerization indicating a constant concentration of the growing chains. The increased molecular weight distribution may be attributed to the higher temperature used in

the butadiene polymerizations. However, being that butadiene has one of the lowest propagation rates, compared to other vinylic monomers (acrylates, styrene, methacrylates) compensation needed to be made in order to perform the experiments on a reasonable time scale. Therefore, while lowering the temperature may indeed give much narrower molecular weight distributions, it would also increase the time needed for an experiment to unreasonable lengths.

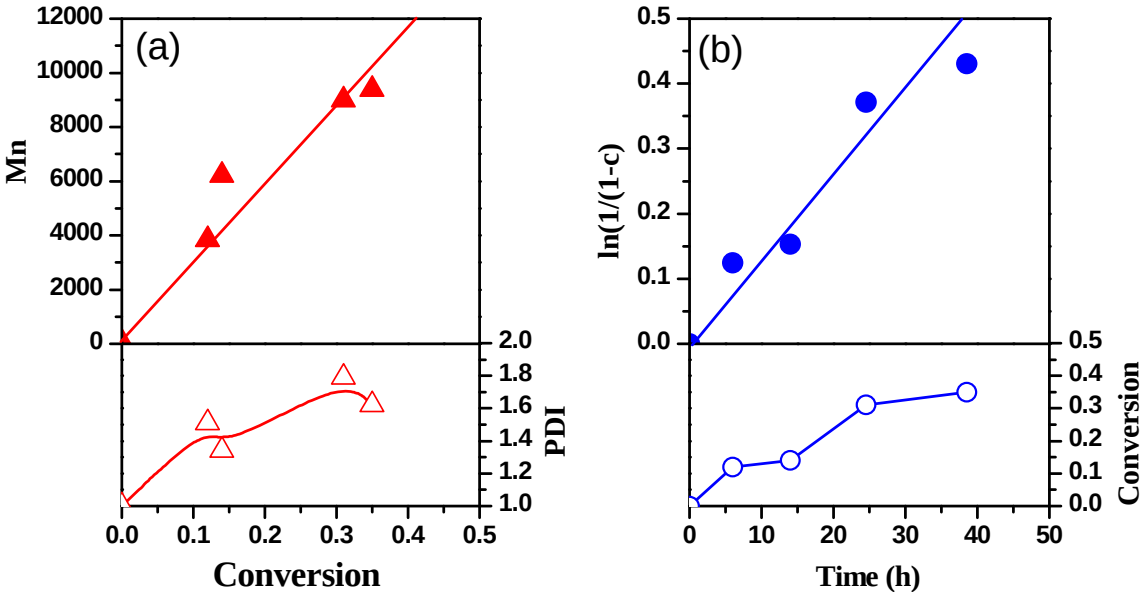

Figure 2.20 The dependence of (a) M_n, M_w/M_n and (b) Ln(1/(1-c)) in the Cp_2TiCl mediated butadiene polymerizations: [BD]/[BA]/[Cp_2TiCl_2]/[Zn] = 200/1/3/3, dioxane, 130 °C.

2.3.11 $Cp_2TiCl^{\bullet}$-Mediated CRP of Butadiene by Halide Abstraction

The polybutadiene initiation from DBPX is demonstrated by the NMR analysis of the chain ends (Figure 2.21). Thus, the characteristic resonances corresponding to a typical free radical butadiene polymerization, such as those corresponding to the 1,2-unit (-[CH_2-C*H*]-, *a*, δ =2.03 ppm, -[CH_2-CH]-, *b,* δ = 1.25-1.45 ppm, -C*H*=CH_2, *c,* δ = 5.56 ppm, and -CH=CH_2, *d*, δ = 4.94 ppm) as well as to the *cis* and *trans* 1,4-enchainement (-[CH_2-C*H*=C*H*-CH_2]-, *f*, δ = 5.35-5.55 ppm and -

[CH_2-C*H*=C*H*-CH_2]-, *e*, δ = 2.05 ppm) are present in the spectrum. With there being an approximate 1,2/1,4 = 20/80 ratio present and typical for a radical butadiene polymerization. Additionally, specific initiator derived peaks such as the aromatic *h*, δ = 7.15 ppm are observed in the polymer spectrum. Interestingly, as indicated by the di-bezylic resonance *i* at δ ~ 2.9 ppm and the absence of the possible benzyl halide group (Ph-C*H*$_2$-Br, ~4.5 ppm), initiator dimerization seems to occur before addition to butadiene, similarly to previous experiments using DBPX. The connectivity between the DBPX fragment and BD is shown by the peaks *g*, δ = 2.73 ppm and *e'*, δ = 2.63 ppm which represent the benzylic linkage to the methylene of the first BD unit. Possible chain ends derived from the hydrolysis of the Ti-endcapped propagating species (such as –CH=CH-C*H*$_2$-*H* or –CH_2-C*H*($CH=CH_2$)-*H* are overlapping with the polymer resonances and could not be observed. Moreover, resonances associated with allyl bromide chain ends (~4 ppm) are absent, indicating that the polymerization do not proceed *via* an ATRP mechanism.

The demonstration of Cp_2TiCl-mediated butadiene polymerization using DBPX as initiator are presented in Figure 2.22 using a [BD]/[DBPX]/[Cp_2TiCl_2]/[Zn] = 200/1/6/20 ratio at 130°C. According to our mechanism, two Ti equivalents are required for halide abstraction from the difunctional initiator and consequently, two more for the reversible endcapping of the growing chains. As seen from Figure 2.22, there is indeed a linear dependence of molecular weight on conversion, which is observed up to about 50 % conversion, with initiator efficiency 0.7. The polydispersity increases with conversion but remains below 1.6. In addition, Figure 2.22b demonstrates the 1st order kinetics of the polymerization indicating a constant concentration of the growing chains and a rate of 0.0059 h^{-1}.

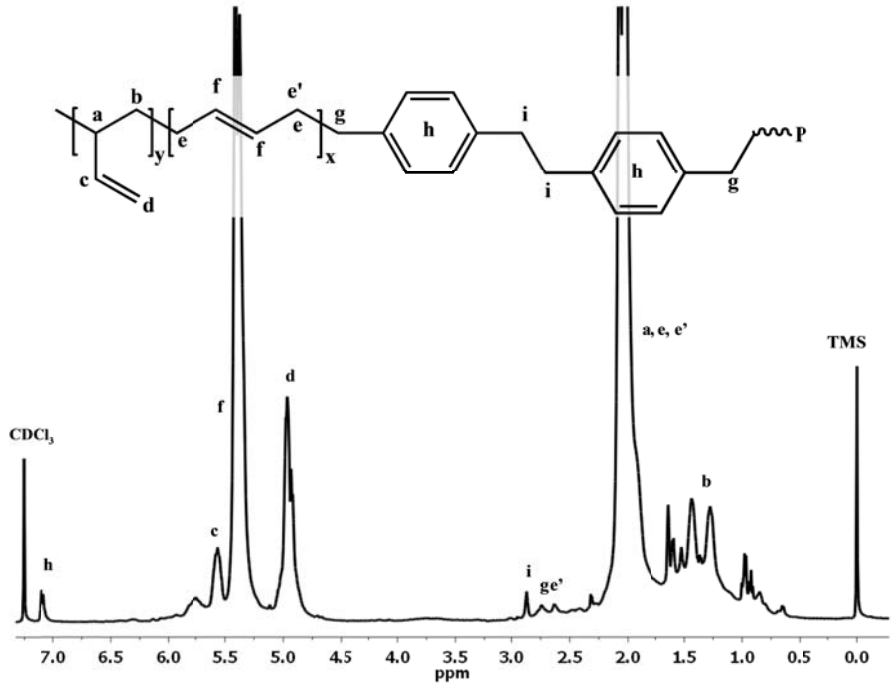

Figure 2.21 500 MHz ^{1}H-NMR spectrum of polybutadiene initiated by DBPX. [BD]/[DBPX]/[Cp_2TiCl_2]/[Zn] = 200/1/6/20 at 130 °C. M_n^{GPC} = 5,418; PDI =1.19 .

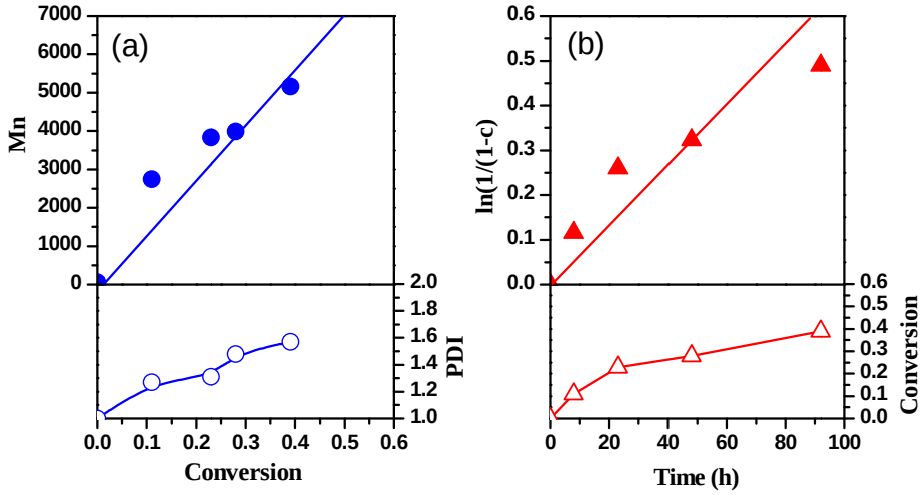

Figure 2.22 The dependence of (a) M_n, M_w/M_n and (b) Ln(1/(1-c)) in Cp_2TiCl mediated butadiene polymerizations: [BD]/[DBPX]/[Cp_2TiCl_2]/[Zn] = 200/1/6/20, dioxane, 130 °C.

2.4 Conclusions

The first examples of transition metal mediated controlled radical polymerizations of isoprene were demonstrated and optimized using the epoxide/Cp_2TiCl initiator/catalyst system. The initiation was supported by NMR investigations, which indicated the presence of epoxide fragments on the chain end and the stereoselectivity of a conventional radical polymerization.

The effect of the reaction variables was studied over a wide range of conditions ([Cp_2TiCl_2]/[epoxide] = 1/1-1/6, ([Cp_2TiCl_2]/[Zn] = 1/0.5-1/8 , [Iso]/[epoxide] = 20/1-1000/1, T = 70-130 °C in THF and dioxane) to reveal a linear dependence of molecular weight on conversion, linear 1st order kinetics as well as moderate polydispersities up to high conversions. The initiator efficiency (IE) and the rate increase, while polydispersity decreases with increasing the [Cp_2TiCl_2]/[epoxide] ratios, with an optimum at [epoxide]/[Cp_2TiCl_2]/[Zn] = 1/3/6-1/4/8 at 90 - 110 °C. While IE is independent of temperature, lower polydispersities (1.3-1.4) were obtained at lower temperatures ~ 90 °C. Furthermore, random and block copolymers with styrene could also be obtained.

The Cp_2TiCl_2/epoxide methodology uses off-the-shelf reagents, and mediates isoprene CRP at lower temperatures (70-110 °C vs. 120-130 °C) than the more expensive nitroxide and dithioester CRP methods, to which it offers a convenient and inexpensive alternative. Moreover, refinement of the ligand systems using examples already available in Ti-coordination polymerization is likely to optimize the polymerization further.

This methodology was expanded further through the use of Cp_2TiCl set-reduction of aldehydes, in addition to halide abstraction to generate initiating radical species for isoprene. All three initiating systems showed promising results, generating a controlled polymerization as well as reasonable rates of polymerization.

This procedure was applied to CRP of butadiene and dimethyl butadiene, each of which was demonstrated for all three classes of initiators. A controlled radical polymerization was observed for all cases with DMBD below 130C. At higher temperatures, it was noted that the polymerization was free radical, most likely attributed to the allylic nature of the monomer and polymer allowing for more significant chain transfer at elevated temperatures. Butadiene exhibited some control over molecular weight, but was the worst among the three monomers

examined. Unfortunately the increased molecular weight distribution may be credited to the higher temperatures used for these polymerizations. However, butadiene has one of the lowest propagation rates, compared to other vinylic monomers and this had to be compensated with a higher temperature in order to perform the experiments on a reasonable time scale. Therefore, while lowering the reaction temperature may indeed give much narrower molecular weight distributions, it drastically increase the time needed for an experiment to unreasonable lengths. It is also possible this system need further optimization to obtain better polymerization control.

2.5 References

1. Hosler, D.; Burkette, S. L.; Tarkanian, M. J. *Science* **1999**, *284*, 1988.
2. Breslow, D. S.; Newburg, N. R. *J. Am. Chem. Soc.* **1957,** *79*, 5072.
3. (a) Schops, M.; Leist, H.; DuChesne, A.; Wiesner, U. *Macromolecules* **1999**, *32*, 2806. (b) Li, W.; Wang, H.; Yu, L.; Morkved, T.; Jaeger, H. M. *Macromolecules* **1999**, *32*, 3034. (c) Allgaier, J.; Poppe, A.; Willner, L.; Richter, D. *Macromolecules* **1997**, *30*, 1582.
4. *Principles of Polymerization*; Odian, G.; Wiley-Interscience: New York, 2004, pp 633-700.
5. Hirao, A.; Hayashi, M. *Acta Polym*. **1999**, *50*, 219.
6. (a) Evans, W. J.; Giarikos, D. G.; Allen, N. T. *Macromolecules* **2003**, *36*, 4256. (b) Miyazawa, A.; Kase, T.; Shibuya, T. *J. Polym. Sci: Part A: Polym. Chem.* **2004**, *42*, 1841.
7. (a) Pintauer, T.; Matyjaszewski, K. *Chem*. *Rev*. **2008**, *37*, 1087–1097. (b) Braunecker, W. A.; Matyjaszewski, K. *Prog. Polym. Sci.* **2007**, 32, 93–146. (c) *Handbook of Radical Polymerization*; Matyjaszewski, K., Davis, T. P., Eds.; Wiley-Interscience: New York, **2002**, pp 361-462.
8. (a) *Handbook of Radical Polymerization*; Matyjaszewski, K., Davis, T. P., Eds.; Wiley-Interscience: New York, 2002, pp 361-462. (b) Matyjaszewski, K.; Xia, J. Chem. Rev. 2001, 101, 2921.
9. Souaille, M.; Fischer, H. *Macromolecules* **2000**, *33*, 7378.
10. Goto, A.; Fukuda, T. *Progr. Polym. Sci.* **2004**, *29*, 329-385.
11. Hawker, C. J.; Bosman, A.W.; Harth, E. *Chem. Rev.* **2001**, *101*, 3661-3688.
12. Gaynor, S.; Wang, J.; Matyjaszewski, K. *Macromolecules* **1995**, *28*, 8051.
13. Moad, G; Rizzardo, E.; Thang, S. *Acc. Chem. Res.* **2008**, 41(9), 1133-1142.
14. Poli, R. *Angew. Chem. Int. Ed. Engl*. **2006**, *45*, 5058–5070.
15. (a) Wayland, B. B.; Poszmik, G.; Mukerjee, S. L.; Fryd, M. *J. Am. Chem. Soc*. **1994**, *116*, 7943. (b) Debuigne, A.; Caille, J. R.; Jerome, R. *Angew. Chem. Int. Ed.* **2005**, *44*, 1101 – 1104.
16. (a) Yamago, S.; Iida, K.; Yoshida, J. I. *J. Am. Chem. Soc.* **2002**, *124*, 2874. (b) Yamago, S.; Ray, B.; Iida, K.; Yoshida, J.; Tada, T.; Yoshizawa, K.; Kwak, Y.; Goto, A.; Fukuda, T. *J. Am. Chem. Soc.*, **2004**, *126*, 13908-13909. (c) Yamago, S.; Kayahara, E.; Kotani, M.; Ray, B.; Kwak, Y.; Goto, A.; Fukuda, T. *Angew. Chem., Int. Ed. Engl*. **2007**, *46*(8), 1304-1306.
17. (a) Le Grognec, E.; Claverie, J.; Poli, R. *J. Am. Chem. Soc.* **2001**, *123,* 9513. (b) Champouret, Y.; Baisch, U.; Poli, R.; Tang, L.; Conway, J. L.; Smith, K. M. *Angew. Chem. Int. Ed.* **2008**, *47*, 6069-6072.
18. (c) Percec, V.; Asandei, A. D.; Asgarzadeh, F.; Bera, T. K. Barboiu, B. *J. Poly. Sci: Part A: Polym. Chem.* **2000**, *38*, 3839. (d) Percec, V.; Asandei. A. D.; Asgarzadeh F.; Barboiu, B.; Holerca, M. N.; Grigoras, C. *J. Poly. Sci: Part A: Polym. Chem.* **2000**, *38*, 4353.
19 Wootthikanokkhan, J.; Peesan, M.; Phinyocheep, P. *Eur. Polym. J.* **2001**, *37*, 2063.
20 Germack, D. S.; Wooley, K. L. *J. Polym. Sci: Part A: Polym. Chem.* **2007,** *45*, 4100.
21 Skaff, H.; Emrick, T. *Angew. Chem. Int. Ed.* **2004**, *43*, 5383.
22 Jitchum, V.; Perrier, S. *Macromolecules*, **2007**, *40,* 1408.
23 (a) Grubbs, R. B.; Wegrzyn, J. K.; Xia, Q. Chem. Commun. 2005, 1, 80. (b) Kamachi, M.; Kajiwara, A. *Macromolecules* **1996**, *29*, 2378. (c) Keosherian, B.; Georges M.; Quinlan, M.; Vergin, R.; Goodbrand, B. Macromolecules **1998**, *31*, 7559. (d) Benoit, D.; Harth, E.; Fox, P.; Waymouth, R. M.; Hawker, C. J. *Macromolecules* **2000**, *33*, 363. (e) Li, I. Q.; Howell, B. A.;

Dineen, M. T.; Kastl, P. E.; Lyons, J. W.; Meunier, D. M.; Smith, P. B.; Priddt, B. B. *Macromolecules* **1997**, *30*, 5195.
24. Mahanthappa, M. ; Waymouth, R. M. *J. Am. Chem. Soc.* **2001**, *123*, 12093.
25. Reetz, M. T. *In Organometallics in Synthesis: A Manual.* Schlosser, M. (Ed.). John Wiley and Sons, Chichester, England, **2002**, p 817-924.
26. (a) Rajanbabu, T.; Nugent, W. *J. Am. Chem. Soc.* **1994**, *116*, 986. (b) Rajanbabu, T.; Nugent, W.; Beattie, M. *J. Am. Chem. Soc.* **1990**, *112*, 6408-6409. (c) RajanBabu, T.; Nugent, W. *J. Am. Chem. Soc* **1989**, *111*, 4525.
27. (a) Gansauer, A.; Rinker, B. *Titanium and Zirconium in Organic Synthesis*; Wiley, **2002**. (b) Cuerva, J. M.; Oller-López, J. L.; Oltra, J. E. *Top. Curr. Chem*. **2006**, *264*, 63–91. (c) Gansäuer, A.; Justicia, J.; Fan, C. A.; Worgull, D.; Piestert, F. *Top. Curr. Chem.* **2007**, 279: 25–52.
28. Spencer, R. P.; Schwartz, J. *Tetrahedron*, **2000**, *56*, 2103-2112.
29. Green, M. L.; Lucas, C. R. *J. Chem. Soc. Dalton Trans.* **1972**, *8*, 1000-1003.
30. Barden, M. C.; Schwartz, J. *J. Am. Chem. Soc.* **1996**, *118*, 5484.
31. (a) Asandei, A. D.; Moran, I. W. *J. Am. Chem. Soc.* **2004**, *126*, 15932. (b) Asandei, A. D.; Moran, I. W. *J. Polym. Sci. Part A: Polym. Chem.* **2005**, *43*, 6028. (c) Asandei, A. D.; Moran, I. W. *J. Polym. Sci. Part A: Polym. Chem.* **2005**, *43*, 6039. (d) Asandei, A. D.; Moran, I. W. *J. Polym Sci. Part A: Polym. Chem.* **2006**, *44*, 1060. (e) Asandei, A. D.; Moran, I. W.; Saha, G.; Chen, Y. *J. Polym. Sci. Part A: Polym. Chem.* **2006**, *44*, 2156. (f) Asandei, A. D.; Moran, I. W.; Saha, G.; Chen, Y. *J. Polym. Sci. Part A: Polym. Chem.* **2006**, *44*, 2015. (g) Asandei, A. D.; Moran, I. W.; Saha, G.; Chen, Y. *ACS Symp. Ser.* **2006***, 944,* 125-139.
32. (a) Asandei, A. D.; Chen, Y. *Macromolecules* **2006**, *39*, 7459. (b) Asandei, A. D.; Saha, G. *J. Polym. Sci. Part A: Polym. Chem.* **2006**, *44*, 1106.
33 (a) Asandei, A. D.; Chen, Y.; Moran, I. W.; Saha, G. *Tetrahedron*, **2008**, 64, 11831-11838. (b) Asandei, A. D.; Chen, Y.; Moran, I. W.; Saha, G. *J. Organomet. Chem.* **2007**, 692, 3174-3182.
34. (a) Asandei, A. D.; Saha, G. *Macromol. Rapid Commun.* **2005**, *26*, 626. (b) Asandei, A. D.; Chen, Y.; Adebolu, O. I.; Simpson, C. P. *J. Polym. Sci.: Part A: Polym. Chem.* **2008**, *46*, 2869-2877.
35. Asandei, A. D.; Saha, G. *Macromolecules,* **2006***, 39*, 8999-9009.
36. (a) Schops, M.; Leist, H.; DuChesne, A.; Wiesner, U. *Macromolecules* **1999**, *32*, 2806. (b) Li, W.; Wang, H.; Yu, L.; Morkved, T.; Jaeger, H. M. *Macromolecules* **1999**, *32*, 3034. (c) Allgaier, J.; Poppe, A.; Willner, L.; Richter, D. *Macromolecules* **1997**, *30*, 1582.
37. Hirao, A.; Hayashi, M. *Acta Polym*. **1999**, *50*, 219.
38. Evans, W. J.; Giarikos, D. G.; Allen, N. T. *Macromolecules* **2003**, *36*, 4256.
39. Wootthikanokkhan, J.; Peesan, M. *Eur. Polym. J.* **2001**, *37*, 2063.
40. Xia, J.; Paik, H.; Matyjaszewski, K. *Macromolecules* **1999**, *32*, 8310-8314.
41. Percec, V.; Popov, A.; Castillo, E.; Monteiro, M.; Barboiu, B.; Asandei A. D.; Mitchell, C. *J. Am. Chem. Soc.* **2002**, *124*, 4940-4941. (b) Asandei, A. D.; Percec, V. *J. Polym. Sci.: Part A: Polym. Chem.* **2001**, *39*, 3392.
42. (a) Grubbs, R. B.; Wegrzyn, J.; Xia, Q. *Chem. Commun*. **2005**, *1*, 80. (b) Kamachi, M.; Kajiwara, A. *Macromolecules* **1996**, *29*, 2378. (c) Keosherian, B.; Georges M.; Quinlan, M.; Vergin, R.; Goodbrand, B. *Macromolecules* **1998**, *31*, 7559.(d) Benoit, D.; Harth, E.; Fox, P.; Waymouth, R. M.; Hawker, C. J. *Macromolecules* **2000**, *33*, 363. (e) Li, I.; Howell, B.;

Dineen, M.; Kastl, P.; Lyons, J.; Meunier, D.; Smith, P.; Priddt, B. *Macromolecules* **1997**, *30*, 5195. (f) Gavranovic, G.; Csihony, S.; Bowden, N. B.; Hawker, C. J.; Waymouth, R. M.; Moerner, W. ; Fuller, G. *Macromolecules* **2006,** *39,* 8121.

43. (a) Germack, D. S; Wooley, K. L. *J. Polym. Sci.: Part A: Polym. Chem.* **2007**, *45*, 4100. (b) Jitchum, V.; Perrier, S. *Macromolecules* **2007**, *40,* 1408.
44. (a) Asandei, A. D.; Simpson, C. P.; Yu, H. S. *Polym. Prepr.* **2008**, *49(2)*, 73-74. (b) Asandei, A. D.; Simpson, C. P. *Polym. Prepr.* **2008**, *49(2)*, 75-76. (c) Asandei, A.D.; Simpson C. *Polym. Prepr*. **2008**, *49(1),* 452-453. (d) Asandei, A. D.; Saha, G. *Polym. Prepr.* **2005**, *46(2)*, 474-475.
45. Gansauer, A.; Bluhm, H. *Chem. Commun*. **1998**, 214-215.
46. Jensen, T. R.; Yoon, S. C.; Dash, A. K.; Luo, L. B.; Marks, T. J. *J. Am. Chem. Soc.* **2003**, *125*, 14482-14494.

47 (a) Yoo, B. W.; Choi, K. W.; Lee,S. J.; Yoon, C. M.; Kim, S. H.; Kim, J. H. *Synth. Commun.* **2002**, 32(1), 63–67. (b) Zhang, Y.; Yu, Y.; Bao, W. *Synth. Commun.* **1995**, *25(12)*, 1825-1830.

48 Blondin, D.; Regis, J.; Prud'homme, J.; *Macromolecules*, **1974**, *7*, 187.

Chapter 3: Towards $Cp_2TiCl^{\bullet}$ Mediated Radical Polymerization of Vinylidene Fluoride

As a prelude to metal mediated systems, a series of typical free radical initiators were first evaluated in the thermal or UV-mediated VDF polymerization in glass tubes, at room temperature (rt) in a variety of solvents. Better polymerization results were obtained with initiators which generate the most reactive radicals (TBPO), in solvents that minimize chain transfer (ACN). The effect of UV irradiation was subsequently investigated to reveal a photocontrolled free radical polymerization. Finally, a series of epoxides, aldehydes, halides and peroxides, known to initiate both styrene and diene polymerizations in the presence of $Cp_2TiCl^{\bullet}$, were tested as potential rt VDF initiators. However, regardless of reaction conditions, no polymer was obtained. This is most likely due to the incompatibility of solvents appropriate for Cp_2TiCl_2 reductions with those conducive of VDF polymerizations. Thus, polar solvents appropriate for Cp_2TiCl_2 are strong chain transfer agents towards VDF (dioxane, THF, diglyme, acetone), while solvents that limit chain transfer to $PVDF^{\bullet}$, react with $Cp_2TiCl^{\bullet}$.

3.1 Introduction

Fluorinated (co)polymers are fundamental specialty materials endowed with wide morphological versatility, high thermal, chemical, ageing and weather resistance, as well as low surface energy, dielectric constant, flammability, refractive index, and moisture absorption. As such, their applications range anywhere from paints and coatings, pipe liners, transmission fluids, O-rings for extreme temperatures, fuel cell membranes and antifouling layers to optical fibers and high power capacitors [1]. A well know example is poly(vinylidene fluoride) (PVDF)[2] which due to its excellent chemical inertness, acid resistance, low water absorptivity, weatherability, low dielectric constant and piezoelectric properties[3,4,5], is a widely used high-performance material for coatings, membranes for fuel cells and Li ion batteries, [6] as well as semiconductor and nuclear applications. To overcome the PVDF high crystallinity and low solubility, various copolymers, especially with non homopolymerizable [7,8] hexafluoropropene [8,9] (HFP) are also used. PVDF is obtained by the high pressure (bp_{VDF} = -86 °C, bp_{HFP} = -29.6 °C) peroxide initiated VDF radical polymerization in metal reactors at 50-100°C.[10,11]

As such, controlled radical polymerizations (CRPs) which limit termination and other side reactions *via* atom transfer (ATRP) [12,13] dissociation-combination (DC) or degenerative transfer (DT) mechanisms and enable control over molecular weight and polydispersity, have been widely applied in the synthesis of complex macromolecular structures [13]. However, while they have recently seen remarkable developments [12], and ATRP, nitroxide or addition-fragmentation methods were successful with acrylates or styrenes, their applicability towards very reactive monomers such as main chain fluorinated alkenes, still awaits demonstration. Moreover, all metal based systems employ only late transition metals and provide initiation only from activated halides or thermal initiators. Thus, a broader selection of initiators and catalysts

would be desirable, especially since they might provide access to novel chain ends derived either from the initiator or catalyst or both.

Thus, as (co)polymers of main chain fluorinated monomers (*e.g.* VDF) are important, the study of their CRPs and the synthesis of the complex polymer architectures thereby derived, is a worthy undertaking[14,15]. Conversely, such polymerizations are quite challenging, especially on a laboratory scale, in view of the low bp of the monomers and the high-pressure metal reactor requirement. As such, while styrene or acrylate CRPs can be conveniently sampled repeatedly from the side arm of a Schlenk tube on a 1 g scale, kinetic studies of VDF polymerizations involve many one-data-point experiments. This is a very time-consuming and expensive process due to the typical lab unavailability of a large number of costly metal reactors, which moreover still require 10-100 g of monomer. Thus, development of methods that would allow few grams-scale polymerizations to proceed at room temperature (rt) in inexpensive, low-pressure glass tubes, would be highly desirable, especially since such procedures would easily lend themselves to the fast screening of a wide range of catalysts and reaction conditions.

VDF polymerization can proceed at rt under organic free radical initiation[16], but only very low molecular weight VDF telomers (DP < 1-3) may be obtained, and only at high temperatures (> 100 °C) from transition metal salts and polyhalides by redox catalysis.[15,17] Moreover, while the 1:1 metal catalyzed addition of R_F-I derived perfluoroalkyl radicals to alkenes using Cu[18], Zn[19], Pd[20], $SnCl_2/CH_3COOAg$[21], Cp_2TiCl[22] occurs readily at high temperatures, the metal catalyzed addition of such electrophilic radicals to electrophilic fluorinated alkene substrates (FMs) at T < 100 °C, and especially at ambient temperatures is to the best of our knowledge, conspicuously absent from the literature. Moreover, there are no reports on metal-mediated VDF polymerizations, let alone VDF-CRP. Consequently, the ability to initiate and control VDF using a transition metal system under mild conditions would be of great synthetic value.

The paramagnetic Cp_2TiCl[23] available in situ by Zn reduction of Cp_2TiCl_2 [24] is a mild one electron transfer agent which catalyzes a variety of radical reactions [25], including epoxide radical ring opening (RRO)[26], aldehyde single electron transfer reduction and halide abstraction. We have demonstrated the Cp_2TiCl-catalyzed LRP of styrene [27] initiated by epoxides, aldehydes [28], halides [29], and peroxides [30], as well as that of dienes [31] initiated from halides [32e,f,i,33] epoxides,[32a,b,g] and aldehydes[32c,d]. The effect of ligands, reducing agents, solvents, additives, reagent ratios and temperature was investigated[27]. This methodology was applied in the synthesis of branched and graft copolymers [34], and Ti alkoxides generated in-situ from epoxides and aldehydes were also shown to catalyze the living ring opening polymerization of cyclic esters[35], epoxides and anhydrides [35].

Encouraged by these results, we decided to evaluate such alternative methods of polymerization initiation and control[36], and explore the scope and limitations of transition metal catalysts in the rt VDF radical polymerization.

3.2 Experimental

3.2.1 Materials.

Vinylidene Fluoride (VDF, 98% min.) and hexafluoropropene (HFP, 99% min.), 1-iodononafluorobutane (PFBI, 98%) and heptafluoro-2-iodopropane (PFipI, 97%), 1, 8-dichloroperfluorooctane (DCPfO, 99%) (all from Synquest Laboratories). Activated Zn powder (Zn, 99+%), glycidyl 4-methoxyphenyl ether (MPEG, 99%), 1,2,7,8-Diepoxyoctane (DEO, 97%), 1,4-butanediol diglycidyl ether (BDE, 95%), Benzaldehyde (BA, 99.5%), 1,10-Dibromodecane (DBD, 97%), methyl iodide (CH_3I, 99.5%), 1-(bromoethyl)benzene (BEB, 95%), azobisisobutyronitrile (AIBN, 98%), H_2O_2 (50% in H_2O), benzoyl peroxide (BPO, 97%), tert-butylperoxy benzoate (TBPB, 95%), t-butyl peroxide (TBPO, 98%), 2,5-bis-(tert-butylperoxy)-2,5–dimethylhexane (BTBDMH, 90%), dicumyl peroxide (DCPO, 99%), and dimethyl carbonate (DMC,

≥ 99%, anhydrous) (all from Aldrich), dilauryl peroxide (DLPO, 99%) methoxybenzene sulfonyl chloride (MBSC, 99%), bis(cyclopentadienyl)titanium dichloride (Cp_2TiCl_2, 97%), bromotrichloromethane ($BrCCl_3$, 99%), ethylene carbonate (EC, 99%) (all from Acros) and carbon tetrachloride (CCl_4, 99%, Fisher) were used as received. Methanol (MeOH, 99%) acetonitrile (ACN, 99%), anisole (99.7%), α,α,α-trifluorotoluene (TFT, 99%), pyridine (Pry, 99%), N-methyl-2-pyrrolidinone (NMP, 99%) (all from Aldrich), N,N'-dimethylacetamide (DMAC, 99%), dioxane (99.7, %), dimethyl sulfoxide (DMSO, 99.8%), benzonitrile (BzN, 99%), and ε-caprolactone (CL, 99%) (all from Acros), diglyme (99.5%, Fluka), N,N'-dimethylformamide (DMF, 99.9%), toluene (Tol, 99.8%) (both from Fisher), and tetrahydrofuran (THF, 99%, J. T. Baker), were dried over CaH_2 overnight. Acetone (99.9%, J. T. Baker) was dried over anhydrous $MgSO_4$.

3.2.2 Techniques.

^1H NMR (500 MHz) spectra were recorded on a Bruker DRX-500 at 24^0C in acetone-d_6. GPC analyses were performed on a Waters gel permeation chromatograph equipped with a Waters 2414 differential refractometer and a Jordi 2 mixed bed columns setup at 80^0C. DMAc (Fisher, 99.9% HPLC grade) was used as eluent at a flow rate of 1 mL/min. Number-average (M_n) and weight-average molecular weights (M_w) were determined from calibration plots constructed with polymethylmethacrylate standards. All reported polydispersities are those of water precipitated samples.

3.2.3 Polymerizations.

A 35-mL Ace Glass 8648 # 15 Ace-Thread pressure tube equipped with bushing and a plunger valve was charged with TBPO (0.16 mL, 0.85 mmol), ACN (3 mL) and degassed. The tube was then cooled, opened under He and charged with VDF (1.1g, 17.18 mmol), re-degassed and the reaction mixture was warmed up to room temperature on a stir plate under UV irradiation

at about 15-20 cm from a UV lamp (Fisher, model B-100AP with a spot bulb, 100W) behind a protective shield. After required amount of time, the tube was cooled in liquid nitrogen, opened and the excess VDF and HFP was allowed to boil off in the hood under maximum air flow. The reaction mixture was precipitated into deionized water. The polymer was centrifuged and dried.

A 35-mL Ace Glass 8648 # 15 Ace-Thread pressure tube equipped with bushing and a plunger valve containing Cp_2TiCl_2 (21.4 mg, 0.09 mmol), Zn (4.2 mg, 0.07 mmol) and dioxane (3.0 mL) was degassed and the Ti reduction was carried out at rt. The tube was then cooled in liquid nitrogen, opened under He and charged with MPEG (15.5 mg, 0.09 mmol) and VDF (1.10g, 17.18 mmol), re-degassed and held at 2 °C. Conversions were determined gravimetrically.

3.3 Results and Discussion

Before evaluating the metal catalyzed systems, we decided to first verify our ability to perform the reactions in glass tubes at rt by carrying out conventional free radical VDF polymerizations. Thus, it is known that UV radiation mediates VDF [2] telomerization with (perfluoro)alkyl iodides [37] or H_2O_2 [38], but there are very few reports on the use of conventional free radical initiators either at mild temperatures or under UV irradiation or on the solvent effect in VDF polymerizations. Thus, we started [39] by exploring VDF polymerizations under such conditions.

Previous investigations of solution properties[40,41] indicated that the best PVDF solvents are polar aprotic and H-bonding capable, and that HH sequences decrease solubility[40d]. A common structural motif is a favorable interaction of the polar Y=O bond (Y = C, S, P) of the solvent, with the mildly acidic Hs in $-CF_2-CH_2-CF_2-$. Accordingly, 2-pentanone, propionitrile, BN, nitrobenzene, $(MeO)_3P$, $(NEt_2)SO_2$, sulfolane $[-(CH_2)_4-]SO_2$ and metylpyridines were classified as bad solvents. $(BuO)_3P=O$ only swells PVDF, whereas γ-butyrolactone, propylenecarbonate, cyclohexanone,

CH_3COPh and $Ph_2C=O$ solutions gel on annealing at rt. Short chain phosphates ($(RO)_3P=O$; R = Me, Et, and $(CH_3)(MeO)_2P=O$) are good solvents, whereas tertiary amides ($HCONR_2$; R = Me (DMF), Et, DMAC, N-formylmorpholine, NMP) and DMSO are very good solvents. Finally, cyclopentanone, N-alkyl cyclic urethanes as well as linear and cyclic ureas ($(Me_2N)_2C=O$, [-$N(CH_3)$-$(CH_2)_{2\text{-}3}$-$N(CH_3)$-]C=O, DMEU and DMPU) dissolve PVDF even at rt, with $[(CH_3)_2N]_3P=O$ (HMPA) and $(CH_3)[(CH_3)_2N]_2P=O$ considered excellent solvents.

However, while VDF "solution" polymerizations are typically carried out in ACN, [42] a non-solvent weak chain transfer (CT) agent, [43] there is in fact very little data [44,45,46] on the solvent effect in VDF polymerizations. Thus, we decided to scan a few common solvents, using typical free radical initiators, noting that while good monomer/polymer solubilization would be desirable, minimization of solvent CT outweighs solubility considerations. Thus, the trends discussed below are the combined result of the solvent CT transfer and swelling ability.

As seen from Table 3.1, no polymer was obtained from AIBN, dilauryl peroxide or TBPB under either thermal (< 90 °C) or irradiation conditions. However, while BPO was also unsuccessful thermally, some polymer was obtained under UV. Dicumyl peroxide was the only initiator which provided polymer at ~ 60 °C. While H_2O_2 can initiate under UV[38] it generated no polymer at 25 °C. Finally, TBPO decomposes thermally or under UV with the formation of methyl radicals which are reactive enough to add to VDF even at ambient temperatures, and was the most efficient of the series. Dialkyl peroxides have quite a long half lifetime (*e.g.* $t_{1/2,TBPO}^{90°C}$ = 543 h)[30], and thus their rt thermal dissociation is negligible. Therefore, any possible rt initiation can only be due to the UV-induced decomposition.

Table 3.1 Free Radical VDF Polymerizations and Solvent Effect.

Ex #	*Initiator*	*[VDF]/ [I]*	*Solvent*	*Temp (°C)*	M_n	*PDI*	*Time (Hrs)*	*Conv %*
1	AIBN	100/1	ACN	60	-	-	15	0
2	AIBN	100/1	ACN	60	-	-	19	0
3	AIBN	20/1	ACN	60	-	-	72	0
4	AIBN	40/1	Diox	60	-	-	18	0
5[a]	AIBN	25/1	ACN	25	-	-	40	0
6[b]	AIBN	20/1	Diox	25	-	-	20	0
7	BPO	20/1	ACN	60	-	-	72	0
8	BPO	100/1	ACN	80	-	-	14	0
9	BPO	100/1	ACN	80	-	-	24	0
10	BPO	100/1	ACN	90	-	-	27	0
11	BPO	10/1	ACN	90	-	-	24	0
12	BPO	100/1	ACN	90	-	-	14	0
13	BPO	20/1	ACN	90	-	-	20	0
14	BPO	100/1	ACN	90	-	-	3	0
15	BPO	50/1	ACN	90	-	-	4	0
16	BPO	100/1	ACN	90	-	-	14	0
17[b]	BPO	20/1	ACN	25	3,265	1.57	20	15
18	DCPO	50/1	ACN	60	3,092	1.14	16	7
19	DLPO	20/1	ACN	90	-		20	0
20[b]	DLPO	20/1	ACN	25	-		20	3
21	H_2O_2	25/1	ACN	25	-		14	0
22	H_2O_2	100/1	ACN	25	-		27	0
23	TBPB	20/1	ACN	90	-		20	0
24[b]	TBPB	20/1	ACN	25	-		20	3
25[a]	TBPO	25/1	BzN	25	-		48	0
26[a]	TBPO	20/1	ACN	25	17,187	1.55	15	37
27[a]	TBPO	25/1	DMAc	25	1,002	1.42	40	10
28[a]	TBPO	25/1	DMF	25	804	1.31	40	17
29[a]	TBPO	25/1	NMP	25	517	1.74	40	17
30[a]	TBPO	25/1	Py	25	-	-	38	0
31[b]	TBPO	25/1	ACN	25	6,300	1.91	22	33
32[b]	TBPO	10/1	ACN	25	-	-	23	47
33[b]	TBPO	20/1	ACN	25	7,074	2.31	20	34
34[b]	TBPO	20/1	BzN	25	-	-	15	0
35[b]	TBPO	20/1	Diox	25	-	-	17	0
36[b]	TBPO	25/1	DMSO	25	-	-	48	0
37[b]	TBPO	25/1	TFT	25	-	-	48	0
38[b]	TBPO	25/1	THF	25	-	-	48	0
39[b]	TBPO	25/1	Tol	25	-	-	48	0

[a)] Oriel Xenon arc lamp [b)] High Intensity UV Lamp 365 nm.

The rest of the experiments evaluated the solvent effect and indicated that unfortunately, the good PVDF solvents (DMF, DMAC) are not necessarily satisfactory for polymerizations, due to their high chain transfer ability. As such, ACN reactions are in fact heterogeneous, precipitation polymerizations. Thus, the prospect of VDF homogeneous solution polymerization without chain transfer under radical conditions appears unlikely.

The effect of UV irradiation on the polymerization kinetics was investigated previously. It was determined that indeed no polymerizations occurs when the UV lamps were switched off, and would continue when turned back on thus under continuous UV irradiation (TBPO), conversion increases with reaction time. Similarly, for the same total reaction time, conversion increases with UV exposure time Thus, as expected, an uninterrupted increase in conversion is observed under continuous irradiation. By contrast, no conversion increase occurs at longer reaction times in the absence of UV irradiation. This indicates that UV irradiation is necessary for the continuous generation of peroxide derived radicals, which support the polymerization.

Having evaluated the conventional VDF-FRP in glass tubes at rt, we then attempted a transition metal mediated radical initiation approach. Similarly to the results we have previously observed with styrene and dienes,[27-34] we expected the VDF polymerization to follow the mechanism outlined in Scheme 3.1. As such, the Zn reduction of Cp_2TiCl_2 occurs readily in dioxane and in many polar solvents to generate $Cp_2Ti(III)Cl$ (eq. 1). Subsequent radical ring opening of epoxides (RRO, eq. 2,3), single electron transfer reduction of aldehydes (eq. 4), halide abstraction (eq. 5) or redox reactions with peroxides (eq. 6, 7) provide radical species which add to alkenes, thereby initiating radical polymerizations. Additionally, polymerization control (eq. 8), can be afforded by the reversible termination of the growing chains with a second equivalent of $Cp_2Ti(III)Cl$ *via* a combination of DC and DT mechanisms (eqs. 9, 10).

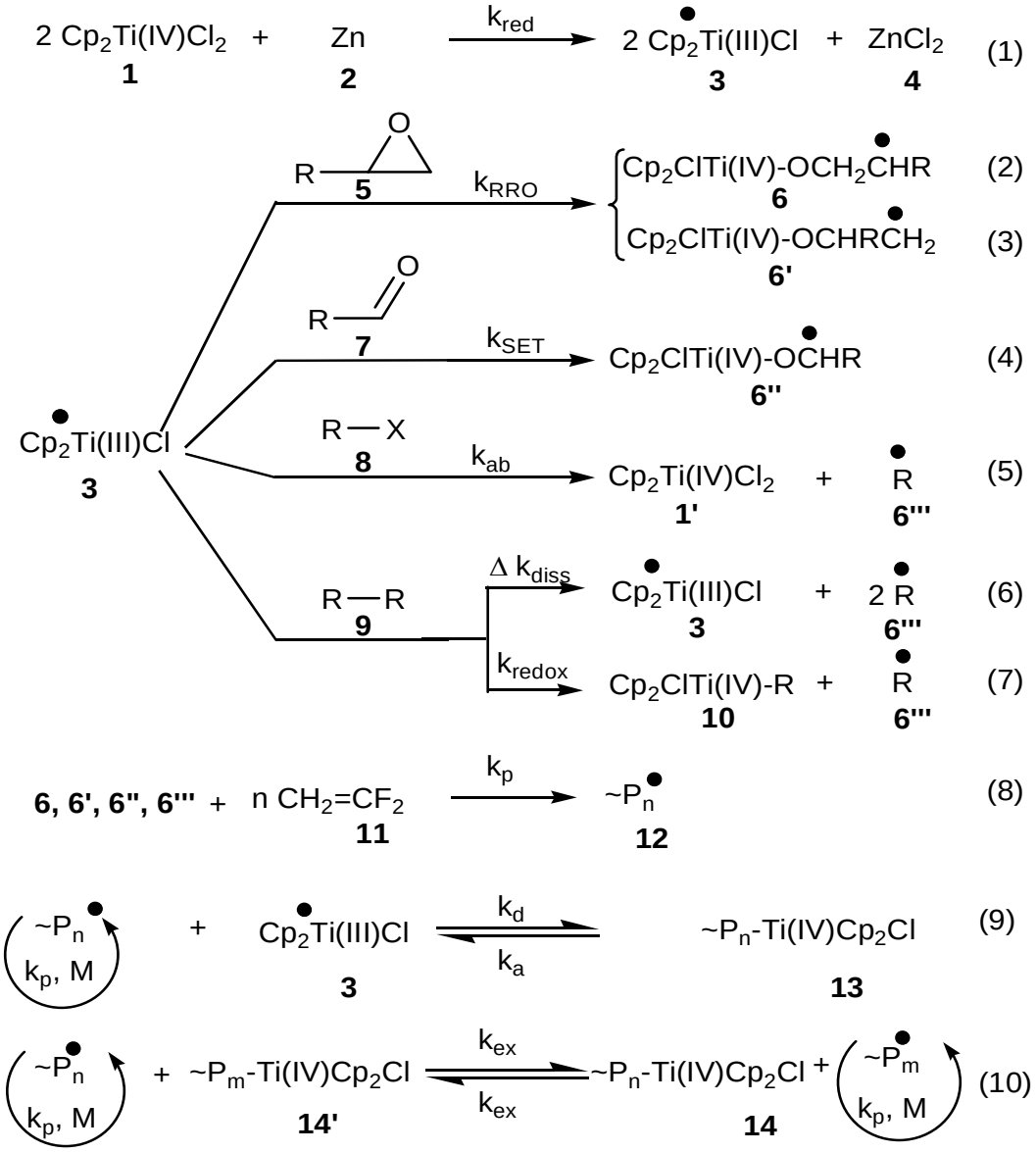

Scheme 3.1. Cp_2TiCl-mediated VDF polymerization mechanism.

Table 3.2. Cp_2TiCl-Mediated Initiating Systems					
Exp	*[VDF]/[I]/ [Cp_2TiCl_2]/[Zn]*	*[I]*	*Solvent*	*Temp °C*	*Time (h)*
1	7.25/0/1/1	-	DMC	50	24
2	0/0/1/0.75	-	DMC	25	24
3	3/0/1/0.6	-	Diox	25	24
4[a,b]	5/0/1/0	-	DMC	40	42
5	100/1/2/4	BPO	ACN	60	14
6	100/1/1/1	BPO	ACN	90	24
7[c]	20/1/.05/.25	TBPB	anisole	25	40
8[c]	100/1/.25/.25	TBPO	Diox	25	21
9[c]	100/1/1/1	TBPO	Diox	25	27
10[c]	100/1/1.5/1.5	TBPO	Diox	25	99
11	100/1/2/4	TBPO	DMF	110	40
12	100/1/1.9/0.95	DEO	Diox	25	18
13	100/1/2/2	BDE	DMF	130	62
14	50/1/2/1.1	BDE	Acetone	40	60
15	200/1/1/0.75	MPEG	Diox	60	48
16	100/1/1/2	BA	DMF	150	62
17	100/1/1/0.6	BA	ACN	90	48
18	50/1/1/0.6	MBSC	ACN	60	12
19	50/1/0.1/1	MBSC	Anisole	25	164
20	100/1/2/1	DBD	ACN	25	20
21	25/1/1/0.6	CCl_4	DMC	25	43
22	100/1/3/6	CCl_4	DMC	40	21
23	50/1/0.3/5	CCl_4	DMC	40	48
24	10/1/0.015/0.05	CCl_4	DMC	50	43
25	50/1/3/1.6	CCl_4	DMC	60	46
26	50/1/3/1.5	CCl_4	DMC	60	62
27	25/1/0.02/1	CCl_3Br	Acetone	40	60
28[a,d]	50/1/1/0	CH_3I	ACN	25	24
29	50/1/0.1/2	BEB	Diox	25	25
30	50/1/2/1.1	DCPfO	DMC	50	24
31	50/1/0.05/0.6	PFBI	DMF	25	24
32	50/1/1/0.6	PFBI	Diox	25	24
33	25/1/0.2/0.4	PFBI	MeOH	25	24
34	25/1/0.1/1	PFBI	H2O	40	44
35	25/1/0.1/1	PFBI	CL	40	44
36	50/1/2/1.1	PFBI	Acetone	40	60
37[b]	50/1/0.2/1	PFBI	DMC	40	72
38	50/1/0.2/0.1	PFBI	DMC	40	48

[a)] no reducing reagent, [b)]30W CFL [c)] High Intensity UV Lamp 365nm, [d)] Oriel Xe Arc Lamp.

Table 3.2. Cp_2TiCl-Mediated Initiating Systems, continued.					
Exp	*[VDF]/[I]/ [Cp_2TiCl_2]/[Zn]*	*[I]*	*Solvent*	*Temp °C*	*Time (h)*
39	75/1/3/6	PFBI	DMC	40	14
40[b]	50/1/0.4/0.21	PFBI	Diglyme	40	18
41[b]	25/1/0.2/0.4	PFBI	Anisole	40	72
42	25/1/0.5/0.6	PFBI	DMC	45	48
43	25/1/0.2/0.4	PFBI	EC	45	48
44	25/1/1.1/2	PFBI	EC	45	48
45	50/1/3/1.6	PFBI	DMC	60	46
46	50/1/3/1.5	PFBI	DMC	60	62
47[a,b]	50/1/0.1/0	PBFI	DMC	40	42
48	50/1/0.1/0.1	PFIpI	DMAC	25	120
49[c]	50/1/0.1/0.6	PFIpI	DMAC	25	96
50	25/1/0.1/1	PFIpI	ACN/Diox	25	63

[a)] no reducing reagent, [b)]30W CFL [c)] High Intensity UV Lamp 365nm, [d)] Oriel Xe Arc Lamp.

Selected examples of the attempts at Cp_2TiCl-mediated radical initiation of VDF from four different classes of initiators (epoxides, aldehydes, halides and peroxides) are presented in Table 3.2. However, in none of these experiments was polymer obtained. Nonetheless, the corresponding radicals can clearly be produced even at r, as evidenced by the green to red color change upon the injection of their precursor into a Cp_2TiCl solution, and by their initiation of the polymerization of styrene and dienes. [27-35] Additionally, the radical polymerization of VDF can proceed at rt as seen above with UV or with other radial generation systems.[16,36]

Hence, what are the reasons for the lack of polymerization? Possible explanations include the absence of a solvent compatible with both VDF polymerizations and Cp_2TiCl, the inability of the initiator radicals to add to VDF at rt, as well as potential organometallic side reactions such as Zn insertion into the carbon halide bond of the initiator[47] or the irreversible deactivation of the chain ends and of the catalyst *via* either β–H (Cp_2TiClH) or β-F (Cp_2TiClF) elimination, assuming initiation does occur. Indeed, in the presence of Zn, perfluoroalkyl iodides may add to the carbonyls of alkyl carbonates such as DMC *via* the intermediary formation of a Grignard-like

R_F-Zn-I species.[47] However, Cp_2TiCl does not abstract F from R_F-X, but mediates the addition $R_F^{\bullet}$ to regular alkenes such as isoprene.[22]

While one can argue that perhaps the radicals derived from aldehydes and sulfonyl or benzyl halides may not be reactive enough for rt initiation, the primary radicals derived from epoxide RRO and those obtained from CH_3-I, CCl_4 and R_F-I are definitely capable of initiation.[36] Thus, the dominant reason is most likely, the solvent effect.

In solution, Cp_2TiCl consist of an equilibrium mixture of the monomer with the dominating $Cp_2Ti(\mu\text{-}Cl)_2TiCp_2$ chloride-bridged dimer,[48] and the relative reactivity of these two species is solvent dependent. While polar, coordinating solvents readily dissociate the dimer,[48a] aromatic, less polar solvents have a lower ability to promote reduction and dimer dissociation. However, too strong of a solvent coordination may also translate in a poor polymerization performance due to blocking of the Ti active site. Amide-based solvents such as DMF, DMAC and NMP and strong nitrogen donors like pyridine and ACN may act as ligands that coordinate $Cp_2TiCl^{\bullet}$ too strongly and irreversibly, or similarly to the single electron transfer reduction of aldehydes and ketones, could directly deactivate the catalyst *via* the single electron transfer reduction and addition of $Cp_2TiCl^{\bullet}$ to the C=O, [25,28] S=O, [49] or CN,[50] groups. Additionally, $Cp_2TiCl^{\bullet}$ can transfer H from water and alcohols and would thus act as CT agents in a polymerization in such -OH solvents. [51]

Under these conditions, for styrene polymerizations,[27d] the best results were obtained with aliphatic ethers such as THF, dioxane and diglyme which coordinate reversibly, and easily stabilize $Cp_2Ti(III)Cl$[48]. The solvent suitability in terms of PDI was: dioxane $\underline{\geq}$ THF > diglyme > PhOMe > Ph_2O $\underline{\geq}$ bulk > toluene >> pyridine > DMF > NMP, DMAC > ethylene carbonate, acetonitrile. One can already see that the best solvents for VDF polymerizations are actually at the bottom of this list.

Thus, in retrospect the above VDF/Cp_2TiCl requirements practically disqualify all the experiments, such as those carried out in anisole, dioxane, and diglyme for VDF, and those in acetone, ACN, BN, DMC, EC, CL, TMP, H_2O and MeOH for Cp_2TiCl, with DMF, DMAC, being unsuitable for both. It appears therefore, that unfortunately, the preferred solvents for the polymerization are incompatible with the ones for the catalyst.

3.4 Conclusions

A series of typical free radical initiators such AIBN, BPO, TBPB, TBPO, DCPO, DLPO, and H_2O_2 were evaluated in the thermal or UV-mediated VDF polymerization in TFT, Py, NMP, DMAC, dioxane, THF, DMSO, BN, DMF, and toluene. Better polymerization results were obtained with initiators which generate the most reactive radicals (TBPO) in solvents that minimize chain transfer (ACN), which however, are not necessarily good PVDF solvent as well. Finally, a series of epoxides, aldehydes, halides and peroxides, known to initiate both styrene and diene polymerizations in the presence of $Cp_2TiCl^{\bullet}$, were tested as potential rt VDF initiators. However, regardless of reaction conditions, no polymer was obtained. This is most likely the combined outcome of a series of factors including lower reactivity of the initiating radicals by comparison with the propagating chain, transfer to the solvent or catalyst, low reaction temperature and of several possible organometallic side reactions. The key reason for the failure of these polymerizations is most likely the solvent effect, *i.e.* the incompatibility of solvents appropriate for Cp_2TiCl_2 reductions with those conducive of VDF polymerizations. Thus, the polar solvents that promote a fast and efficient reduction of Cp_2TiCl_2 are strong chain transfer agents towards VDF (dioxane, THF, diglyme, acetone), while solvents that limit chain transfer to $PVDF^{\bullet}$, will react with $Cp_2TiCl^{\bullet}$.

3.5 References

1 Ameduri, B. *Macromolecules*, **2010**, *43*, 10163–10184.
2. *Well-Architectured Fluoropolymers: Synthesis, Properties and Applications.* Ameduri, B.; Boutevin, B; Elsevier, **2004**.
3. Souzy, R.; Ameduri, B.; Boutevin, B. *J. Polym. Sci.: Part A: Polym. Chem.* **2004**, *42*, 5077.
4. Shi, Z.; Holdcroft, S. *Macromolecules* **2004**, *37*, 2084.
5. Guiot, J.; Ameduri, B.; Boutevin, B. *Macromolecules* **2002**, *35,* 8694.
6. Yang, Z.; Rajendran, R. G. *Angew. Chem. Int. Ed.* **2005**, *44*, 564.
7. Chambers, R. D.; Fuss, R. W.; Spink, R. C. H.; Greenhall, M. P.; Kenwright, A. M.; Batsanov, A. S.; Howard, J. A. K. *J. Chem. Soc., Perkin Trans.* **2000**, *1*,1623.
8. Souzy, R.; Ameduri, B.; Boutevin, B. *Macromol. Chem. Phys.* **2004**, *205*, 476.
9. Apostolo, M.; Arcella, V.; Storti, G.; Morbidelli, M. *Macromolecules* **1999**, *32*, 989.
10. Guiot, J.; Neouze, M. A.; Sauguet, L.; Ameduri, B.; Boutevin, B. *J. Polym. Sci.: Part A: Polym. Chem.* **2005**, *43*, 917.
11. Kostov, G.; Petrov, P. *J. Polym. Sci. Part A: Polym. Chem.* **1992**, *30*, 1083.
12. Di Lena, F.; Matyjaszewski, K. *Prog. Polym. Sci*. **2010**, *35*, 959–1021.
13. *Handbook of Radical Polymerization*; Matyjaszewski, K., Davis, T. P., Eds.; Wiley-Interscience: New York, **2002**, pp 361-462.
14. Ameduri, B. *Chem. Rev.* **2009**, *109*, 6632–6686.
15. Hansen, N.; Jankova, K.; Hvilsted, S. *Eur. Polym. J.* **2007**, *43*, 255.
16. Zhang, Z. C.; Chung, T. C. *Macromolecules*. **2006**, *39*, 5187-5189.
17. Balague, J.; Ameduri, B.; Boutevin, B.; Caporiccio, G. *J. Fluorine Chem.* **1995**, *70*, 215-223.
18. Nguyen, B. V.; Yang, Z. Y.; Burton, D. J. *J. Org. Chem.* **1998**, *63*, 2887.
19. Li, A. R.; Chen, Q. Y. *J. Fluorine Chem.* **1997**, *81(2)*, 99-101.
20. Chen, M. Y.; Yang, Z. Y.; Zhao, C. X.; Qiu, Z. M. *J. Chem. Soc. Perkin Trans. I*. **1988**, 3, 563-567.
21. (a) Metzerg, J. O.; Linker, U. *Liebigs Ann. Chem.* **1992**, *3*, 209-16. (b) Ishihara, T.; Kuroboshi, M. *Synth. Commun.* **1989**, *19(9&10)*, 1611-1617.
22. (a) Hu, C.; Qiu, Y. L. *J. Chem. Soc. Perkin Trans. 1.* **1992**, *13*, 1569. (b) Xiao, F.; Wu, F.; Yang, X.; Shen, Y.; Shi, X. *J. Fluorine Chem.* **2005**, *126*, 319. (c) Kitazume, T.; Ishikawa, N. *J. Am. Chem. Soc.* **1985**, *107*, 5186.
23. Spencer, R. P.; Schwartz, J. *Tetrahedron*, **2000**, *56*, 2103-2112.
24. Green, M. H.; Lucas, C. R. *J. Chem. Soc. Dalton Trans.* **1972**, *8*, 1000.
25. Barden, M. C.; Schwartz, J. *J. Am. Chem. Soc.* **1996**, *118*, 5484.
26. Rajanbabu, T. V.; Nugent, W. *J. Am. Chem. Soc.* **1994**, *116*, 986.
27. (a) Asandei, A. D.; Moran, I. W.; Chen, Y.; Saha, G. *J. Organomet. Chem.* **2007**, *692*, 3174-3182. (b) Asandei, A. D.; Moran, I. W.; Saha, G.; Chen, Y. *ACS Symp. Ser.* **2006**, *944*, 125. (c) Asandei, A. D.; Moran, I. W.; Saha, G.; Chen. Y. *J. Polym. Sci.: Part A: Polym. Chem.* **2006**, *44*, 2156. (d) Asandei, A. D.; Moran, I. W.; Saha, G.; Chen. Y. *J. Polym. Sci.: Part A: Polym. Chem.* **2006**, *44*, 2015. (e) Asandei, A. D.; Moran, I. W. *J. Polym. Sci.: Part A: Polym. Chem.* **2006**, *44*, 1060. (f) Asandei, A. D.; Moran, I. W. *J. Polym. Sci.: Part A: Polym. Chem.* **2005**, *43*, 6039. (g) Asandei, A. D.; Moran, I. W. *J. Polym. Sci.: Part A: Polym. Chem.* **2005**, *43*, 6028. (h) Asandei, A. D.; Moran I. W. *J. Am. Chem. Soc.* **2004**, *126*, 15932. (i) Asandei; A.D.; Moran; I.W.; Castro, M.A. *Polym. Prepr.* **2003**, *44(1)*, 829. (j) Asandei, A. D.; Chen, Y.; Saha, G.; Moran, I. W.; *Tetrahedron*, **2008**, *64,* 11831.
28. Asandei; A. D; Chen, Y. *Macromolecules* **2006**, *39*, 7549.

29. (a) Asandei, A. D.; Chen, Y. *Polym. Mater.: Sci. Eng.* **2007**, *97*, 450. (b) Asandei, A. D.; Saha, G. *Polym. Prepr.* **2007**, *48*, 272.
30. Asandei, A. D.; Saha, G. *J. Polym. Sci.: Part A: Polym. Chem.* **2006**, *44*, 1106.
31. Asandei, A. D.; Simpson, C. P.; Yu, H. S.; Adebolu, O. I.; Saha, G.; Chen, Y. *ACS Symp. Ser.* **2009**, *1024*, 149-166.
32. (a) Asandei, A. D.; Saha, G. *Polym. Prepr*. **2005**, *46(2)*, 474 (b) Asandei, A.D.; Simpson C. *Polym. Prepr*. **2008**, *49(1)*, 452. (c) Asandei, A. D.; Simpson, C. P.; Yu, H. S. *Polym. Prepr.* **2008**, *49(2)*, 73. (d) Asandei, A. D.; Adebolu, O.; Yu, H. S; Simpson, C. P.; Gilbert, M. *Polym. Prepr.* **2009**, *50(1)*, 177. (e) Asandei, A. D.; Simpson, C. P. *Polym. Prepr.* **2008**, *49(2)*, 75. (f) Asandei, A. D.; Yu, H. S; Adebolu, O.; Simpson, C. P.; Duong, O. *Polym. Mater.: Sci. Eng.* **2009**, *100*, 366. (g) Asandei, A. D.; Yu, H. S*; Polym. Prepr*. **2009**, *50(2)*, 601. (h) Asandei, A. D.; Yu, H. S; Adebolu, A. *Polym. Mater.: Sci. Eng.* **2009**, *101*, 1377. (i) Asandei, A. D.; Yu, H. S; Simpson, C. P. *Polym. Mater.: Sci. Eng.* **2009**, *101*, 1379.
33. (a) Asandei, A. D.; Yu, H. S.; Simpson, C. P. *Polym. Prepr.* **2010**, *51(1)*, 545. (b) Asandei, A. D.; Yu, H. S.; Simpson, C. P. *Polym. Mater.: Sci. Eng.* **2010**, *103*, 511. (c) Asandei, A. D.; Yu, H. S.; Simpson, C. P. *Polym. Prepr.* **2010**, *51(2)*, 584. (d) Asandei, A. D.; Yu, H. S.; Simpson, C. P. *Polym. Prepr.* **2010**, *51(2)*, 586. (e) Asandei, A. D.; Simpson, C. P.; Olumide, A.; Yu, H. S. *Polym. Mater.: Sci. Eng.* **2010**, *102*, 425. (f) Asandei, A. D.; Yu, H. S.; Simpson, C. P. *Polym. Mater.: Sci. Eng.* **2010**, *102*, 68. (g) Asandei, A. D.; Yu, H. S. *Polym. Prepr.* **2011**, *52(1)*, 415. (h) Asandei, A. D.; Yu, H. S. *Polym. Prepr.* **2011**, *52(1)*, 413. (i) Asandei, A. D.; Yu, H. S. *Polym. Mater.: Sci. Eng.* **2011**, *104*, 619. (j) Asandei, A. D.; Yu, H. S. *Polym. Mater.: Sci. Eng.* **2011**, *104*, 627. (k) Asandei, A. D.; Simpson, C. P.; Olumide, A.; Yu, H. S. *Polym. Prepr.* **2010**, *51(1)*, 553. (l) Asandei, A. D.; Simpson, C. P.; Olumide, A.; Yu, H. S. *Polym. Prepr.* **2010**, *51(1)*, 498.
34. Asandei, A. D.; Saha, G. *Macromolecules* **2006**, *39,* 8999.
35. (a) Asandei, A. D.; Saha, G. *Macromol. Rapid Commun*. **2005**, 26, 626. (b) Asandei, A. D.; Chen, Y.; Adebolu, O. I.; Simpson, C. P. *J. Polym. Sci.: Part A: Polym. Chem.* **2008**, *46*, 2869. (c) Asandei, A. D.; Chen, Y.; Adebolu, O. I.; Simpson, C. P. *Polym. Prepr.* **2008**, *49(2)*, 740.
36. Asandei, A. D.; Olumide, O. I.; Simpson, C. P. *J. Am. Chem. Soc*. **2012**, *134*, 6080-6083.
37. Haszeldine, R. N.; Steele, B. R. *J. Chem. Soc.* **1954**, 923.
38. Saint-Loup, R.; Ameduri, B. *J. Fluorine Chem*. **2002**, *116*, 27.
39. (a) Asandei, A. D.; Chen, Y.; *Polym. Mater.: Sci. Eng.* **2008**, *98*, 346. (b) Asandei, A. D.; Chen, Y. *Polym. Prepr.* **2007**, *48(2)*, 452-453. (c) Asandei, A. D.; Chen, Y. *Polym. Mater.: Sci. Eng.* **2007**, *97*, 270-271. (d) Asandei, A. D.; Chen, Y. *Polym. Prepr.* **2005**, *46(2)*, 633. (e) Asandei; A. D.; Weiss, R. A.; Moran, I. W.; Chen, Y.; Saha, G. *Polym. Prepr.* **2004**, *45(1)*, 1010. (f) Asandei, A. D.; Yu, S. H.; Adebolu, O.; Simpson, C. P.; *Polym. Prepr.* **2011**, *52(2)*, 470-471. (g) Asandei, A. D.; Simpson, C. P.; Adebolu, O.; Chen, Y. *Polym. Prepr.* **2011**, *52(2)*, 759-560. (h) Asandei, A. D.; Simpson, C. P.; Adebolu, O.; Chen, Y. *Polym. Prepr.* **2011**, *52(2)*, 728-729. (i) Asandei, A. D.; Simpson, C. P.; Adebolu, O.; Chen, Y. *Polym. Prepr.* **2011**, *52(2)*, 732-733.
40. (a) Galin, M.; Maslinkot, L. *Macromolecules* **1985**, *18*, 2192-2196. (b) Galin, J. C.; Lutringer, G.; Galin, M. *J. Appl. Polym. Sci.* **1989**, *37*, 487-498. (c) Kutringer, G.; Weill, G. *Polymer* **1991**, *32*, 877- 883. (d) Lutringer, G.; Meurer, B.; Weill, G. *Polymer* **1991**, *32*, 884-891. (e) Bottino, A.; Campanelli, G.; Munari, S.; Turturro, A. *J. Polym. Sci.: Part B: Polym. Phys.* **1988**, *26*, 785-794.
41 W. H. Lee, in *Chemistry of Nonaqueous Solvents Vol. 4,* by *J* . J. Lagowski, Ed., *Academic Press, NY, 1976*, p 167.
42. Ameduri, B.; Boutevin, B. *Top. Curr. Chem*. **1997**, *192*, 165-233.

43. Wormald, P.; Ameduri, B.; Harris, R. K.; Hazendonk, P. *Polymer* **2008**, *49*, 3629–3638.
44. Doll, W. W.; Lando, J. B. J. Appl. Polym. Sci. **1970**, *14*, 1767-73.
45. Russo, S.; Behari, K.; Chengji, S.; Pianca, M.; Barchiesi, E.; Moggi, G. *Polymer* 34, **1993**, *22*, 4777-4781
46. Duc, M.; Ameduri, B.; Boutevin, B.; Kharroubi, M.; Sage, J. M. *Macromol. Chem. Phys.* **1998,** *199*, 1271–1289.
47. (a) Benefice, S.; Blancou, H.; Commeyras, A. *Tetrahedron*. **1984**, *40(9)*, 1541. (b) Yang, Z. Y.; Burton, D. J. *J. Org. Chem.* **1991**, *56*, 1037-1041.
48. (a) Spencer, R. P.; Schwartz, J. *Tetrahedron*. **2000**, *56*, 2103. (b) Jungst, R.; Sekutowski, D.; Davis, J. Luly, M.; Stucky, *J. Inorg. Chem*. **1977**, *16*, 1645. (c) Enemaerke, R. J.; Larsen, J.; Skrydstrup, T.; Daasbjerg, K. *J. Am. Chem. Soc*. **2004**, *126*, 7853. (d) Enemaerke, R. J.; Larsen, J.; Skrydstrup, T.; Daasbjerg, K. *Organometallics*. **2004**, *23*, 1866. (e) Enemaerke, R.; Larsen, J.; Hjollund, G. H.; Skrydstrup, T.; Daasbjerg, K. *Organometallics*. **2005**, *24*, 1252-1262.
49. Yoo, B. W.; Choi, K. H.; Lee, S. J.; Yoon, C. M.; Kim, S. H.; Kim, J. H. *Synth Commun.* **2002**, *32*, 63.
50. Fernandez-Mateos, A.; Madrazo, S. E.; Teijon, P. H.; Gonzalez, R. R. *J. Org. Chem.* **2009**, *74*, 3913–3918.
51. Paradas, M.; Campana, A. G.; Marcos, M. L.; Justicia, J.; Haidour, A.; Robles, R.; Cardenas, D. J.; Oltra, J. E.; Cuerva, J. M. *Dalton Trans.* **2010**, *39*, 8796–8800.

Chapter 4: Metal Carbonyl Photomediated Iodine Degenerative Transfer Controlled Radical Polymerization of Vinylidene Fluoride and Synthesis of Well Defined Block Copolymers.

A series of transition metal carbonyl complexes ($Re_2(CO)_{10}$, $Mn_2(CO)_{10}$, $Cp_2W_2(CO)_6$, $Cp_2Mo_2(CO)_6$, $Fe(CO)_5$, $Cp_2Fe_2(CO)_4$, $Cp^*_2Cr_2(CO)_4$, $Co_2(CO)_8$ $Mo(CO)_6$, $Cr(CO)_6$) in conjunction with alkyl or perfluoroalkyl halides ($CH_3(CH_2)_5Cl$, $CH_3(CH_2)_5Br$, $CH_3(CH_2)_5I$, CH_3I, CCl_4, CCl_3Br, $CF_3(CF_2)_3I$ $Cl(CF_2)_8Cl$, $Br(CF_2)_6Br$, and $I(CF_2)_6I$) were evaluated in the initiation and respectively control of vinylidene fluoride (VDF) polymerization. A free radical polymerization (FRP) process was observed for alkyl halides ($CH_3(CH_2)_5Br$, $CH_3(CH_2)_5I$, CH_3I, CCl_4, CCl_3Br, $Br(CF_2)_6Br$), with $Br(CF_2)_6Br$ exhibiting a decrease in molecular weight with respect to conversion, while perfluoroalkyl iodides (R_FI = $CF_3(CF_2)_3I$, $I(CF_2)_6I$) mediated the VDF controlled radical polymerization (CRP) via iodine degenerative transfer (IDT). The fastest rates were observed with R_FI used in conjunction with $Re_2(CO)_{10}$ and $Mn_2(CO)_{10}$. The effect of various [VDF]/[PFBI]/[$Mn_2(CO)_{10}$], [VDF]/[solvent], and [PFBI]/[$Mn_2(CO)_{10}$] ratios were evaluated and confirmed DMC was indeed the superior solvent, while the [VDF]/[solvent] ratio had little effect on the polymerization rate. A selection of the metal complexes were then evaluated in the PVDF-I activation, where $Re_2(CO)_{10}$, $Mn_2(CO)_{10}$, $Cp_2W_2(CO)_6$, $Cp_2Mo_2(CO)_6$, and $Cp_2Fe_2(CO)_4$ provided complete activation of both PVDF-CH_2-CF_2-I and PVDF-CF_2-CH_2-I chain ends and were subsequently used towards the synthesis of well-defined block copolymers with vinyl acetate, t-butyl acrylate, methyl methacrylate, isoprene, styrene, and acrylonitrile, from their respective metal carbonyls.

4.1 Introduction

Fluorinated (co)polymers constitute a fundamental class of specialty materials endowed with a wide range of high-end applications[1] demanding their precise synthesis. However, while controlled radical polymerizations (CRPs) have undergone remarkable developments for typical vinyl monomers such as (meth)acrylates or styrene,[2,3] they remain ineffective for highly reactive, gaseous main chain fluorinated monomers (FMs: CH_2=CF_2, vinylidene fluoride, (VDF), CF_2=CF(CF_3), CF_2=CF_2, etc.). As such, due to the current lack of suitable chemistry, the synthesis and fundamental understanding of the properties and applications of well-defined complex fluoropolymer architectures, lag considerably behind those associated with conventional alkenes. Moreover, since metal mediated alkyl halide radical initiation and FM-CRP was not available until very recently,[4] industrial FM-CRP is still accomplished at high temperatures and pressures with the oldest CRP method,[5] the iodine degenerative transfer[1,3,6,7] using perfluorinated alkyl iodides (R_F-I)[8-11] chain transfer agents (CTAs),[6] and peroxide free radical initiators.[1,6,9]

However, IDT always demands a free radical source (*e.g.* ^{t}butyl peroxide)[1], as *direct* metal catalyzed initiation from R_F-I or any other R-X is not available. Indeed, while electrophilic $R_F^{\bullet}$ radicals add readily to alkenes with metal catalysis,[12] their addition to electrophilic, fluorinated substrates (FMs) at room temperature (rt) is absent. Thus, even though VDF polymerizes at rt,[13] only low VDF oligomers result even at T > 100 °C from transition metal complexes and polyhalides.[1,7,14] Moreover, by contrast to the CRP of acrylates or styrene, VDF-IDT produces two different halide chain ends, P_n-CH_2-CF_2-I and P_m-CF_2-CH_2-I having dissimilar reactivity.[4,10] Consequently, surpassing the limitations of the current chemistry by providing the ability to initiate directly from halides, mediate rt FM-CRP and activate both PVDF-I termini, is an essential

requirement towards the synthesis of well-defined, architecturally rich fluoropolymers, which are otherwise unavailable or inevitably end up as inseparable mixtures.

Accordingly, the development of FM-CRP, the synthesis of elaborate architectures and the mapping the resulting fluoromaterials remain worthy endeavors.[1,5,6-10,15,16] Such polymerizations are quite challenging, as all FMs are gases (b_p^{VDF} = -83 °C) and typical reactions are performed at T ~ 100-200 °C,[1] in expensive, high-pressure metal reactors. Moreover, by contrast with conventional CRPs which can be sampled even on a 1g scale, FM polymerizations kinetics involve many time-consuming, large scale, one-data-point experiments. Thus, the development of mild temperature protocols for low pressure, small-scale polymerizations in inexpensive glass tubes, would be very appropriate for fast catalyst and reaction conditions screening and amenable to photochemistry.[4]

To address the above concerns, we started to examine rt VDF-CRP.[17,4] However, none of the conventional CRP methods proved effective in glass tubes at moderate temperatures (25-60 °C), most likely due to the inability to generate radicals reactive enough to add to VDF, or to reactivate the potentially dormant PVDF-Y chain end, as well as catalyst/polymer solvent incompatibility.[18] We thus subsequently considered alternative means of radical photo-generation and set out to investigate[4] a mild, photomediated metalloradical formation,[19] using low power ($\leq$ 30 W) white light compact fluorescent bulbs.

As such, while high power UV VDF telomerizations exist,[1,6,20,21] prior to our work,[4] there were are no reports on VDF polymerizations under visible light. As VDF is a very reactive monomer, it is expected that successful rt initiators should provide highly reactive, destabilized alkyl, semifluorinated, or perfluoroalkyl radicals. Additionally, the visible light generated $L_nMt^{\bullet}$ metal radical species should be a very good halide abstractor, and, for possible catalyzed CRP, L_nMt-X should also be a very good halide donor (X = most likely iodine).

Suitable examples[19] of radically photolyzable transition metal complexes are based on $(CO)_nMt\text{-}Mt(CO)_n$ type dimers. Out of the many know examples, the following $Re(CO)_5$ > $Mn(CO)_5$ > $CpW(CO)_3$ >$CpMo(CO)_3$ > $CpFe(CO)_2$ > $Co(CO)_4$ order is available in terms of their ability to abstract halides.[22] Although $Re(CO)_5^{\bullet}$ (λ_{max} = 535-550 nm) abstracts Cl from CCl_4 ~65 times faster than $Mn(CO)_5^{\bullet}$[23] the stronger bond dissociation energy (BDE) of Re-Re[24] and the higher cost, make the relatively inexpensive $Mn_2(CO)_{10}$[25] dimer[26] the most popular reagent in the series. At room temperature, in the dark, the dimer[27] is stable, ($K_{eq} < 2.4 \times 10^{-19}$),[28] but as the Mn-Mn linkage is relatively weak (20-40 kcal/mol),[29,30,31] (and further decreased by extra ligands),[32] $Mn_2(CO)_{10}$ undergoes facile thermolysis at T > 80 °C and rt photolysis. UV irradiation promotes CO loss forming $Mn_2(CO)_9$ and $Mn(CO)_5^{\bullet}$, but near-UV and rt visible longer wavelength (λ= 366-400 nm, $\lambda_{max}^{Mn2(CO)10}$ = 324 nm)[35] provide the $Mn(CO)_5^{\bullet}$ 17e$^-$ metalloradical ($\lambda_{max}^{Mn(CO)5}$ = 780-830 nm)[33] with good quantum efficiency.[34-36]

$Mn(CO)_5^{\bullet}$ cleanly effects both hydride and halide abstraction from good RH donors [37] and respectively, from halides with moderate BDE (< 310 kJ/mol)[38] such as polyhalides[38] (CCl_4)[39] allyl and benzyl halides,[38,39b] CH_3I,[40] I_2,[39] and, by contrast with other reagents, reacts faster with primary rather than with secondary or tertiary ones.[38] Phosphine ligands (PPh_3) depress the rates of such reactions.[41] While Mn-alkyls photolyze, they are not effective in radical reactions.[4,30b] In addition, to the best of our knowledge, there is no examples of the use $Mn_2(CO)_{10}$ for the radical activation of perfluoroalkyl halides.

Early reports have described the photo/thermal $Mn_2(CO)_{10}$ or $Re_2(CO)_{10}$ mediated polymerizations initiated *via* either H abstraction from monomer,[42] or $Mn(CO)_5^{\bullet}$ addition of the metalloradical to tetrafluoroethylene to initiate its polymerization,[43] MMA[44] block copolymerization,[45] or addition to 1,2-disubstituted acetyls and alkenes.[46] However, while preliminary polymerizations with $Mn_2(CO)_{10}$ or $Re_2(CO)_{10}$ and CCl_4[47] as well as grafting from N-

halogenated polyamides[48] were carried out in the 1960s, $Mn_2(CO)_{10}$ was only recently employed in the thermal (60-90 °C)[49] free radical polymerization of MMA or photografting of PMMA form side-chain CCl_3 groups on chitosan[50] or polystyrene-Br.[51] While the addition of Mn or Re to the VDF monomer may be possible,[52] this was deemed unlikely to occur for any of the other weaker activators, and was examined with some[4] control experiments to reveal that with Mn no polymerization occurs in the presence of the metal carbonyl without initiator. Additionally,[52] these metal carbonyls only appear to have the possibility of addition to the vinyl substrate in the absence of an easily activated halide, such as the typical examples used within this work (e.g. perfluoroalkyl halides, and CCl4), making addition of the metal carbonyls to VDF even more unlikely.

Very recently, $Mn_2(CO)_{10}$ was used as a photo-coinitiator for activated alkyl iodides,[53,54] I_2[54] or RAFT reagents,[55] in the photo IDT-CRP[1, 7] of VAc, and acrylates, styrene and alkenes where $Mn(CO)_5^\bullet$ irreversibly activates iodine terminated chains,[53]where the in-situ generated $Mn(CO)_5$-I[39] (*i.e.* Q-I) was not involved in IDT.[53] Therefore, since prior to our work,[4] there were no examples of the use $Mt_2(CO)_x$ for the radical activation of perfluoroalkyl iodides or in VDF polymerizations, we decided to investigate its suitability we decided to assess their scope and limitations as photo-coinitiators and to demonstrate such L_nMt-MtL_n photolyzable transition metal complexes afford the initiation of VDF polymerization *directly* from a variety of regular and (per)fluorinated alkyl halides (Cl, Br, I) even at rt to 40 °C, thus opening up novel synthetic avenues for the photomediated synthesis of block and graft copolymers based on VDF and other fluorinated monomers. Second, we also set to kinetically explore such polymerization and investigate the possibility of L_nMt-MtL_n mediated IDT-VDF-LRP.

This system indeed enabled our recent demonstation[4] of the first examples of metal mediated, controlled (IDT-CRP), and respectively free radical (FRP) VDF polymerizations, carried

out at 40 °C, in low pressure glass tubes, and using $Mn_2(CO)_{10}$[4,56] as a visible light photoactivator in conjunction with R_FIs and respectively, with a wide variety of alkyl halides. Moreover, $Mn_2(CO)_{10}$ afforded the complete activation of both -CH_2-CF_2-I and -CF_2-CH_2-I PVDF chain ends, towards the synthesis of the first examples of well-defined PVDF block copolymers with a variety of monomers.[4]

An especially notable result was the $Mn_2(CO)_{10}$ activation of the models of the "bad" PVDF-I chain ends (*i.e.* $R_{H/Alk}$-CH_2-I and H-CF_2-CF_2-CH_2-I) which concurred with the demonstration of the quantitative activation of the corresponding macromolecular PVDF-CH_2-CF_2-I and PVDF-CF_2-CH_2-I chain ends towards the synthesis of well-defined block copolymers.

While inactivated R_{alk}-I alkyl iodides could successfully generate initiating radicals in the presence of $Mn_2(CO)_{10}$, only traces of polymer were obtained with similar Br and Cl substrates. Moreover, $Mn(CO)_5$-I was not involved in the catalysis of IDT, and except for direct halide activation, the polymerization mechanism was essentially the same as conventional IDT. However, availability of initiation from even the least activated halides and IDT catalysis would be of great value in the synthesis of block or other complex fluoropolymer architectures.

Out of many formally zero valet or (+1) metal carbonyls that photolyze (visible light, laser flash, or high intensity Xe arc lamps) to metalloradicals, the following; $Re(CO)_5$ > $Mn(CO)_5$ > $CpW(CO)_3$ >$CpMo(CO)_3$ > $CpFe(CO)_2$ > $Co(CO)_4$ order is available in terms of halide abstraction ability in flash photolysis.[57,58] While some of these complexes have previously been investigated in the redox or high power UV photoinitiation of radical polymerizations,[59-65] the metal carbonyls $Mo(CO_6)$, $Cr(CO)_6$, $Mn_2(CO)_{10}$[66], and $Fe(CO)_5$[67,68] have been shown to mediate radical addition of CCl_4 and CCl_3Br to alkenes and subsequent polymerization of vinyl monomers (*ie*, Methyl methacrylate (MMA), Styrene (STY), acrylonitrile (ACyN)) *via* UV photolysis or thermally above 80°C while $Co_2(CO)_8$[66a] instead acts as an effective inhibitor preventing its use in radical

polymerizations. $Mn_2(CO)_{10}$ or $Re_2(CO)_{10}$ have also been shown to mediate polymerizations initiated by H abstraction[69], addition to tetrafluoroethylene[70], styrene, acrylonitrile, MMA[70,71], block copolymerization,[72] and alkenes.[73] Additionally, $Mn_2(CO)_{10}$, $Co_2(CO)_8$, $Fe(CO)_5$, $Mo(CO)_6$, $Cr(CO)_6$, $Re_2(CO)_{10}$ have been used as catalysts for the carbonylation of alkyl iodides with high power UV irradiation.[74] The accepted mechanism is an activation of the metal carbonyl by either homolysis of a metal-metal bond or loss of a carbonyl, which gives rise to a radical with the ability to abstract a halide from the initiator. To the best of our knowledge, aside from $Mn_2(CO)_{10}$[75], there is no available information on the radical activation under continuous low power ($\leq$ 30W) visible light irradiation of $CH_3(CH_2)_5Cl$, $CH_3(CH_2)_5Br$, $CH_3(CH_2)_5I$, CH_3I, CCl_4, CCl_3Br, $CF_3(CF_2)_3I$ $Cl(CF_2)_8Cl$, $Br(CF_2)_6Br$, and $I(CF_2)_6I$ in conjunction with $Re_2(CO)_{10}$, $Cp_2W_2(CO)_6$, $Cp_2Mo_2(CO)_6$, $Fe(CO)_5$, $Cp_2Fe_2(CO)_4$, $Cp^*_2Cr_2(CO)_4$, $Co_2(CO)_8$, $Mo(CO)_6$, or $Cr(CO)_6$.

Being that very little is known about the radical reactions of such $Mt_x(CO)_y$ under continuous low power ($\leq$30 W) visible light irradiation, we thus wondered, in addition to possible initiation and polymerization of fluorinated monomers *via* halide abstraction, if these compounds are also capable of quantitative activation of both PVDF chain ends and useful in the synthesis of more complex macromolecular structures (i.e. block, star, and graft copolymers).

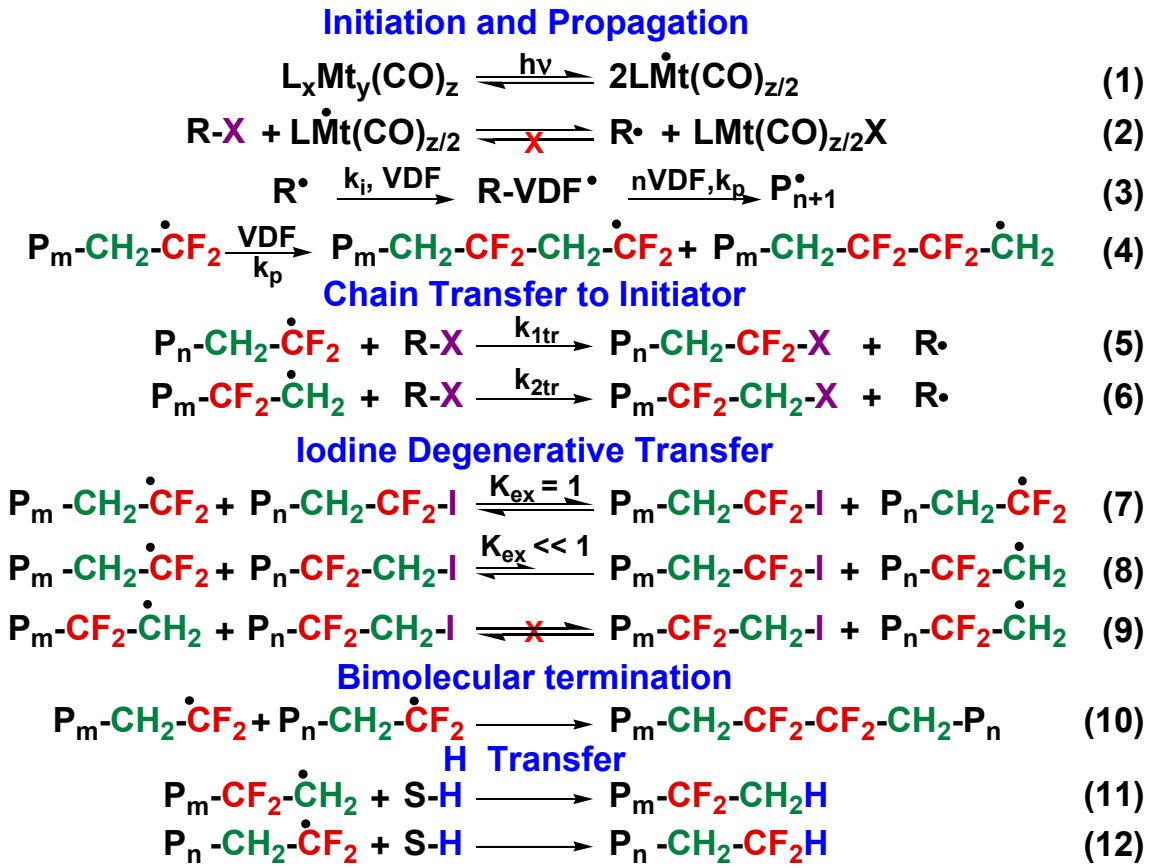

Scheme 4.1. $Mt_x(CO)_Y$-Photomediated VDF-CRP

The proposed reaction mechanism is outlined in Scheme 4.1. Following photolysis of $L_xMt_y(CO)_z$ (eq. 1), irreversible[53] halide abstraction from R-X (driven by the formation of high BDE Mt-X, X = Cl, Br, I, eq. 2)[76] affords $LMt(CO)_z$-X and R$^\bullet$, which, if reactive enough, initiates VDF polymerization (eq. 3). As VDF is asymmetrical, both 1,2- and 2,1-modes of propagation (eq. 4, head to tail HT, ~95 %[1,8,77] and respectively head to head, HH) are possible in free radical polymerizations. Thus, the polymerization is controlled by the carbon-halide bond strength, which determines the RX chain transfer (CT) ability (eqs. 5, 6).

Thus, initiators with high BDEs (alkyl iodides, $CHCl_3$, R_F-Cl), do not undergo chain transfer with PVDF$^\bullet$, require stoichiometric activation and yield PVDF with no halide chain ends. By

contrast, substrates with weak R-X bonds (e.g. R-CCl_3, R_F-X, X = Br, I) do undergo CT to the initiator (eqs. 5, 6), require reduced amounts of metal carbonyl and afford halide functionalized PVDF-X (X = Br, I).[4] As such, high CT R_F-I initiators suitable for IDT-CRPs,[7] are converted early in the process into macromolecular PVDF-I CT agents,[10] where the terminal P_m-CF_2-CH_2-I[7-11,] 2-1 unit is about 25 times less reactive towards IDT than the P_n-CH_2-CF_2-I 1,2-unit.[10]

Once all the R_F-I initiator is consumed via chain transfer, no new PVDF-I chains are generated, and the thermodynamically neutral (degenerative), reversible iodine exchange (IDT, K_{equil} = 1), between equally reactive, propagating and dormant P_n-CH_2-$CF_2^{\bullet}$ and P_m-CH_2-CF_2-I terminal 1,2-units (eq. 7), is in operation. While IDT catalysis would lead to lower PDI,[3,6] experiments revealed[4] that similarly to PVAc-IDT,[53] $Mn(CO)_5$-I is incapable of reversibly transferring iodine. Additionally, although R_F-$Mn(CO)_5$ (R_F = CH_2F, CF_2H)[29] are known, organometallic controlled radical polymerization mediated by PVDF-$Mn(CO)_5$ can be discounted based on the observed -I not -H or -$Mn(CO)_5$ chain ends. That the successful controlled radical polymerization was performed with *catalytic* not stoichiometric $Mn_2(CO)_{10}$ *vs.* R_F-I and considering the BDE order (R_F-$Mn(CO)_5$ < $(CO)_5$Mn-$Mn(CO)_5$ < R_F-I < I-$Mn(CO)_5$, *i.e.* 34,[29] 38,[76b] 48,[78] 54[76] kcal/mol), consistent with the instability of Mn alkyls under irradiation.[30,37,76b] control experiments already available for VAc polymerizations.[53] As such, in IDT, potential HH defects become dramatically suppressed[4], being trapped as P_m-CF_2-CH_2-I. I-R_F-I initiators are particularly suitable for such FM-CRPs, as bidirectional growth from difunctional propagating species,[5] in conjunction with initiator or chain end halide activation by the continuously photogenerated $LMt(CO)_{z/2}^{\bullet}$,[77] (eq. 2) help compensate for termination by radical coupling,[5] and maintain a steady state radical concentration.

Nonetheless, due to the much stronger -CH_2-I bond, the cross-IDT between the 1,2- and 2,1-units (eq. 8) is shifted towards the irreversible buildup of P_n-CF_2-CH_2-I chain ends, whereas the

IDT of the 2,1- terminal units is virtually inexistent (eq. 9).[9-10] We had previously shown[4] that the -CH_2-CF_2-I termini decreases and unreactive -CF_2-CH_2-I species accumulate with conversion and contribute to PDI broadening,[10,11,53] although the total (-CH_2-CF_2-I + -CF_2-CH_2-I) iodine functionality remains >90%, which is satisfactory for block copolymer synthesis, if both halide chain ends can be activated completely. Furthermore to expand the list of viable metal carbonyl compounds suitable for this type of chemistry, a series various carbonyl compounds were examined in their ability to initiate polymerization from various R-X (Cl,Br,I) substrates. Additionally each representative metal carbonyl was examined for its ability to activate the PVDF-I terminal units. As such, any catalyst that was shown to completely and cleanly activate both -CH_2-CF_2-I and -CF_2-CH_2-I iodine terminated polymer chain ends was subsequently used in the synthesis of block copolymers.

4.2 Experimental

4.2.1 Materials.

Manganese carbonyl ($Mn_2(CO)_{10}$), rhenium carbonyl ($Re_2(CO)_{10}$), cyclopentadienyl molybdenum tricarbonyl dimer ($Cp_2Mo_2(CO)_6$), iron pentacarbonyl ($Fe(CO)_5$), cyclopentadienyl iron dicarbonyl dimer ($Cp_2Fe_2(CO)_4$), pentamethylcyclopentadienyl chromium dicarbonyl dimer ($Cp^*_2Cr_2(CO)_4$), molybdenum hexacarbonyl ($Mo(CO)_6$), chromium hexacarbonyl ($Cr(CO)_6$) (all from *Strem Chemicals*, $\geq$98%). 1,8-dichloroperfluorooctane (DCPFO, $Cl(CF_2)_8Cl$), 1,6-dibromododecafluoro hexane (DBPFH, $Br(CF_2)_6Br$), vinylidene fluoride (VDF,99.9%), 1-iodononafluorobutane (perfluorobutyl iodide, PFBI, 98%), 1,6-diiododododecafluorohexane (DIPFH, $I(CF_2)_6I$ 98%), methyl 2-(trifluoromethyl)acrylate (MTFMA, 97%) and 2,2,2-trifluoroethyl methacrylate (TFEMA, 99%) (all from *Synquest Laboratories*), 4-methoxybenzenesulfonyl chloride (MBSC, 99%), iodoform (CHI_3 99+%), N,N'-dimethylacetamide, (DMAc, 99%), vinyl

acetate (VAc, 99+%), acrylonitrile (AN, 99+%), styrene (Sty, 99%), methyl acrylate (MA, 99%), cyclopentadienyl tungsten tricarbonyl dimer ($Cp_2W_2(CO)_6$, 97%) (all from *Acros Organics*); iodomethane (CH_3I, ReagentPlus, 99.5%), bromotrichloromethane ($BrCCl_3$, 99%), 1-Iodohexane ($CH_3(CH_2)_5I$, 98+), acetonitrile (ACN, 99%), 1H,1H,7H-dodecafluoroheptyl acrylate (95%), dimethyl carbonate (DMC, ≥ 99% anhydrous), methanol (MeOH, 99%), 2-Methyl-1,3-butadiene (Isoprene, Iso, ≥99%) cobalt carbonyl ($Co_2(CO)_8$, >90%), 1-chlorohexane ($CH_3(CH_2)_5Cl$, 99%) 1-bromohexane ($CH_3(CH_2)_5Br$, 98%) (all from *Sigma-Aldrich*); vinyl chloride (≥99.5%) (all from Fluka); 1,10-diiododecane (97%), carbon tetrachloride (CCl_4), N,N'-Dimethylformamide (DMF, 99.9%), diethylether (anhydrous, 99%), (all from *Fisher Scientific*); DMSO-d_6, acetone-d_6 (Cambridge Isotope Laboratories, Inc., D, 99.9%), all were used as received. Mn(CO)-I was synthesized by reaction of $Mn_2(CO)_{10}$ with I2 in DMC, at 75C for 24hours, followed by purification via successive sublimations.

4.2.2 Techniques.

^{1}H NMR (500 MHz) and ^{19}F-NMR (400 MHz) spectra were recorded on a Bruker DRX-500 and respectively on a Bruker DRX-400 at 24 ^{0}C in acetone-d_6 typically between 32-128 scans. 2D-$^{19}F\{^1H\}$,-Heteronuclear correlation (HETCOR) spectra were recorded on a Bruker DRX-400 at 24 ^{0}C with a scan set of 16x256 using typical Bruker pulse sequences for HETCOR. GPC analyses were performed on a Waters gel permeation chromatograph equipped with a Waters 2414 differential refractometer and a Jordi 2 mixed bed columns setup at 80^{0}C. DMAc (Fisher, 99.9% HPLC grade) was used as eluent at a flow rate of 1 mL/min. Number-average (M_n) and weight-average molecular weights (M_w) were determined from calibration plots constructed with polymethylmethacrylate standards. All reported polydispersities are those of water precipitated samples. While narrower PDIs could be obtained by MeOH precipitation, this may also lead to partial fractionation, especially for lower molecular weight samples.

4.2.3 Polymerization.

In a typical reaction, a 35-mL Ace Glass 8648 # 15 Ace-Thread pressure tube equipped with a bushing, and plunger valve with two O-rings and containing a magnetic stir bar, $Mn_2(CO)_{10}$, (53.6 mg, 0.14 mmol) and solvent (*e.g.* DMC, 3 mL) was degassed with He and placed in a liquid nitrogen bath. Note that it is important to use He for degassing, as N_2 or Ar would actually condense in the tube in a liquid nitrogen bath. The tube was subsequently opened, and the initiator (*e.g.* CF_3-$(CF_2)_3$-I (PFBI), 0.12 mL, 0.69 mmol) was added, followed by the condensation of VDF (1.1 g, 17.2 mmol), directly into the tube, which was then re-degassed with He. The amount of condensed VDF was determined by weighing the closed tube before and after the addition of the monomer. The tube was then placed in behind a plastic shield, in a thermostated oil bath illuminated with a commercial GE Helical 26 W fluorescent white light Hg spiral bulb, from about 2-4 cm. For polymerization kinetics, identical reactions were set up simultaneously and stopped at different polymerization times. At the end of the reaction, the tube was carefully placed in liquid nitrogen, slowly opened behind the shield, and allowed to thaw to room temperature in the hood, with the concomitant release of unreacted VDF. The contents were poured in water, filtered and dried. The polymer was than dissolved in DMAC, and the residual inorganics (which may interfere with the NMR signals) were removed by flash column chromatography. The polymer was finally precipitated in water, filtered and dried. While precipitation in MeOH is feasible, it will also lead to fractionation and narrowing of the polydispersity by about 0.2, especially on lower molecular weight samples. Thus, all reported GPC results are from water precipitation. The monomer conversion was determined as the ratio of the differences of the tube weight before and after the reaction and respectively before and after VDF charging (*i.e.* $c = (Wt_{\text{after VDF condensation}} - Wt_{\text{after VDF release}})/(Wt_{\text{after VDF condensation}} - Wt_{\text{before VDF}}$

$_{addition}$), as well as the ratio of the dry polymer to the condensed VDF. Both procedures gave conversions within < 5% of each other.

4.2.4 Synthesis of PVDF Block Copolymers.

A Schlenk tube containing a DMAC solution of I-PVDF-I (I-PVDF-I, M_n = 2,500, PDI = 1.34, with a total halide chain end functionality of F = 95% ($F_{1,Pn\text{-}CH2\text{-}CF2\text{-}I}$ = 0.64 and $F_{2,Pm\text{-}CF2\text{-}CH2\text{-}I}$ = 0.31, 100 mg, 0.05 mmol in 2 mL of DMAC), a second monomer (*e.g.* styrene, 215 mg, 2.1 mmol) and $Mn_2(CO)_{10}$ (36 mg, 0.1 mmol) was degassed under Ar then heated to 110 ^oC under visible light irradiation for 5 h. The solution was precipitated in MeOH, filtered and dried. M_n = 14,500, PDI = 2.25 conv. = 67%, and composition, VDF/St = 30/70.

PVDF-*b*-TFEMA: A Schlenk tube containing a DMAC solution of CF_3-PVDF-I (M_n = 1,400, PDI = 1.81, with a total halide chain end functionality of F = 96% ($F_{1,Pn\text{-}CH2\text{-}CF2\text{-}I}$ = 0.38 and $F_{2,Pm\text{-}CF2\text{-}CH2\text{-}I}$ = 0.58, 33 mg, 0.02 mmol in 2 mL of DMAC), 2,2,2-trifluoroethyl methacrylate (TFEMA, 296 mg, 1.8 mmol) and $Mn_2(CO)_{10}$ (9.2 mg, 0.02 mmol) was degassed under Ar then heated to 60 ^oC in a thermostated oil bath, illuminated with a commercial GE Helical 26 W fluorescent white light Hg spiral bulb, from about 2-4 cm for 18h. The solution was precipitated in MeOH, filtered and dried to provide PVDF-*b*-PTFEMA, M_n = 6,500 PDI = 2.02, conversion = 65%, composition, VDF/TFEMA = 60/40.

PVDF-*b*-MTFMA: A Schlenk tube containing a DMAC solution of CF_3-PVDF-I (M_n = 1,400, PDI = 1.81, with a total halide chain end functionality of F = 96% ($F_{1,Pn\text{-}CH2\text{-}CF2\text{-}I}$ = 0.38 and $F_{2,Pm\text{-}CF2\text{-}CH2\text{-}I}$ = 0.58, 15 mg, 0.01 mmol in 2 mL of DMAC), methyl 2-(trifluoromethyl)acrylate (MTFMA, 126 mg, 0.8 mmol) and $Mn_2(CO)_{10}$ (4.3 mg, 0.01 mmol) was degassed under Ar then heated to 60 ^oC in a thermostated oil bath, illuminated with a commercial GE Helical 26 W fluorescent white light Hg spiral bulb, from about 2-4 cm for 18h. The solution was precipitated in MeOH, filtered and

dried to provide PBDF-*b*-PMTFMA, M_n = 2,500, PDI = 1.5 conversion = 30%, and composition, VDF/MTFMA = 75/25.

4.3 Results and Discussion

4.3.1 Effect of catalyst and initiator on the photo-IDT VDF-CRP.

During the course of our work[4] with $Mn_2(CO)_{10}$ we investigated over 40 solvents while highlighting dimethyl carbonate (DMC) as a particularly suitable VDF-CRP media,[4] with a polymerization temperature of 40°C as a reasonable balance between reaction rate and pressure. Additionally evaluated were a wide variety of over 50 halide structures, in order to determine the ones capable of affording VDF initiation at or around rt.[4] As such, no initiation occurred from I_2, ^tBu-I, CH_3-SO_2Cl, CH_3O-Ph-SO_2Cl, CH_2Cl_2, CH_2I_2, $CHCl_2$-$CHCl_2$, $CHBr_3$, CHI_3, CBr_4, CH_2=CH-CH_2-Cl/Br/I, Ph-CH_2-Cl/Br/I, Ph-CH(CH_3)-Br, Ph(CH_2-Br/I)$_2$, CH_3-CH(CN)-Br, CH_2(CN)-I, $(CH_3)_2$C(COOEt)-Br/I, NBS and I-Ph-O-CH_3. As $Mn(CO)_5^\bullet$ has a very high halide affinity,[56] abstraction is available in all cases. Thus, the lack of initiation resulted from the higher relative stability of the corresponding radicals by comparison with that of the propagating PVDF$^\bullet$ radicals, which impeded their addition to VDF at moderate temperatures.

By contrast, reactive alkyl, polyhalide, as well as semi- and perfluorinated halide counterparts of the above structures *i.e.* $CHCl_3$, CCl_4, CCl_3-CCl_3, $CF_3(CF_2)_2CO$-Cl, CF_3-SO_2-Cl, Cl-CF_2-CClF-Cl, Cl-$(CF_2)_8$-Cl, -$(CF_2$-$CFCl)_n$-, CCl_3-Br, EtOOC-CF_2-Br, Br-$(CH_2)_{10}$-Br, Br-CF_2-CH_2-CF_2-Br, Br-$(CF_2)_4$-Br, CH_3-I, $CH_3(CH_2)_5$-I, I-$(CH_2)_{4,10}$-I, C_6F_5-CF_2-I, H-CF_2-CF_2-CH_2-I, EtOOC-CF_2-I, Cl-CF_2-CFCl-I, CF_3-I, CF_3CF_2-I, $(CF_3)_2$CF-I, $(CF_3)_3$C-I, $CF_3(CF_2)_3$-I and I-$(CF_2)_{4,6}$-I, all led to polymer formation, where R_F-I also afforded VDF-IDT-CRP.[4]

While the known trends are based on high power laser flash photolysis, little is known about the radical reactions of $Mt_x(CO)_y$ under continuous low power ($\leq$30W) visible light irradiation. Thus, in addition to $Mn_2(CO)_{10}$, evaluated were an extended set of commercially available

monomeric and dimeric metal carbonyls such as $Re_2(CO)_{10}$, $Cp_2W_2(CO)_6$, $Mo(CO)_6$, $Cp_2Mo_2(CO)_6$, $Fe(CO)_5$, $Cp_2Fe_2(CO)_4$, $Cr(CO)_6$, $Cp^*_2Cr_2(CO)_4$ and $Co_2(CO)_8$, in conjunction with a representative set of alkyl or perfluoroalkyl halides ($CH_3(CH_2)_5Cl$, $CH_3(CH_2)_5Br$, $CH_3(CH_2)_5I$, CH_3I, CCl_4, CCl_3Br, $CF_3(CF_2)_3$-I, Cl-$(CF_2)_8$-Cl, Br-$(CF_2)_6$-Br, I-$(CF_2)_6$-I) as VDF initiators. While $Mo(CO)_6$, $Fe(CO)_5$, $Cr(CO)_6$ are monomeric in the dark, irradiation leads to CO expulsion[79-86] and can also yield rearrangement in to carbonyl bridged dimers which then photolyze to generate radical species. The results are summarized in Table 4.1 and Chart 4.1. An initial scan of all catalysts was performed using primarily C_4F_9-I (PFBI) as a low C-I BDE initiator standard already proven successful with $Mn_2(CO)_{10}$.[4] As expected, no reaction was observed *in the dark* at 40 °C for over > 24 h with either catalytic or stoichiometric amounts of any of the complexes investigated. Moreover, no polymer was obtained under visible light in the presence of $Co_2(CO)_8$, $Cr(CO)_6$, $Cp^*_2Cr_2(CO)_4$, $Mo(CO)_6$, $Fe(CO)_5$, or $Cp_2Fe_2(CO)_4$, regardless of reaction conditions or reagent ratios. This was likely due to the inability of the radical generated to abstract halides at an appreciable rate, or in fact no radicals were generated from the low power irradiation used. Historically, these photolysis were conducted with high power/intensity light sources ($\geq$200W)[79] ($Cr(CO)_6$, $Mo(CO)_6$, $Fe(CO)_5$).(Table 4.1 Exp. 1-30). Additionally, there is the possibility of oxidative insertion to the R_F-I initiators, thus consuming the metal carbonyl activator.[85] Therefore, with the exception of CCl_4, other higher BDE halides were not explored further with these compounds.

Table 4.1 Effect of $Mt_x(CO)_y$ Photoactivator and Initiator on the VDF Polymerization.

Exp	Initiator	Activator	[VDF]/[I]/ $[Mt_x(CO)_y]$	Mn	P.D.I.	Time (Hrs)	Conv.	K_p^{APP}	I.E.
1	CH_2I_2	$Co_2(CO)_8$	20/1/0.1	--	--	90.0	0.0%	0.0000	--
2	CH_3I	$Co_2(CO)_8$	50/1/0.15	--	--	94.0	0.0%	0.0000	--
3	MBSC	$Co_2(CO)_8$	20/1/0.1	--	--	90.0	0.0%	0.0000	--
4	$(CH_3)_3COCl$	$Co_2(CO)_8$	20/1/0.1	--	--	90.0	0.0%	0.0000	--
5	C_4F_9I	$Co_2(CO)_8$	50/1/0.15	--	--	26.0	0.0%	0.0000	--
6	C_4F_9I	$Co_2(CO)_8$	25/1/0.15	--	--	100.0	0.0%	0.0000	--
7	C_4F_9I	$Co_2(CO)_8$	25/1/0.1	--	--	115.0	0.0%	0.0000	--

Table 4.1 Effect of $Mt_x(CO)_y$ Photoactivator and Initiator on the VDF Polymerization.

Exp	Initiator	Activator	[VDF]/[I]/ $[Mt_x(CO)_y]$	Mn	P.D.I.	Time (Hrs)	Conv.	K_p^{APP}	I.E.
8	$I\text{-}(CF_2)_6\text{-}I$	$CpCo(CO)_2$	25/1/0.2	--	--	90.0	0.0%	0.0000	--
9	C_4F_9I	$Cr(CO)_6$	50/1/0.2	--	--	22.0	0.0%	0.0000	--
10	C_4F_9I	$Cr(CO)_6$	25/1/0.2	--	--	67.5	0.0%	0.0000	--
11	C_4F_9I	$Cr(CO)_6$	50/1/0.2	--	--	22.0	0.0%	0.0000	--
12	CH_3I	$Mo(CO)_6$	50/1/0.15	--	--	94.0	0.0%	0.0000	--
13	C_4F_9I	$Mo(CO)_6$	25/1/0.2	--	--	67.5	0.0%	0.0000	--
14	C_4F_9I	$Mo(CO)_6$	50/1/0.3	--	--	26.0	0.0%	0.0000	--
15	C_4F_9I	$Mo(CO)_6$	25/1/0.15	--	--	100.0	0.0%	0.0000	--
16	CCl_4	$Cp^*_2Cr_2(CO)_4$	25/1/0.4	--	--	24.0	0.0%	0.0000	--
17	C_4F_9I	$Cp^*_2Cr_2(CO)_4$	50/1/0.2	--	--	14.5	0.0%	0.0000	--
18	C_4F_9I	$Cp^*_2Cr_2(CO)_4$	25/1/0.15	--	--	45.5	0.0%	0.0000	--
19	C_4F_9I	$Cp^*_2Cr_2(CO)_4$	50/1/0.2	--	--	14.5	0.0%	0.0000	--
20	C_4F_9I	$Cp^*_2Cr_2(CO)_4$	25/1/0.4	--	--	16.5	0.0%	0.0000	--
21	CCl_4	$Fe(CO)_5$	25/1/0.6	--	--	20.5	0.0%	0.0000	--
22	C_4F_9I	$Fe(CO)_5$	50/1/0.2	--	--	61.0	0.0%	0.0000	--
23	C_4F_9I	$Fe(CO)_5$	25/1/0.2	--	--	140.0	0.0%	0.0000	--
24	C_4F_9I	$Fe(CO)_5$	50/1/0.2	--	--	70.0	0.0%	0.0000	--
25	I-PVDF-I	$Fe(CO)_5$	500/1/0.6	--	--	90.0	0.0%	0.0000	--
26	CCl_4	$Cp_2Fe_2(CO)_4$	25/1/0.4	--	--	24.0	0.0%	0.0000	--
27	C_4F_9I	$Cp_2Fe_2(CO)_4$	50/1/0.25	--	--	65.0	0.0%	0.0000	--
28	C_4F_9I	$Cp_2Fe_2(CO)_4$	25/1/0.15	--	--	45.5	0.0%	0.0000	--
29	C_4F_9I	$Cp_2Fe_2(CO)_4$	50/1/.15	--	--	48.0	0.0%	0.0000	--
30	C_4F_9I	$Cp_2Fe_2(CO)_4$	25/1/0.15	--	--	100.0	0.0%	0.0000	--
31	$Cl\text{-}(CF_2)_8\text{-}Cl$	$Cp_2W_2(CO)_6$	50/1/0.4	--	--	38.5	0.0%	0.0000	--
32	CCl_3Br	$Cp_2W_2(CO)_6$	25/1/0.2	--	--	38.5	0.0%	0.0000	--
33	CCl_3Br	$Cp_2W_2(CO)_6$	25/1/0.2	--	--	66.5	0.0%	0.0000	--
34	CCl_4	$Cp_2W_2(CO)_6$	25/1/0.2	--	--	38.5	0.0%	0.0000	--
35	$Br\text{-}(CF_2)_6\text{-}Br$	$Cp_2W_2(CO)_6$	50/1/0.4	4,700	3.37	38.5	25.0%	0.0075	0.27
36	C_4F_9I	$Cp_2W_2(CO)_6$	25/1/0.2	--	--	19.5	0.0%	0.0000	--
37	$C_4F_9I^{\text{acetone}}$	$Cp_2W_2(CO)_6$	25/1/0.1	700	1.35	16.5	8.0%	0.0051	0.68
38	C_4F_9I	$Cp_2W_2(CO)_6$	50/1/0.4	1,750	1.98	40.0	25.0%	0.0072	0.65
39	$I\text{-}(CF_2)_6\text{-}I$	$Cp_2W_2(CO)_6$	50/1/0.4	1,700	1.28	64.3	25.0%	0.0045	0.79
40	$C_6H_{13}Cl$	$Cp_2Mo_2(CO)_6$	50/1/0.5	--	--	60.0	0.0%	0.0000	--
41	$C_6H_{13}Br$	$Cp_2Mo_2(CO)_6$	50/1/0.5	--	--	60.0	0.0%	0.0000	--
42	$C_6H_{13}I$	$Cp_2Mo_2(CO)_6$	50/1/0.5	--	--	60.0	0.0%	0.0000	--
43	CH_3I	$Cp_2Mo_2(CO)_6$	25/1/0.2	--	--	22.5	0.0%	0.0000	--
44	CCl_3Br	$Cp_2Mo_2(CO)_6$	25/1/0.2	--	--	19.0	0.0%	0.0000	--
45	CCl_3Br	$Cp_2Mo_2(CO)_6$	25/1/0.2	--	--	66.5	0.0%	0.0000	--
46	$Cl\text{-}(CF_2)_8\text{-}Cl$	$Cp_2Mo_2(CO)_6$	50/1/0.4	--	--	24.0	0.0%	0.0000	--
47	$C_4F_9I^{\text{No light 80C}}$	$Cp_2Mo_2(CO)_6$	50/1/0.5	--	--	20.0	0.0%	0.0000	--
48	$C_4F_9I^{\text{No light 40}}$	$Cp_2Mo_2(CO)_6$	25/1/0.2	--	--	91.0	0.0%	0.0000	--
49	$I\text{-}(CF_2)_6\text{-}I^{\text{No light 80C}}$	$Cp_2Mo_2(CO)_6$	50/1/0.1	--	--	23.0	0.0%	0.0000	--
50	$I\text{-}(CF_2)_6\text{-}I^{\text{No light 40}}$	$Cp_2Mo_2(CO)_6$	50/1/0.1	--	--	94.5	0.0%	0.0000	--
51	$I\text{-}(CF_2)_6\text{-}I^{\text{No Light 40}}$	$Cp_2Mo_2(CO)_6$	50/1/0.2	--	--	94.5	0.0%	0.0000	--
52	CCl_4	$Cp_2Mo_2(CO)_6$	25/1/0.2	3,400	1.16	17.8	5.0%	0.0029	0.02
53	$Br\text{-}(CF_2)_6\text{-}Br$	$Cp_2Mo_2(CO)_6$	50/1/0.4	1,500	3.03	20.8	18.3%	0.0097	0.39
54	C_4F_9I	$Cp_2Mo_2(CO)_6$	25/1/0.2	800	1.28	15.0	20.0%	0.0192	0.44
55	C_4F_9I	$Cp_2Mo_2(CO)_6$	25/1/0.2	600	1.34	23.3	25.2%	0.0097	0.65
56	C_4F_9I	$Cp_2Mo_2(CO)_6$	100/1/1	2,000	2.08	23.3	20.0%	0.0096	0.64
57	C_4F_9I	$Cp_2Mo_2(CO)_6$	100/1/1	2,000	1.89	49.5	21.0%	0.0048	0.67
58	C_4F_9I	$Cp_2Mo_2(CO)_6$	100/1/1	1,900	1.92	67.0	21.0%	0.0035	0.71

Table 4.1 Effect of $Mt_x(CO)_y$ Photoactivator and Initiator on the VDF Polymerization.									
Exp	**Initiator**	**Activator**	**[VDF]/[I]/ [$Mt_x(CO)_y$]**	**Mn**	**P.D.I.**	**Time (Hrs)**	**Conv.**	**K_p^{APP}**	**I.E.**
59	I-$(CF_2)_6$-I	$Cp_2Mo_2(CO)_6$	50/1/0.2	700	1.42	15.5	14.0%	0.0097	0.64
60	I-$(CF_2)_6$-I	$Cp_2Mo_2(CO)_6$	50/1/0.2	750	1.34	28.5	16.0%	0.0061	0.68
61	I-$(CF_2)_6$-I	$Cp_2Mo_2(CO)_6$	50/1/0.2	800	1.33	51.0	19.5%	0.0043	0.78
62	I-$(CF_2)_6$-I	$Cp_2Mo_2(CO)_6$	50/1/0.2	1,000	1.38	75.0	23.0%	0.0040	0.83
63	I-$(CF_2)_6$-I	$Cp_2Mo_2(CO)_6$	50/1/0.5	900	1.19	94.5	12.0%	0.0014	0.43
64	I-$(CF_2)_6$-I	$Cp_2Mo_2(CO)_6$	100/1/1	3,100	1.82	20.8	21.0%	0.0114	0.43
65	I-$(CF_2)_6$-I	$Cp_2Mo_2(CO)_6$	100/1/1	3,900	1.85	46.5	24.0%	0.0059	0.39
66	I-$(CF_2)_6$-I	$Cp_2Mo_2(CO)_6$	100/1/1	3,800	1.79	67.0	30.0%	0.0053	0.51
67	$C_6H_{13}Cl$	$Mn_2(CO)_{10}$	50/1/0.5	--	--	50.0	0.0%	0.0000	--
68	$C_6H_{13}Br$	$Mn_2(CO)_{10}$	50/1/0.5	3,100	1.81	50.0	15.3%	0.0033	0.16
69	$C_6H_{13}I$	$Mn_2(CO)_{10}$	50/1/0.5	5,700	1.89	50.0	26.7%	0.0062	0.15
70	CH_3I	$Mn_2(CO)_{10}$	50/1/0.2	4,900	1.8	13	11.0%	0.0090	0.07
71	CCl_3Br	$Mn_2(CO)_{10}$	25/1/0.2	2,500	1.70	22.5	35.0%	0.0191	0.28
72	Cl-$(CF_2)_8$-Cl	$Mn_2(CO)_{10}$	50/1/0.4	4,800	3.04	24.0	5.0%	0.0021	0.14
73	CCl_4	$Mn_2(CO)_{10}$	25/1/0.2	3,600	2.22	22.5	43.0%	0.0250	0.19
74	Br-$(CF_2)_6$-Br	$Mn_2(CO)_{10}$	50/1/0.4	3,500	2.33	20.8	69.3%	0.0569	0.63
75	$C_4F_9I^{no\ light\ 40}$	$Mn_2(CO)_{10}$	25/1/0.2	--	--	93.0	0.0%	0.0000	--
76	$C_4F_9I^{no\ light\ 75C}$	$Mn_2(CO)_{10}$	25/1/0.2	--	--	93.0	0.0%	0.0000	--
77	C_4F_9I	$Mn_2(CO)_{10}$	50/1/0.2	4,200	1.56	18.5	60.9%	0.0508	0.46
78	C_4F_9I	$Mn_2(CO)_{10}$	25/1/0.2	950	1.31	10.0	22.7%	0.0250	0.52
79	C_4F_9I	$Mn_2(CO)_{10}$	25/1/0.2	1,200	1.56	23.3	72.4%	0.0554	0.97
80	C_4F_9I	$Mn_2(CO)_{10}$	25/1/0.25	1,550	1.62	3.0	50.0%	0.2310	0.47
81	C_4F_9I	$Mn_2(CO)_{10}$	25/1/0.25	1,700	1.85	6.0	64.0%	0.1700	0.60
82	C_4F_9I	$Mn_2(CO)_{10}$	25/1/0.25	1,900	1.85	9.0	75.0%	0.1540	0.67
83	I-$(CF_2)_6$-I	$Mn_2(CO)_{10}$	50/1/0.2	1,200	1.48	3.0	34.0%	0.1387	0.91
84	I-$(CF_2)_6$-I	$Mn_2(CO)_{10}$	50/1/0.2	1,700	1.39	7.0	50.0%	0.0990	0.94
85	I-$(CF_2)_6$-I	$Mn_2(CO)_{10}$	50/1/0.2	2,200	1.40	11.0	63.0%	0.0910	0.92
86	I-$(CF_2)_6$-I	$Mn_2(CO)_{10}$	200/1/0.4	6,800	1.55	1.0	28.0%	0.3285	0.53
87	I-$(CF_2)_6$-I	$Mn_2(CO)_{10}$	200/1/0.4	8,200	1.56	4.0	35.0%	0.1077	0.55
88	I-$(CF_2)_6$-I	$Mn_2(CO)_{10}$	200/1/0.4	9,400	1.67	15.0	47.0%	0.0423	0.64
89	I-$(CF_2)_4$-I	$Mn_2(CO)_{10}$	50/1/0.2	1,500	1.63	6.5	44.0%	0.0892	0.94
90	I-$(CF_2)_4$-I	$Mn_2(CO)_{10}$	50/1/0.2	1,800	1.46	22.0	64.0%	0.0464	1.14
91	I-$(CF_2)_4$-I	$Mn_2(CO)_{10}$	50/1/0.2	2,300	1.51	30.0	80.0%	0.0536	1.11
92	$C_6H_{13}Cl$	$Re_2(CO)_{10}$	50/1/0.5	--	--	48.0	0.0%	0.0000	--
93	$C_6H_{13}Br$	$Re_2(CO)_{10}$	50/1/0.5	5,700	2.03	88.7	26.0%	0.0034	0.17
94	$C_6H_{13}I$	$Re_2(CO)_{10}$	50/1/0.5	7,500	1.62	48.0	42.0%	0.0113	0.09
95	CH_3I	$Re_2(CO)_{10}$	50/1/0.2	15,000	1.82	22.0	26.0%	0.0137	0.07
96	CCl_3Br	$Re_2(CO)_{10}$	25/1/0.2	3,000	1.37	20.0	37.0%	0.0231	0.44
97	Cl-$(CF_2)_8$-Cl	$Re_2(CO)_{10}$	50/1/0.5	9,300	2.01	88.7	17.0%	0.0021	0.10
98	CCl_4	$Re_2(CO)_{10}$	25/1/0.2	6,400	1.60	20.0	43.9%	0.0289	0.24
99	Br-$(CF_2)_6$-Br	$Re_2(CO)_{10}$	50/1/0.4	8,200	1.69	20.8	68.5%	0.0557	0.27
100	$C_4F_9I^{no\ light\ 40}$	$Re_2(CO)_{10}$	25/1/0.2	--	--	91.0	0.0%	0.0000	--
101	$C_4F_9I^{no\ light\ 40}$	$Re_2(CO)_{10}$	50/1/0.5	--	--	20.0	0.0%	0.0000	--
102	I-$(CF_2)_6$-$I^{no\ light\ 80}$	$Re_2(CO)_{10}$	50/1/0.1	--	--	23.0	0.0%	0.0000	--
103	C_4F_9I	$Re_2(CO)_{10}$	25/1/0.2	800	1.27	1.7	23.0%	0.1537	0.46
104	C_4F_9I	$Re_2(CO)_{10}$	25/1/0.2	1,250	1.38	3.0	58.0%	0.2892	0.71
105	C_4F_9I	$Re_2(CO)_{10}$	25/1/0.2	1,400	1.55	6.0	78.0%	0.2524	0.89
106	I-$(CF_2)_6$-I	$Re_2(CO)_{10}$	50/1/0.2	1,000	1.31	2.0	22.0%	0.1242	0.70
107	I-$(CF_2)_6$-I	$Re_2(CO)_{10}$	50/1/0.2	2,900	1.37	4.0	56.0%	0.2052	0.62
108	I-$(CF_2)_6$-I	$Re_2(CO)_{10}$	50/1/0.2	4,100	1.50	8.0	77.0%	0.1837	0.60
109	I-$(CF_2)_6$-I^{65C}	$Re_2(CO)_{10}$	50/1/0.1	700	1.35	2.5	12.0%	0.0511	0.85

Table 4.1 Effect of $Mt_x(CO)_y$ Photoactivator and Initiator on the VDF Polymerization.									
Exp	**Initiator**	**Activator**	**[VDF]/[I]/ $[Mt_x(CO)_y]$**	**Mn**	**P.D.I.**	**Time (Hrs)**	**Conv.**	**K_p^{APP}**	**I.E.**
110	I-$(CF_2)_6$-I[65C]	$Re_2(CO)_{10}$	50/1/0.1	1,800	1.36	8.5	38.0%	0.0562	0.86
111	I-$(CF_2)_6$-I[65C]	$Re_2(CO)_{10}$	50/1/0.1	2,500	1.39	16.5	65.0%	0.0636	0.96
112	I-$(CF_2)_6$-I	$Re_2(CO)_{10}$	200/1/0.4	3,000	1.43	2.0	13.0%	0.0696	0.55
113	I-$(CF_2)_6$-I	$Re_2(CO)_{10}$	200/1/0.4	6,100	1.61	4.0	30.0%	0.0892	0.63
114	I-$(CF_2)_6$-I	$Re_2(CO)_{10}$	200/1/0.4	7,200	1.63	15.0	41.0%	0.0352	0.73
115	I-$(CF_2)_4$-I	$Re_2(CO)_{10}$	50/1/0.2	1,100	1.56	3.3	41.0%	0.1584	1.19
116	I-$(CF_2)_4$-I	$Re_2(CO)_{10}$	50/1/0.2	1,300	1.57	5.0	58.0%	0.1735	1.43
117	I-$(CF_2)_4$-I	$Re_2(CO)_{10}$	50/1/0.2	2,100	1.60	7.0	84.0%	0.2618	1.28

*All in dimethyl carbonate at 40°C under low power (≤ 30W) visible light irradiation with a compact fluorescent bulb unless otherwise stated

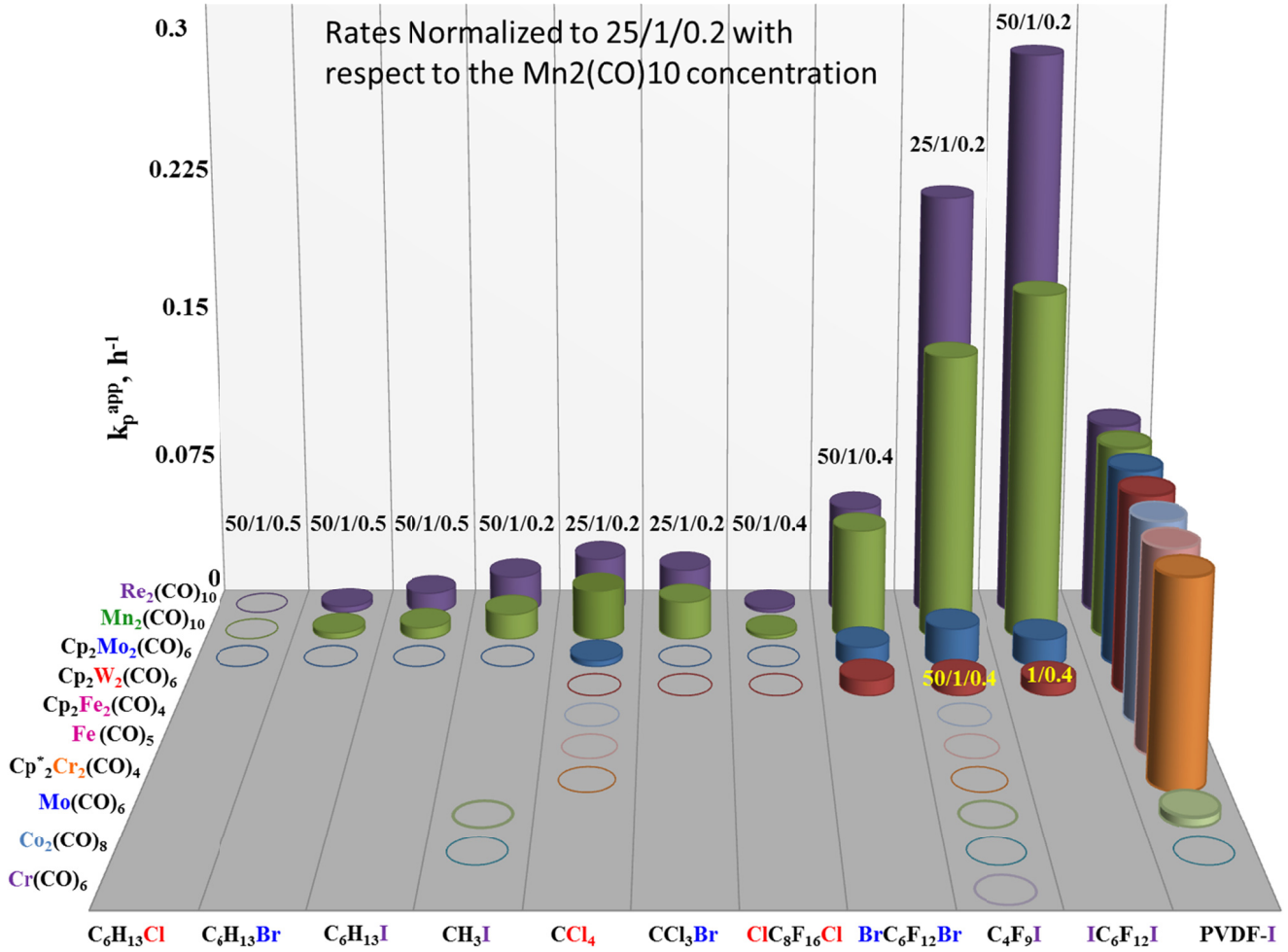

Chart 4.1. Effect of catalyst initiator system on the rate of VDF polymerization at 40C in dimethyl carbonate. [monomer]/[initiator]/[catalyst] ratios are given for each initiator, *[50]/[1]/[0.4]

$Cp_2W_2(CO)_6$: $Cp_2W_2(CO)_6$ did not afford polymer with medium BDE halides (CCl_3-Cl, CCl_3-Br, and Cl-$(CF2)_8$-Cl) (Table 4.1 Exp. 31-34), but only with Br-$(CF_2)_6$-Br, $CF_3(CF_2)_3$-I, and I-$(CF_2)_6$-I (Table 4.1 Exp. 35, 37-39) while requiring at least twice the amount *vs*. a typical $Mn_2(CO)_{10}$ ratio. (*i.e.* $[R_f\text{-}I]\backslash[Cp_2W_2(CO)_6] = [1]\backslash[0.4]$ *vs.* $[R_f\text{-}I]\backslash[Mt_x(CO)_y] = [1]\backslash[0.1\text{-}0.2]$). This was attributed to the poor solubility of the catalyst in DMC, where no polymer is obtained in DMC with 20 mole % $Cp_2W_2(CO)_6$. However, in acetone 10 mole % $Cp_2W_2(CO)_6$ affords PVDF, although still with very low conversion. (Table 4.1 Exp. 36-37). While it was expected the $Cp_2W_2(CO)_6$ would fall between $Mn_2(CO)_{10}$ and $Cp_2Mo_2(CO)_6$ in the ability to abstract halides and thus initiate polymerization, the poor solubility in the our best polymerization solvent likely inhibited this.

$Cp_2Mo_2(CO)_6$: While UV irradiation (λ < 400 nm) forces CO loss without Mo-Mo bond scission,[87] visible light (λ > 400 nm), readily promotes $Cp_2Mo_2(CO)_6$ homolysis[88] to $CpMo(CO)_3^{\bullet}$. The resulting $17e^-$ metalloradical can then undergo recombination and hydride or halide abstraction. By contrast to $Mn(CO)_5^{\bullet}$ which reacts faster with primary over secondary or tertiary halides,[4] the Mo abstraction rates follow the expected RI > RBr > RCl and benzyl > allyl > 3° > 2° > 1° > CH_3[89] trend. However, as for Mn, no previous examples of abstraction from fluorinated or semi fluorinated halides are available. Additionally the $CpMo(CO)_3^{\bullet}$ recombination rate constant ($k = 3.1x10^9$) is larger than for $Mn(CO)_5^{\bullet}$ ($k = 1.9x10^9$) [28, 90] thus upon irradiation the lifetime of $Mn(CO)_5^{\bullet}$ is nearly twice that of $CpMo(CO)_3^{\bullet}$ allowing for a decreased ability to react with a halide.[90] Moreover the quantum yield of Mo-X bond homolysis is negligible ($\Phi = 9 \times 10^{-4}$).[91] Thus, it is very unlikely that Mo can mediate a reversible iodine transfer. While $Cp_2Mo_2(CO)_6$ is considered a weaker halide abstractor than $Cp_2W_2(CO)_6$,[22,57,58] it may compensate in rate *via* the better solubility in DMC. However, under visible light, even with up to stoichiometric amounts of $Cp_2Mo_2(CO)_6$ no polymer was obtained from the higher BDE halides ($CH_3(CH_2)_5Cl$, $CH_3(CH_2)_5Br$, $CH_3(CH_2)_5I$, CH_3I, CCl_3Br, and $ClC_8F_{16}Cl$) (Table 4.1 Exp. 40-46) or in the dark, at 40°C - 80°C, from

R_F-I (Table 4.1 Exp. 47-51). As such, $Cp_2Mo_2(CO)_6$ generated PVDF from Br-$(CF_2)_6$-Br, $CF_3(CF_2)_3$-I, I-$(CF_2)_6$-I, and also activated CCl_4, although very poorly (Table 4.1 Exp. 52-66), confirming that $Cp_2Mo_2(CO)_6$ is indeed a weak abstractor and no thermal homolysis is present.

Interestingly, fluxionally active $Cp_2Mo_2(CO)_6$ presents itself with both *trans* and *gauche* conformers possessing different reactivity.[92] The dominant *trans* conformation is the major species in the dimer and in solution. However, upon recombination following visible light irradiation, and due to in-cage recombination, ~30 % of the *trans* conformer is instantly converted to the higher energy *gauche* conformation. This also results in a shift to a higher energy (UV region) absorption wavelength, which significantly depresses its homolysis under visible light. Moreover, the thermal rotation about the Mo-Mo bond back to the *trans* conformer ($k = 2 \times 10^2\ s^{-1}$),[92] is 7 orders of magnitude slower than *trans* dissociation and recombination ($k = 3 \times 10^9\ M^{-1}\ s^{-1}$). Thus, under continuous visible light irradiation, a buildup of the *gauche* conformer occurs, causing a rapid decrease in the ability of $Cp_2Mo_2(CO)_6$ to homolyze and abstract halides. Unfortunately, while UV irradiation could promote the *gauche* homolysis, this would also cause CO loss. This is consistent with the observed trends using $Cp_2Mo_2(CO)_6$, *i.e.* a fast increase in initial conversion of monomer to polymer (higher initial k_p^{app}) followed by a rapid decrease in polymerization rate (Table 4.1 Exp. 59-62, 64-66; Figure 4.1 a-b) yielding non-linear 1st order kinetic, although there is a linear dependence of M_n on conversion indicating that the IDT-CRP is functioning.

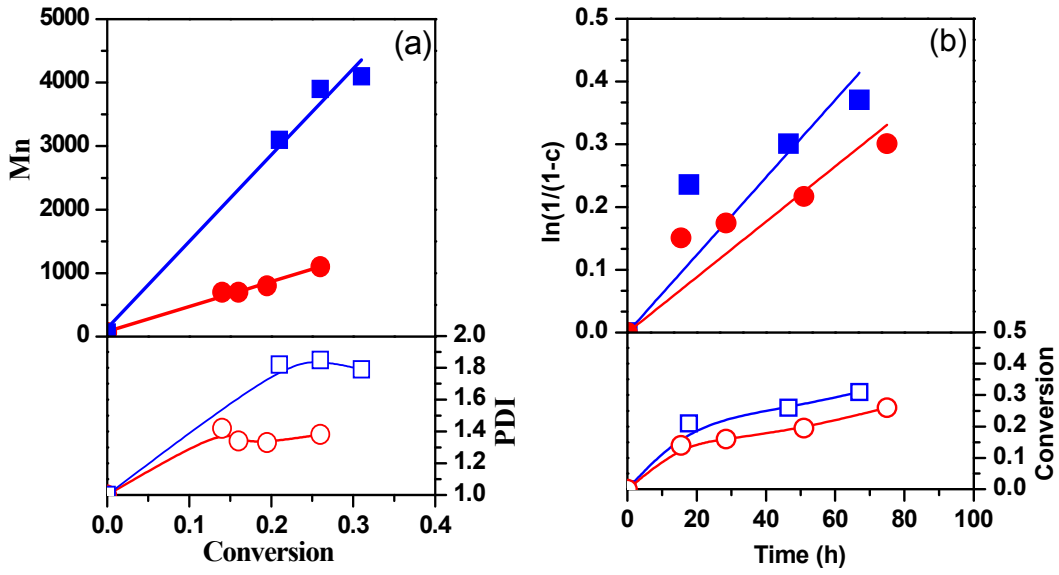

Figure 4.1: Dependence of (a) M_n and M_w/M_n on conversion and (b) ln(1/1-c) vs. Time for [VDF]/[DIPFH]/[$Cp_2Mo_2(CO)_6$] = [50]/[1]/[0.2] (● ○); [VDF]/[DIPFH]/[$Cp_2Mo_2(CO)_6$] = [100]/[1]/[1] (■ □)

$Mn_2(CO)_{10}$: $Mn_2(CO)_{10}$ afforded polymer with all initiators except the inactivated $C_6H_{13}Cl$ (Table 4.1 exp. 67). While, $C_6H_{13}Br$, $C_6H_{13}I$, CH_3I, CCl_3Br, Cl-$(CF_2)_8$-Cl, and CCl_4, yielded polymer, they were much slower than the lower BDE initiators, had poor initiator efficiency (<30%), and for the alkyl halides, required stoichiometric $Mn_2(CO)_{10}$ (Table 4.1 Exp. 69-73). The Br-$(CF_2)_6$-Br, generated polymer with a faster rate and higher initiator efficiency then the polyhalides, alkyl halides, and Cl-$(CF_2)_8$-Cl (Table 4.1 exp. 74). Control experiments (Table 4.1 Exp. 75-76) revealed that at both 40°C and 75°C in the absence of light there is no polymerization, thus photoactivation of the $Mn_2(CO)_{10}$ is required. The fastest rates and highest initiator efficiencies were obtained with the use of the lowest BDE strongest chain transfer agents, the perfluoroalkyliodides (Table 4.1 Exp. 77-91). The use of the monofunctional initiator PFBI yielded a free radical polymerization, while the difunctional DIPFH initiator exhibits trends of a CRP (Figure 4.2-4.3). This is likely due to a few reasons, first are the inherent defects which exist in VDF polymerizations (i.e. the reverse 2,1-addition) which are shown[4] to build up during the

course of a VDF-IDT polymerization. Regardless of the [VDF]/[Initiator]/[$Mn_2(CO)_{10}$] ratio, in all cases the 1,2-terminus decreases, 2,1-terminus increases, and with higher [Initiator]/[$Mn_2(CO)_{10}$] ratios the total functionality rapidly drops with conversion. These ~CH_2-CF_2-CF_2-CH_2-I terminal units have a considerably higher BDE, thus rendering them unable to participate in the DT (Scheme 4.1 eq, 7-9) process, and are in effect "dead" chains, thus increasing termination. Although It is known that $Mn_2(CO)_{10}$ can activate the ~CH_2-CF_2-CF_2-CH_2-I terminal units of the polymer this requires a larger amount of $Mn_2(CO)_{10}$ present at the start of the reaction thus leading to a FRP as can be seen in a M_n which does not increase with conversion, as well as their low % of iodo-chain ends[4]. Additionally, the unavailability of iodine on the $Mn(CO)_5$-I generated in (scheme 4.1, eq. 2) is further evidenced by these reactions in which higher amounts of $Mn_2(CO)_{10}$ do not yield a CRP, supported by the demonstration that additional $Mn(CO)_5$-I added to a FRP of VDF generates no iodine chain ends of any type.[4] (appendix 4.A, Figure 4.A4, 4.A5) Thus, the only means by which to obtain a CRP while maintaining a high total functionality is to use difunctional initiators. This can be reasoned, in that all difunctional initiators have a means of maintaining a functional chain end even following typical termination events which occur throughout the polymerization. As represented in Scheme 4.2 eq. 1, 3, 5 monofunctional initiators that undergo termination, no longer maintain any functionality, while Scheme 4.2. eq. 2, 4, 6 difunctional initiators have the ability to maintain a functional chain end.

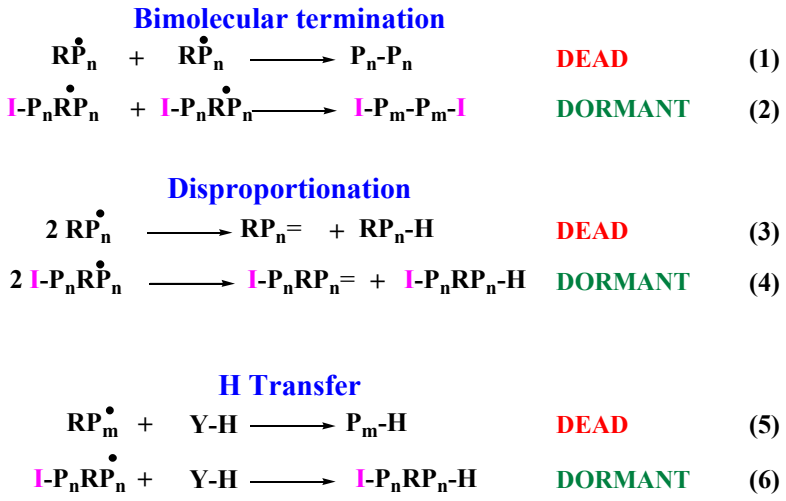

Scheme 4.2: Termination in the presence of monofunctional *vs*. difunctional initiators.

$Re_2(CO)_{10}$: Similar to $Mn_2(CO)_{10}$, $Re_2(CO)_{10}$ afforded polymer with all initiators except the inactivated $C_6H_{13}Cl$ (Table 4.1 exp. 92). $C_6H_{13}Br$, $C_6H_{13}I$, CH_3I, Cl-$(CF_2)_8$-Cl, Br-$(CF_2)_6$-Br, and CCl_4, yielded polymer, but with poor initiator efficiency (<25%), and for the alkyl halides, required stoichiometric $Re_2(CO)_{10}$ (Table 4.1 exp 93-95, 97-99). Interestingly the CCl_3Br generated polymer with a faster rate and higher initiator efficiency then other initiators aside from the perfluoroalkyliodides, (Table 4.1 exp 96). Control experiments (Table 4.1 exp 100-102) revealed that at both 40C and 80C in the absence of light there is no polymerization, thus similarly to $Mn_2(CO)_{10}$, photoactivation is required. The fastest rates and highest initiator efficiencies were obtained with the use of the lowest BDE strongest chain transfer agents, the perfluoroalkyliodides (Table 4.1 exp 103-117). As observed with Mn2(CO)10 the use of the monofunctional initiator PFBI yielded a free radical polymerization, while the difunctional DIPFH initiator exhibits results typical of a CRP (Figure 4.2-4.3), for the same reasons as previously discussed.

Comparison of $Mn_2(CO)_{10}$ and $Re_2(CO)10$ in the IDT-CRP of VDF: Figure 4.2 and 4.3 demonstrate the linear dependence of molecular weight of the polymers on conversion (i.e. IDT-CRP) for both manganese and rhenium carbonyls, in conjunction with DIPFH, a difunctional initiator over a range of [Monomer]/[Initiator] ratios, with the rhenium carbonyl yielding the fastest overall rates. In addition to revealing the monofunctional PFBI trends more towards a FRP.

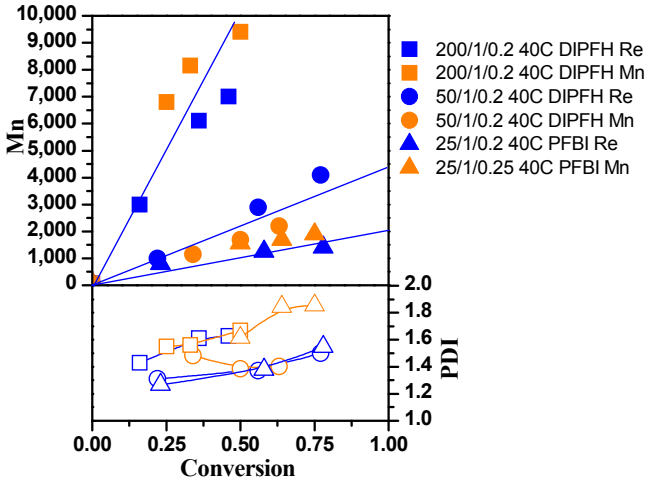

Figure 4.2 Dependence of M_n and M_w/M_n on conversion. Comparison of $Mn_2(CO)_{10}$ (■ ●▲) and $Re_2(CO)_{10}$ (■ ●▲) for [VDF]/[Initiator] = 200/1 (■,■); 50/1 (●●); 25/1 (▲▲)

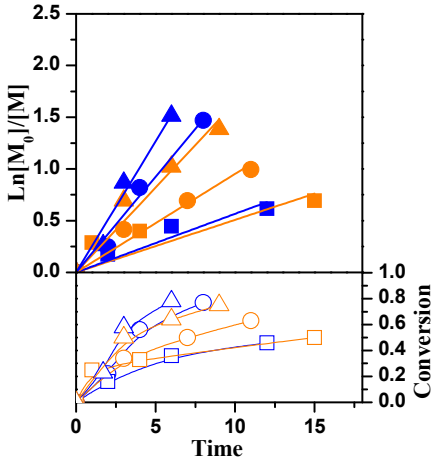

Figure 4.3 Dependence of ln(1/1-c) vs. Time. Comparison of $Mn_2(CO)_{10}$ (■ ●▲) and $Re_2(CO)_{10}$ (■ ●▲) for [VDF]/[Initiator] = 200/1 (■,■); 50/1 (●●); 25/1 (▲▲)

$Mn_2(CO)_{10}$ Mediated VDF Polymerization Initiated from Br-$(CF_2)_4$-Br or CCl_4:

By contrast to the difunctional perfluoroalkyl iodide IDT-CRP of VDF, no increase of molecular weight is observed as a function of conversion for CCl_4 or Br-$(CF_2)_4$-Br. It was expected these would lead to a typical free radical polymerization, exhibiting a constant molecular weight with increasing conversion. This result is indeed observed for the initiation from CCl_4 (Figure. 4.4)

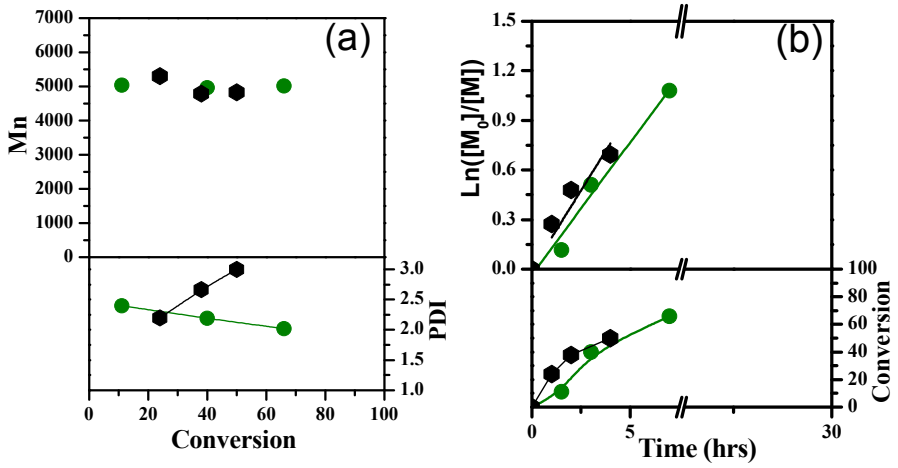

Figure 4.4: (a) M_n and PDI vs conversion (b) Kinetics of free Radical polymerization-[VDF]/[I]/[cat], using CCl_4 (30/1/0.5 ⬢, 50/1/0.2 ●).

However, this was not the case for Br-$(CF_2)_6$-Br, and in fact a decrease in molecular weight was observed. This behavior is in fact consistent with typical telomerization reactions where the chain transfer to initiator leads to an unreactive polymer chain ends (i.e. the Br terminated PVDF cannot be reactivated either by degenerative transfer to another chain or by the initiating radical) and the rate of consumption of monomer is greater than that of the initiator. Thus in Figure 4.5 we can clearly see a decreasing molecular weight with respect to conversion for both a high ([VDF]/[Br-$(CF_2)_6$-Br]= 200/1) and low ([VDF]/[Br-$(CF_2)_6$-Br] = 50/1) DP reaction. In both cases the M_w/M_n is increasing with conversion as expected due to the shorter chains being produced as the reaction proceeds.[93]

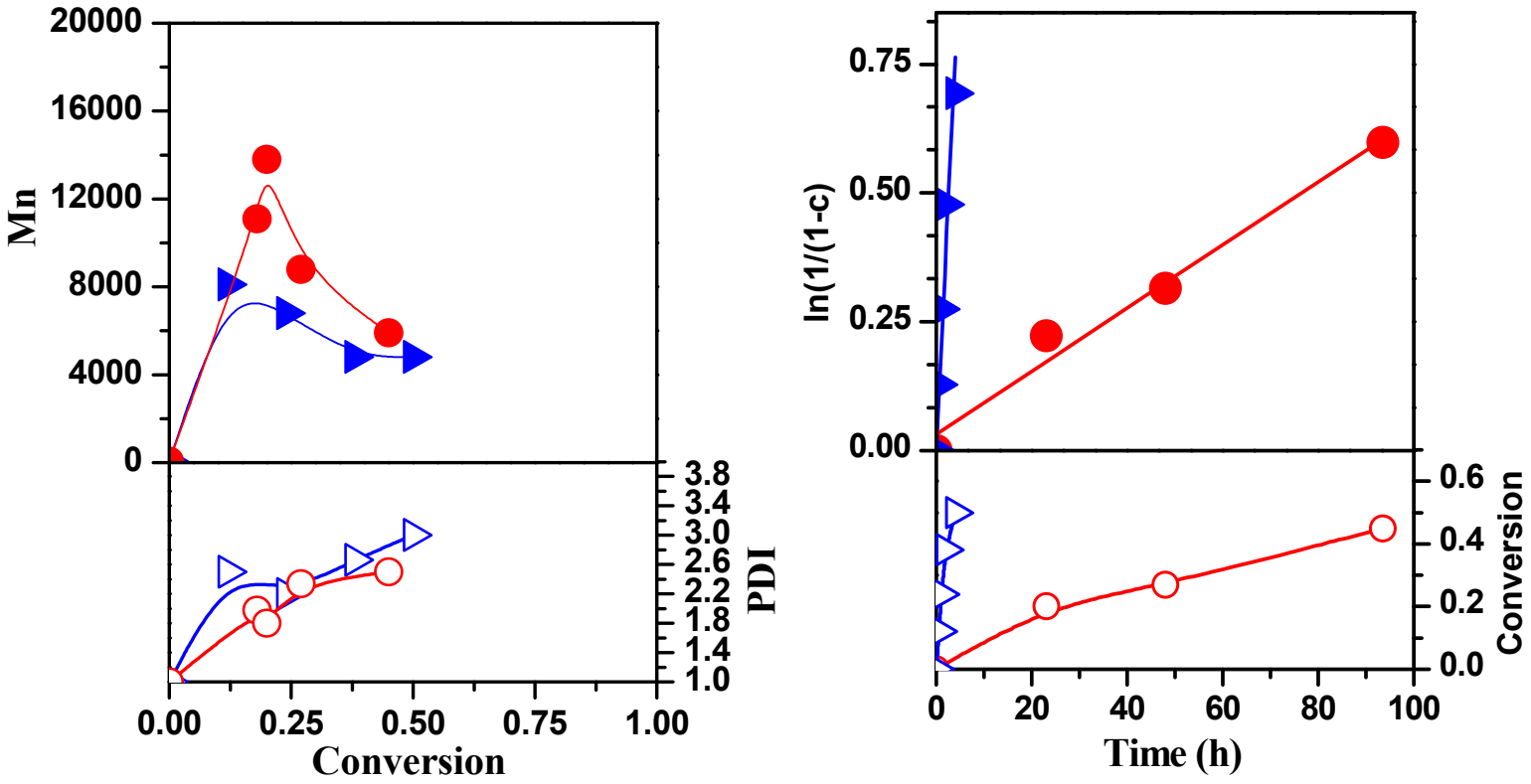

Figure 4.5: (a)Dependence of M_n and M_w/M_n on conversion and (b) dependence of ln(1/(1-C)) and conversion on time for (●) [VDF]/[Br-$(CF_2)_4$-Br]/[$Mn_2(CO)_{10}$] = 200/1/0.2 and (▶) [VDF]/[Br-$(CF_2)_4$-Br]/[$Mn_2(CO)_{10}$] = 50/1/0.1 in dimethyl carbonate at 40C with visible light irradiation (30W Compact fluorescent light bulb) .

4.3.2 Effect of [VDF]/[PFBI]/[$Mn_2(CO)_{10}$] ratio and solvent on the VDF Polymerization.

As discussed previously[4] the most suitable solvent for the metal carbonyl mediated VDF polymerization was dimethyl carbonate. Therefore this was the chosen solvent to perform a series of kinetic experiments in order to explore the effects of various [VDF]/[PFBI]/[$Mn_2(CO)_{10}$] ratios on the polymerizations.(Figure 4.6 and Table 4.2) Examining the [PFBI]/[$Mn_2(CO)_{10}$] ratio it can be seen that, as expected, the k_p^{app} indeed increases with higher amounts of manganese, (Figure 4.7) however no increase of molecular weight as a function of conversion is observed, (Figure 4.8) demonstrating simply a free radical polymerization (FRP) is present under these conditions. This FRP is also seen when increasing the [VDF]/[PFBI] ratio (i.e. for higher degree of polymerization DP) in conjunction with larger amounts of activator [PFBI]/[$Mn_2(CO)_{10}$] =1/0.25 .(Figure 4.9) As such these results were not typical of a controlled radical polymerization (CRP) (i.e. linear dependence of Mn on conversion) for reasons discussed previously. For experiments where both the DP ([VDF]/[PFBI]) was increased and [Initiator]/[$Mn_2(CO)_{10}$] ratio decreased, the polymerizations trend towards CRP, by beginning to show an increase of molecular weight with conversion(Figure 4.10) in fact only these experiments with less activator and higher DP appear to show any increase of molecular weight with conversion in conjunction with a monofunctional initiator. The inherent defects which exist in VDF polymerizations (i.e. the reverse 2,1-addition) which has been shown[4] to build up during the course of an VDF-IDT polymerization. These ~CH_2-CF_2-CF_2-CH_2-I terminal units have a considerably higher BDE, thus rendering them unable to participate in the DT (Scheme 4.1) process, and are in effect “dead” chains, thus increasing termination. It is known that $Mn_2(CO)_{10}$ can in fact activate the ~CH_2-CF_2-CF_2-CH_2-I terminal units of the polymer, however this requires a larger amount of $Mn_2(CO)_{10}$ present at the start of the reaction thus leading to a typical FRP, as such, the experiments with higher amounts of $Mn_2(CO)_{10}$ proceed via FRP, as can be seen in an initially high Mn which does not increase with

conversion, as well as their low % of iodo- chain ends[4]. The unavailability of iodine on the $Mn(CO)_5$-I generated in (scheme 4.1, eq. 2) is further evidenced by these reactions in which higher amounts of $Mn_2(CO)_{10}$ do not yield a CRP, supported by the demonstration that additional $Mn(CO)_5$-I added to a FRP of VDF generates no iodine chain ends of any type. (appendix 4.A, Figure 4.A4, 4.A5).

Table 4.2 $Mn_2(CO)_{10}$ Mediated VDF Polymerizations:

Exp #	Temp °C	[VDF]/[PFBI] /[$Mn_2(CO)_{10}$]	Solvent	Time (Hrs)	Conv (%)	k_p^{app} (h^{-1})	Mn	PDI
1	40	25/1/0.05	DMC	26.00	38%	0.0184	760	1.21
2	40	25/1/0.1	DMC	8.33	27%	0.0378	720	1.25
3	40	25/1/0.1	ACN	6.00	8%	0.0139	2,300	1.10
4	40	25/1/0.25	DMC	7.00	64%	0.1460	1,700	1.85
5	40	25/1/1	ACN	6.00	40%	0.0851	2,180	1.10
6	40	50/1/0.1	DMC	15.75	42%	0.0346	1,500	1.34
7	40	50/1/0.25	DMC	7.67	58%	0.1131	2,600	1.43
8	75	50/1/0.2	DMC	1.00	49%	0.6733	2,600	1.45
9	40	50/1/0.5	DMC	7.00	75%	0.1980	2,500	1.52
10	40	100/1/0.2	DMC	24.00	28%	0.0137	3,800	1.68

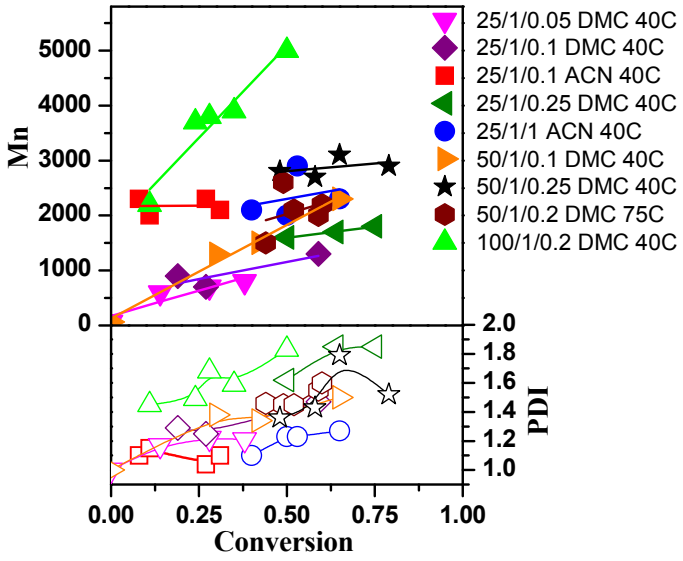

Figure 4.6 Dependence of M_n and M_w/M_n on conversion of VDF polymerizations at various [VDF]/[PBFI]/[$Mn_2(CO)_{10}$] ratios. Polymerizations were carried out in acetonitrile or dimethyl carbonate.

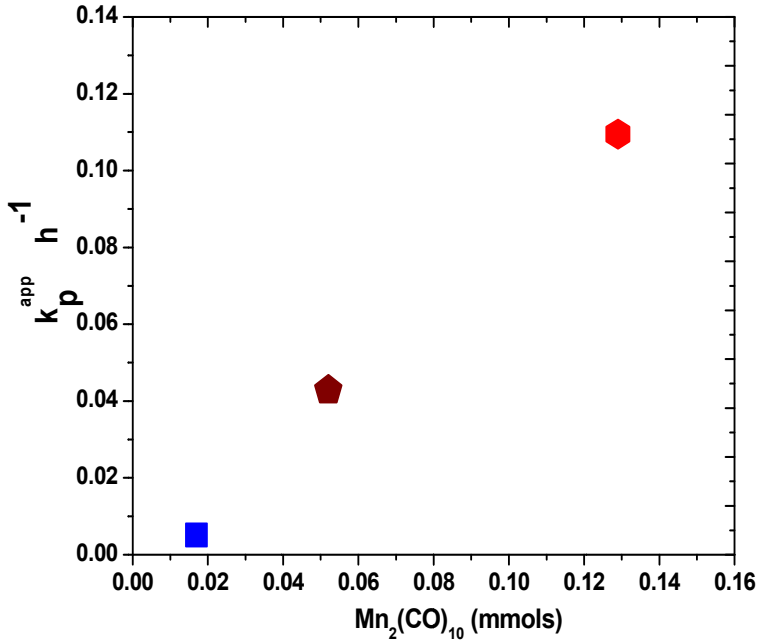

Figure 4.7 Dependance of k_p^{app} on the [Initiator]/[Activator] ratio, [VDF]/[I]/[cat] : 50/1/0.05 ■, 50/1/0.1 ⬟ and 50/1/0.25 ⬢

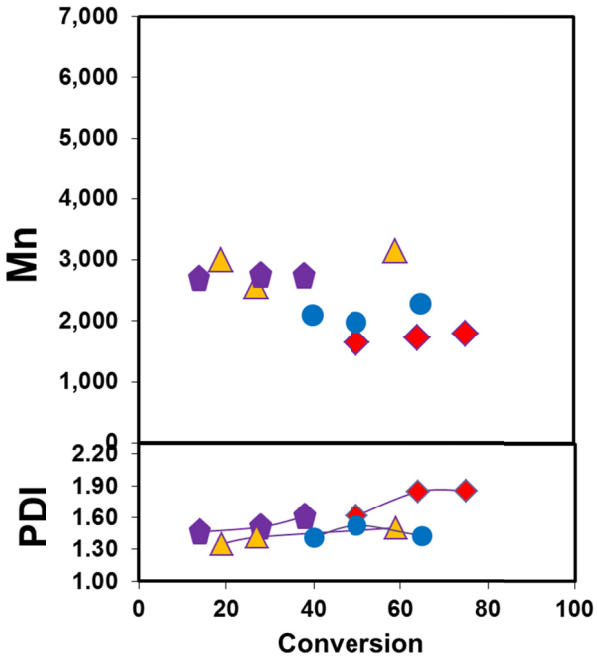

Figure 4.8 Effect of [PFBI]/[$Mn_2(CO)_{10}$] ratio on the M_n and PDI dependence on conversion in VDF-FRP : [VDF]/[PFBI]/[$Mn_2(CO)_{10}$] = 25/1/0.05 (⬟), 25/1/0.1 (▲), 25/1/0.25 (◆), 25/1/1 (●).

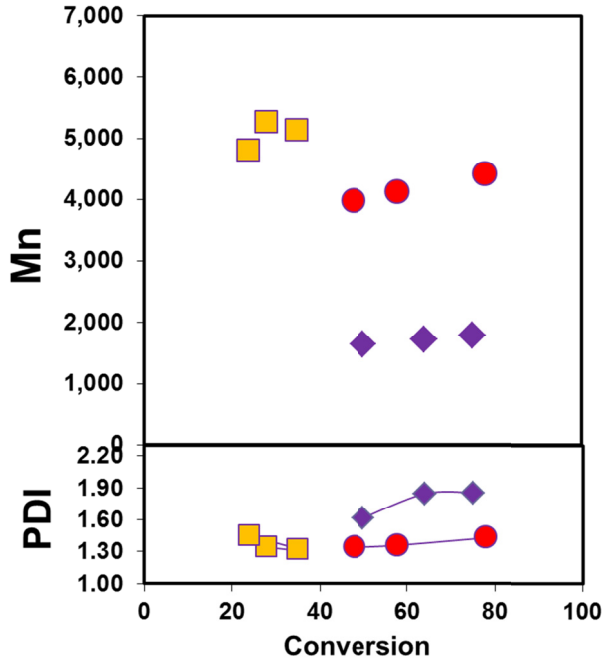

Figure 4.9 Effect of [VDF]/[PFBI] ratio on the M_n and PDI dependence on conversion in VDF-FRP : [VDF]/[PFBI]/[$Mn_2(CO)_{10}$] = 25/1/0.25 (◆), 50/1/0.25 (●), 100/1/0.25 (■).

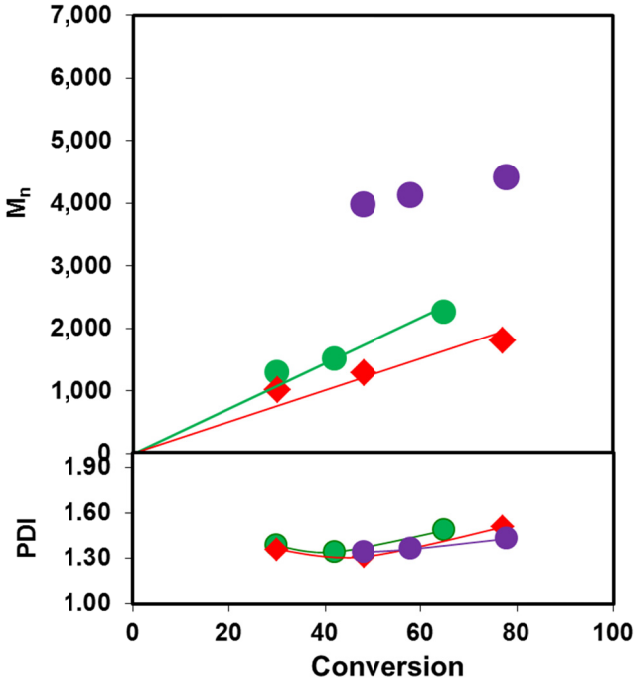

Figure 4.10: Demonstration of CRP at low activator amount for monofunctional initiators; M_n and PDI dependence on conversion in VDF-CRP: [VDF]/[PFBI]/[$Mn_2(CO)_{10}$] = 50/1/0.25 (●) [VDF]/[PFBI]/[$Mn_2(CO)_{10}$] = 50/1/0.1 (●) [VDF]/[Cl-CF_2CFCl-I]/[$Mn_2(CO)_{10}$] = 50/1/0.1 (◆).

4.3.3 Effect of [PFBI]/[$Mn_2(CO)_{10}$] ratio on k_p^{app} In Acetonitrile

The effect of [PFBI]/[$Mn_2(CO)_{10}$] on the rates of polymerization was also examined in acetonitrile. (Table 4.3) The results observed here corroborate those found in DMC. As the amount of $Mn_2(CO)_{10}$ is increased in turn the k_p^{app} increases as expected. Interestingly we see a lower limit at [PFBI]/[$Mn_2(CO)_{10}$] = 1/0.05. Lowering the manganese further resulted in no polymer formation. Conversely, above [PFBI]/[$Mn_2(CO)_{10}$] = 1/0.5 there appears to be a maximum reached with the k_p^{app} of polymerization, thus subsequent increases in the amount of manganese used affected the rate very little. Although in (exp. 5) [PFBI]/[$Mn_2(CO)_{10}$] = 1/0.75, the k_p^{app} appears to decrease, this example had a lower initiator efficiency, leading to an effective higher [VDF]/[PFBI] ratio. Ultimately, although the polymerizations do proceed in acetonitrile, and similar trends are observed, DMC is by far the superior polymerization solvent for VDF. This can be explained as previously discussed, DMC minimizes chain transfer, and both the monomer, polymer, and likely $Mn_2(CO)_{10}$ are more soluble in DMC than acetonitrile.

Table 4.3 Effect of [PFBI]/[$Mn_2(CO)_{10}$] ratio on the VDF polymerization in acetonitrile:

Exp #	Temp °C	[VDF]/[PFBI] /[$Mn_2(CO)_{10}$]	Solvent	Time (Hrs)	Conv (%)	k_p^{app} (h^{-1})	Mn	PDI	IE
1	40	50/1/0.0015	ACN	120	-	0			
2	40	50/1/0.015	ACN	120	-	0			
3	40	50/1/0.25	ACN	20	15%	0.0081	2,200	1.23	0.38
4	40	50/1/0.5	ACN	24	56%	0.0350	2,200	1.48	0.84
5	40	50/1/0.75	ACN	20	42%	0.0272	4,200	1.76	0.41
6	40	50/1/1	ACN	24	53%	0.0310	2,200	1.54	0.79
7	40	50/1/1.5	ACN	23	50%	0.0301	2,400	1.71	0.69
8	40	25/1/0.05	ACN	70	12%	0.0018	2,900	1.04	0.19
9	40	25/1/0.15	ACN	90	16%	0.0019	1,900	1.06	0.32
10	40	25/1/0.2	ACN	70	22%	0.0035	2,600	1.04	0.28

4.3.4 Effect of [VDF]/[Solvent] ratios on k_p^{app}

Upon investigation of the effect of [VDF]/[Solvent] ratios on the rates of polymerization, (Table 4.4, Figure 4.11) it can be seen that contrary to typical liquid monomers, increasing the amount of solvent while maintaining a constant VDF mass has little to no effect on the k_p^{app}. (Table 4.4, exp 1-6, ●) In fact a very slight increase of rate is observed when additional solvent is present and likely due to the decrease in volume of the head space above the reaction mixture in the pressure tube. Furthermore, while maintaining a constant ratio ([VDF]/[Solvent] = 0.34) with increasing scale (1.1g to 4.4g VDF) a 100-fold rate increase is observed.(Table 4.4, exp. 7, 9, 11, 13 ■) Additionally, these rates are similar to their analogous experiments in which the solvent is kept constant with increasing scale.(Table 4.4, exp. 8, 10, 12, ■, Figure 4.11,) This can be attributed to the monomer being gaseous, therefore the only effective means of increasing the concentration of the monomer in solution is to increase the internal pressure of the reaction vessel. (*i.e.* the addition of larger quantities of monomer). Attempts were carried out to further increase the rate of the polymerization with 6.6g and 8.8g levels; however the resulting pressures were above the rating of our equipment and caused a failure in the seals and bushing of the reaction vessels, as such subsequent reactions were limited to a maximum of 4.4g of VDF.

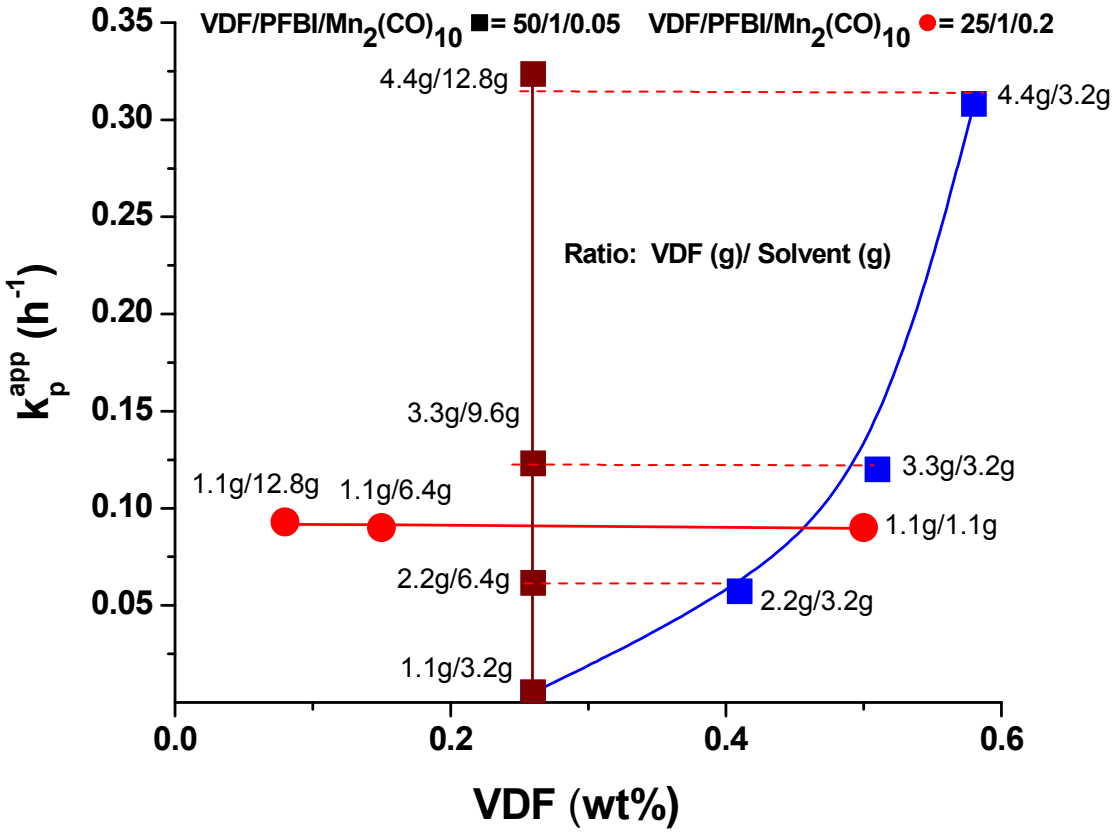

Figure 4.11 Dependence of k_p^{app} on the [VDF]/[DMC] ratio at 40°C under visible light irradiation.

Table 4.4 Effect of [VDF]/[DMC] ratio on the VDF polymerization:

Exp #	Temp °C	[VDF]/[PFBI] /[$Mn_2(CO)_{10}$]	Solvent	Time (h)	Conv (%)	k_p^{app} (h^{-1})	Mn	PDI	VDF (g)	Solvent (g)
1	40	25/1/0.2	DMC	18.0	80%	0.089	1,270	1.8	1.1	1.1
2	40	25/1/0.2	DMC	22.0	81%	0.074	1,700	1.41	1.1	1.1
3	40	25/1/0.2	DMC	18.0	80%	0.089	1,220	1.58	1.1	6.4
4	40	25/1/0.2	DMC	22.0	87%	0.094	2,300	1.49	1.1	6.4
5	40	25/1/0.2	DMC	18.0	83%	0.098	1,670	1.47	1.1	12.8
6	40	25/1/0.2	DMC	22.0	87%	0.092	2,500	1.41	1.1	12.8
7	40	50/1/0.05	DMC	69.5	30%	0.005	870	1.33	1.1	3.2
8	40	50/1/0.05	DMC	7.0	33%	0.057	1,110	1.48	2.2	3.2
9	40	50/1/0.05	DMC	7.3	36%	0.062	1,100	1.44	2.2	6.4
10	40	50/1/0.05	DMC	4.0	38%	0.120	N/A	N/A	3.3	3.2
11	40	50/1/0.05	DMC	4.0	38%	0.123	N/A	N/A	3.3	9.6
12	40	50/1/0.05	DMC	2.3	50%	0.308	1,840	1.63	4.4	3.2
13	40	50/1/0.05	DMC	2.3	60%	0.407	2,100	1.68	4.4	12.8

4.3.5 Chain end Activation of ~CH_2-CF_2-I and ~CF_2-CH_2-I

While ethyleneation,[94] azidation,[95] and block copolymer synthesis via ATRP[96] or IDT[11] have been attempted previously with iodine terminated PVDF, all such undertakings were essentially flawed due to the failure of the respective chemistries to activate the stronger and dominant -CF_2-CH_2-I termini. Thus, the products were always inseparable, ill-defined mixtures of PVDF-CF_2-CH_2-I homopolymer, and PVDF-CH_2-CF_2-*b*-P_m block copolymer. We have recently demonstrated the $Mn_2(CO)_{10}$ quantitative activation of both -CH_2-CF_2-I and -CF_2-CH_2-I chain ends, and the subsequent synthesis of well-defined block copolymers.[4] In an attempt to expand this methodology further, the metal carbonyl compounds; $Co_2(CO)_8$, $Mo(CO)_6$, $Fe(CO)_5$, $Cp^*_2Cr(CO)_4$, $Mn_2(CO)_{10}$, $Re_2(CO)_{10}$, $Cp_2Mo_2(CO)_6$, $Cp_2W_2(CO)_6$, and $Cp_2Fe_2(CO)_4$ were evaluated as -CH_2-CF_2-I and -CF_2-CH_2-I activators. The screening was done by monitoring the disappearance of the resonances associated with the PVDF-CF_2-C*H*$_2$-I and PVDF-C*H*$_2$-CF_2-I chain ends (Figure 4.12a*;* c δ = 3.66 and c' δ = 3.87 ppm) while looking for the appearance of -CH_2-CF_2*H* and -CF_2-C*H*$_3$, **d**, **d'**. (Figure 4.12g)

A typical PVDF-I sample is presented in (Figure 4.12a). In addition to acetone (δ = 2.05 ppm),[97] the head-to-tail (HT) -CF_2-[C*H*$_2$-CF_2]$_n$-CH_2-, **a** and head to head (HH), -CF_2-C*H*$_2$-C*H*$_2$-CF_2- **a'** resonances [94,98] are observed at δ = 2.8-3.1 ppm and respectively δ = 2.2-2.3. Resonance **b** (δ = 3.25 ppm) verifies the R_F-C*H*$_2$-CF_2- connectivity with the first polymer unit. The PVDF-C*H*$_2$-CF_2-I **c** and PVDF-CF_2-C*H*$_2$-I **c'**, iodine chain ends are seen at δ = 3.62 ppm and respectively δ = 3.87 ppm[4].

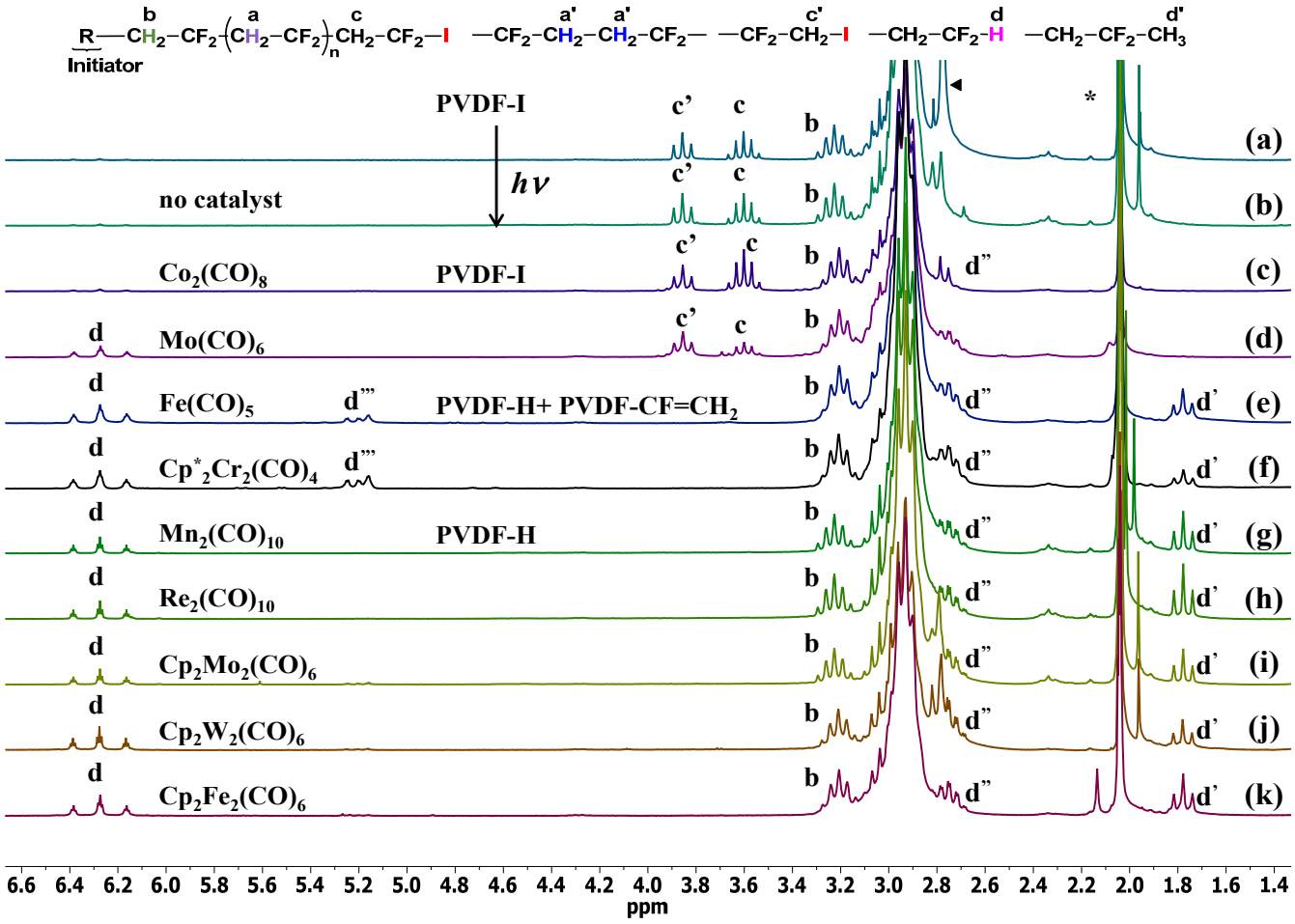

Figure 4.12. 500-MHz ^{1}H-NMR spectra in d_6-acetone. Effect of metal carbonyls on the photo-activation of polyvinylidene fluoride iodine terminated chain ends. (a) PVDF-I (b) No Metal Carbonyl (c) $Co_2(CO)_8$ (d) $Mo(CO)_6$ (e) $Fe(CO)_5$ (f) $Cp^*_2Cr(CO)_4$ (g) $Mn_2(CO)_{10}$ (h) $Re_2(CO)_{10}$ (i) $Cp_2Mo_2(CO)_6$ (j) $Cp_2W_2(CO)_6$ (k) $Cp_2Fe_2(CO)_4$ * = acetone.

While VDF-FRP terminates primarily by the recombination of the 1,2-units (eq. 10),[1,7-11,99] in VDF-IDT, trace termination by H transfer (eq. 11, 12), (i.e. -CH_2-CF_2-H and -CF_2-CH_3, peaks **d**, **d'**) can be seen at δ = 6.30 ppm and 1.80 ppm.[98c](Figure 4.12a)

As such, in the absence of another monomer, complete iodine chain end activation, upon treatment with stoichiometric metal carbonyl, followed by H transfer to the solvent should result in the disappearance of the resonances **c** and **c'** and their conversion into **d** and respectively **d'** and a resolved –CH_2-CF_2-C*H*$_2$-CF_2-H **d"**, δ = 2.77 ppm.[98e] A control experiment (Figure 4.12b) establishes that at 40°C, and for t > 24 h, there is no photoinduced homolysis of the iodine chain ends in the absence of a metal carbonyl. Spectra Figure 4.12c-k detail the effect of each individual compound examined.

Interestingly, while some of the metal carbonyl compounds, ($Fe(CO)_5$, $Cp_2Fe_2(CO)_6$, or $Cp^*_2Cr_2(CO)_4$) failed to generate polymer in conjunction with R_F-I initiators at substoichiometric levels, at stoichiometric amounts with respect to PVDF-I, complete activation was observed in ($Fe(CO)_5$, $Cp^*_2Cr_2(CO)_4$, $Mn_2(CO)_{10}$, $Re_2(CO)_{10}$, $Cp_2Mo_2(CO)_6$, $Cp_2W_2(CO)_6$, and $Cp_2Fe_2(CO)_4$). Partial activation of PVDF-CH_2-CF_2-I with no activation of the stronger PVDF-CF_2-CH_2-I was exhibited by $Mo(CO)_6$ while no activation at all was seen with $Co_2(CO)_8$. In an effort to be thorough some metal (0) and other compounds were tested as well(Figure 4.A9-10) but not examined further.

As experiments (Table 4.1 exp. 5-7, 17-20, 22-25, 27-30) show that no polymerization is obtained from any R_f-I source with $Fe(CO)_5$, $Cp_2Fe_2(CO)_6$, $Cp^*_2Cr_2(CO)_4$, or $Co_2(CO)_8$ it was expected that these results would simply correlate with the chain end activation experiments (*i.e.* no polymer-I activation), this was indeed observed with $Co_2(CO)_8$. However, it was not the case with $Fe(CO)_5$, $Cp_2Fe_2(CO)_6$, or $Cp^*_2Cr_2(CO)_4$, as all three of these materials indeed were able to activate completely the PVDF-I halide chain ends. This apparent contradiction can be explained via the stoichiometry of the reagents, i.e. under polymerization conditions a typical

[I]/[$Mt_x(CO)_yL_z$] ratio of [1]/[0.1-0.2] was employed, while [1]/[1] was used in the activation of the polymer halide chain ends. Therefore the inability to initiate VDF polymerization was attributed to these catalysts having much lower activity. Additionally, in the R_F-I initiated polymerizations; there is a critical radical concentration or rate of I abstraction that must be met in order for polymerization to occur. This critical rate is one which is greater than the rate of photolysis of R_f-I under constant low power visible light irradiation. If the radical generation via metal carbonyl is slower than that of the R_f-I homolysis, there will be a consumption of the activator resulting in an iodine concentration greater than that of the metal carbonyl activator in solution leading to the persistent radical effect, thus inhibiting the polymerization. This presence of I_2 in solution is the likely explanation for the lack of polymerization in the $Cp_2Fe_2(CO)_6$ or $Cp^*_2Cr_2(CO)_4$ experiments (Table 4.1, exp. 17-20, 27-30), as well as the rapid decrease in polymerization rate discussed previously for $Cp_2Mo_2(CO)_6$ as the transformation of trans to gauche isomers subsequently decreases the rate of radical generation. While, although there is not a complete stop in the formation of radicals, but rather a drastic decrease in their generation, to which we end up with a higher concentration of free iodine in the polymerization. Unfortunately in all our reactions the highly colored solutions do not allow us to easily verify whether there was in fact free iodine present visually. We know from control experiments that irradiation of PVDF-I solutions yields no observable photoinduced PVDF-I hemolytic cleavage. (Figure 4.12b) As such, the slowly generated radicals can still continue to consume quantitatively all the iodine from the chain ends.

Additionally the resonance assigned **d'''** δ = 5.2 ppm has an interesting origin and helps to explain one of the more puzzling aspect of the chain end activation and subsequent block copolymerization initiated from PVDF-I. The origins of resonance **d'''**, enabled the ability to develop an explanation for this phenomenon. It is know that $Fe(CO)_5$, will in fact react directly

with R_f-I compounds via an oxidative insertion of the metal carbonyl into the CF_2-I bond to yield R_f-$Fe(CO)_5$-I which are relatively stable compounds, and would indeed prevent the formation of the required metalloradical needed to start the initiation process.[85,86] It is evidenced previously that PVDF-I has two distinct chain ends, ~CF_2-CH_2-I and ~CH_2-CF_2-I, thus it is very likely we are in fact obtaining the oxidative insertion product with $Cp^*_2Cr_2(CO)_4$ and $Fe(CO)_5$. However, due to the relative stability of the oxidative insertion products (R_f-$Mt(CO)_x$-I > ~CH_2-CF_2-$Mt(CO)_x$-I >> ~CF_2-CH_2-$Mt(CO)_x$-I) it is very likely the ~CF_2-CH_2-$Mt(CO)_x$-I can quickly decompose by β-fluoride elimination yielding a metal fluoride and ~CF=C*H*$_2$ (**d'''** δ = 5.20 ppm). Upon aqueous workup of the reaction, hydrolysis of the more stable ~CH_2-CF_2-$Mt(CO)_x$-I would then yield -CH_2-CF_2-C*H*$_2$-CF_2-H **d"** δ = 2.77 ppm. This is supported by the NMR spectra (Figure 4.12 e-f,) where we indeed see the resonances associated with the elimination and in the $^{19}F\{^1H\}$ HETCOR spectra.(Figure 4.13) This allows us to pinpoint the resonances in the ^{19}F-NMR which correspond to the unsaturated chain ends derived from the elimination. Additionally, while insertion to R_{alk}-I and R_F-I exist, these represent the first examples of $Fe(CO)_5$ insertion into semifluorinated alkyl iodides, which can be envisioned as means of addition reactions to other substrates, such as aldehydes.[100](Barbier type addition to electrophilic substrates)

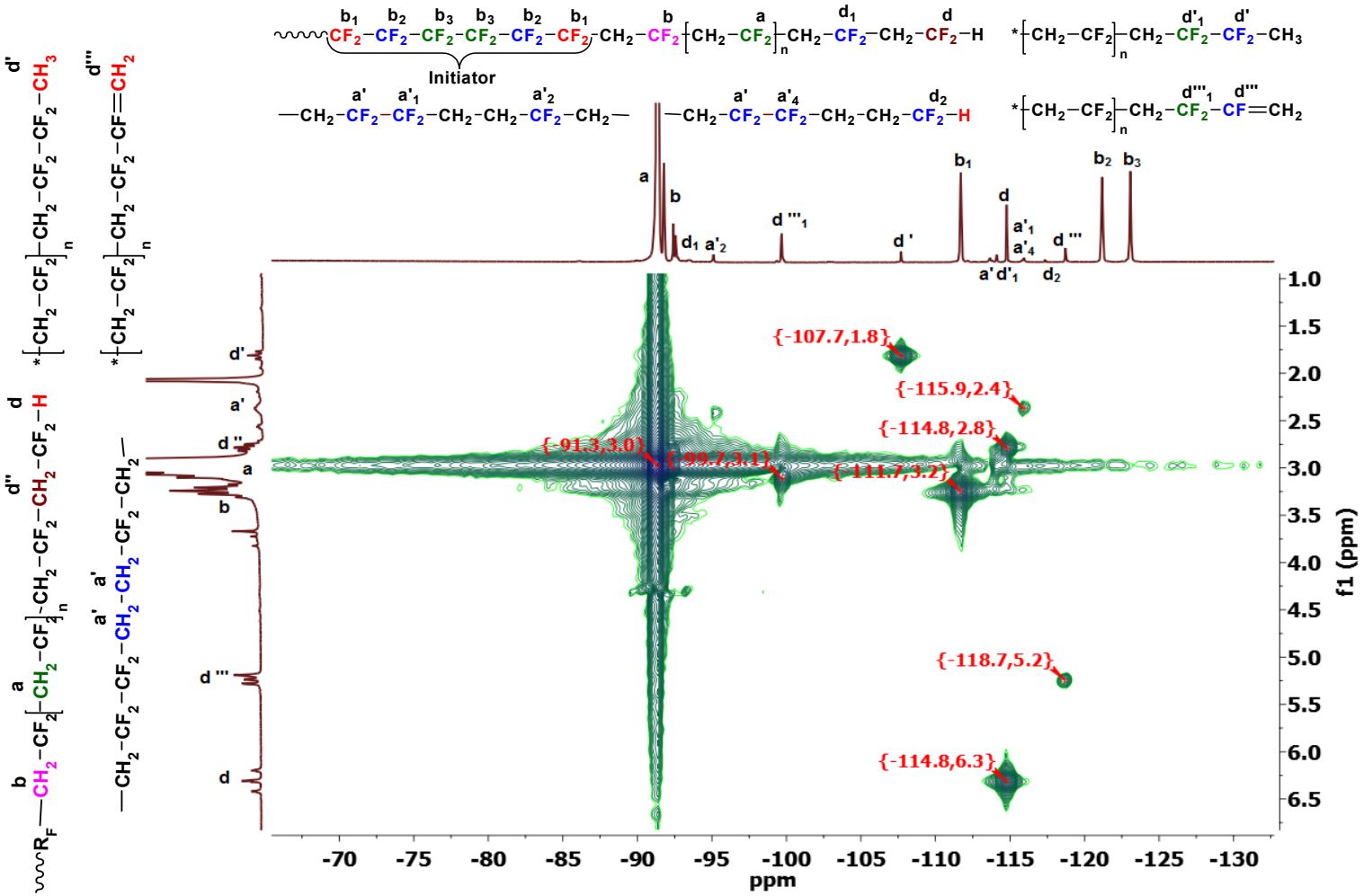

Figure 4.13. $^{19}F\{^{1}H\}$ Heteronuclear Correlation Spectra, β-fluoride elimination from $Fe(CO)_5$

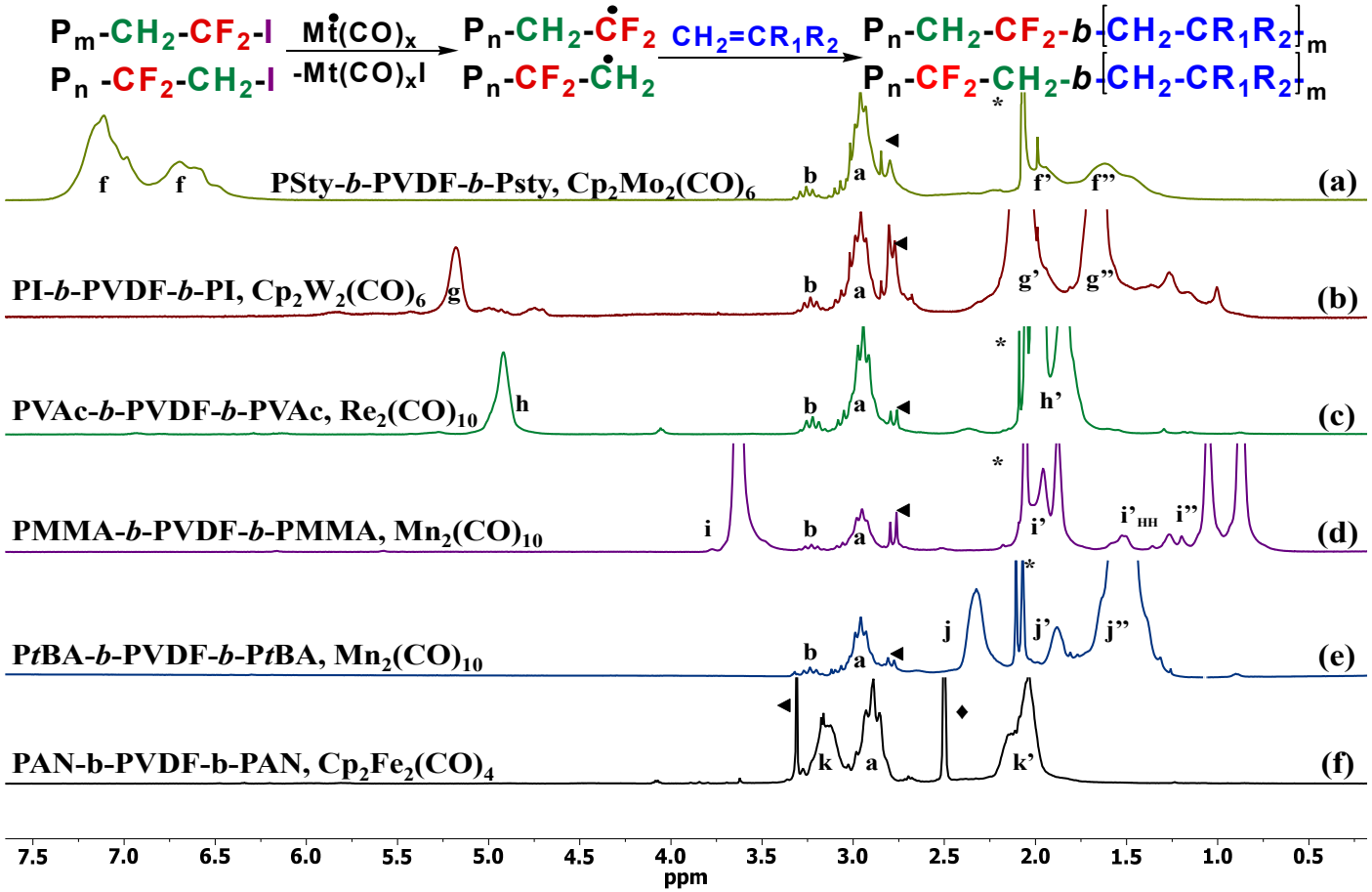

Figure 4.14 500 MHz ^{1}H-NMR spectra in d_6-acetone except PAN in d_6-DMSO of various PVDF block copolymers using selected metal carbonyls shown to give complete activation of PVDF-I chain ends. (a) $Cp_2Mo_2(CO)_6$, (b) $Cp_2W_2(CO)_6$, (c) $Re_2(CO)_{10}$, (d-e) $Mn_2(CO)_{10}$, (f) $Cp_2Fe_2(CO)_4$. ◀ = H_2O, * = acetone, ♦ = DMSO.

4.3.6 Synthesis of Well-Defined PVDF Block Copolymers

Block Copolymers from Alkenes: Subsequently, carrying out the chain end activation reactions in the presence of a radically polymerizable alkene (styrene, isoprene, vinyl acetate, methyl methacrylate, methyl acrylate, t-butyl acrylate, and acrylonitrile) and the metal carbonyls shown, to quantitatively activate both ~CF_2-CH_2-I and ~CH_2-CF_2-I, ($Mn_2(CO)_{10}$, $Re_2(CO)_{10}$, $Cp_2Mo_2(CO)_6$, $Cp_2W_2(CO)_6$ and, $Cp_2Fe_2(CO)_4$), leads to further examples of well-defined, ABA-type PVDF block copolymers. (Figure 4.14 a-f) Evidence of block copolymer synthesis is presented, and in addition to molecular weight increases via seen via GPC there is no longer the tell-tale sign of PVDF homopolymer in the refractive index signal (i.e. negative trace). The DSC thermographs (Figure 4.A7) of selected examples show typical glass transitions associated with each polymer. However, due to the connectivity and relatively low molecular weights (needed in order to accurately examine NMR spectra), PVDF is slightly higher than for typical bulk homopolymer, while the other blocks are lower than for their typical homopolymers. The resonances associated with each alkene, styrene (**f**, **f'**), isoprene (**g**, **g'**, **g''**), vinyl acetate (**h**, **h', h''**), methyl methacrylate (**i**, **i'$_{HH}$, I''**), *t*-butyl acrylate (**j**, **j', j''),** and acrylonitrile (**k**, **k'**) initiated from *both* PVDF halide chain ends are presented (Figure 4.14 a-f). Additionally, hydrolysis of the P*t*BA-*b*-PVDF-*b*-P*t*BA block copolymer was demonstrated (Figure 4.A8) by the disappearance of resonance **j''** associated with the tertiary butyl group, yielding the first example of the amphiphilic block copolymer PAA-*b*-PVDF-*b*-PAA copolymer. While here the metal carbonyls simply act as a photoactivator and there is no IDT, control of the block copolymerization can be envisioned by other CRP methods.

$^{19}F\{^1H\}$ Heteronuclear Correlation Spectra Analysis of PVDF Block Copolymers.

Having PVDF block copolymers with a nonfluorinated or semi-fluorinated second block afford us the unique situation and first examples, demonstrating very clearly, via ^{19}F and $^{19}F\{^1H\}$

HETCOR analysis, the exact connectivity between the two blocks by NMR.(Figure 4.15-4.20, 4.24-4.25) Examining the available and known chemical shifts for various PVDF structures in fluorine NMR allowed for the development of this method.[102] As such, ^{19}F-NMR demonstrates the block copolymerization by the disappearance and conversion of the PVDF-CH_2-***CF_2***-I ***c, c_1, c_2*** and PVDF-***CF_2***-CH_2-I ***c'*** and ***c'_1*** iodine chain ends into the ***a'_4***, δ = -90 - 93 ppm and respectively ***a'_5***, δ = -114.0 ppm and ***a'_6*** δ = -116.22 ppm resonances associated specifically with the block connectivity. Upon examination of the cross peak in the 2D spectra it can be seen that all the unique protons that would normally be associated with the connectivity resonances in fact overlap with either polymer main chain resonances. Thus, although proton NMR does not allow the ability to demonstrate the connectivity, in conjunction with fluorine NMR we have provided a valuable tool in the understanding and characterization of these block copolymers. While the results were similar in all HETCOR figures, there are some slight variations in where some of the chemical shift appear and whether a cross peak is highly visible or more pronounced. For instance, polyisoprene (Figure 4.16) has six possible modes of addition from the PVDF-I starting material, thus broadening the possible chemical shifts, the use of starting material with a low content of CF_2-CH_2-I can make it difficult to see a'_5 and a'_6 resonances and subsequent cross peaks. Finally the deuterated solvent used will have an effect on these chemical shifts as well, as seen in Figure 4.20, where DMSO was required to dissolve the PAN-b-PVDF-b-PAN block copolymer completely; there is a shift present *vs* what is typically seen in d_6-acetone.

Table 4.5 Characterization of Metal Carbonyl Photomediated Synthesis of PVDF Block Copolymers									
Exp.	Monomer	PVDF-I M_n	PDI	[M]/[PVDFI]/ [$Mn_2(CO)_{10}$]	Conv (%)	Composition M/VDF	M_n	PDI	Temp (C)
1	Styrene	1,500	1.38	100/1/1	56	58/42	5,900	1.49	90
2	Isoprene	2,100	1.28	200/1/1	12	62/38	4,300	1.48	100
3	Vinyl acetate	2,100	1.28	100/1/1	58	56/44	5,400	1.52	40
4	Methyl methacrylate	2,100	1.28	100/1/1	28	67/33	7,800	1.65	90
5	*t*-Butyl acrylate	2,100	1.28	50/1/1	40	64/36	8,400	1.75	60
6	Acrylonitrile	2,100	1.28	175/1/1	30	66/34	5,200	1.85	40
All in DMAC from I-PVDF-I samples.									

The NMR assignments corresponding to the copolymers from Figure 4.14 are as follows:

Polystyrene:
f, δ = 6.4-7.4 ppm, -CH_2-CH(C_6***H_5***)-,
f' δ = 1.94 ppm , -CH_2-C***H***(C_6H_5)-,
f" δ = 1.63 ppm , -C***H_2***-CH(C_6H_5)-,

Polyisoprene:
g δ = 5.44 ppm -CH_2-C***H***=C***H***-CH_2- 1,4-*cis* and -*trans*;
g δ = 5.6 ppm, 1,2 -CH_2-CH(C***H***=CH_2)- and δ = 4.99 ppm, -CH_2-CH(CH=C*H_2*)-;
g' δ = 2.1 ppm -C*H_2*-CH=CH-C***H_2***- and -CH_2-C***H***(CH=CH_2)-
g" δ = 1.3-1.5 ppm, -C***H_2***-CH(CH=CH_2)-

Poly(vinyl acetate):
h δ = 4.92 ppm, -CH_2-C***H***($OCOCH_3$)-
h' δ = 1.98 ppm, -CH_2-CH(OCOC***H_3***)-
h' δ = 1.83 ppm, -C*H_2*-C***H***($OCOCH_3$)-,

Poly(methyl methacrylate):
i δ = 3.67 ppm, -CH_2-C(CH_3)(COOC***H_3***)-,
i' δ = 1.8-1.9 ppm, -C***H_2***-C(CH_3)($COOCH_3$)-,
i" δ = 0.8-1.4 ppm, -CH_2-C***(CH_3)***($COOCH_3$)-,

Poly(t-butyl acrylate):
j δ = 2.3 ppm, -C***H_2***-CH($COOC(CH_3)_3$)-,
j' δ = 1.8 ppm, -CH_2-C***H***($COOC(CH_3)_3$)-,
j" δ = 1.4 ppm, -CH_2-CH($COOC(CH_3)_3$)-,

Polyacrylonitrile:
k δ = 3.0-3.2 ppm, -CH_2-C***H***(CN)-
k' δ = 1.9-2.2 ppm, -C***H_2***-CH(CN)-

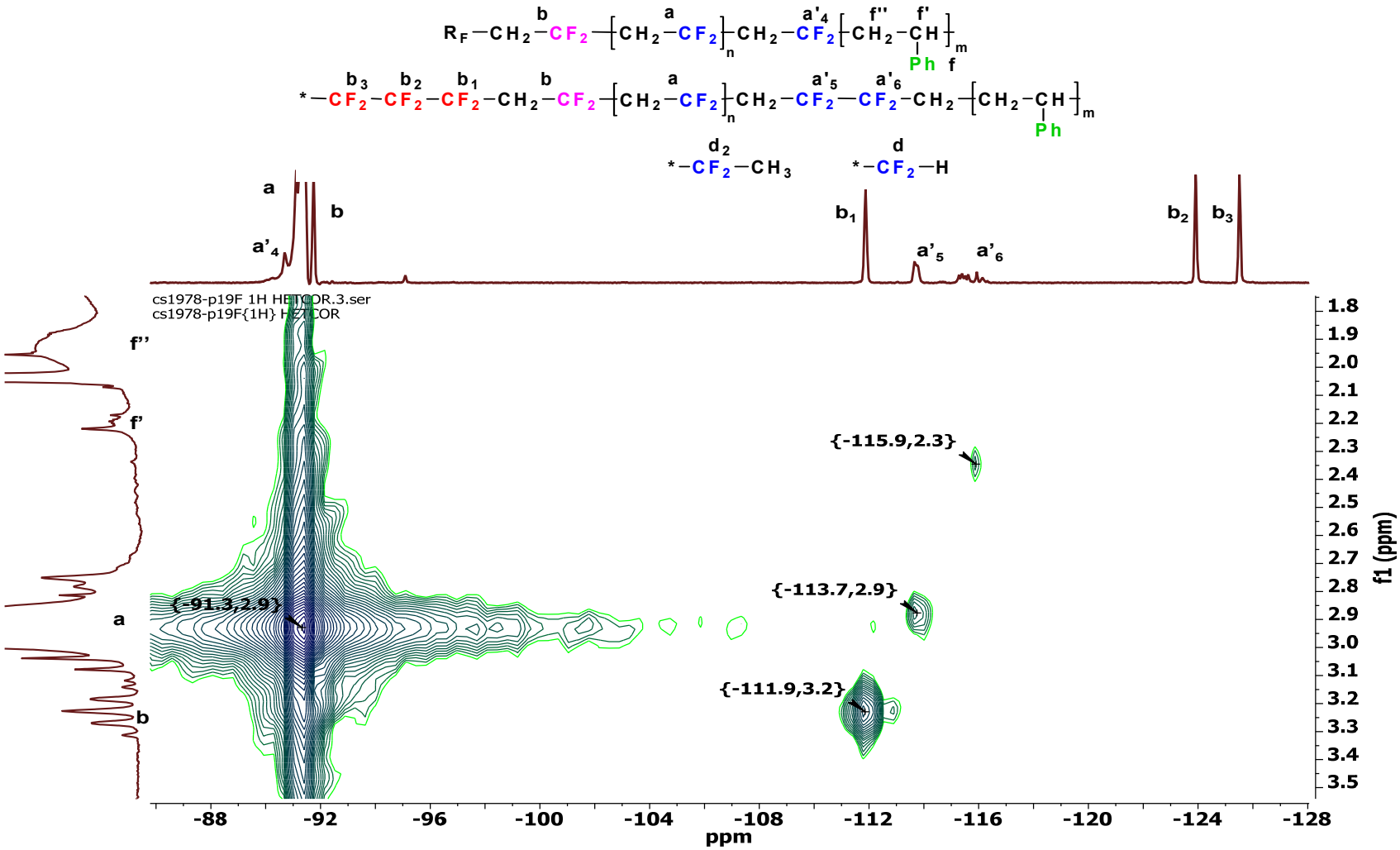

Figure 4.15. $^{19}F\{^{1}H\}$ Heteronuclear Correlation Spectra of PSty-PVDF- PSty Block Copolymer, Demonstration of Connectivity

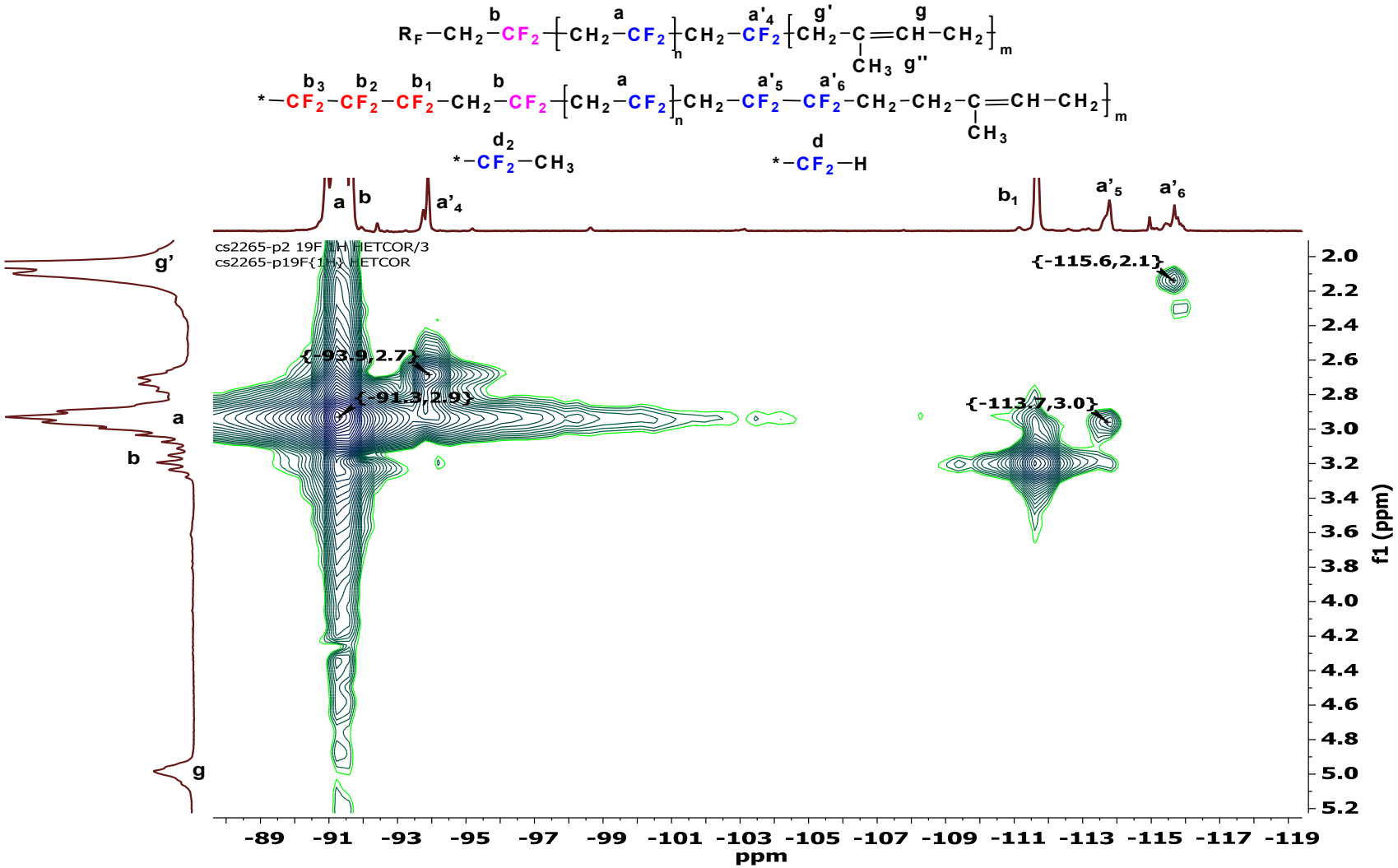

Figure 4.16. $^{19}F\{^{1}H\}$ Heteronuclear Correlation Spectra of PI-PVDF-PI Block Copolymer, Demonstration of Connectivity

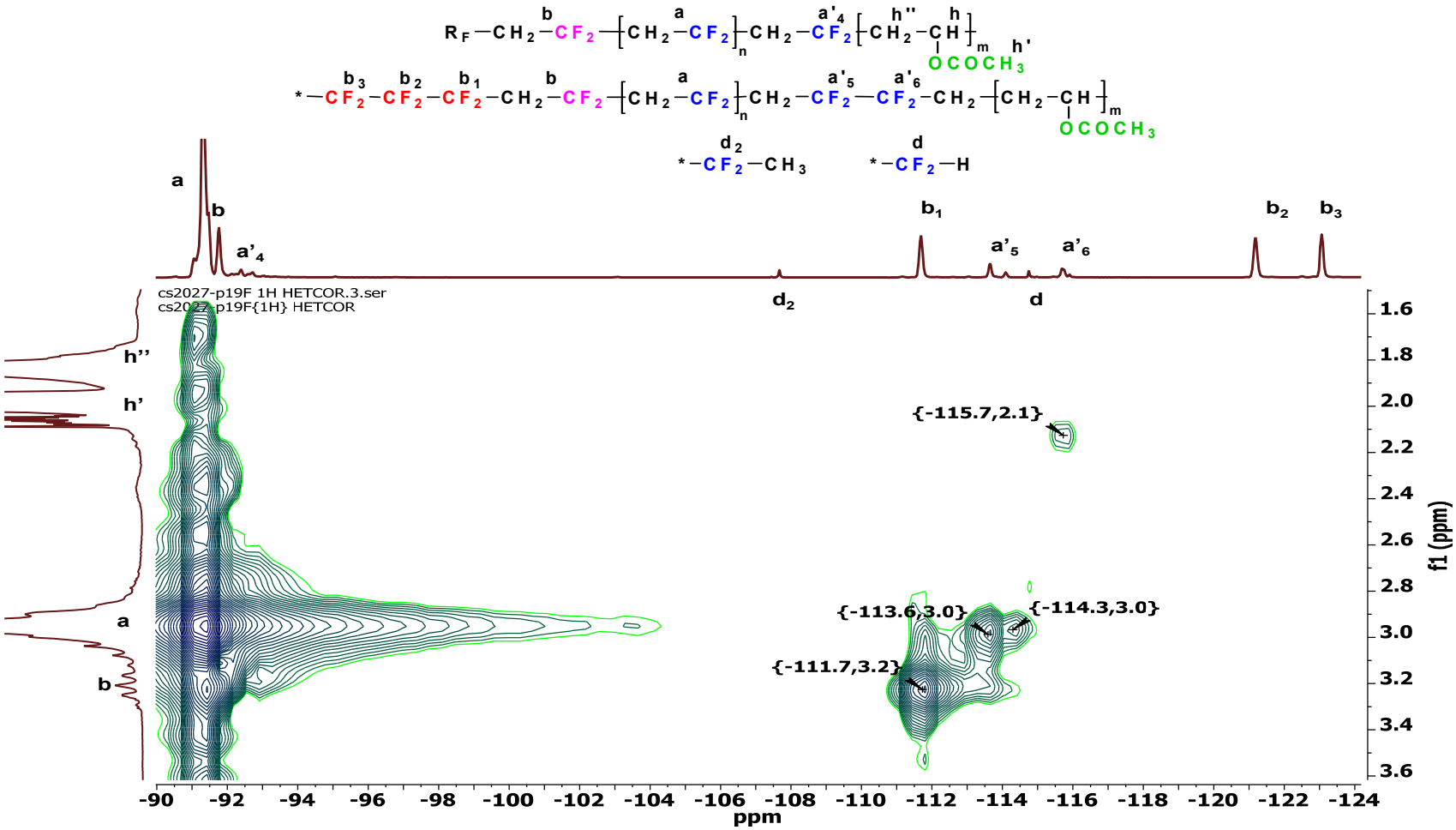

Figure 4.17. $^{19}F\{^{1}H\}$ Heteronuclear Correlation Spectra of PVAc-PVDF-PVAc Block Copolymer, Demonstration of Connectivity.

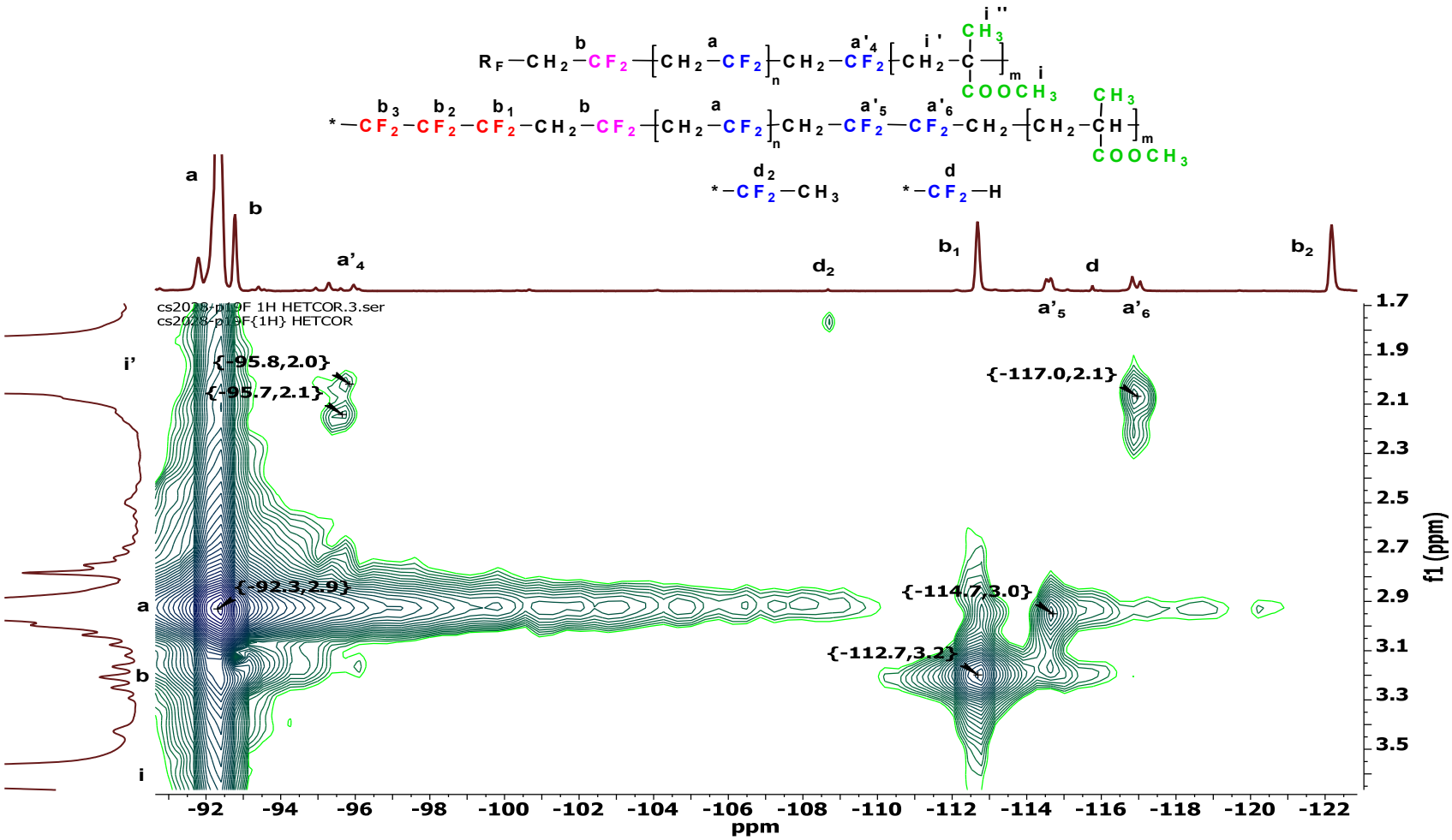

Figure 4.18. $^{19}F\{^{1}H\}$ Heteronuclear Correlation Spectra of PMMA-PVDF-PMMA Block Copolymer, Demonstration of Connectivity

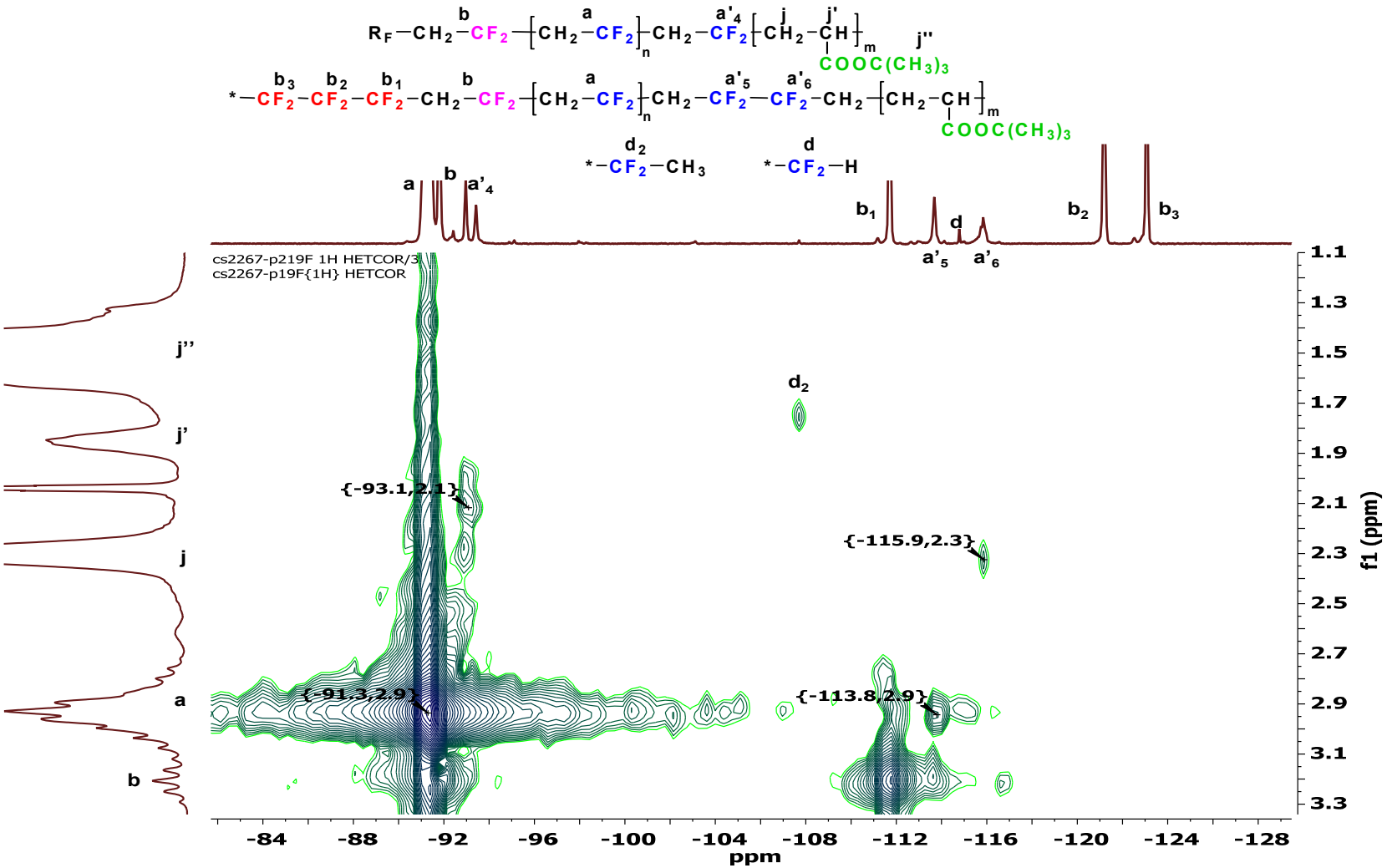

Figure 4.19. $^{19}F\{^{1}H\}$ Heteronuclear Correlation Spectra of P*t*Bu-PVDF- P*t*Bu Block Copolymer, Demonstration of Connectivity

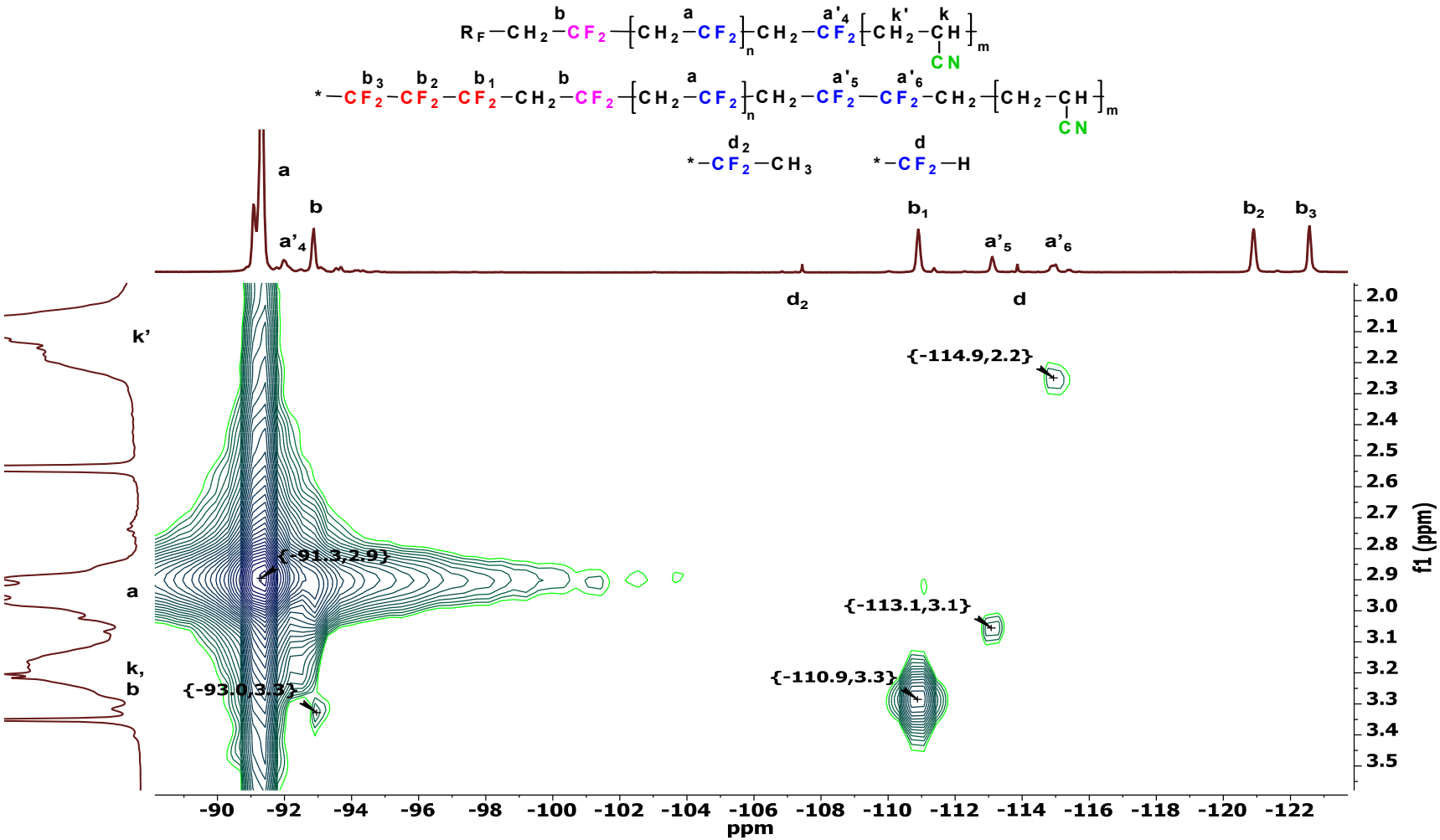

Figure 4.20 $^{19}F\{^{1}H\}$ Heteronuclear Correlation Spectra of PAN-PVDF-PAN Block Copolymer, Demonstration of Connectivity.

Block Copolymers from Fluorinated Side Chain Alkenes: Two CF_3-containing monomers (CH_2=C(CH_3)(COO-CH_2-CF_3), TFEMA and CH_2=C(CF_3)(COO-CH_3) MTFMA) were selected for this example. The block copolymerization is demonstrated first by the increase in molecular weight from M_n = 1,400 for CF_3-PVDF-I to M_n = 6,500 for PVDF-*b*-PTFEMA and respectively M_n = 2,500 for PVDF-*b*-PMTFMA, and second, by the presence of the resonances associated with the new polymer structures, but most importantly, by the disappearance of the PVDF-I chain end resonances and their replacement with resonances associated with the VDF-TFEMA and VDF-MTFMA connectivity, as follows:

^{1}H-NMR: In addition to typical PVDF resonances, the block copolymerization is first demonstrated (Figure 4.21) by the disappearance of the PVDF-CH_2-CF_2-I ***c*** (δ = 3.62 ppm, *q*, $^3J_{HF}$ = 16 Hz) and PVDF-CF_2-CH_2-I ***c'*** (δ = 3.87 ppm, t, $^3J_{HF}$ = 18.2 Hz) peaks, and by the presence of new resonances associated with the PTFEMA block *i.e.* ***f***, δ = 4.5-4.75 ppm, -CH_2-C(CH_3)(COO-***CH_2***-CF_3)-, ***f'$_{HT}$***, δ = 1.96-2.25 ppm and ***f'$_{HH}$***, δ = 1.65-1.78 ppm, -***CH_2***-C(CH_3)(COO-CH_2-CF_3)-, and ***f''***, δ = 0.86-1.43 ppm, -CH_2-C(***CH_3***)(COO-CH_2-CF_3)-, and respectively with MTFMA block, such as ***g***, δ = 3.62-3.90 ppm -CH_2-C(CF_3)(COO-***CH_3***)- and ***g'***, δ = 2.63 ppm, -C***H_2***-C(CF_3)(COO-CH_3)-.

^{19}F-NMR: Additionally, ^{19}F-NMR (Figure 4.22-4.23) demonstrates the block copolymerization by the disappearance and conversion of the PVDF-CH_2-***CF_2***-I ***c, c$_1$, c$_2$*** and PVDF-***CF_2***-CH_2-I ***c'*** and ***c'$_1$*** iodine chain ends into the ***a'$_4$***, δ = -94.93 ppm and ***a''$_4$*** δ = -92.5 ppm and respectively ***a'$_5$***, δ = -116.0 ppm and ***a'$_6$*** δ = -116.22 ppm resonances associated with the block connectivity, and by the resonances corresponding to the PTFEMA and PMTFMA CF_3 group, *i.e.* ***f***, δ = -72.2 to -73.71 ppm, -CH_2-C(CH_3)(COO-CH_2-***CF_3***)-, and ***g$_{HH}$***, δ = -64.2 to -66.9 ppm and ***g$_{HT}$***, δ = -67.01 to -69.4 ppm, -CH_2-C(***CF_3***)(COO-CH_3)-. Also included, are the 2D-HETCOR NMR spectra further showing the connectivity and correlations between the both blocks**.**

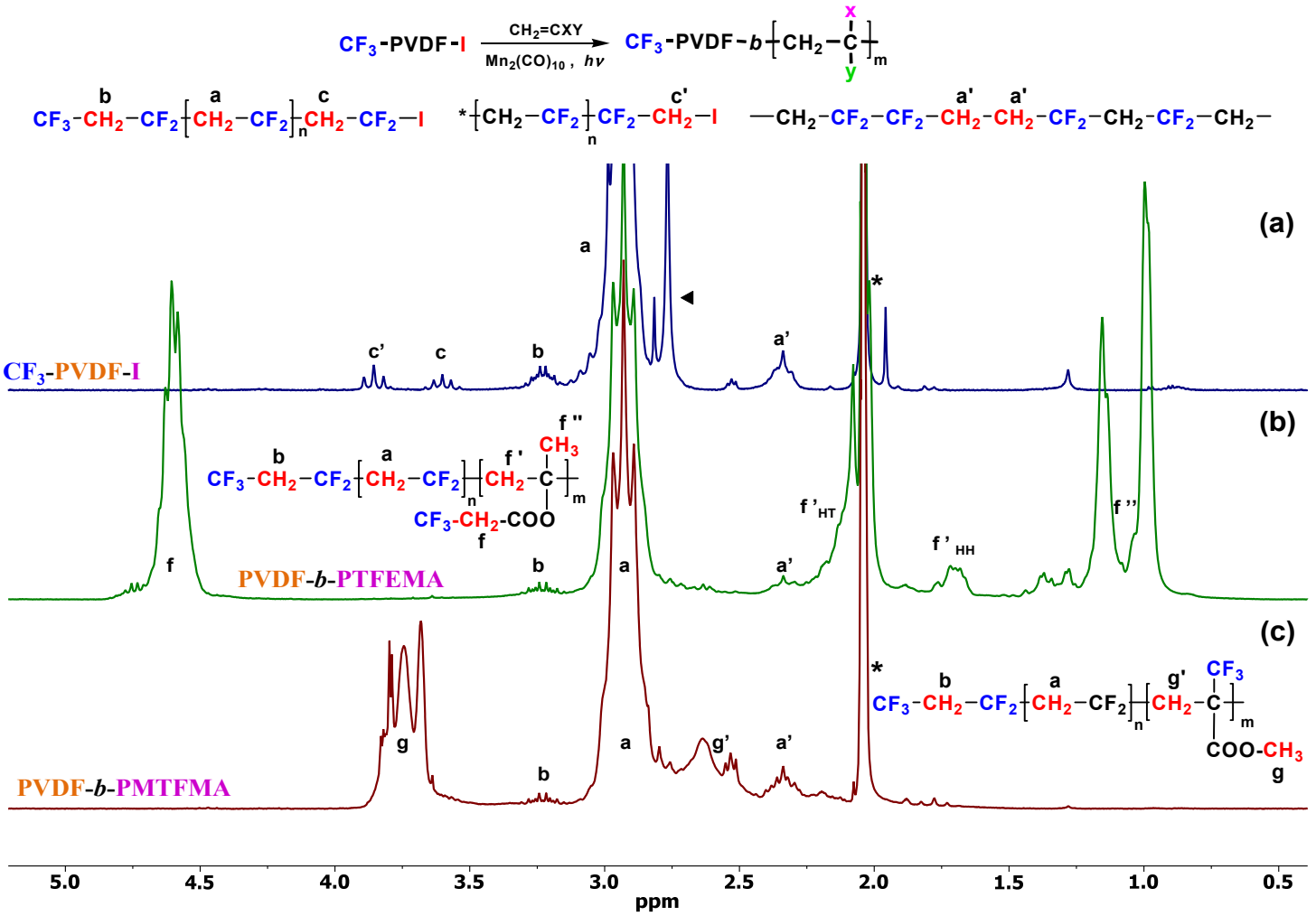

Figure 4.21 ^{1}H-NMR of PVDF-I and of the corresponding block copolymers with TFEMA and respectively, with MTFMA.

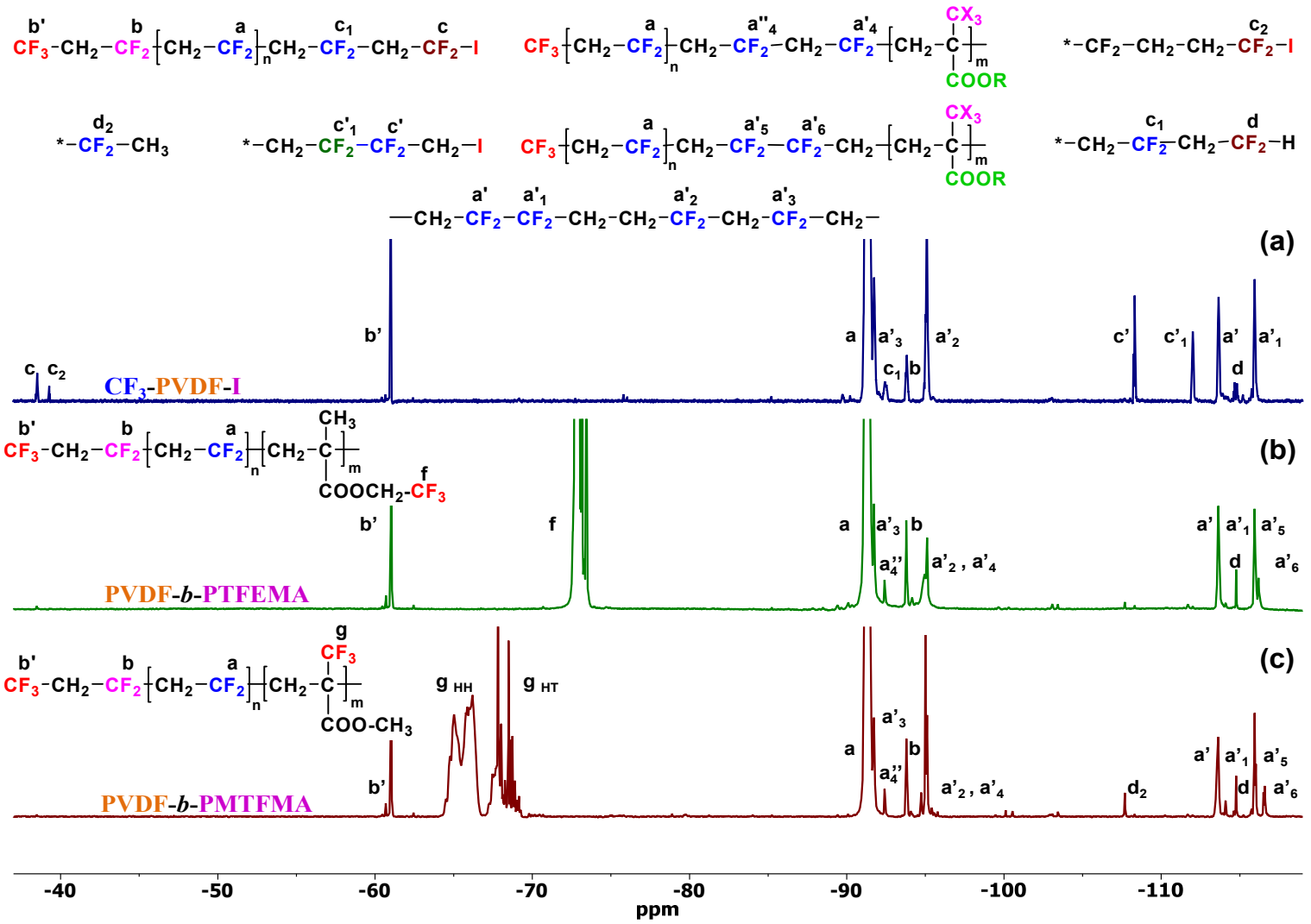

Figure 4.22 ^{19}F-NMR of PVDF-I and of the corresponding block copolymers with TFEMA and respectively, with MTFMA.

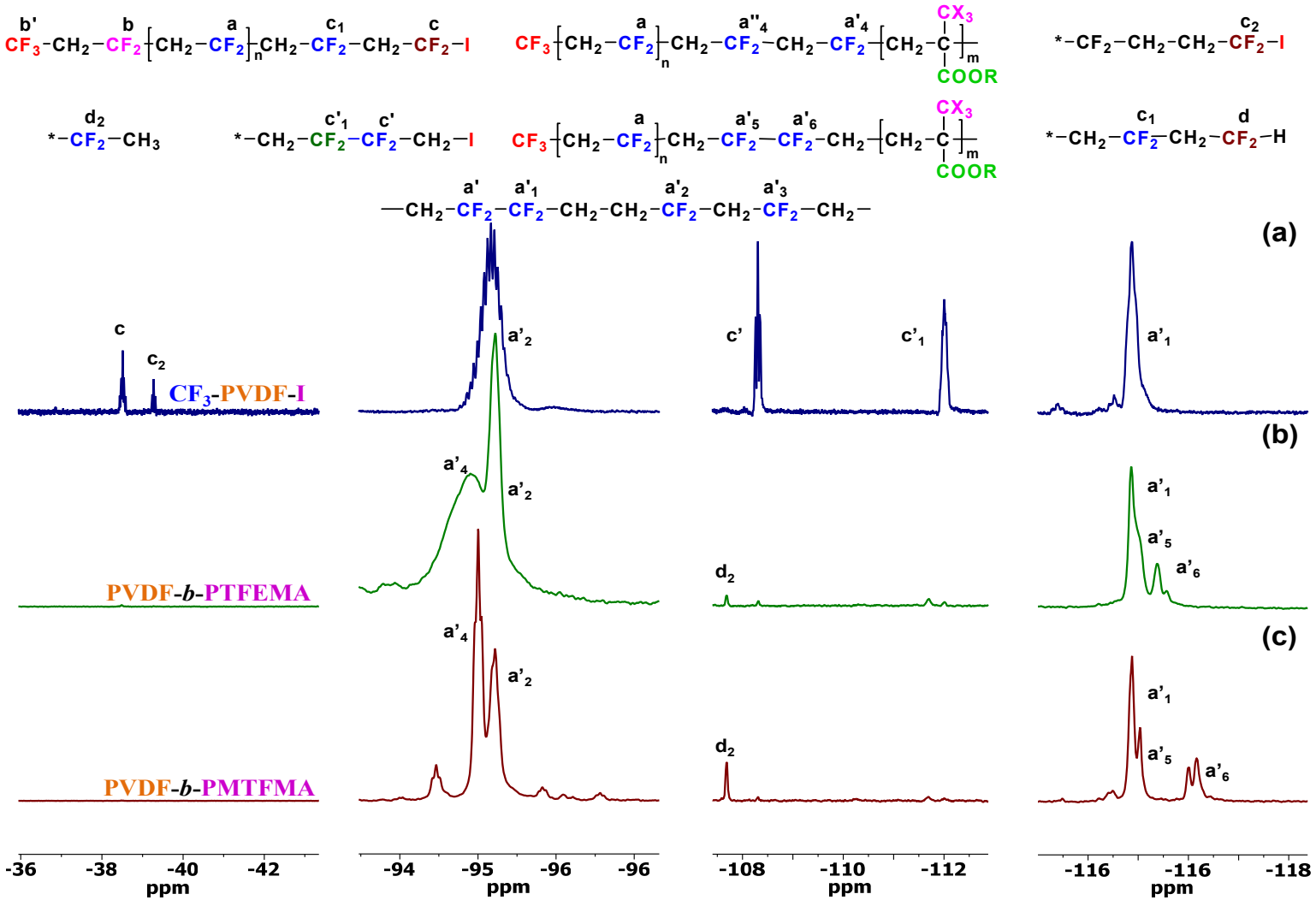

Figure 4.23 Expansion of the ^{19}F-NMR of PVDF-I and of the block copolymers with TFEMA and respectively, with MTFMA.

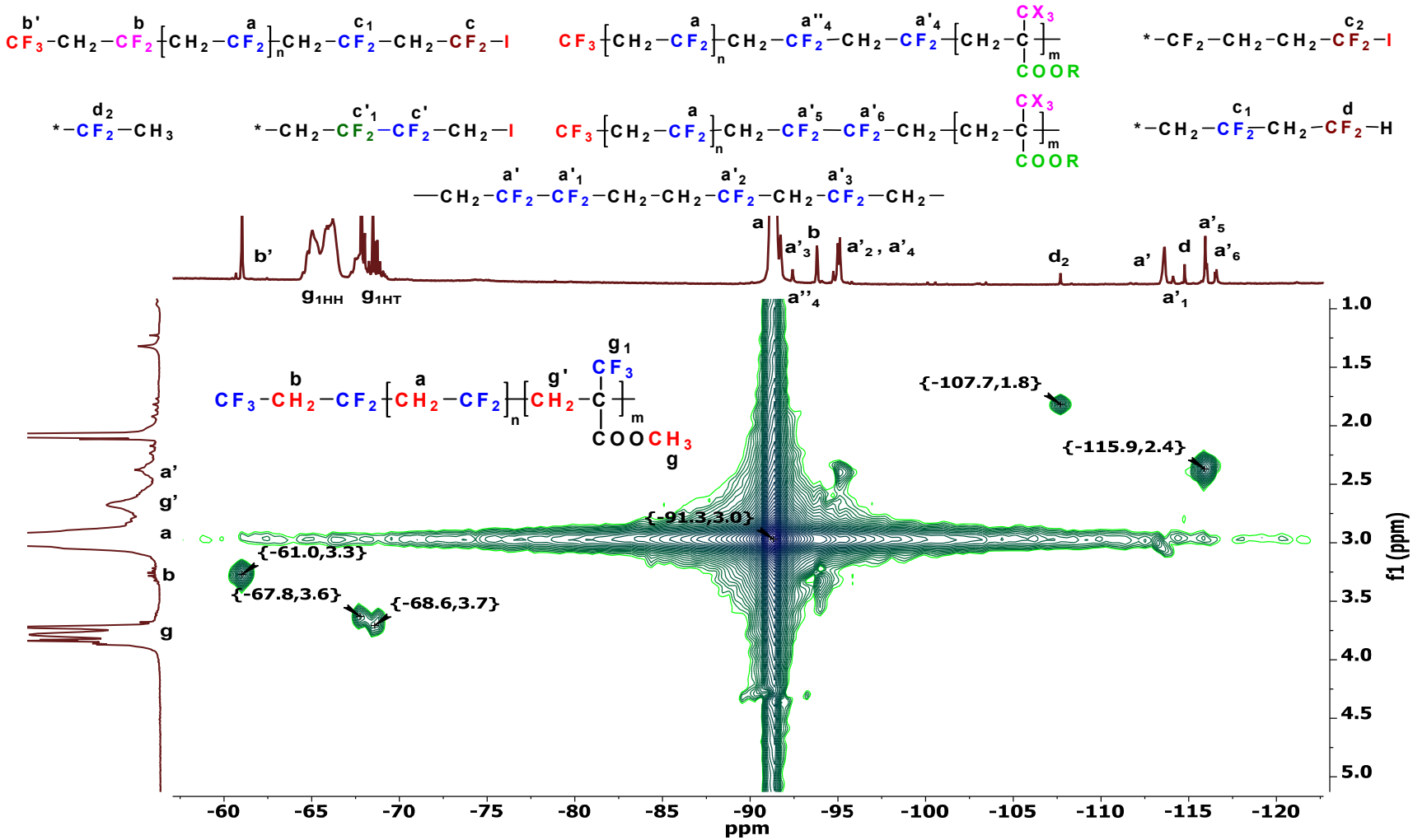

Figure 4.24 $^{19}F\{^{1}H\}$ Heteronuclear Correlation Spectra of PVDF-PMTFMA Block Copolymer, Demonstration of Connectivity.

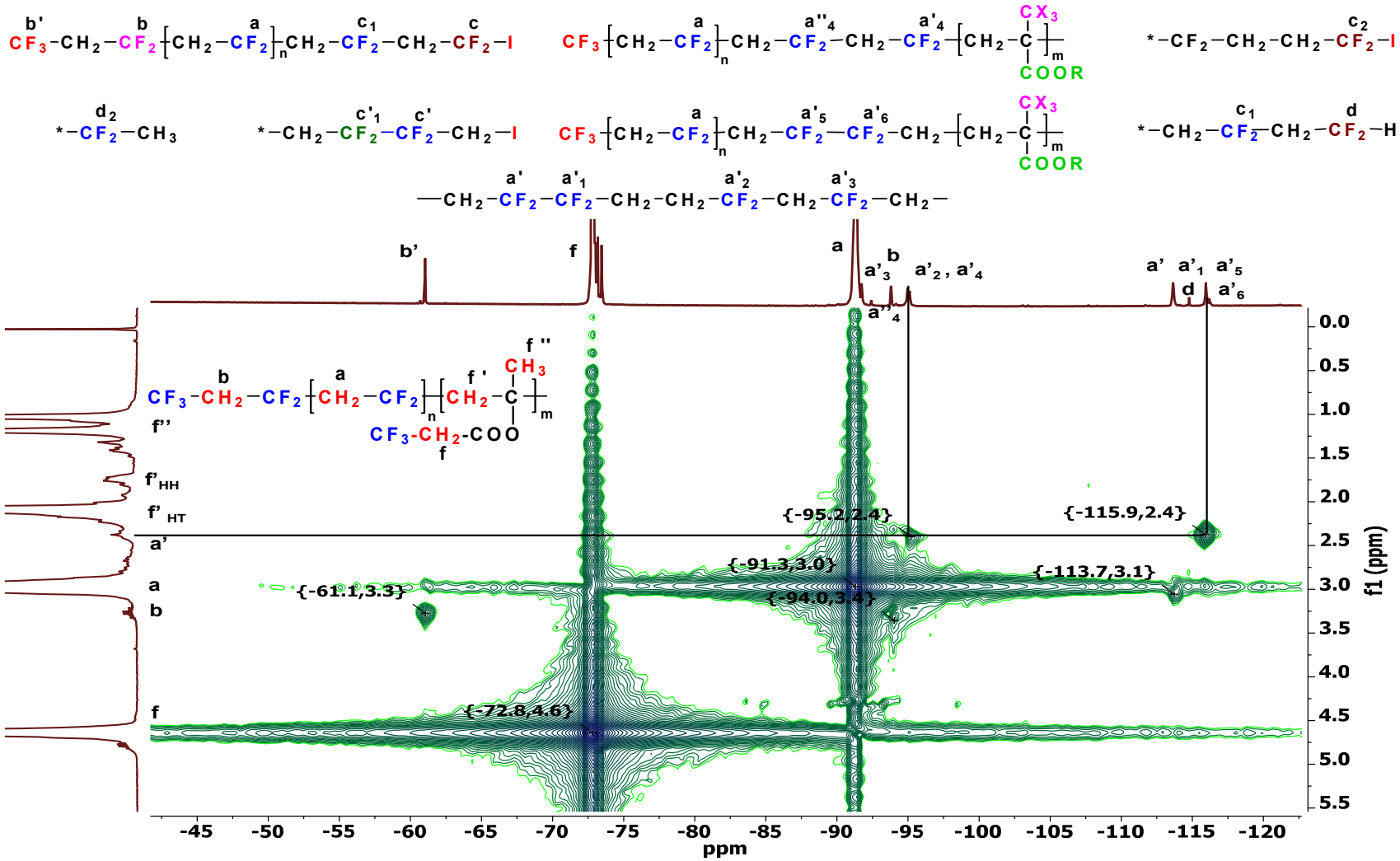

Figure 4.25 $^{19}F\{^{1}H\}$ Heteronuclear Correlation Spectra of PVDF-PTFEMA Block Copolymer, Demonstration of Connectivity.

4.4 Conclusions

To summarize, we have demonstrated that the photoinduced initiation of vinylidene fluoride can easily be obtained using vinylidene fluoride, at relatively mild temperatures, directly from alkyl or perfluoroalkyl halides ($CH_3(CH_2)_5Br$, $CH_3(CH_2)_5I$, CH_3I, CCl_4, CCl_3Br, $CF_3(CF_2)_3I$ $Cl(CF_2)_8Cl$, $Br(CF_2)_6Br$, and $I(CF_2)_6I$) using low power visible light irradiation ($\leq$30W) in conjunction with the transition metal carbonyl complexes ($Re_2(CO)_{10}$, $Mn_2(CO)_{10}$, $Cp_2W_2(CO)_6$, $Cp_2Mo_2(CO)_6$). The perfluoroalkyl iodides $CF_3(CF_2)_3I$ and especially $I(CF_2)_6I$) with $Mn_2(CO)_{10}$ or $Re_2(CO)_{10}$ mediated the VDF controlled radical polymerization (CRP) via iodine degenerative transfer (IDT) mechanism, while all other combinations yielded either FRP, telomerization, or no reaction at all. The effect of various [VDF]/[PFBI]/[$Mn_2(CO)_{10}$] ratios demonstrated again that poor or no control was obtained with PBFI in either ACN or DMC, with only the higher [VDF]/[PFBI] and lower [PFBI]/[$Mn_2(CO)_{10}$] ratios beginning to show slight IDT-CRP character, and confirming DMC as the superior solvent. The effect of [PFBI]/[$Mn_2(CO)_{10}$] revealed a lower limit of [1]/[0.05] below which no polymerization occurs, and an upper limit of [1]/[0.5] above which no further increases in k_p^{app} were observed. The [VDF]/[solvent] ratio had little effect on the polymerization rate *i.e.* maintaining a constant amount of VDF while increasing the solvent twelve-fold yielded similar k_p^{app}. While, maintaining a constant [VDF]/[solvent] ratio with increasing amounts of VDF, brought forth a significant increase in k_p^{app}. This was attributed to the monomer being gaseous, therefore the only effective means of increasing (decreasing) the concentration of the monomer in solution is to increase (decrease) the internal pressure of the reaction vessel. (*i.e.* the addition of larger(smaller) quantities of monomer). Subsequently, a selection of the metal carbonyl complexes were evaluated in the PVDF-CH_2-CF_2-I and PVDF-CF_2-CH_2-I activation, where $Re_2(CO)_{10}$, $Mn_2(CO)_{10}$, $Cp_2W_2(CO)_6$, $Cp_2Mo_2(CO)_6$, and $Cp_2Fe_2(CO)_4$ provided complete activation of both halide polymer chain ends, while $Fe(CO)_5$ and $Cp^*_2Cr_2(CO)_4$ generated β-elimination

products following the oxidative insertion into PVDF-CH_2-CF_2-I and PVDF-CF_2-CH_2-I. Finally, $Re_2(CO)_{10}$, $Mn_2(CO)_{10}$, $Cp_2W_2(CO)_6$, $Cp_2Mo_2(CO)_6$, and $Cp_2Fe_2(CO)_4$ provided the synthesis of well-defined block copolymers with vinyl acetate, t-butyl acrylate (and subsequent acrylic acid), methyl methacrylate, isoprene, styrene, and acrylonitrile. In addition, evidenced here were the first examples to demonstrate block copolymer connectivity *via* a combination of ^{19}F and $^{19}F\{^1H\}$ HETCOR NMR spectroscopy. The ability to not only see connectivity but to distinguish between the connection from both -CH_2-CF_2-I and -CF_2-CH_2-I is unique to these fluorinate/non(semi)fluorinated block copolymer architectures, and opens up a pathway to further develop complex polymer architecture characterization.

4.5 Chapter 4: Appendix

4.A: General NMR Discussion for the Structural Assignments of Typical ^1H and ^{19}F PVDF NMR Spectra and Previously Demonstrated Block Copolymers.

Examples of the d_6-acetone comparison of the ^1H and ^{19}F-NMR of I-PVDF-I is presented in Figure 4.A1a-b and Table 4.A1, while a comparison of the ^{19}F-NMR spectra of PVDF-I vs. PVDF-H is shown in Figure 4.A2-4.A3 and Table 4.A1.

1H-NMR: In addition to known PVDF H-NMR resonances,[103-106] acetone is seen at δ = 2.05 ppm and H_2O at δ = 2.84 ppm.[107] The other sets of signals are associated with PVDF propagation and termination events and initiator used.

PVDF Typical Main Chain Resonances: Two dominant, propagation derived PVDF main chain signals are observed: First, the head to tail (HT), -CF_2-[C*H*$_2$-CF_2]$_n$-CH_2-, broad multiplet ***a***, appears at δ = 2.8 - 3.1 ppm. Second, the head to head (HH) -(CH_2-CF_2)$_n$-CF_2-C*H*$_2$-C*H*$_2$-CF_2-(CH_2-CF_2)$_m$- linkage (typically HH = 5-10 % in free radical VDF polymerizations)[104,105,108,109,110,111] ***a'*** is observed at δ = 2.3 - 2.4 ppm. The resonances derived from typical PVDF termination by the

recombination[112] of terminal HT or HH units cannot be easily identified due to overlap, as follows: HT/HT (-CH_2-CF_2-C*H*$_2$-CF_2-CF_2-C*H*$_2$-CF_2-CH_2-, overlap with the HT main chain), HT/HH (-CH_2-CF_2-C*H*$_2$-CF_2-C*H*$_2$-CF_2-CF_2-CH_2-, identical to HT propagation), or HH/HH (-CH_2-CF_2-CF_2-C*H*$_2$-C*H*$_2$-CF_2-CF_2-CH_2-, identical to HH propagation). Interestingly, such termination is dramatically suppressed in the presence of active perfluoroiodo CT agents,[103,113-115] and is visualized by the disappearance of the HH peak ***a'***[114] which becomes -CF_2-C*H*$_2$-I (***c'*** *vide infra*).

Initiator Derived Chain Ends: The signal, ***b*** corresponds to the first VDF unit connected with R_F (R_F-C*H*$_2$-CF_2-) and confirm the predominantly regiospecific[115-117] 1,2-connectivity (R_F-C*H*$_2$-CF_2-).

Iodine Chain Ends: The ***c*** and ***c'*** resonances represent the corresponding PVDF halide chain ends (*i.e.* HT: ***c***, -CH_2-CF_2-C*H*$_2$-CF_2-I and HH: ***c'***, -CH_2-CF_2-CF_2-C*H*$_2$-I). Since $Mn(CO)_5$-I is not a halide donor[118] the concentration of ***c*** and ***c'*** may decrease with increasing the amount of $Mn_2(CO)_{10}$ employed, and their ratio will also depend on conversion. However, similarly to VAc,[118] it does change in the favor of the less reactive -CH_2-CF_2-CF_2-CH_2-I for pefluoroiodo derivatives.[4]

Hydrogen Chain Ends: While dramatically suppressed in IDT, termination may also occur by H transfer to the "good" ~CH_2-$CF_2^{\bullet}$ or to a smaller extent to the "bad" ~CF_2-$CH_2^{\bullet}$ propagating units to form -CH_2-CF_2-*H* (peak ***d***, triplet of triplets at δ = 6.3 ppm $^3J_{HH}$ = 4.6 Hz $^2J_{HF}$ = 54.7 Hz) and respectively, -CH_2-CF_2-*H* (peak ***d'***, triplet at δ = 1.80 ppm, $^3J_{HF}$ = 19.2 Hz).[104,119] Such H-transfers may arise from either the solvent, the main chain (inter or intramolecular), or by disproportionation with the terminal HT unit, to also give a -CH_2-CF_2-C*H*=CF_2 unsaturation, observed in a few cases as a trace multiplet at **d'"** at ~ 5.2 ppm.

Solvent-derived chain ends: Chain transfer to an R_S-H solvent may occur by H abstraction leading to the -CH_2-CF_2-*H* and -CF_2-CH_2-*H* chain ends described above. This will happen especially when the C-X bond of the initiator or the chain end is very strong, *i.e.* for very weak CT agents (Cl, Br). For most typical R_S-H solvents, the resulting $R_S^{\bullet}$ radicals are not reactive enough to

reinitiate VDF and are consumed by dimerization. Thus, the solvent fragment will not be observed in NMR. This is the case of ACN ($NC-CH_2-H$). Indeed, while $Mn_2(CO)_{10}$ clearly activates the corresponding iodide $NC-CH_2-I$[4] no polymer is obtained, as the resulting CN-stabilized radical dimerizes without addition to VDF (*i.e.* chain breaking and transfer without reinitiating) and is thus absent from the NMR of the polymer. By contrast, a more reactive $CH_3-O-CO-O-CH_2-^{\bullet}$ radical is generated by H abstraction from DMC. Thus, DMC provides chain transfer *with reinitiation*, (*i.e.* without breaking the radical chain) and this can be seen as trace signals as $C\boldsymbol{H_3}-O-CO-O-C\boldsymbol{H_2}-CH_2-CF_2-$ at δ = 3.74 s, 3H and respectively at δ = 4.33 ppm, t, 2H. However, this transfer is not observed for the linear perfluoroalkyl iodides suitable for VDF-CRP.

^{19}F-NMR Characterization of I-PVDF-I, PVDF-I and PVDF-H: A comparison of ^{1}H- and ^{19}F-NMR proton decoupled spectra of I-PVDF-I is provided in Figure A1, while a comparison of the ^{19}F-NMR spectra of PVDF-I initiated from $CF_3-CF_2-CF_2-CF_2-I$ with the corresponding PVDF-H (obtained by reacting PVDF-I with excess $Mn_2(CO)_{10}$ and corresponding to the top of Figure 4.2, chain end activation discussion) is shown in Figure 4.A1-A3. The corresponding assignments are presented in Table 4.A1. The same notation was used as with the ^{1}H-NMR spectra. The ^{19}F assignments are discussed below.

The main chain polyvinylidene fluoride head to tail $-CF_2-[\boldsymbol{CH_2}-\boldsymbol{CF_2}]_n-CH_2-$ unit ***a*** is observed at δ = -91.3 ppm. While the head to head units are greatly minimized in VDF-IDT, *trace* internal HH are seen as a set of 3 resonances $-CH_2-CF_2-CH_2-\boldsymbol{CF_2}-CF_2-CH_2-CH_2-CF_2-CH_2-CF_2-$, $-CH_2-CF_2-CH_2-CF_2-\boldsymbol{CF_2}-CH_2-CH_2-CF_2-CH_2-CF_2-$ and $-CH_2-CF_2-CH_2-CF_2-CF_2-CH_2-CH_2-\boldsymbol{CF_2}-CH_2-CF_2-$, peaks ***a', a'$_1$*** and ***a'$_2$*** at δ = -113.5 ppm, δ = -115.9 ppm and respectively, δ = - 95.1 ppm. Interestingly, *penultimate* $-CH_2-CF_2-\boldsymbol{CF_2}-CH_2-CH_2-CF_2-I$ and respectively $-CH_2-CF_2-\boldsymbol{CF_2}-CH_2-CH_2-CF_2-H$ units can also be distinguished as ***a'$_3$*** and ***a'$_4$*** at δ = -115.2 ppm and δ = -115.8 ppm.

The connectivity of the R_F initiators with the main chain is demonstrated by the resonance ***b***, PVDF-***CF$_2$***-CH_2-CF_2-CF_2-CF_2-CF_2-CF_2-CH_2-***CF$_2$***-PVDF and respectively CF_3-CF_2-CF_2-CF_2-CH_2-***CF$_2$***-PVDF associated with the first VDF unit. The R_F initiator resonances are clearly distinguished as PVDF-CF_2-CH_2-***CF$_2$***-CF_2-CF_2-CF_2-CF_2-***CF$_2$***-CH_2-CF_2-PVDF, PVDF-CF_2-CH_2-CF_2-***CF$_2$***-CF_2-CF_2-***CF$_2$***-CF_2-CH_2-CF_2-PVDF and PVDF-CF_2-CH_2-CF_2-CF_2-***CF$_2$***-***CF$_2$***-CF_2-CF_2-CH_2-CF_2-PVDF peaks ***b$_1$***, ***b$_2$*** and ***b$_3$*** at δ = -111.7 ppm, δ = -121.2 ppm and δ = -123.1 ppm for I-PVDF-I and respectively as ***CF$_3$***-CF_2-CF_2-CF_2-CH_2-CF_2-PVDF, CF_3-***CF$_2$***-CF_2-CF_2-CH_2-CF_2-PVDF, CF_3-CF_2-***CF$_2$***-CF_2-CH_2-CF_2-PVDF and CF_3-CF_2-CF_2-***CF$_2$***-CH_2-CF_2-PVDF peaks ***b$_4$***, ***b$_5$***, ***b$_6$*** and ***b$_7$*** at δ = -80.9 ppm δ = -125.5 ppm, δ = -123.9 ppm and δ = -111.9 ppm for PVDF-I The more reactive 1,2- iodide chain ends (“good”) are seen as -CH_2-CF_2-CH_2-CF_2-CH_2-***CF$_2$***-I and -CH_2-CF_2-CH_2-***CF$_2$***-CH_2-CF_2-I, peaks ***c*** and ***c$_1$*** at δ = -38.5 ppm and respectively δ = -92.5 ppm, as well as a weaker, penultimate -CH_2-CF_2-CF_2-CH_2-CH_2-***CF$_2$***-I reversed addition unit, ***c$_2$*** at δ = -39.3 ppm. The less reactive 2,1- iodide chain ends (“bad”) are observed as -CH_2-CF_2-***CF$_2$***-CH_2-I and -CH_2-***CF$_2$***-CF_2-CH_2-I peaks ***c’*** and ***c’$_1$*** at δ = -108.3 ppm and respectively δ = -112.0 ppm.

Finally, the complete activation of both iodine chain ends by metal carbonyl activator and subsequent H transfer to solvent figure 4.A2-A3, enables the definitive verification of all “***c***” peaks associated with iodine, *via* their disappearance, as well as the comparative increase in intensity in PVDF-H, that of the -CH_2-CF_2-CH_2-***CF$_2$***-H, -CH_2-CF_2-CF_2-CH_2-CH_2-***CF$_2$***-H, -CH_2-CF_2-***CF$_2$***-CH_3 and -CH_2-***CF$_2$***-CF_2-CH_3 H chain ends, peaks ***d, d$_2$, d’*** and ***d’$_1$*** at δ = -114.7 ppm, δ = -116.8 ppm, δ = -108.2 ppm and respectively δ = -114.1 ppm. Interestingly, as seen in Figure 4.2 and 4.4, there is also the presence of the resonances d’’’, and d’’’$_1$ associated with the β-elimination, following the oxidative insertion of the complexes $Fe(CO)_5$ and $Cp^*_2Cr_2(CO)_6$ yielding the

subsequent unsaturated polymer chain ends -CH_2-CF_2-***CF=CH$_2$***, δ = -118.9 ppm and -CH_2-***CF_2***-CF=CH_2 δ = -99.7 ppm.

Functionality and Mn calculations.

Comparative integrations of the resonances ***a, a' b, c, c'***, ***d*** and ***d'*** allow for the determination of the halide and hydride chain end functionality, as well as that of M_n^{NMR}, as outlined below and reported in Table A1:

$$(1) M_n^{NMR} = R_F + N\left\{64.04\left[\frac{\int a+\int a'+\int b+\int c+\int c'+{}^2/_3\int d'}{\int b}\right] + 1.008\left(\frac{2\int d+{}^2/_3\int d'}{\int b}\right) + Y\left(\frac{\int c+\int c'}{\int b}\right)\right\}$$

$$(2)\%\ total\ Iodine\ Functionality = \frac{\int c+\int c\prime}{\int b} = \frac{\int c+\int c\prime}{\int c+\int c\prime+{}^2/_3\int d'+2\int d}$$

$$(3)\%\ CH_2\text{-}CF_2\text{-}I\ Functionality = \frac{\int c}{\int b} = \frac{\int c}{\int c+\int c\prime+{}^2/_3\int d'+2\int d}$$

$$(4)\ \%\ CF_2\text{-}CH_2\text{-}I\ Functionality = \frac{\int c\prime}{\int b} = \frac{\int c\prime}{\int c+\int c\prime+{}^2/_3\int d'+2\int d}$$

$$(5)\ \%\ CF_2\text{-}CH_2\text{-}H\ Functionality = \frac{{}^2/_3\int d'}{\int b} = \frac{{}^2/_3\int d'}{\int c+\int c\prime+{}^2/_3\int d'+2\int d}$$

$$(6)\ \%\ CH_2\text{-}CF_2\text{-}H\ Functionality = \frac{2\int d}{\int b} = \frac{2\int d}{\int c+\int c\prime+{}^2/_3\int d'+2\int d}$$

Where 1.008 and 64.04, represent the molar masses of H and VDF while Y is the atomic weight of the halide chain end (*e.g.* Y = 126.9 for iodine chain ends); N = 1, 2 (initiator functionality); and R_F is the molecular weight of the initiator fragment (without the halides). All integrals are normalized to 2 protons.

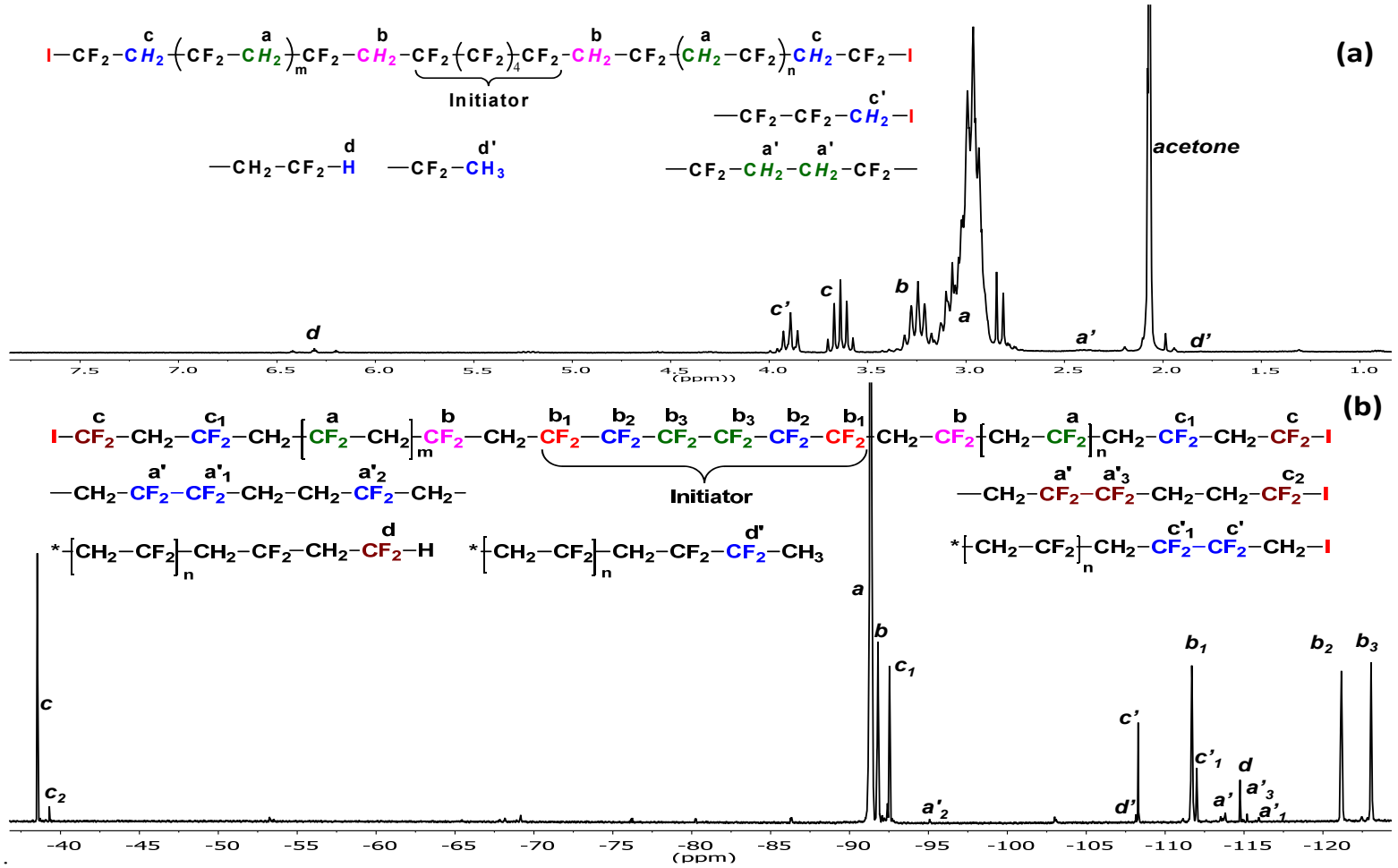

Figure 4.A1. Comparison of the ^{1}H and ^{19}F-NMR spectra of I-PVDF-I initiated from I-$(CF_2)_6$-I. VDF/I-$(CF_2)_6$-I/$Mn_2(CO)_{10}$ = 50/1/0.1.

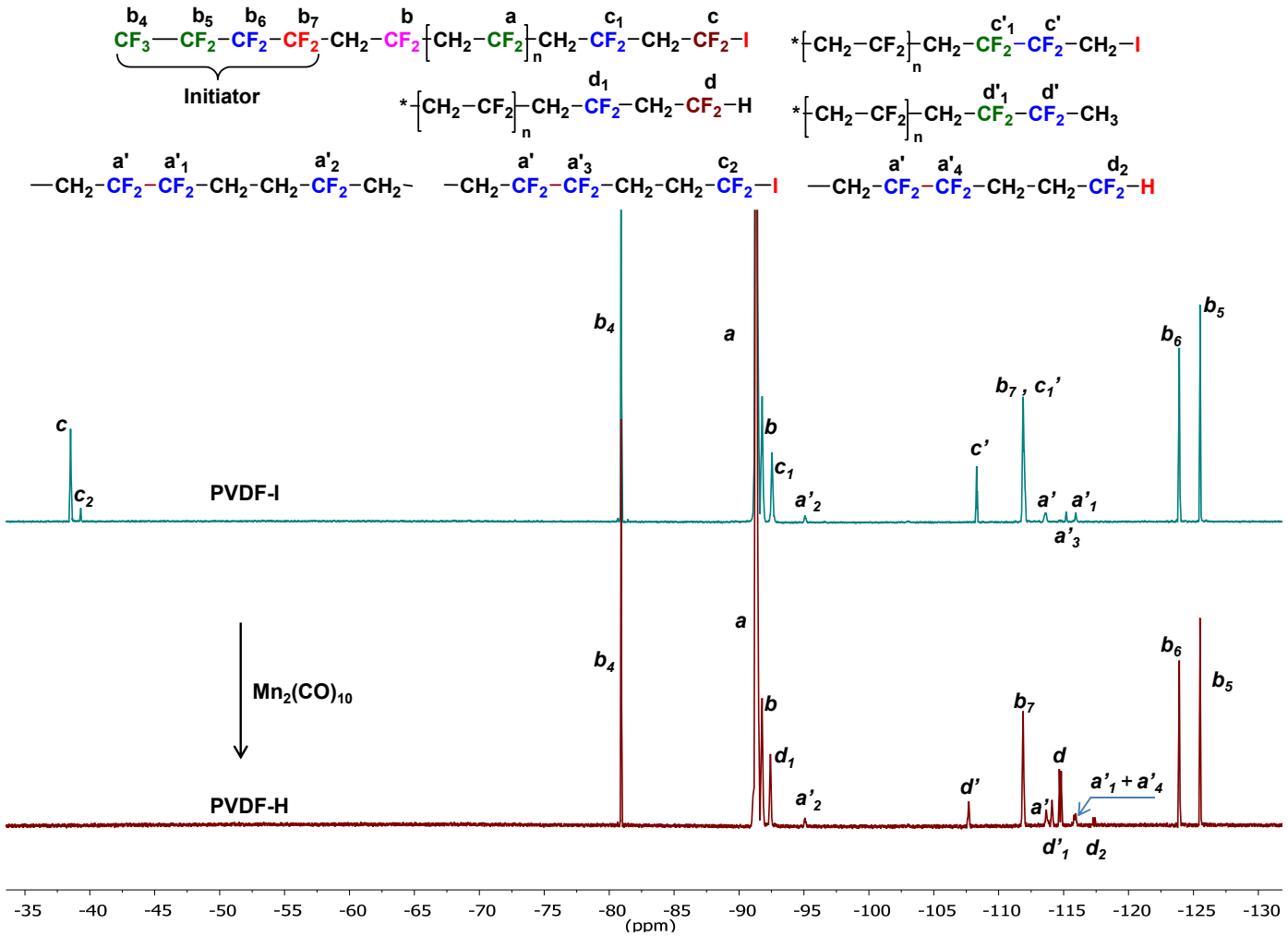

Figure 4.A2. Comparison of the ^{19}F-NMR spectra of PVDF-I initiated from CF_3-$(CF_2)_3$-I with the corresponding PVDF-H sample obtained after complete iodide abstraction by $Mn_2(CO)_{10}$.

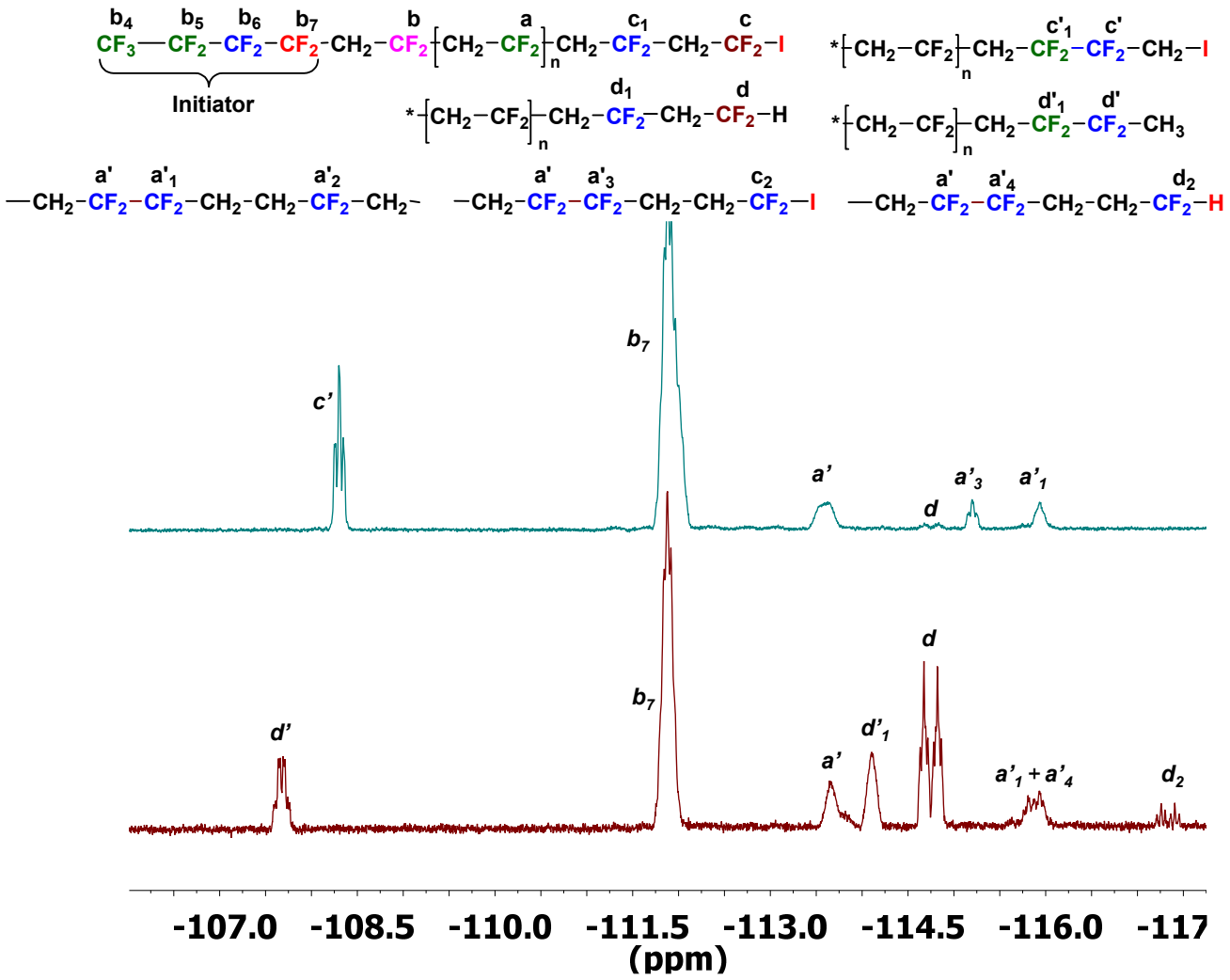

Figure 4.A3. Expansion of the -107 ppm to -117 ppm region from Figure A2

Table 4.A1. PVDF typical structural assignments of ^{1}H and ^{19}F NMR resonances. The δ values correspond to red italics.

Signal	Structure	^{1}H-NMR	^{19}F-NMR
a	$-CF_2-[\mathit{CH_2}-\mathit{CF_2}]_n-CH_2-$ HT	m, δ = 2.9 ppm	m, δ = -91.3 ppm
a'	$-CH_2-CF_2-CH_2-\mathit{CF_2}-CF_2-\mathit{CH_2}-\mathit{CH_2}-CF_2-CH_2-CF_2-$ HH	m, δ = 2.35 ppm	m, δ = -113.5 ppm
a'$_1$	$-CH_2-CF_2-CH_2-CF_2-\mathit{CF_2}-CH_2-CH_2-CF_2-CH_2-CF_2-$ HH	< 0.5 %	m, δ = -115.9 ppm
a'$_2$	$-CH_2-CF_2-CH_2-CF_2-CF_2-CH_2-CH_2-\mathit{CF_2}-CH_2-CF_2-$ HH		m, δ = - 95.1 ppm < 0.4 %
a'$_3$	$-CH_2-CF_2-\mathit{CF_2}-CH_2-CH_2-CF_2-I$		m, δ = -115.2 ppm
a'$_4$	$-CH_2-CF_2-\mathit{CF_2}-CH_2-CH_2-CF_2-H$		m, δ = -115.8 ppm
b	$PVDF-\mathit{CF_2}-\mathit{CH_2}-CF_2-CF_2-CF_2-CF_2-CF_2-CF_2-\mathit{CH_2}-\mathit{CF_2}-PVDF$	q, δ = 3.22 ppm	m, δ = -91.8 ppm
b	$CF_3-CF_2-CF_2-CF_2-\mathit{CH_2}-\mathit{CF_2}-PVDF$	q, δ = 3.24 ppm	m, δ = -91.8 ppm
b$_1$	$PVDF-CF_2-CH_2-\mathit{CF_2}-CF_2-CF_2-CF_2-CF_2-\mathit{CF_2}-CH_2-CF_2-PVDF$	N/A	m, δ = -111.7 ppm
b$_2$	$PVDF-CF_2-CH_2-CF_2-\mathit{CF_2}-CF_2-CF_2-\mathit{CF_2}-CF_2-CH_2-CF_2-PVDF$	N/A	m, δ = -121.2 ppm
b$_3$	$PVDF-CF_2-CH_2-CF_2-CF_2-C\mathit{F_2}-C\mathit{F_2}-CF_2-CF_2-CH_2-CF_2-PVDF$	N/A	m, δ = -123.1 ppm
b$_4$	$\mathit{CF_3}-CF_2-CF_2-CF_2-CH_2-CF_2-PVDF$	N/A	m, δ = -80.9 ppm
b$_5$	$CF_3-\mathit{CF_2}-CF_2-CF_2-CH_2-CF_2-PVDF$	N/A	m, δ = -125.5 ppm
b$_6$	$CF_3-CF_2-\mathit{CF_2}-CF_2-CH_2-CF_2-PVDF$	N/A	m, δ = -123.9 ppm
b$_7$	$CF_3-CF_2-CF_2-\mathit{CF_2}-CH_2-CF_2-PVDF$	N/A	m, δ = -111.9 ppm
c	$-CH_2-CF_2-CH_2-CF_2-\mathit{CH_2}-\mathit{CF_2}-I$	q, δ = 3.62 ppm	t, δ = -38.5 ppm
c$_1$	$-CH_2-CF_2-CH_2-\mathit{CF_2}-\mathit{CH_2}-CF_2-I$	$f^{H}_{CF2\text{-}I}$ = 70 %	q, δ = -92.5 ppm, $f^{F}_{CF2\text{-}I}$ = 68 %
c$_2$	$-CH_2-CF_2-CF_2-CH_2-CH_2-\mathit{CF_2}-I$		m, δ = -39.3 ppm,
c'	$-CH_2-CF_2-\mathit{CF_2}-\mathit{CH_2}-I$	t, δ = 3.87 ppm	m, δ = -108.3 ppm $f^{F}_{CH2\text{-}I}$ = 24 %
c'$_1$	$-CH_2-\mathit{CF_2}-CF_2-CH_2-I$	$f^{H}_{CH2\text{-}I}$ = 25 %	m, δ = -112.0 ppm,
d	$-CH_2-CF_2-CH_2-\mathit{CF_2}-\mathit{H}$	tt, δ = 6.3 ppm $f^{H}_{CF2\text{-}\mathit{H}}$ = 4%	dt, δ = -114.7 ppm $f^{F}_{\mathit{CF2}\text{-}H}$ = 6%
d$_1$	$-CH_2-\mathit{CF_2}-CH_2-CF_2-H$	N/A	q δ = -92.6 ppm
d$_2$	$-CH_2-CF_2-CF_2-CH_2-CH_2-\mathit{CF_2}-H$		dt, δ = -116.8 ppm
d'	$-CH_2-CF_2-\mathit{CF_2}-\mathit{CH_3}$	t, δ = 1.80 ppm	dd, δ = -108.2 ppm, $f^{F}_{\mathit{CF2}\text{-}CH3}$ = 2%
d'$_1$	$-CH_2-\mathit{CF_2}-CF_2-CH_3$	$f^{H}_{CF2\text{-}\mathit{CH3}}$ = 1%	δ = -114.1 ppm
d''	$-CH_2-CF_2-\mathit{CH_2}-CF_2-H$	m, δ = 2.77 ppm	N/A
d'''	$-CH_2-CF_2-\mathit{CF}=\mathit{CH_2}$	m, δ = 5.3 ppm	m, δ = -118.9 ppm
d'''$_1$	$-CH_2-\mathit{CF_2}-CF=CH_2$	N/A	d, δ = -99.7 ppm

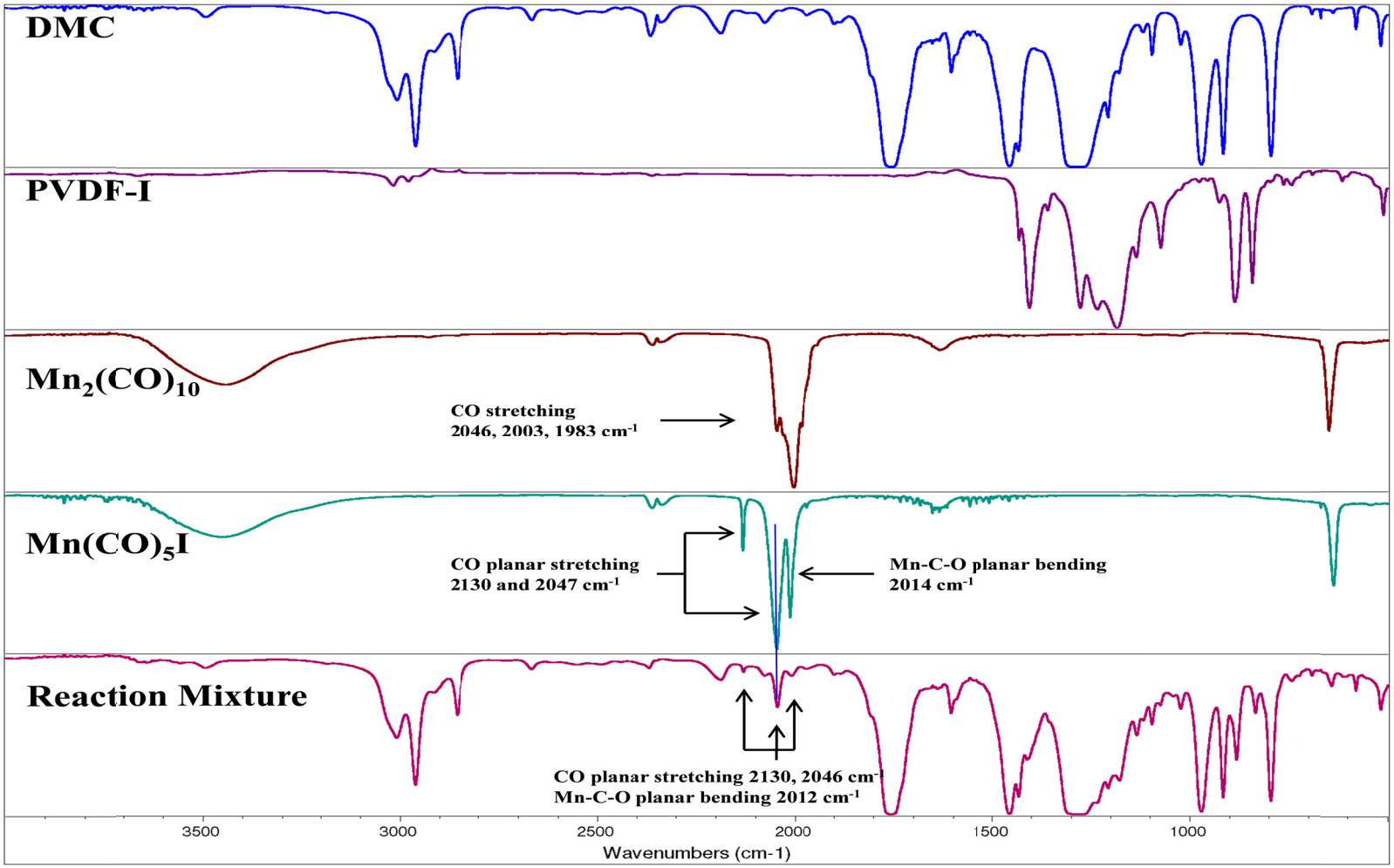

Figure 4.A4. Comparison of IR spectra of DMC, PVDF-I, $Mn_2(CO)_{10}$, $Mn(CO)_5$-I and of a typical polymerization mixture (VDF/PFBI/ $Mn_2(CO)_{10}$ = 25/1/0.2, after evaporation of VDF, ~ 80 % conversion).

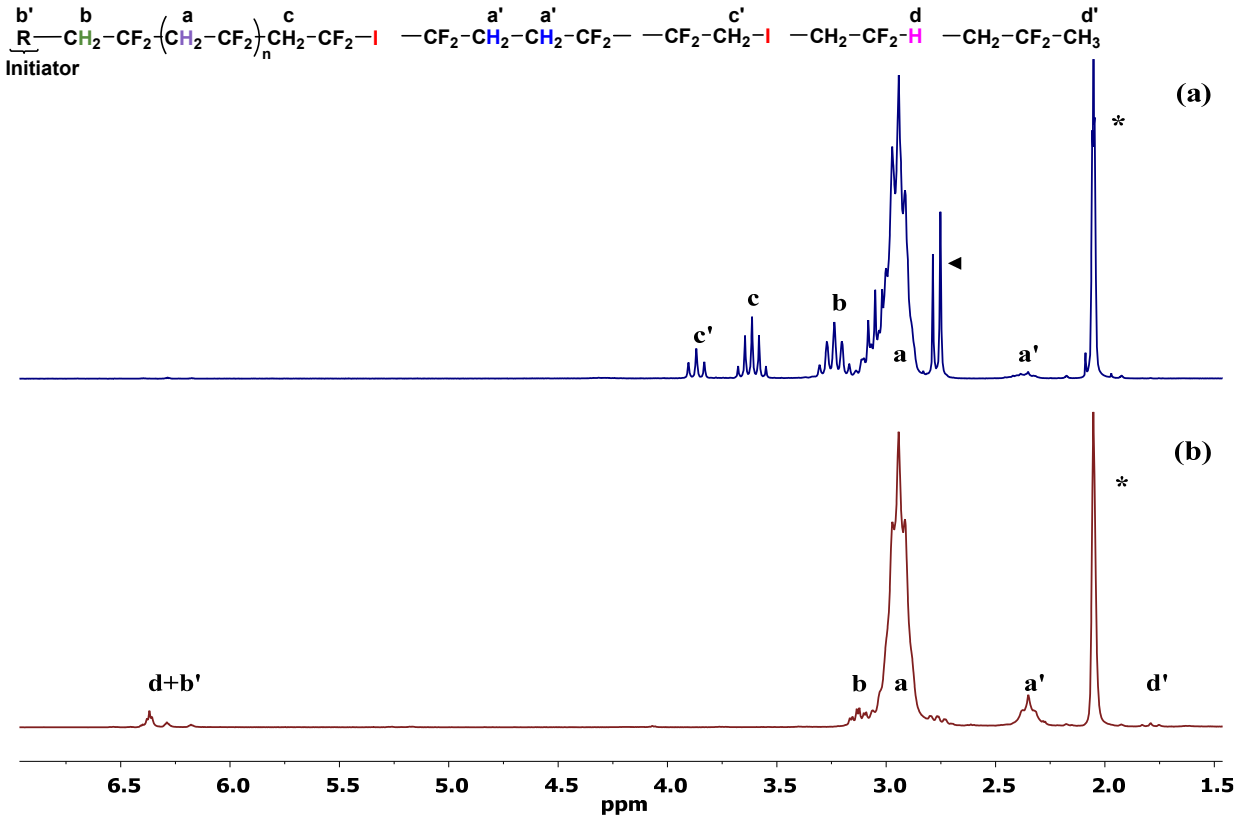

Figure 4.A5. Effect of excess $Mn(CO)_5$-I: Comparison of the 500 MHz ^{1}H-NMR d_6-acetone spectra of (a) PVDF-I obtained from VDF/PFBI/$Mn_2(CO)_{10}$ = 50/1/0.1 with (b) PVDF obtained from VDF/$CHCl_3$/$Mn_2(CO)_{10}$/$Mn(CO)_5$-I = 50/1/0.2/1, ◀ = H_2O, * = acetone.

Discussion: Figure 4.A4-A5: $Mn_2(CO)_5$-I Yields no Iodine Chain Ends

Figures A4 and A5 addresses the issue of whether or not $Mn_2(CO)_5$-I can donate I back to the propagating chain. In fact, this is not possible under the reaction conditions, since the BDE of $Mn_2(CO)_5$-I (54 kcal/mol)[120] is larger than that of typical R_F-I (*e.g.* for $CF_3CF_2CF_2CF_2$-I, BDE = 48.4 kcal/mol).[121] In addition, R-I compounds are most likely already in a photoexcited state, activated towards homolysis,[122] prior to their interaction $Mn_2(CO)_5^{\bullet}$. By contrast, the Mn-I bond of $Mn(CO)_5$-I does not photolyze homolytically under visible irradiation.[123]

Thus, in Figure 4.A4 the characteristic IR frequencies of $Mn_2(CO)_5$-I (2130, 2046, 2012 cm-^{1})[39,124] are clearly observed in both the $Mn_2(CO)_5$-I pure sample and in the reaction mixture.

As such, Figure 4.A5 is the comparison of a typical PVDF-I sample with PVDF synthesized from $CHCl_3$, (a poor chain transfer agent and cannot generate any PVDF-Cl chain ends) in the presence of a large excess of $Mn_2(CO)_5$-I. Thus, if any iodine abstraction by the propagating chain from $Mn_2(CO)_5$-I would be possible, the corresponding PVDF-I chain ends PVDF-C*H*$_2$-CF_2-I and PVDF-CF_2-C*H*$_2$-I (**c** and **c'** δ = 3.62 ppm δ = 3.87 ppm) would be visible. This is clearly not the case. Together, these control experiments indicate that similarly to the IDT of vinyl acetate,[125] the reversible iodine transfer is not mediated by $Mn_2(CO)_5$-I.

PVDF Block Copolymers Initiated by $Mn_2(CO)_{10}$ Activation:

Shown previously[4] AB or ABA-type PVDF block copolymers with styrene (**e**, **e'**), butadiene (**f**, **f'**, **f''**,**f'''**), vinyl chloride (**g**, **g'**), vinyl acetate (**h**, **h'**), methyl acrylate (**i**, **i', i''**), and acrylonitrile (**j**, **j'**), initiated from *both* PVDF halide chain ends (Table 4.A2 and Figure 4.A6 c-h). Again $Mn_2(CO)_{10}$ only role here is photoactivator and no IDT is considered. Although, control of the block copolymerization can be anticipated with other typical CRP methodologies, such as ATRP, RAFT, and TEMPO (nitroxide mediated).

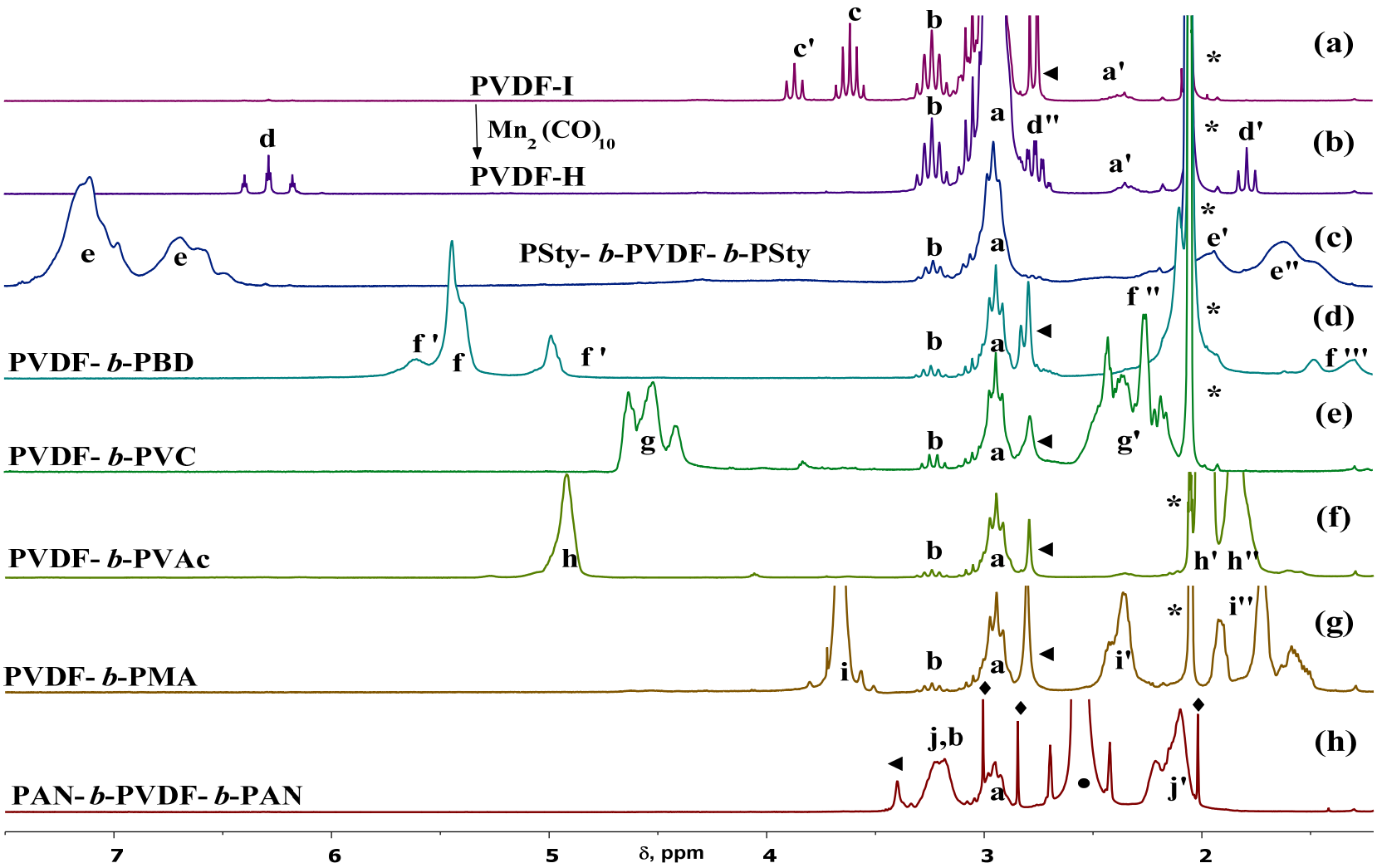

Figure 4.A6. 500 MHz 1H-NMR spectra of PVDF-I, PVDF-H and various PVDF block copolymers. All in d_6-acetone except PAN in d_6-DMSO. ◀ = H_2O, * = acetone, ♦ = DMAC, ● = DMSO

Table 4.A2 Characterization of $Mn_2(CO)_{10}$ Photomediated Synthesis of PVDF Block Copolymers

Exp.	Monomer	PVDF-I M_n	PVDF-I PDI	[M]/[PVDFI]/ [$Mn_2(CO)_{10}$]	Conv (%)	Composition M/VDF	M_n	PDI
1	Styrene[a,b)]	2,500	1.34	60/1/2	67	70/30	14,500	2.25
2	Butadiene[b)]	1,400	1.48	200/1/1	25	62/38	4,700	2.00
3	Vinyl Chloride[c)]	1,800	1.29	100/1/1	35	77/23	20,100	1.52
4	Vinyl Acetate	1,500	1.49	100/1/0.2	30	65/35	11,000	1.70
5	Methyl Acrylate	2,300	1.52	75/1/4	40	72/28	9,000	2.46
6	Acrylonitrile[a)]	2,100	1.31	50/1/1	25	74/26	25,800	2.33

T = 40 °C and solvent = DMAC except where noted. [a)]Block copolymers from I-PVDF-I samples. [b)]Polymerization was carried out at 110 °C, [c)] in dioxane

The NMR assignments corresponding to the copolymers from Figure 2 are as follows:

Polystyrene:
e, δ = 6.4-7.4 ppm, -CH_2-CH(C_6***H_5***)-,
e' δ = 1.94 ppm , -CH_2-C***H***(C_6H_5)-,
e" δ = 1.63 ppm , -C***H_2***-CH(C_6H_5)-,

Polybutadiene:
f, δ = 5.44 ppm -CH_2-C***H***=C***H***-CH_2- 1,4-*cis* and -*trans*;
f' δ = 5.6 ppm, 1,2 -CH_2-CH(C***H***=CH_2)- and δ = 4.99 ppm, -CH_2-CH(CH=C*H_2*)-;
f" δ = 2.1 ppm -C*H_2*-CH=CH-C***H_2***- and -CH_2-C***H***(CH=CH_2)-
f'" δ = 1.3-1.5 ppm, -C***H_2***-CH(CH=CH_2)-

Polyvinyl chloride:
g δ = 4.35-4.71 ppm, -CH_2-C***H***Cl-
g' δ = 2.11-2.52 ppm, -C***H_2***-CHCl-

Poly(vinyl acetate):
h δ = 4.92 ppm, -CH_2-C***H***($OCOCH_3$)-
h' δ = 1.98 ppm, -CH_2-CH(OCOC***H_3***)-
h' δ = 1.83 ppm, -C*H_2*-C***H***($OCOCH_3$)-,

Poly(methyl acrylate):
i δ = 3.67 ppm, -CH_2-CH(COOC***H_3***)-,
i' δ = 2.42 ppm, -CH_2-C***H***($COOCH_3$)-,
i' δ = 1.51-1.97 ppm, -C***H_2***-CH($COOCH_3$)-,

Polyacrylonitrile:
j δ = 4.35-4.71 ppm, -CH_2-C***H***(CN)-
j' δ = 2.2-2.28 ppm, -C***H_2***-CH(CN)-

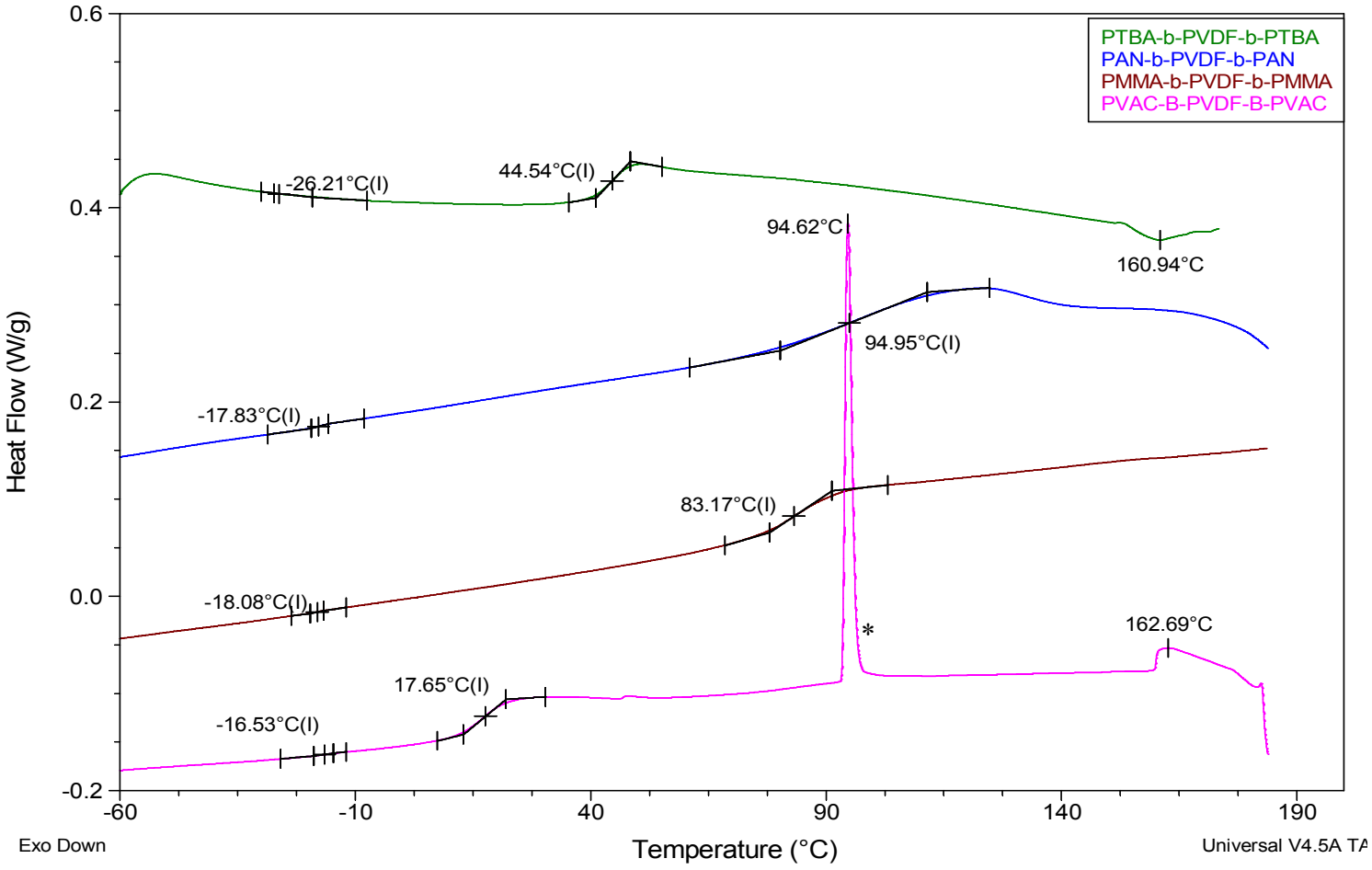

Figure 4.A7. DSC Thermographs of selected PVDF block copolymers. *Impurity likely due to $Re(CO)_5$-I that was difficult to remove.

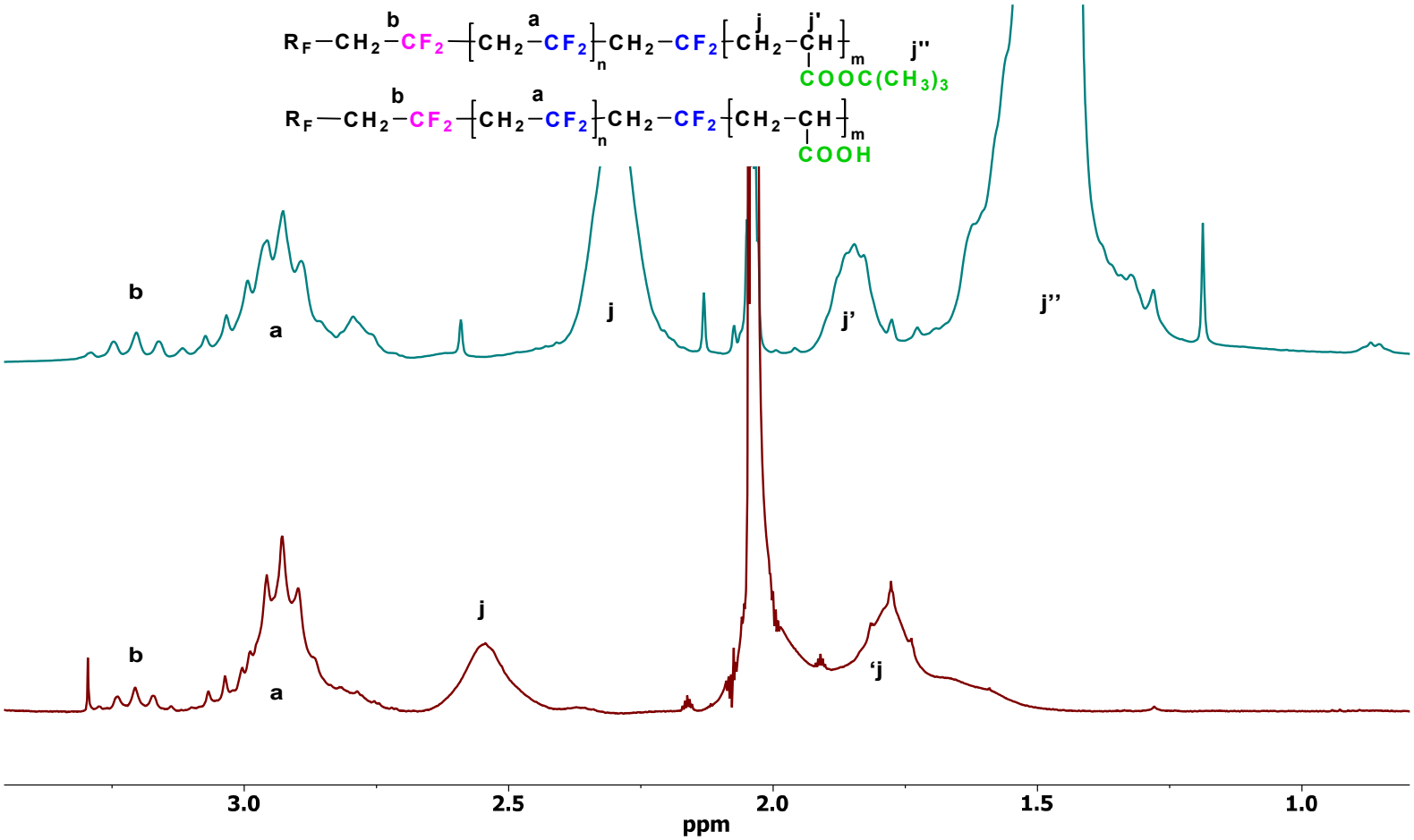

Figure 4.A8. 500 MHz ^{1}H-NMR spectra of PtBA-PVDF-PtBA (top) after hydrolysis PAA-b-PVDF-b-PAA (bottom) in d_6-acetone hydrolysis PAA-b-PVDF-b-PAA (bottom) in d_6-acetone.

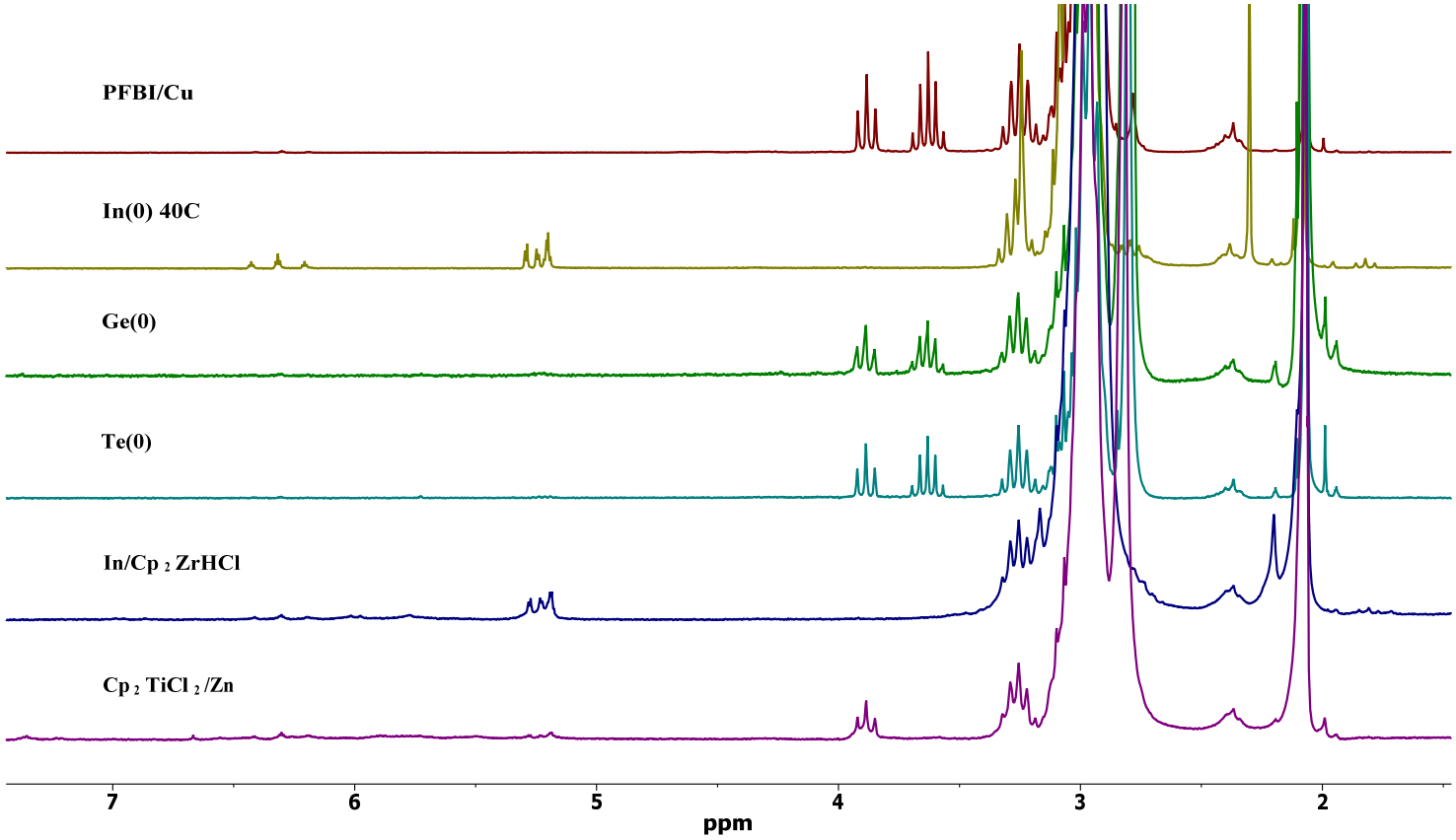

Figure 4.A9. 500 MHz ^{1}H-NMR spectra of PVDF-I activation attempted by various other metal compounds and metal (0).

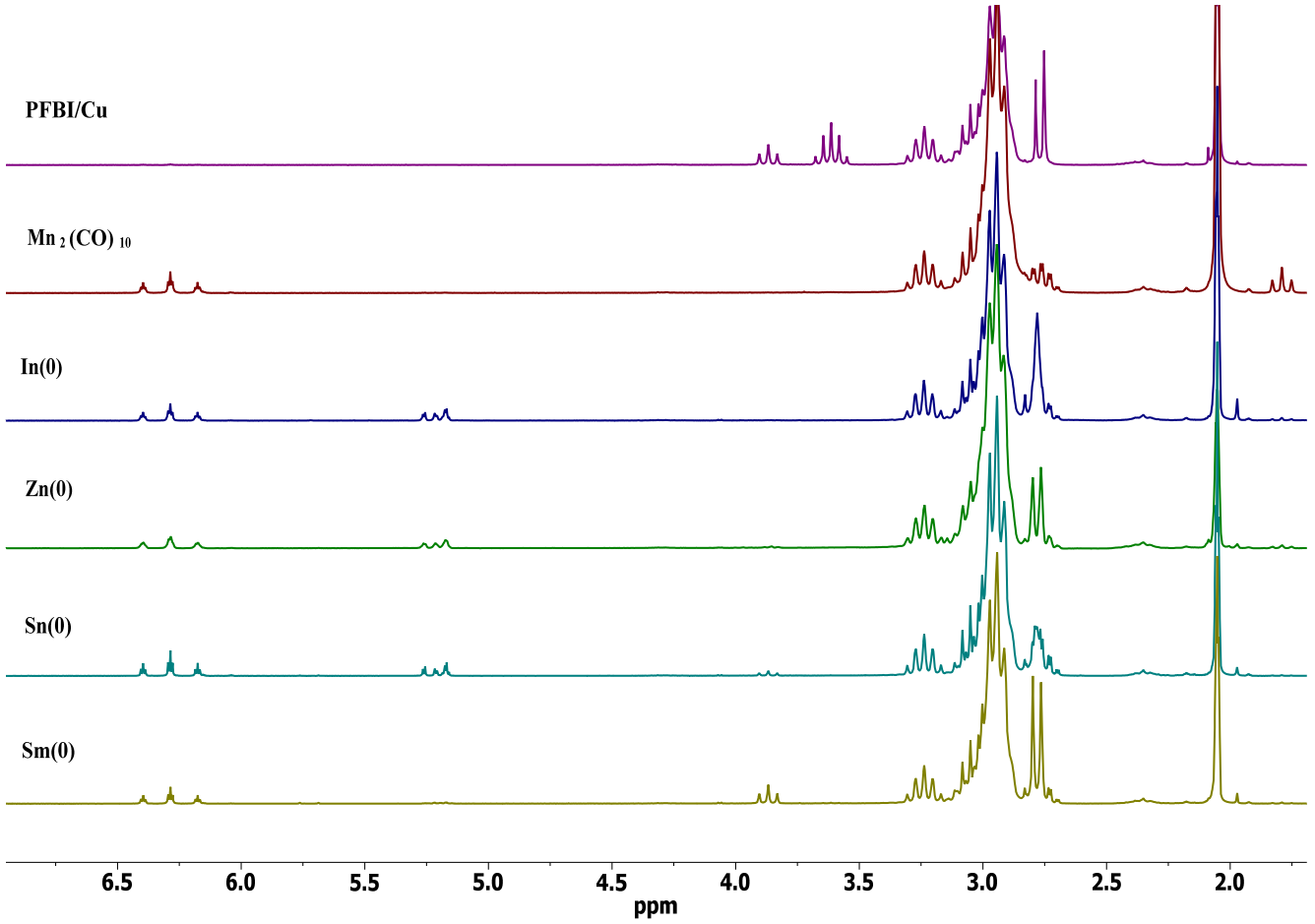

Figure 4.A10. 500 MHz ^{1}H-NMR spectra of PVDF-I activation attempted by various other metal compounds and metal (0)

4.6 References

1 (a) Ameduri, B. *Macromolecules*, **2010**, *43*, 10163–10184. (b) *From Vinylidene Fluoride (VDF) to the Applications of VDF-Containing Polymers and Copolymers: Recent Developments and Future Trends*. Ameduri, B. *Chem. Rev.* **2009**, *109*, 6632–6686. (c) *Well Architectured Fluoropolymers: Synthesis, Properties and Applications*. Ameduri, B.; Boutevin, B.; Elsevier, Amsterdam, **2004**, p 1-99. (d) *Fluoropolymer materials and architectures prepared by controlled radical polymerizations*. Hansen, N. M. L.; Jankova, K.; Hvilsted, S. *Eur. Polym. J.* **2007**, *43*, 255–293. (e) *Thermal Syntheses of Telomers of Fluorinated Olefins. 11. 1,1-Difluoroethylene*. Hauptschein, M.; Braid, M.; Lawlor, F. E. *J. Am. Chem. Soc*., **1958**, *80(4)*, 846–851.

2 Braunecker, W. A.; Matyjaszewski, K. *Prog. Polym. Sci*. **2007**, *32*, 93–146.

3 Goto, A.; Fukuda, T. *Progr. Polym. Sci*. **2004**, *29*, 329.

4 (a) *Mild-Temperature $Mn_2(CO)_{10}$-Photomediated Controlled Radical Polymerization of Vinylidene Fluoride and Synthesis of Well-Defined Poly(vinylidene fluoride) Block Copolymers*. Asandei, A. D.; Olumide, O. I.; Simpson, C. P. *J. Am. Chem. Soc*. **2012**, *134*, 6080-6083. (b) *Visible Light Hypervalent Iodide Carboxylate Photo-Iodo(Trifluoro)Methylations and Controlled Radical Polymerization of Fluorinated Alkenes*. Asandei, A. D.; Adebolu, O. I.; Simpson, C. P.; Kim, J. S. *Angew. Chem. Int. Ed.* **2013**, *52*, 10027-10030. (c) *Towards Metal Mediated Radical Polymerization of Vinylidene Fluoride* Asandei, A. D.; Simpson, C. P.; Adebolu, O. I.; Chen, Y. *Advances in Fluorine-Containing Polymers.* **2012**, *1106*, 47-63.

5 (a) *Vinylidene fluoride-hexafluoropropylene copolymer having terminal iodines*. Oka, M.; Tatemoto, M.; in *Contemporary Topics in Polymer Science.* Bailey, W. J.; Tsuruta, T.; Eds. Plenun Press, New-York, **1984**, *4*, pp.763-781. (b) *Fluorinated Thermoplastic Elastomers* Tatemoto, M. *Int. Poly. Sc. Tech*. **1985**, *12*, 85-98. (c) Tatemoto, M. in *Polymeric Materials Encyclopedia*. Salamone, J. C. Ed., CRC Boca Raton, FL, **1996**, *5*, pp. 3847-3862. (d) *Thermoplastic Elastomers*. Tatemoto, M.; Shimizu, T.; in *Modern Fluoropolymers*. Scheirs, J.; Ed, Wiley, New-York, **1997**, pp. 565-576. (e) *Segmented Polymers Containing Fluorine and Iodine and their Production*. Tatemoto, M.; Nakagawa, T.; U.S. Patent 4,158,678, **1979**.

6 (a) *Kinetics of Living Radical Polymerization*. Fukuda, T.; Goto, A.; Tsujii, Y. in *Handbook of Radical Polymerization*. Matyjaszewski, K.; Davis, T. P. Eds. Wiley, New York, **2002**, pp. 407-462. *(b) Controlled Radical Polymerization by Degenerative Transfer: Effect of the Structure of the Transfer Agent*. Gaynor, S. G.; Wang, J. S.; Matyjaszewski, K. *Macromolecules*. **1995**, *28*, 8051-8056.

7 *Use of Iodocompounds in Radical Polymerization*. David, G.; Boyer, C.; Tonnar, J.; Ameduri, B.; Lacroix-Desmazes, P.; Boutevin, B. *Chem. Rev.* **2006**, *106*, 3936–3962.

8 *First MALDI-TOF Mass Spectrometry of Vinylidene Fluoride Telomers Endowed with Low Defect Chaining*. Ameduri, B.; Ladavière, C.; Delolme, F.; Boutevin, B.; *Macromolecules*. **2004**, *37*, 7602-7612.—can cut

9 *Iodine Transfer Polymerization (ITP) of Vinylidene Fluoride (VDF). Influence of the Defect of VDF Chaining on the Control of ITP*. Boyer, C.; Valade, D.; Sauguet, L.; Ameduri, B.; Boutevin, B. *Macromolecules*. **2005**, *38*, 10353-10362.

10 *Kinetics of the Iodine Transfer Polymerization of Vinylidene Fluoride*. Boyer, C.; David, V.; Lacroix-Desmazes, P.; Ameduri, B.; Boutevin, B. *J. Polym. Sci.: Part A: Polym. Chem*. **2006**, *44*, 5763–5777.

11 *Poly(vinylidenefluoride)-b-poly(styrene) Block Copolymers by Iodine Transfer Polymerization (ITP): Synthesis, Characterization, and Kinetics of ITP*. Valade, D.; Boyer, C.; Ameduri, B.; Boutevin, B. *Macromolecules*. **2006**, *39*, 8639-8651.

12 (a) *Studies on Fluoroalkylation and Fluoroalkoxylation. Part 3. Perfluoroalkylation of Olefins with Perfluoroalkyl-Iodides and Copper in Various Solvents*. Chen, Q. Y.; Yang, Z. Y. *J. Fluorine Chem*. **1985**, *28(4)*, 399-411. (b) *Studies on Fluoroalkylation and Fluoroalkoxylation. Part 28. Palladium(o)-induced Addition of Fluoroalkyl Iodides to Alkenes: an Electron Transfer Process.* Chen, M. Y.; Yang, Z. Y.; Zhao, C. X.; Qiu, Z. M. *J. Chem. Soc. Perkin Trans. I*. **1988**, 3, 563-567. (c) *Polyfluoroalkylation of Octa-1,7-diene Promoted by Dichlorobis(π-cyclopentadienyl)Titanium and Iron Powder*. Hu, C. M.; Qiu, Y. L. *J. Chem. Soc. Perkin Trans. 1*. **1992**, *13*, 1569-1572.

13 *Reaction Mechanism of Borane/Oxygen Radical Initiators during the Polymerization of Fluoromonomers*. Zhang, Z. C.; Chung, T. C. *Macromolecules*. **2006**, *39*, 5187-5189.

14 *Synthesis of fluorinated telomers.1. Telomerization of vinylidene fluoride with Perfluoroalkyl Iodides*. Balague, J.; Ameduri, B.; Boutevin, B.; Caporiccio, G. *J. Fluorine Chem.* **1995**, *70*, 215-223.

15 *From Vinylidene Fluoride (VDF) to the Applications of VDF-Containing Polymers and Copolymers: Recent Developments and Future Trends*. Ameduri, B. *Chem. Rev.* **2009**, *109*, 6632-86.

16 *Fluoropolymer materials and architectures prepared by controlled radical polymerizations*. Hansen, N. M. L.; Jankova, K.; Hvilsted, S. *Eur. Polym. J.* **2007**, *43*, 255–293.

17 Asandei, A. D.; Adebolu, O. I.; Simpson, C. P. *Acs. Symp. Ser.: Advances in Fluorine-Containing Polymers; Smith, D. et al. Eds;* **2012**, *1106*, Chapter 4, p 47-63.++ all the preprints

18 *$Mn_2(CO)_{10}$-Visible Light Photomediated, Controlled Radical Polymerization of Main Chain Fluorinated Monomers and Synthesis of Block Copolymers Thereof*. Asandei, A. D.; Adebolu, O. I.; Simpson, C. P. *Handbook of Fluoropolymer Science and Technology*. **2014**, 21-42.

19 (a) Rowlands, G. J. *Tetrahedron*. **2009**, *65*, 8603–8655. (b) Gilbert, B. C.; Parsons, A. F. *J. Chem. Soc*., *Perkin Trans. 2*, **2002**, *3*, 367–387. *(c) Initiation of radical cyclisation reactions using dimanganese decacarbonyl. A flexible approach to preparing 5-membered rings.* Gilbert, B. C.; Kalz, W.; Lindsay, C. I.; McGrail, P. T.; Parsons , A. F.; Whittaker, D. T. E. *J. Chem. Soc., Perkin Trans. 1,* **2000***, 1187–1194*.

20 (a) *Addition of free radicals to unsaturated systems. Part VII. 1,1-Difluoroethylene*. Haszeldine, R. N.; Steele, B. R. *J. Chem. Soc.* **1954**, 923-925.(b) *Photochemical induced polymerization of VDF with hydrogen peroxide to obtain original telechelic PVDF*. Saint-Loup, R.; Ameduri, B. *J. Fluorine Chem*. **2002**, *116*, 27-34.

21 (a) Haszeldine, R. N.; Steele, B. R. *J. Chem. Soc.* **1954,** 923-25. (b) *Photolysis of trifluoromethyl iodide in the presence of ethylene and 1,1-difluoroethylene.* Braslavsky , S. E. Casas F. and Cifuentes O. *J. Chem. Soc. B*, **1970**, 1059-1060, (c) Saint-Loup, R.; Ameduri, B. *J. Fluorine Chem*. **2002**, *116*, 27. (d) Ameduri, B.; Billard, T.; Langlois, B. *J. Polym. Sci., Part A: Polym. Chem.* **2002,** *40*, 4538.

22 *Ordering the Reactivity of Photogenerated, 17 Valence Electron, Metal Carbonyl Radicals.* Harmon **B.** Abrahamson, Mark **S.** Wrighton. *J. Am. Chem. Soc*. **1977**, *99*, 5510-5512.

23 *Fast Reaction Studies of Rhenium Carbonyl Complexes: The Pentacarbonylrhenium(0) Radical*. Meckstroth, W. K.; Walters, R. T.; Waltz, W. L.; Wojcicki, A.; Dorfman, L. M. *J. Am. Chem. Soc.* **1982**, *104,* 1842-1846.

24 *Reaction mechanisms of metal-metal bonded carbonyls. Part 23. Thermal homolytic fission of decacarbonyldirhenium (Re-Re).* Fawcett, J. P.; Poe, A.; Sharma, K. R. *J. Chem. Soc., Dalton Trans.: Inorg. Chem.* **1979**, *12*, 1886-90.

25 (a) *Preparation and Properties of Manganese Carbonyl*. Brimm, E. O.; Lynch Jr., M. A.; Sesny, W. J *J. Am. Chem. Soc.*, **1954**, *76 (14)*, 3831–3835. (b) *The Chemistry of Manganese Carbonyl*. K.N .Anisirnov, K. N.; Loganson, A. A.; Kolobova, N. E. *Russ. Chem . Rev*. **1968**, *37*, 184-197.

26 (a) *Manganese Carbonyls and Manganese Carbonyl Halides.* Treichel, P. M. in *Comprehensive Organometallic Chemistry II vol 6, Manganese group.* Abel, E. W.; Stone, F. G. A.; Wilkinson, G.; Casey C. P, Eds. **1995**, pp. 1-19.

27 (a) *Manganese Carbonyls and Manganese Carbonyl Halides.* Treichel, P. M. in *Comprehensive Organometallic Chemistry II vol 6, Manganese group.* Abel, E. W.; Stone, F. G. A.; Wilkinson, G.; Casey C. P, Eds. **1995**, pp. 1-19.

28 *Equilibrium Constants for Homolysis of Metal-Metal-Bonded Organometallic Dimers in Cyclohexane Solution. Reaction of the (MeCp)Mo(CO)3 Radical with the Nitroxide Radical Trap TMIO*. Tenhaeff, S. C.; Covert, K. J.; Castellani, M. P.; Grunkemeier, J.; Kunz, C. Weakley, T. J. R.; Koenig, T.; Tyler, D. R. *Organometallics*. **1993**, *12,* 5000-5004.

29 The experimental measurements of *D*(Mn-Mn) by a variety of methods range from 19 to 42 kcal mol^{-1} and have been reviewed critically: (a) *Transition metal-hydrogen and metal-carbon bond strengths: the keys to catalysis*. Martinho Simoes, J. A.; Beauchamp, J. A. *Chem. Rev.* **1990**, *90*, 629-688. Here, the value was 38.5 kcal/mol by photoacoustic calorimetry: *The determination of the manganese-manganese bond strength in Mn2(CO)10 using pulsed time-resolved photoacoustic calorimetry.* Goodman, J. L.; Peters, K. S.; Vaida, V. *Organometallics* **1986**, *5*, 815-816. (c) Bond strengths *D*(Mn-X) for I-Mn(CO)5, Br-Mn(CO)5, and Cl-Mn(CO)5 are 54, 66, and 78kcal/mol, respectively (d) *Principles and Applications of Organotransition Metal Chemistry.* Collman, J. P.; Hegedus, L. S.; Norton, J. R.; Finke, R. G.; University Science Books: Mill Valley, California, **1987**; pp 368. (e) Reaction Mechanisms of Metal-Metal Bonded Carbonyls. Haines, L. I. B.; Hopgood, D.; Poe, A. J. *J. Chem. Soc. (A). Inorg. Phys. Theor.* **1968**, *2*, 421-8.

30 (a) *Intermolecular Alkyl Radical Addition to Chiral N-Acylhydrazones Mediated by Manganese Carbonyl*. Friestad, G. K.; Qin, J. *J. Am. Chem. Soc.* **2001**, *123,* 9922-9923.(b) *Mn-Mediated Coupling of Alkyl Iodides and Chiral N-Acylhydrazones: Optimization, Scope, and Evidence for a Radical Mechanism*. Friestad, G. K.; Marie, J. C.; Suh, Y. S.; Qin, J. *J. Org. Chem.* **2006**, *71*, 7016-7027.

31 *The determination of the manganese-manganese bond strength in Mn2(CO)10 using pulsed time-resolved photoacoustic calorimetry.* Goodman, J. L.; Peters, K. S.; Vaida, V. *Organometallics* **1986**, *5*, 815-816.

32 *Reaction Mechanisms of Metal-Metal Bonded Carbonyls. 18. Kinetic Measurement of the Strengths of Some Metal-Metal Bonds*. Jackson, R. A.; Poe, A. *Inorg.Chem*. **1978**, *17(4)*, 997-1003.

33 (a) *Pulse Radiolysis Studies of Decacarbonyldimanganese(0) and Halopentacarbonylmanganese (I). The Pentacarbonylmanganese(0) Radical*. Waltz, W. L.; Hackelberg, O.; Dorfman, L. M.; Wojcicki, A. *J. Am. Chem.* Soc. **1978**, *100*, 7259-7264.(b) *Picosecond Dynamics of Solution-Phase Photofragmentation of Mn2(CO)10.* Rothberg, L. J.; Cooper, J. N.; Peters, K. S.; Vaida, V. *J. Am. Chem. Soc.* **1982**, *104*, 3536-3537.

34 *Comprehensive Organometallic Chemistry III, volume 5*. Robert, H. C.; Michael, P. Eds. **2007** Elsevier, Providence, RI, 440-746, (b) *Photodissociation dynamics of Mn2(CO)10 in solution on ultrafast time scales.* Zhang, J. Z.; Harris, C. B. *J. Chem. Phys*. **1991**, *95(6)*, 4024-4032.

35 *Photophysical Features of the M2(CO)10, M = Mn and Re, Solution* Photochemistry. Sarakha, M. Ferraudi, G. *Inorg. Chem.* **1999**, *38,* 4605-4607.

36 Hughey, J. L.; Anderson, C. P.; Meyer, T. J. *J. Organomet. Chem.* 1977, *125 C49-C52.*

37 *Encyclopedia of Reagents for Organic Synthesis.* Pauson, P. L.; Friestad, G. K. **2008**, John Wiley & Sons (b) *Preparation, properties, and kinetics of the reaction of manganese(0) radicals Mn(CO)3(R3P)2 with tributyltin hydride.* McCullen, S. B.; Brown, T. L. *J. Am. Chem. Soc.* **1982**, *104*, 7496-7500. (c) *Photochemical Reaction of Dinuclear Manganese Carbonyl Compounds with Tributyltin Hydride and with Silanes* Sullivan, R. J.; Brown, T. L. *J. Am. Chem. Soc.* **1991**, *113,* 9155-9161.

38 *Initiation of radical cyclisation reactions using dimanganese decacarbonyl. A flexible approach to preparing 5-membered rings.* Gilbert, B. C.; Kalz, W.; Lindsay, C. I.; McGrail, P. T.; Parsons , A. F.; Whittaker, D. T. E. *J. Chem. Soc., Perkin Trans. 1,* **2000***, 1187–1194*.

39 (a) *Photochemistry of Metal-Metal Bonded Complexes. II. The Photochemistry of Rhenium and Manganese Carbonyl Complexes Containing a Metal-Metal Bond*. Wrighton, M. S.; Ginley, D. S. *J. Am. Chem.* Soc. **1975**, *97(8)*, *2065-2072.* **DOI:** 10.1021/ja00841a012 *(b) Efficient Radical Coupling of Organobromides Using Dimanganese Decacarbonyl*. Gilberta, B. C.; Lindsay, C. I.; McGrail, P. T.; Parsons, A. F.; Whittaker, D. T. E. *Synth. Commun*. **1999***, 29(15)*, 2711-2718.

40 *Photochemically induced reactions of decacarbonyldimanganese(0).* Hallock, S. A.; Wojcicki, A. *J. Organomet. Chem.* **1979**, *182(4)*, 521-35.

41 *Rates of Halogen Atom Transfer to Manganese Carbonyl Radicals*. Herrick, R. S.; Herrinton, T. R.; Walker, H. W.; Brown, T. L. *Organometallics*. **1985**, *4,* 42-45.

42 *Photoinitiation of polymerization and hydrogen abstraction by metal carbonyls*. Bamford, C. H.; Mahmud, M. U. *J. Chem. Soc., Chem. Commun*.**1972**, *13*, 762-3.

43 *Metal carbonyls as photoinitiators for the polymerizations of tetrafluoroethylene and vinyl monomers containing tetrafluoroethylene*. Bamford, C. H.; Mullik, S. U. *Polymer*. **1973**, *14(1)*, 38-9. (b) *Polymerization of tetrafluoroethylene in acetic acid photoinitiated by metal carbonyls*. Bamford, C. H.; Mullik, S. U. *Polymer*. **1976**, *17(3)*, 225-30.

44 (a) Photoinitiated polymerization. Aliwi, S. M.; Bamford, C. H.; Mullik, S. U. J. Polym. Sci., Polym. Symp. **1975**, *50*, 33-50. (b) *Photoinitiation of free- radical polymerization by rhenium carbonyl in the presence of tetrafluoroethylene.* Bamford, C. H.; Mullik, S. U*. J. Chem. Soc., Faraday Trans. 1.* **1975**, *71(3)*, 625-36.

45 *New thermal initiators of free-radical polymerization and block copolymerization*. Bamford, C. H.; Mullik, S. U. *Polymer* **1976**, *17(1)*, 94-5.

46 *Photoinitiation of free- radical polymerization by transition metal carbonyls in systems without halides*. Bamford, C. H.; Mullik, S. U. *J. Chem. Soc., Faraday Trans. 1* **1976**, *72(2)*, 368-75.

47 (a) *Initiation of free radical polymerization by manganese carbonyl and carbon tetrachloride*. Bamford, C. H.; Denyer, R. *Nature*. **1968**, *217(5123)*, 59-60. (b) *Polymerization. XVI. The photosensitized initiation of vinyl polymerization by the carbonyls of Group VII metals.* Bamford, C. H.; Crowe, P. A.; Hobbs, J.; Wayne, R. P. *Proceedings of the Royal Society of London, Series A: Mathematical, Physical and Engineering Sciences.* **1966**, *292(1429)*, 153-67. (c) *Initiation of Vinyl Polymerization By Manganese Carbonyl And Related Compounds.* Bamford, C. H.; Finch, C. A. *J. Chem. Soc., Faraday Trans. 1.* **1963**, 59, 540-7.

48 *A new technique for polymer grafting*. Bamford, C. H.; Duncan, F. J.; Reynolds, R. J. W.; Seddon, J. D. *J. Poly. Sci.: Part C. No.* **1968**, *23*, 419-432.

49 (a) *Reactivity, Mechanism and Structure in Polymer Chemistry;* Jenkins, A. D., Ledwith, A., Eds., Wiley, New York, **1974**, ch 3. (b) Bamford, C. H.; Dyson, R. W.; Eastmond, G. C. *J. Polym. Sci., Part C* **1967**, *16*, 2425.(c) Bamford, C. H.; Dyson, R. W.; Eastmond, G. C.; Whittle, D. *Polymer* **1969**, *10*, 759. (d) Bamford, C. H.; Eastmond, G. C.; Whittle, D. *Polymer* **1969**, *10*, 771. (e) Bamford, C. H.; Dyson, R. W.; Eastmond, G. C. *Polymer* **1969**, *10*, 885. (f) *Polymerization of Methyl Methacrylate and Vinyl Acetate Initiated by the Manganese Carbonyl–1,2-Epoxy-4,4,4-trichlorobutane System*. Kireev, V. V.; Pudskov, B. M.; Filatov, S. N.; Lipendina, O. L. *Vysokomolekulyarnye Soedineniya, Ser. B,* **2006***, 48(6), 1024 – 1028.* (g) *Polymerization of Methyl Methacrylate Using Dimanganese Decacarbonyl in the Presence of Organohalides.* Gilbert, B. C.; Harrison, R. J.; Lindsay, C. I.; McGrail, P. T.; Parsons, A. F.; Southward, R.; Irvine, D. J. *Macromolecules.* **2003**, *36*, 9020-9023.

50 *Heterogeneous Graft Copolymerization of Chitosan Powder with Methyl Acrylate Using Trichloroacetyl-Manganese Carbonyl Co-initiation Mn grafting.* Jenkins, D. W.; Hudson, S. M. *Macromolecules.* **2002**, *35*, 3413.

51 *Synthesis of Block Copolymers by Combination of Atom Transfer Radical Polymerization and Visible Light Radical Photopolymerization Methods*. Acik, G.; Kahveci, M. U.; Yagci, Y. *Macromolecules* **2010**, *43*, 9198–9201.

52 Bamford, C. H.; Mullik, S. U. *J. Chem. Soc., Faraday Trans. 1.* **1977**, *73(8)*, 1260

53 (a) *Manganese-Based Controlled/Living Radical Polymerization of Vinyl Acetate, Methyl Acrylate, and Styrene: Highly Active, Versatile, and Photoresponsive Systems*. Koumura, K.; Satoh, K.; Kamigaito, M. *Macromolecules*, **2008**, *41 (20)*, 7359-7367. (b*) Mn2(CO)10-Induced Controlled/Living Radical Copolymerization of Vinyl Acetate and Methyl Acrylate:Spontaneous Formation of Block Copolymers Consisting of Gradient and Homopolymer Segments*. Koumura, K.; Satoh, K.; Kamigaito, M. *J. Polym. Sci.: Part A: Polym. Chem*. **2009**, *47*, 1343–1353.

54 *$Mn_2(CO)_{10}$-Induced Controlled/Living Radical Copolymerization of Methyl Acrylate and 1-Hexene in Fluoroalcohol: High α-Olefin Content Copolymers with Controlled Molecular Weights*. Koumura, K.; Satoh, K.; Kamigaito, M. *Macromolecules* **2009**, *42*, 2497-2504.

55 *$Mn_2(CO)_{10}$-Induced RAFT Polymerization of Vinyl Acetate, Methyl Acrylate, and Styrene.* Kimura, K.; Satoh, K, Kamigaito, M. *Polym. J.* **2009**, *41*, 595-603..

56 (a) Rowlands, G. J. *Tetrahedron*. **2009**, *65*, 8603–8655. (b) Gilbert, B. C.; Parsons, A. F. *J. Chem. Soc*., *Perkin Trans. 2*, **2002**, *3*, 367–387. *(c) Initiation of radical cyclisation reactions using dimanganese decacarbonyl. A flexible approach to preparing 5-membered rings.* Gilbert, B. C.; Kalz, W.; Lindsay, C. I.; McGrail, P. T.; Parsons , A. F.; Whittaker, D. T. E. *J. Chem. Soc., Perkin Trans. 1,* **2000***, 1187–1194*.

57 *Electron-Transfer Reactions of Re(CO)5: Atom-Transfer-Concerted Mechanism vs. Bimetallic Intermediate Formation*. Sarakha, M.; Ferraudi, G. *Inorg. Chem.* **1996**, *35,* 313-317
58 Abrahamson, H. B.; Wrighton, M. S. *J. Am. Chem. Soc.* **1977**, *99*, 5510-5512.
59 *Stereoregulation in the Free Radical Polymerization of Polar Monomers*. Bamford, C. H.; Blackie, M. S.; Finch, C. A. *Chem. Ind. (Chichester, U. K.)*, **1962**, 1763-64.
60 *A Highly Active Fe(I) Catalyst for Radical Polymerisation and Taming the Polymerisation with Iodine.* Kamigaito, M.; Onishi, I.; Kimura, S.; Kotani, Y.; Sawamoto, M. *Chem. Commun.* **2002**, *22*, 2694-2695.
61 *Iron-Catalyzed Radical Polymerization of Acrylamides in the Presence of Lewis Acid for Simultaneous Control of Molecular Weight and Tacticity*. Sugiyama, Y.; Satoh, K.; Kamigaito, M.; Okamoto, Y. *J. Polym. Sci. Part A: Polym. Chem.* **2006**, *44(6)*, 2086-2098.
62 *Dicarbonyl Pentaphenylcyclopentadienyl Iron Complex for LivingRadical Polymerization: Smooth Generation of Real Active Catalysts Collaborating with Phosphine Ligand*. Ishio, M.; Ouchi, M.; Sawamoto, M. *J. Polym. Sci. Part A: Polym. Chem.* **2011**, *49(2)*, 537-544.
63 *On the Favorable Interaction of Metal Centered Radicals with Hydroperoxides for an Enhancement of the Photopolymerization Efficiency Under Air*. Lalevee, J.; Tehfe, M.; Gigmes, D.; Fouassier, J. P. *Macromolecules* **2010**, *43*, 6608–6615.
64 *Possibility of Living Radical Polymerization of Vinyl Acetate Catalyzed by Iron(I) Complex*. Wakioka, M.; Baek, K.; Ando, T.; Kamigaito, M.; Sawamoto, M. *Macromolecules* **2002**, *35*, 330-333.
65 *Preparation of Antibacterial Polymer-grafted Nano-sized Silica and Surface Properties of Silicone Rubber Filled with the Silica*. Yamashita, R.; Takeuchi, Y. Kikuchi, H.; Shirai, K.; Yamauchi, T.; Tsubokawa, N. Polymer Journal, **2006**, *38(8)*, 844–851.
66 (a)*Some Novel Initiators of Vinyl Polymerization*. Bamford, C. H. *J. Polym. Sci: Part C*. **1964**, *4*, 1571. (b) *Oxidation of Molybdenum Carbonyl and Related Derivatives by Organic Halides; Thermal and Photochemical Activation*. Bamford, C. H.; Eastmond, G.C.; Fildes, F. J. T. *J. Chem. Soc., Chem. Commun.* **1970**, *3*, 145.
67 (a) *Stereoregulation in the Free Radical Polymerization of Polar Monomers*. Bamford, C. H.; Blackie, M. S.; Finch, C. A. *Chem. Ind*. **1962**, 1763. (b) *Phosphine-metal carbonyl derivatives as free radical sources*. Bamford, C. H.; Maltman, W. R. *Trans. Faraday Soc*. **1966**, *61(10),* 2823.
68 Davis, R.; Groves, I. F. *J. Chem. Soc., Dalton Trans. Inorg. Chem.* **1982**, *11*, 2281-7.
69 Bamford, C. H.; Mahmud, M. U. *J. Chem. Soc., Chem. Commun*. **1972**, *13*, 762-3.
70 Bamford, C. H.; Mullik, S. U. *Polymer*. **1973**, *14(1)*, 38-9. (b) Bamford, C. H.; Mullik, S. U. *Polymer*. **1976**, *17(3)*, 225-30.
71 (a) Aliwi, S. M.; Bamford, C. H.; Mullik, S. U. *J. Polym. Sci., Polym. Symp.* **1975**, *50*, 33-50. (b) Bamford, C. H.; Mullik, S. U. *J. Chem. Soc., Faraday Trans. 1.* **1975**, *71(3)*, 625-36.
72 Bamford, C. H.; Mullik, S. U. *Polymer* **1976**, *17(1)*, 94-5.
73 Bamford, C. H.; Mullik, S. U. *J. Chem. Soc., Faraday Trans. 1* **1976**, *72(2)*, 368-75.
74 *Photo-, Electro-, And Thermal Carbonylation Of Alkyl Iodides In The Presence Of Group 7 And 8-10 Metal Carbonyl Catalysts* Teruyuki, K.; Yoshitsugu, S.; Yasushi, T.; Yoshihisa, Y. *J. Organomet. Chem*. **1994**, *473(1-2)*, 163-73.
75 Asandei, A. D.; Adebolu, O. I.; Simpson, C. P. *J. Am. Chem. Soc.* **2012**, *134*, 6080−6083.
76 (a) Drago, R. S.; Wong, N. M.; Ferris, D. C. *J. Am. Chem. Soc.* **1992**, *114,* 91-98. (b) Bond strengths *D*(Mn-X) for I-Mn(CO)5, Br-Mn(CO)5, and Cl-Mn(CO)5 are 54, 66, and 78kcal/mol,

respectively (c) *Principles and Applications of Organotransition Metal Chemistry.* Collman, J. P.; Hegedus, L. S.; Norton, J. R.; Finke, R. G.; University Science Books: Mill Valley, California, **1987**; pp 368-372.

77 (a) *Radiation-initiated solution polymerization of vinylidene fluoride***.** Doll, W. W.; Lando, J. B. *J. Appl. Poly. Sci.* **1970**, *14(7)*, 1767-73. (b) *Synthesis and microstructural characterization of low-molar-mass poly(vinylidene fluoride).* Russo, S.; Behari, K.; Chengji, S.; Pianca, M.; Barchiesi, E.; Moggi, G. *Polymer* 34, **1993**, *22*, 4777-4781.

78 Okafo, E. N.; Whittle, E. *Int. J. Chem. Kinet*. **1975**, *7(2)*, 287-300

79 *Photo-, electro-, and thermal carbonylation of alkyl iodides in the presence of Group 7 and 8-10 metal carbonyl catalysts*. Kondo, T.; Sone, Y.; Tsuji, Y.; Watanabe, Y. *J. Organomet. Chem.* **1994**, *473*, 163-73.

80 *Photoinduced Reactions of (CF3S)3N and CF3SeSeCF3 with Mn2(CO)10 and Fe(CO)5*. Chaudhuri, M. K.; Hass, A.; Wensky, A. *J. Organomet. Chem.* **1976**, *116*, 323-26.

81 *A Radical Mechanism for the Photochemical Iron Pentacarbonyl Catalyzed Hydrogenation Of Octenes*. Nagorski, H. *J. Organomet. Chem.* **1985**, *291*, 199-204.

82 Pulse Radiolysis of Iron Pentacarbonyl Solutions: The Role of the Tetracarbonyl Radical Anion. Reed, D. T.; Meckstroth, W. K. J. Phys. Chem. **1985**, 89, 4578-4580.

83 *Reduction of Metal Carbonyls via Electron Transfer. Formation and Chain Decomposition of Formylmetal Intermediates*. Narayanan, B. A.; Amatore, C.; Kochi, J. K. *Organometallics*, **1986**, *5*, 926-935.

84 *On Iron Carbonyls*. Mond, L. *J. Chem. Soc., Trans.* **1891**, *59*, 1090-3

85 *Mechanism of the Photochemical Oxidation of Fe(CO)5 and CpW(CO)3Cl (Cp = 5-C5H5) by Chlorocarbons.* Goldman, A. S.; Tyler, D. R. *Organometallics*, **1984**, *3*, 449-456.

86 *F-Alkyliron(II) Compounds*. Krespan, C. G. *J. Fluor. Chem.* **1988**, *40*, 129-137**.**

87 Bitterwolf, T. E.; Linehan, J. C.; Shade, J. E. Organometallics, 2000, 19, 4915-4817. (b) Sun, X. Z.; Nikiforov, S. M.; Dedieu, A.; George, M. W. Organometallics, 2001, 20, 1515-1520.

88 (a) Wrighton, M. S.; Hepp, A. F. *J. Am. Chem. Soc.* **1981**, *103*, 1258-1261. (b) Espenson, J. H. *J. Mol. Liq*. 1995, 65/66, 205-212.

89 Bitterwolf, T. E. Coord. CHem. Rev. 2001, 211, 235-254.

90 Meyer, T. J.; Caspar, J. V. Chem. Rev. 1985, 85, 187-218.

91 Tyler, D.R.; Castellani, M.P.; Philbin, C. E.; Pan, X. Inorg. Chem. 1988, 27, 671-676.

92 Peters, J.; George, M. W.; turner, J. J. Organometallics, 1995, 14, 1503-1506.

93 (a) Boutevin *J. Polym. Sci.*: *Part A: Polym. Chem.* 2000, *38*, 3235–3243. (b*)* Reghunadhan Nair, C. P.; Sivadasan, P.; Balagangadharan, V. P. *J. Macromol. Sci., Part A: Pure Appl. Chem.* **1999**, *A36(1)*, 51–72. (c) *Kinetics and Modeling of Vinyl Acetate Graft Polymerization from Poly(ethylene glycol)* Zhu, X.; Li, B. G.; Wu, l.; Zheng, Y.; Zhu, S.; Hungenberg, K. D.; Mussig, S.; Reinhard, B. *Macromol. React. Eng*. **2008**, *2*, 321–333.

94 (a) *Controlled step-wise telomerization of vinylidene fluoride, hexafuoropropene and trifuoroethylene with iodofluorinated transfer agents*. Balague, J.; Ameduri, B.; Boutevin, B.; Caporiccio, G. *J. Fluorine Chem.* **2000**, *102*, 253-268. (b) *Use of Telechelic Fuorinated Diiodides to Obtain Well-Defined Fuoropolymers*. Ameduri, B.; Boutevin, B. *J. Fluorine. Chem*. **1999**, *100*, 97-116. (c) *Synthesis of fluorinated telomers.1. Telomerization of vinylidene fluoride with Perfluoroalkyl Iodides*. Balague, J.; Ameduri, B.; Boutevin, B.; Caporiccio, G. *J. Fluorine Chem.* **1995**, *70*, 215-223.

95 *Fullerenes Decorated with Poly(vinylidene fluoride)* Vukicevic, R.; Beuermann, S. *Macromolecules*. **2011**, *44*, 2597–2603.
96 *New AB or ABA type block copolymers: atom transfer radical polymerization (ATRP) of methyl methacrylate using iodine terminated PVDFs as (macro)initiators.* Seong-Mu Jol, S. M.; Lee, W. S.; Byoung-Sung Ahn, B.S.; Park, K Y.; 2, Kim, K. A.; Paeng, I. R. *Polym. Bull.* **2000**, *44*, 1–8.
97 *NMR Chemical Shifts of Trace Impurities: Common Laboratory Solvents, Organics, and Gases in Deuterated Solvents Relevant to the Organometallic Chemist*. Fulmer, G. R.; Miller, A. J. M.; Sherden, N. H.; Gottlieb, H. E.; Nudelman, A.; Stoltz, B. M.; Bercaw, J. E.; Goldberg, K. I. *Organometallics* **2010**, *29*, 2176–2179.
98 (a) *Effect of molecular weight and chain end groups on crystal forms of poly(vinylidenefluoride) oligomers*. Herman; Uno, T.; Kubono, A.; Umemoto, S.; Kikutani, T.; Okui, N. *Polymer*. **1997**, *38(7)*, 1677-1683. (b) *High Resolution Nuclear Magnetic Resonance of Fluoro Polymers. 2. Fluorine-19 Spectra and Chain Structure of Poly(vinylidene fluoride)*. Ferguson, R. C.; Brame, E. G. *J. Phys. Chem*.**1979**, *83(11)*, 1397-1401. (c) *Radical Homopolymerization of Vinylidene Fluoride Initiated by tert-Butyl Peroxypivalate. Investigation of the Microstructure by 19F and 1H-NMR Spectroscopies and Mechanisms*. Guiot, J.; B. Ameduri, B.; B. Boutevin, B. *Macromolecules* **2002,** *35,* 8694-8707. (d) *End groups in Fluoropolymers*. Pianca, M.; Barchiesi, E.; Esposto, G.; Radice, S. *J. Fluorine Chem*. **1999**, *95*, 71-84. (e) Wormald, P.; Ameduri, B.; Harris, R. K.; Hazendonk, P. *Polymer* **2008**, *49*, 3629–3638.
99 (a) Boutevin, B. *J. Polym. Sci., Part A: Polym. Chem*. **2000**, *38*, 3235. (b) Ameduri, B.; Boutevin, B. *Top. Curr. Chem*. **1997**, *192*, 165.
100 Vasil'eva, T. T.; Mysova, N. E.; Chakhovskaya, O. V.; Terent'ev, A. B. *Russ. J. Org. Chem.* **2002**, *38(7)*, 1014-1017.
102 (a) *Characterization of end groups and branching structures in copolymers of vinylidene fluoride with hexafluoropropylene using multidimensional NMR spectroscopy*. Twum, E. B.; McCord, E. F.; Lyons, D. F.; Fox, P. A.; Rinaldi, P. L. *Eur. Poly. J.*, **2014**, ***51***, 136. (b) *Poly(vinylidenefluoride-co-tetrafluoroethylene).* Li, L.; Twum, E. B.; Li, X.; McCord, E. F.; Lyons, D. F.; Fox, P. A.; Rinaldi, P. L. *Macromol*. **2013**, *46*, 7146−7157.
103 (a) Balague, J.; Ameduri, B.; Boutevin, B.; Caporiccio, G. *J. Fluorine Chem.* **1995**, *70*, 215-223. (b) Balague, J.; Ameduri, B.; Boutevin, B.; Caporiccio, G. *J. Fluorine Chem.* **2000**, *102*, 253-268.
104 Wormald, P.; Ameduri, B.; Harris, R. K.; Hazendonk, P. *Polymer* **2008**, *49*, 3629–3638.
105 Guiot, J.; B. Ameduri, B.; B. Boutevin, B. *Macromolecules* **2002,** *35,* 8694-8707.
106 Pianca, M.; Barchiesi, E.; Esposto, G.; Radice, S. *J. Fluorine Chem*. **1999**, *95*, 71-84.
107 Fulmer, G. R.; Miller, A. J. M.; Sherden, N. H.; Gottlieb, H. E.; Nudelman, A.; Stoltz, B. M.; Bercaw, J. E.; Goldberg, K. I. *Organometallics* **2010**, *29*, 2176–2179.
108 Herman, X.; Uno, T.; Kubono, A.; Umemoto, S.; Kikutani, T.; Okui, N. *Polymer* **1997**, *38*, 1677-1683.
109 Bovey, F. A.; Jelinski, L. W.; Academic Press: New York, **1982**, p 157.
110 Ferguson, R. C.; Brame, E. G. *J. Phys. Chem*. **1979**, *83*, 1397-1401.
111 Russo, S.; Behari, K.; Chengji, S.; Pianca, M.; Barchiesi, E.; Moggi, G. *Polymer* 34, **1993**, *22*, 4777-4781
112 Timmerman, R.; Greyson, W.; *J. Appl. Polym. Sci.* **1962**, *6(22)*, 456-460.

113 David, G.; Boyer, C.; Tonnar, J.; Ameduri, B.; Lacroix-Desmazes, P.; Boutevin, B. *Chem. Rev.* **2006**, *106*, 3936–3962.
114 Boyer, C.; David, V.; Lacroix-Desmazes, P.; Ameduri, B.; Boutevin, B. *J. Polym. Sci.: Part A: Polym. Chem*. **2006**, *44*, 5763–5777.
115 Ameduri, B.; Ladavière, C.; Delolme, F.; Boutevin, B.; *Macromolecules* **2004**, *37*, 7602-7612.
116 El Soueni, A.; Tedder, J. M.; Walton, J. C. *J. Fluorine Chem.* **1978**, 11, 407—417
117 Duc, M.; Ameduri, B.; Ghislain, D.; Boutevin, B. *J. Fluorine Chem*. **2007**, *128*, 144–149.
118 (a) Koumura, K.; Satoh, K.; Kamigaito, M. *Macromolecules* **2008**, *41 (20)*, 7359-7367. (b) Koumura, K.; Satoh, K.; Kamigaito, M. *J. Polym. Sci.: Part A: Polym. Chem*. **2009**, *47*, 1343–1353.
119 Imran-ul-haq, M.; Beuermann, S. *Macromol. Symp*. **2009**, *275-276*, 102–111.
120 Drago, R. S.; Wong, N. M.; Ferris, D. C. *J. Am. Chem. Soc.* **1992**, *114,* 91-98
121 (a) Okafo, E. N.; Whittle, E. *Int. J. Chem. Kinet*. **1975**, *7(2)*, 287-300; (b) Ahonkhai, S. I. *Int. J. Chem. Kinet*. **1984**, *16(5)*, 543-58.
122 Anslyn, E. V.; Dougherty, D. A. *Modern Physical Organic Chemistry*, Chapter 16, *Photochemistry* p. 955-956, University Science Books, **2006**.
123 Pan, X.; Philbin, C. E.; Castellani, M. P.; Tyler, D. R. *Inorg. Chem.* **1988**, *27*, 671-676.
124 (a) Mamooda, Z.; Azama, M.; Mushtaqa, A.; Kausara, R.; Kausara, S.; Gilanib, S. R. *Spectrochim. Acta, Part A.* **2006**, *65(2*), 445-452. (b) Kaesz, H. D.; Bau, R.; Hendrickson, D.; Smith, J. M. *J. Am. Chem. Soc.* **1967**, *89*, 2844.
125 (a) Koumura, K.; Satoh, K.; Kamigaito, M. *Macromolecules*, **2008**, *41*, 7359. (b*)* Koumura, K.; Satoh, K.; Kamigaito, M. *J. Polym. Sci.: Part A: Polym. Chem*. **2009**, *47*, 1343. (c) Koumura, K.; Satoh, K.; Kamigaito, M. *Macromolecules* **2009**, *42*, 2497.

Chapter 5. Evaluation of Cu-Mediated Room Temperature Radical Polymerization of Vinylidene Fluoride: from Atom Transfer Radical Polymerization to Iodine Degenerative Transfer.

A series of various alkyl, fluoro, and sulfonyl halides were evaluated as room temperature initiators for vinylidene fluoride controlled radical polymerization. The polymerizations were attempted in a number of ways; direct ATRP, ARGET-like, as well as a Cu-initiated iodine degenerative chain transfer, including activation by irradiation. However, in none of these experiments was polymer obtained. There are a few explanations which are likely. First, it is possible that the rate of radical generation is just too, not all alkyl radicals may be reactive enough to add to VDF at rt, and copper failing to activate Fluoroalkyl halides or side reactions with the amine ligands. Additionally, strong chain transfer to solvent, ligand etc. may stop the polymerization in its incipient phase. Ultimately a new methodology was developed with a photo-IDT system, and thus enabled PVDF-I synthesis which make use of perfluoroalkyl iodides as photo-iniferters in conjunction with Cu(0) as a iodine "sink". The role of copper is solely there to inhibit the persistent radical effect that would otherwise normally prevent these materials from initiating polymerizations. Under irradiation it was demonstrated that in the absence of an iodine "sink" such as copper these alkyl iodides had extremely low decomposition rates, which was nearly 100 times faster in the presence of metal zero. This system was then utilized to produce I-PVDF-I. These preliminary experiments showed typical CRP properties, having a linear dependence of molecular weight on conversion, and most importantly generated the highest total %-functionality of any system previously studied, yielding $\geq$ 99%. This system can surely be envisioned as applicable and tailored to use with other monomers and various polymerizations and being CRP process is very tolerant of functional groups and solvent, even allowing for the use of emulsion polymerizations.

5.1 Introduction

Controlled radical polymerization (CRP) has been widely applied in the synthesis of complex macromolecular structures.[1] While catalytic systems based on late transition metals were successful in CRP mediated by atom transfer radical polymerization (ATRP)[1,2,] dissociation-combination (DC) and degenerative transfer (DT) and initiated from activated halides or thermal initiators, a broader selection of initiators and catalysts is still needed for the controlled polymerization of fluorinated monomers.

Fluorinated (co)polymers are specialty materials with wide morphological versatility, high thermal, chemical, ageing and weather resistance, as well as low surface energy, dielectric constant, flammability, refractive index, and moisture absorption. As such, their applications range anywhere from paints and coatings, pipe liners, transmission fluids, O-rings for extreme temperatures (rocket engines), fuel cell membranes, antifouling layers etc., to optical fibers and high power capacitors.[3] Therefore, their precise synthesis is very relevant. However, while controlled/living radical polymerizations (C/LRPs) have recently seen remarkable developments,[2] and classic ATRP, nitroxide or addition-fragmentation methods are successful with acrylates or styrenes, their applicability in the CRP of very reactive monomers such as main chain fluorinated alkenes, still awaits demonstration.

The paramagnetic Cp_2TiCl,[4] available in situ by Zn reduction of Cp_2TiCl_2[5] is a mild one electron transfer agent which catalyzes a variety of radical reactions[6] including epoxide radical ring opening (RRO)[7], aldehyde SET reduction and halide abstraction. We have demonstrated the Cp_2TiCl-catalyzed CRP of styrene[8] initiated by epoxides, aldehydes,[9] halides[10] and peroxides,[11] as well as that of dienes[12] initiated from halides,[13e,f,l,14] epoxides,[13a,b,g] and aldehydes.[13c,d] The effect of all reaction variables was also investigated.[8] This methodology was also applied in the synthesis of branched and graft copolymers.[15] Ti alkoxides generated in-situ from epoxides and

aldehydes also catalyze the living ring opening polymerization of cyclic esters,[16] epoxides and anhydrides.[16] Unfortunately, as discussed previously, this system fails when being used for the polymerization of fluorinated monomers.

Thus, as (co)polymers based on main chain fluorinated monomers (*e.g.* vinylidene fluoride (VDF), are industrially significant, the study of their CRPs and the synthesis of the complex polymer architectures derived thereby is a worthy endeavor.[17,18] However, such polymerizations are quite challenging on a laboratory scale, in view of the fact that *e.g.* VDF boils at -83 °C. Since typical telo/polymerizations are carried out at 80-100 °C or more,[3] they require specialized, high-pressure metal reactors.

Accordingly, and by contrast to styrene or acrylate CRPs which can be conveniently sampled repeatedly from the side arm of a Schlenk tube on *e.g.* a 1 g scale, kinetic studies of VDF polymerizations involve many one-data-point experiments. This is very time-consuming and expensive due to the typical lab unavailability of a large number of costly metal reactors, which moreover still require tens of grams of monomer. Thus, development of methods that would allow small, gram-scale polymerizations to proceed at room temperature (rt) in inexpensive, low-pressure, glass tubes, would be highly desirable, especially since they could easily be adapted for the fast screening of a wide range of catalysts and reaction conditions.

Interestingly, VDF polymerization was shown to proceed in the presence of alkylboron/O_2, in a poorly controlled radical manner at ambient temperature.[19] Nonetheless, bock copolymers could be synthesized. We have also described the room temperature UV free radical polymerization of VDF initiated from TBPO.[20] However, only very low molecular weight VDF telomers (DP < 1-3) may be obtained, and only at high temperatures (> 100 °C) from transition metal salts and polyhalides by redox catalysis.[18,21]

Moreover, while the 1:1 thermal and or metal catalyzed addition of R_F-I derived perfluoroalkyl radicals to alkenes using Cu,[22] Zn,[23] Pd,[24] $SnCl_2/CH_3COOAg$,[25] Cp_2TiCl,[26] PPh_3,[27] AIBN,[28,29] $(NH_4)_2S_20_8/HCOONa$[30] or of the corresponding Grignard-like Zn[31, 32] or Zn/Cu[33] derived organometallics to carbonyls and amides occurs under a wide range of conditions, and especially at high temperatures, the metal catalyzed addition of such electrophilic radicals to electrophilic fluorinated alkene substrates such as FMs at T < 100 °C, and especially at ambient temperatures is to the best of our knowledge, conspicuously absent from the literature.

Therefore, the ability to carry out such reactions under mild conditions, would be of great synthetic value, especially in the initiation of the CRP of FMs. Thus, since to the best of our knowledge, while copper complexes have proven extremely successful in ATRP, there are no reports on metal-mediated VDF polymerizations let alone Cu-Mediated/assisted VDF-CRP. As such we decided to explore the scope and limitations of late-transition metal catalysts in the initiation of room temperature radical VDF polymerizations *via* typical ATRP protocols, making use of the persistent radical effect (PRE).

The persistent radical effect (PRE)[34] states that if two radicals with widely different stability (*i.e.* a conventional unstable X• and a persistent Y• ; where the lifetimes of which are orders of magnitude different) are formed in a homolysis (X-Y $\rightarrow$ X + Y) reaction, or produced independently and allowed to react, then their cross-coupling X-Y product will dominate over X-X and of course over Y-Y which is unstable and negligible. Such features have been widely exploited in both organic chemistry as well as controlled radical polymerizations (CRPs) by the dissociation-combination (DC) or atom-transfer (ATRP) mechanisms, where the bimolecular termination of the growing chains is dramatically suppressed by their cross coupling with a persistent radical (nitroxide or a halide radical supported by a transition metal complex)[34]

Alternatively, CRPs based on degenerative transfer (RAFT, IDT, titanium,[8-16] tellurium,[35] mediated polymerizations do not require PRE, and irreversible bimolecular termination is suppressed *via* reversible exchange of a transferable group (I, RAFT, Ti, Te) between propagating and dormant chains. Indeed, IDT,[36,37] may in fact be the oldest CRP method,[38] Moreover, since metal mediated alkyl halide radical initiation and VDF-CRP was not available until very recently,[39] industrial VDF-CRP is still accomplished at high temperatures and pressures using perfluorinated alkyl iodides (R_F-I)[40-43] chain transfer agents (CTAs),[36] and peroxide free radical initiators.[36,41]

Iodine degenerative transfer (IDT) involves the reversible exchange of iodine between dormant and propagating chains and is typically set-up either by a free radical initiator in the presence of an iodine chain transfer agent (R-I), by direct transition metal *irreversible* activation of an alkyl iodide ($Mn_2(CO)_{10}$),[39] or by the in-situ generation of the alkyl iodide via trapping of the growing chains with iodine. However, to the best of our knowledge, (except for $Mn_2(CO)_{10}$) there are no reports of photo mediated IDT or Cu(0) photo IDT in the absence of a ligand. Moreover, the concept of PRE of iodine has not been recognized by the organic or polymer community.

While I_2 is not a radical, and I$^\bullet$ is clearly not a persistent species, the I-I bond is extremely weak and, moreover, I_2 is known to intercept radicals at diffusion controlled rates. Thus, while I_2 does not add to VDF,[44] it traps radicals at diffusion controlled rates,[45] by intercepting[46] $CX_3^\bullet$ and PVDF$^\bullet$. In fact the cross coupling of radicals with iodine is higher than with CuX_2 or nitroxides. Indeed, I_2 is considered a very strong inhibitor of radical reactions, including polymerizations.

However, to the best of our knowledge, the occurrence of the PRE was never considered to explain the outcome of iodine radical reactions. We thus theorize that while indeed I_2 is not a radical, but for all intents and purposes it behave like one, and in fact does support the PRE. This

was demonstrate using the well-known photodecomposition/homolysis of alkyl and perfluoroalkyl iodides.

Indeed, due to the very weak C-I BDE, most conventional alkyl iodides will easily photolyze on standing and the orange/pink iodine color is easily identifiable upon exposure to lab light overnight. Accordingly, all suppliers of alkyl iodides (Sigma-Aldrich, Strem, etc.) ship such compounds in brown glass containers. Moreover, they also ship it allegedly "stabilized" with copper pellets or turnings. However, there is no literature evidence or understanding in what way copper may "stabilize" against such photodecomposition. We believe that such statements are in fact wrong and misleading. It is known that at room temperature and in the absence of ligands Cu(0) does not insert into the C-I bond. What we believe is happening, is that if fact copper merely serves as a "sponge" to trap iodine generated via dissociation and thus give the perception of a "pure", "clean" sample.

In reality, no inhibitor that can *chemically* prevent photolysis. However, one can push the dissociation equilibrium back to the R-I starting material. This is indeed where the iodine PRE (IPRE) comes into play. Thus, after R-I homolysis, a few couplings of R into R-R quickly leads to the accumulation of the corresponding amount of I_2, which will suppress any subsequent R dimerization by trapping it back into R-I. Thus we believe that the addition of copper is not necessary, and that while iodine colored, the samples are more stable than in the presence of copper. Before use, as demonstrated herein, the iodine color can be easily removed by stirring with Cu(0).

It is known from our control experiments with VDF/RFI under visible light irradiation for over a week produced no polymer, but rather turned orange, which is the color of I_2 in DMC. Therefore adding copper should inhibit the PRE and allow polymerization to occur. Finally the most illustrative experiments are based on the kinetics of the photolysis of a variety of alkyl and

perfluoroalkyl iodides in the presence of copper. Thus also introduced below is the Cu(0) inhibition of the persistent radical effect of iodine in the photolysis of (fluoro)alkyl iodides as a universal and chemically simple (VDF) IDT-CRP method.

5.2 Experimental

5.2.1 Materials.

1-(bromoethyl)benzene (BEB, 95%), bromoform ($CHBr_3$, 99%), tin(II)-2-ethylhexanoate($Sn(Oct)_2$, 95%), tris(2-aminoethyl) amine (TREN, 96%), pentamethyldiethylene triamine (PMDETA, 99%), sodium dodecyl sulfate (SDS, 99%), copper(I) bromide (CuBr, 98%), copper(0) (Cu(0) 99%), α,α,α-trifluorotoluene (TFT, 99%), acetonitrile (ACN, 99%) and anisole (99.7%) (all from Aldrich), Iodoform (CHI_3, 98%), copper(II) bromide ($CuBr_2$, 99%), copper(II) chloride ($CuCl_2$, 98%), dioxane (99.7, %) 99%), 4-methoxybenzene sulfonyl chloride (MBSC, 99%) (all from Acros),vinylidene fluoride (VDF, 99%), 1-iodononafluorobutane (PFBI, 98%) (all from Synquest), and N,N'-dimethylformamide (DMF, 99.9%, Fisher), bipyridyl (BiPy, 98%, Alfa Aesar), were used as received. Ethyl-2-iodoisobutyrate (EIIB) and α,α-diiodo-p-xylene (DIPX) were prepared from ethyl-2-bromoisobutyrate (EBIB, 98%, Acros), α,α-dibromo-p-xylene, (DBPX, 98%, Fluka) and NaI (99%, Fisher) respectively.

5.2.2 Techniques.

^{1}H NMR (500 MHz) and ^{19}F-NMR (400 MHz) spectra were recorded on a Bruker DRX-500 and respectively on a Bruker DRX-400 at 24 ^{0}C in acetone-d_6 typically between 32-128 scans. 2D-^{19}F{^{1}H},-Heteronuclear correlation (HETCOR) spectra were recorded on a Bruker DRX-400 at 24 ^{0}C with a scan set of 16x256 using typical Bruker pulse sequences for HETCOR. GPC analyses were performed on a Waters gel permeation chromatograph equipped with a Waters 2414 differential refractometer and a Jordi 2 mixed bed columns setup at 80^{0}C. DMAc (Fisher, 99.9% HPLC grade) was used as eluent at a flow rate of 1 mL/min. Number-average (M_n) and weight-

average molecular weights (M_w) were determined from calibration plots constructed with polymethylmethacrylate standards. All reported polydispersities are those of water precipitated samples. While narrower PDIs could be obtained by MeOH precipitation, this may also lead to partial fractionation, especially for lower molecular weight samples.

5.2.3 Polymerizations.

A 35-mL Ace Glass 8648 # 15 Ace-Thread pressure tube equipped with bushing and a plunger valve containing CuBr (4.9 mg, 0.04 mmol), BiPy (16.1 mg, 0.12 mmol) and ACN (3.0 mL) was degassed then cooled, opened under Ar and charged with PFBI (0.06 mL, 0.34 mmol) and vinylidene fluoride (1.10g, 17.18 mmol), re-degassed and placed in an oil bath at 25 C. Conversions were determined gravimetrically. 150W Oriel Xenon Arc lamp model 66060 (with PTI Lamp power supply model lps200).

5.3 Results and Discussion

The selected examples of the attempts at radical initiation of VDF at various temperatures from all initiators are presented in Table 5.1. The polymerization was attempted in many different ways, either as a direct ATRP, ARGET-like, as well as a Cu-initiated iodine degenerative chain transfer, including extra activation by low (BLB), medium (UV), or high intensity UV lamps (oriel), and visible light irradiation. However, in none of these experiments was polymer obtained for which there are several likely explanations (also depicted in scheme 5.1). First, it is possible that the rate of radical generation is just too slow under these conditions. However, sulfonyl chlorides are known to be easily activated by Cu even at rt.[47] However, the carbon-halide bond in the -CH_2-CF_2-X terminal dormant unit may also be too hard to homolyze at low temperatures leading to irreversible deactivation. Second, not all of the possible resulting alkyl radicals may be reactive enough to add to VDF at rt. Nevertheless, perfluoro alkyl iodides do add to VDF, but here there was again no polymer formed which can be attributed to either copper

not activating or a side reaction with the amine ligands.[24] Third, strong chain transfer to solvent, ligand etc. may stop the polymerization in its incipient phase. Thus, DMF may be a good PVDF solvent, but also is a good chain transfer agent, especially for a reactive propagating chain. Similarly, dioxane and anisole may also be conducive to chain transfer. Lastly, while the high temperature Cu-catalyzed grafting from PVDF was previously reported,[48] we believe that the activation of C-F bond and formation of unreactive CuF_2, is extremely unlikely at rt.

Table 5.1: Cu Mediated Redox Initiating Systems (25°C)

Exp	Initiator	Cat.	Co-Cat.	Ligand	Ratio	Solvent	Temp.(°C)	Light Source
1	BEB	nCu	$Sn(Oct)_2$	PMEDTA	50/1/0.1/2/4	ACN/Diox	25	N/A
2	CCl4	CuBr		BiPy	25/1/0.5/1.5	DMC	25	UV
3	CCl4	CuBr		Me6TREN	50/1/1/1	DMC	25	UV
4	CCl4	CuBr		Me6TREN	50/1/0.25/0.25	DMC	40	N/A
5	CCl4	CuBrPhenPPh3			50/1/0.25	DMC	40	Vis
6	CCl4	CuCl2	Zn(0)/Cu(0)	Me6TREN	1/2/0.001/2/2/0.001	CCl4	40	N/A
7	CCl4	nCu	CuBr	Me6TREN	25/1/1/1/2	DMC	40	Vis
8	CCl4	nCu		Me6TREN	50/1/1/1	DMC/DMSO	50	N/A
9	CCl4	nCu		PMDETA	25/10/2/2	DMC	40	Vis
10	CH3I	CuBr2	SnOct	PMDETA	50/1/0.05/0.1/0.1	ACN	25	N/A
11	CHBr3	nCu	SnOct	TREN	10/1/1/1/1	ACN	25	N/A
12	CHBr3	nCu	SnOct	TREN	40/1/1/1/1	ACN	25	N/A
13	CHBr3	nCu	SnOct	TREN	40/1/1/1/1	DMSO	25	N/A
14	CHCl3	nCu	CuBr	BiPy	25/1/1/1/3	DMC	40	Vis
15	DBPFH	CuBr		BiPy	50/1/5/15	DMC	40	N/A
16	DBPFH	CuBr	Cu(0)	TREN	50/1/0.2/0.2	DMSO	50	N/A
17	DBPFH	CuBr2	Vit C	PMDETA	50/1/0.1/1/0.1	ACN	40	N/A
18	DBPFH	CuBr2		TREN	50/1/0.05/0.3	ACN	40	Blb
19	DBPFH	CuCl2	Vit C	PMDETA	50/1/0.075/5/0.075	ACN	40	N/A
20	DBTFP	CuBr2	SnOct	PMDETA	50/2/0.005/0.1/0.1	ACN	25	UV
21	DCPFH	CuBr		Me4Cyclam	25/1/0.3/0.3	DMC	50	N/A
22	DCPFH	CuBr		Me6TREN	25/1/0.3/0.3	DMC	50	N/A
23	DCPFH	CuBr		PMDETA	25/1/0.3/0.3	DMC	50	N/A
24	DIPFH	CuBr		Me6TREN	50/1/0.1/0.1	H2O	40	N/A
25	DIPFH	CuBr	CuWire	methoxy Bipy	100/1/0.1/xs/0.3	DMC	40	Vis
26	DIPFH	CuBr2	SnOct	BiPy	75/1/.2/1.35/3	anisole	25	N/A
27	DIPFH	CuBr2	SnOct	BiPy	75/1/.2/1.35/2	DMF	25	N/A
28	DIPX	nCu	SDS	TREN	50/1/2/2/2	ACN/H2O	25	N/A
29	EBDFA	CuBr		TREN	40/1/.5/.5	ACN	25	N/A
30	EIDFA	CuBr		BiPy	25/1/0.1/0.3	ACN	60	N/A
31	EIIB	CuBr2	Vit C	BiPy	50/1/.1/2/.3	ACN	25	N/A
32	MBSC	CuBr		BiPy	75/1/1/3	DMF	25	N/A
33	MBSC	CuBr	SnOct	BiPy	75/1/.1/1/2	DMF	25	N/A

Table 5.1: Cu Mediated Redox Initiating Systems (25°C)

Exp	Initiator	Cat.	Co-Cat.	Ligand	Ratio	Solvent	Temp.(°C)	Light Source
34	MBSC	CuBr	SnOct	BiPy	75/1/.1/1/2	Dioxane	25	N/A
35	MBSC	CuBr	SnOct	BiPy	75/1/.1/1/2	Trifluoro Toluene	25	N/A
36	MBSC	CuBr2	TBPB	BiPy	20/1/.1/1/2	anisole	25	UV
37	MBSC	CuBr2	SnOct	BiPy	20/1/.1/1/2	anisole	25	N/A
38	MBSC	CuBr2	SnOct	BiPy	20/1/.1/1/2	DMF	25	N/A
39	MBSC	CuBr2	SnOct	BiPy	20/1/1/1/3	anisole	25	N/A
40	PFBI	ClCu(PPh3)3	nZn	PPh3	50/1/0.05/0.5/0.5	ACN	25	Vis
41	PFBI	ClCu(PPh3)3			25/1/0.05	Anisole	25	Oriel
42	PFBI	ClCu(PPh3)3			25/1/0.05	Ethylene Carb	45	N/A
43	PFBI	Cu(OAc)2	Hydrazine		25/1/0.1/1	ACN	25	N/A
44	PFBI	CuBr		BiPy	25/1/0.1/0.3	DMC	25	Dark
45	PFBI	CuBr		BiPy	50/1/0.1/0.3	ACN	25	Oriel
46	PFBI	CuBr	Bu3SnI	BiPy	25/1/0.1/0.2/0.3	ACN	25	N/A
47	PFBI	CuBr		BiPy	25/1/0.5/1.5	Ethylene Carb	45	N/A
48	PFBI	CuBr	Na2S2O3	BiPy	25/1/0.3/1/0.9	DMC/H2O	50	N/A
49	PFBI	CuBr	Bu3SnI	BiPy	50/1/0.1/0.1/0.3	DMC	25	N/A
50	PFBI	CuBr		dinonyl Bipy	50/1/0.25/0.75	DMC	40	N/A
51	PFBI	CuBr	Hexadecyl Ammonium Br	PMDETA	50/1/1/0.05/1	DMC/H2O	25	N/A
52	PFBI	CuBr		TetraMethylCyclam	25/1/0.1/0.1	DMC	25	N/A
53	PFBI	CuBr		TPMA	20/1/0.01/0.01	Propylene Carb	25	UV
54	PFBI	CuBr		TPMA	25/1/0.05/0.05	DMC	45	N/A
55	PFBI	CuBr		TPMED	25/1/0.1/0.1	DMC	50	N/A
56	PFBI	CuBr/Cu(0)	Bu3SnI	BiPy	50/1/0.1/0.1/0.2/0.6	DMC	40	Vis
57	PFBI	CuBr2	SnOct	BiPy	50/1/0.05/0.1/0.1	ACN	25	UV
58	PFBI	CuBr2		BiPy	25/1/0.4/1.2	MeOH	25	UV
59	PFBI	CuBr2	SnOct	BiPy	20/1/0.01/0.1/0.1	DMC	50	N/A
60	PFBI	CuBr2	SnOct	Me6TREN	50/1/0.05/0.1/0.1	ACN	25	N/A
61	PFBI	CuBr2	SnOct	PMDETA	500/1/0.005/0.1/0.1	ACN	25	UV
62	PFBI	CuBr2	SnOct	PMDETA	50/1/0.05/0.1/0.1	Acetonitril	25	UV
63	PFBI	CuBr2	SnOct	PMDETA	25/1/0.005/0.1/0.1	DMF	25	UV
64	PFBI	CuBr2	TBPO	PMDETA	50/1/0.005/0.1/0.1	ACN	25	UV
65	PFBI	CuBr2		PMDETA	25/1/0.2/0.2	MeOH	25	UV
66	PFBI	CuBr2	SnOct	PMDETA	50/1/0.005/0.1/0.1	ACN	100	Vis

Table 5.1: Cu Mediated Redox Initiating Systems (25°C)

Exp	Initiator	Cat.	Co-Cat.	Ligand	Ratio	Solvent	Temp.(°C)	Light Source
67	PFBI	CuBr2	SnOct	PMDETA	50/1/0.005/0.1/0.1	ACN	40	N/A
68	PFBI	CuBr2	SnOct	TPMA	50/1/0.05/0.1/0.1	ACN	25	UV
69	PFBI	CuBr2	Sn(Oct)	TPMA	50/1/0.1/0.1/2	Ethylene carbonate	40	Vis
70	PFBI	CuBr2	SnOct	PMDETA	50/1/0.005/1/1	ACN	25	UV
71	PFBI	CuBrPhen	nZn	PPh3	50/1/0.05/0.5/0.5	ACN	25	Vis
72	PFBI	CuBrPhenPPh3			50/1/0.05	ACN	25	Oriel
73	PFBI	nCu		BiPy	50/1/1/3	ACN	25	N/A
74	PFBI	nCu	Na2S2O3	BiPy	25/1/1/1/3	DMC/H2O	50	N/A
75	PFBI	nCu		TetraMethylCyclam	25/1/0.1/0.1	DMC	25	N/A
76	PFBI	nCu	SDS	TREN	50/1/2/2/2	ACN/H2O	25	N/A
77	PFBI	nCu		TREN	25/1/0.1/0.1	DMSO	25	N/A
78	PFBI	nCu		TREN	50/1/1/1	ACN/H2O	25	N/A
79	PFBI	nCu		TREN	25/1/0.25/0.25	H2O/Propylene Carb	25	N/A
80	PFBI	nCu			50/1/0.5	DMC	25	UV
81	PFIpI	CuBr		BiPy	50/1/0.1/0.3	DMSO	25	UV
82	PFIpI	CuBr		BiPy	50/1/0.1/0.3	DMSO	25	N/A
83	PFIpI	CuBr2	SnOct	BiPy	50/1/0.005/0.1/0.1	ACN	70	UV
84	PFIpI	CuBr2	SnOct	BiPy	50/1/0.1/0.1/0.3	ACN	70	UV
85	PFIpI	CuBr2	SnOct	PMDETA	50/1/0.005/0.1/0.1	ACN	25	UV
86	PFIpI	nCu		TREN	25/1/1/1	ACN	60	N/A
87	PFtBI	CuBr2	SnOct	BiPy	50/1/0.1/0.1/0.3	ACN	70	UV
88	TBPO	CuBr2		BiPy	20/1/1/3	anisole	25	UV
89	TBPO	CuBr2	SnOct	BiPy	20/1/1/1/3	anisole	25	UV
90	TBPO	CuBr2	SnOct	BiPy	20/1/.1/1/1	anisole	25	UV
91	TBPO	CuBr2	SnOct	BiPy	10/1/.05/.05/.2	ACN	25	UV
92	TBPO	CuBr2		BiPy	10/1/.05/.2	ACN	25	UV
93	TBPO	CuBr2	SnOct	TREN	20/1/.1/1/1	Toluene	25	UV
94	TBPO	CuBr2	SnOct	TREN	20/1/.1/1/1	DMSO	25	UV
95	TBPO	CuBr2	SnOct	TREN	10/1/.1/.1/.1	ACN	25	UV

Bipyridyl(BiPy), Oriel; xenon arc lamp, UV; high intensity UV lamp 365 nm, Dark; foil wrapped, Blb; black light compact fluorescent bulb, vis; 30W compact fluorescent bulb

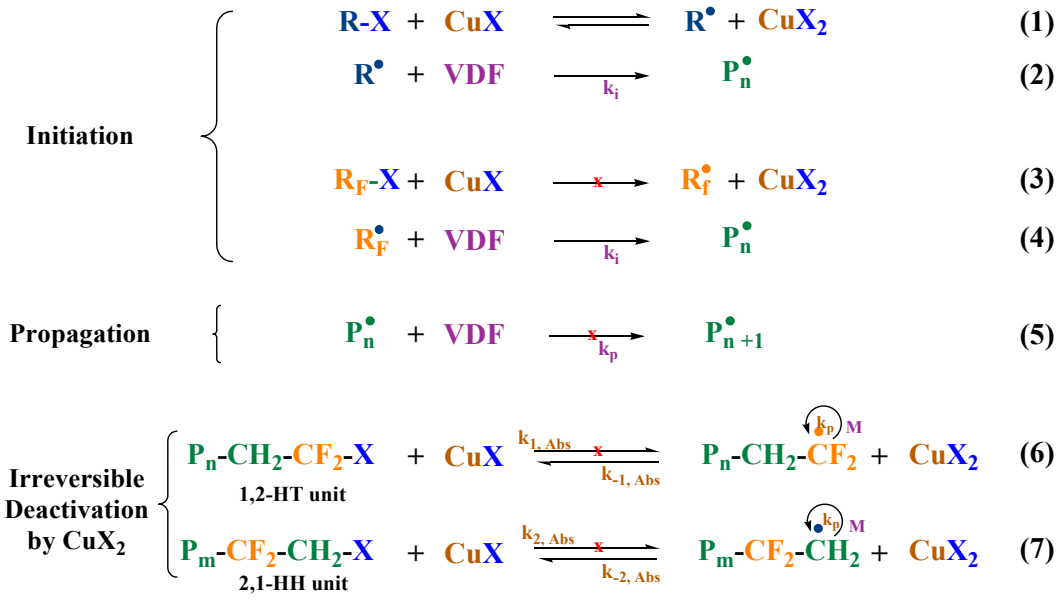

Scheme 5.1 Faults in the Cu-mediated ATRP of VDF with fluorinated/nonfluorinated initiators.

While the typical copper mediated experiments yielded no polymer in any attempt, we were able to develop a new unique methodology for this to succeed with a photo-IDT system, and thus enabled PVDF-I synthesis. In previous control experiments[49] with perfluoroalkyl iodides, upon irradiation of the reaction mixture containing solvent, monomer, and initiator (R_F-I) it was always observed that indeed these mixtures eventually became colored with a faint shade of orange/pink, typical of I_2 present in solution. This led us to believe that if in fact we were generating I_2, then the initiator itself, under visible light irradiation undergoes photo-induced homolytic cleavage. Which is in fact typical with alkyl iodides, as their syntheses and storage generally always state to protect from light sources and store in the dark. This was a puzzling result, as the presence of I_2 would indicate that we were generating radicals, yet no polymerization was ever observed, and this seemed counterintuitive. To explain this we realized that I_2 is in fact a persistent species, such that any radical generated in the presence of I_2 will immediately be trapped. In the control experiments as the perfluoroalkyl iodides start to cleave

slowly under irradiation, even a few of the typical primary radical termination events will quickly lead to an excess of I_2 in solution (PRE), thus inhibiting any further degradation of the initiator, and if it does add to monomer, propagation. The relatively small amount of photo-degradation that takes place, even if it were to add to monomer, would not be measurable as a conversion gravimetrically on the scale of our experiments. Interestingly, often times commercially available alkyl and perfluoroalkyl iodides come stabilized with copper turnings or beads. As such, it occurred to us to try adding some copper(0) to the reaction (copper wire, figure 5.1) to see whether a noticeable reaction would occur. As seen below, after just a few minutes the copper has scavenged all the free iodine in solution, thus allowing us a clear means of removing iodine.

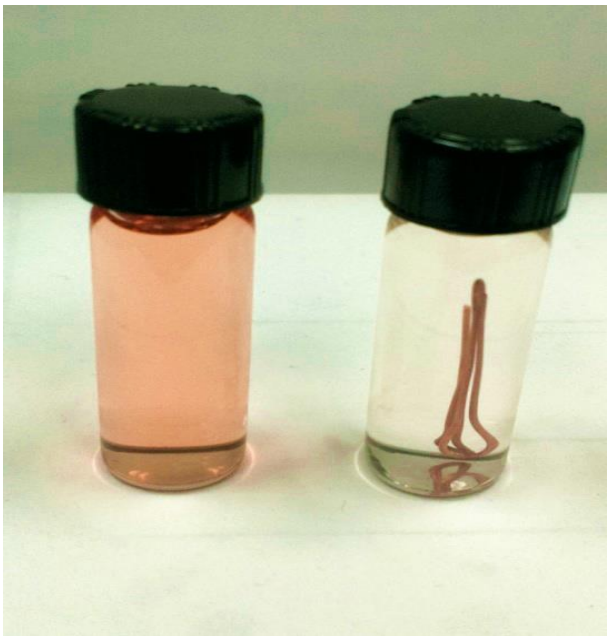

Figure 5.1 Two identical solutions of I_2 in DMC, left; no copper, right; 5 min. after Cu addition

A series of kinetic experiments for a set of alkyl and perfluoroalkyl iodides are shown in Figure 5.2) and indeed, under irradiation, and without the presence of copper wire, the photodecomposition is extremely slow. There was less than 10% loss (decomposition) of CF_2-I

(based on ^{19}F-NMR) after nearly 300 hour (Figure 5.2 ▲). This indicates, that while initially some of the material is decomposed, the I_2 generated is self-inhibiting and prevents further degradation, and this mixture indeed exhibited the typical orange/pink color of free I_2 in solution. The same experiment in the presence of copper wire gave vastly different results. When comparing the analogous experiment (Figure 5.2 ◆) for PFBI under irradiation with copper there is a 65x increase in the rate of decomposition of PFBI. We then proceeded to examine further various other alkyl iodides.(Figure 5.2) in every case there was relatively fast decomposition in the presence of copper wire, with iodoform and perfluoroisopropyl iodide being the fastest with the most stable compound, iodohexane, being the slowest. For polymerization applications the proposed mechanism is presented in scheme 5.2. First we see the photo-induced bond homolysis of the R_f-I (eq 1) followed by irreversible Cu(0) trapping of the initial excess iodine formed (eq 2). Once this occurs the remainder of the mechanism is consistent with typical VDF IDT-CRP.

Initiation and Propagation

$$R_f\text{-}I \underset{}{\overset{h\nu}{\rightleftharpoons}} R_f^{\bullet} + I^{\bullet} \quad (1)$$

$$I^{\bullet} + Cu(0) \overset{X}{\rightleftharpoons} CuI_{(S)} \quad (2)$$

$$R_f^{\bullet} + VDF \xrightarrow{k_i} P_n^{\bullet} \xrightarrow{VDF} P_m^{\bullet} \overset{k_p}{\circlearrowleft} M \quad (3)$$

$$P_n\text{-}CH_2\text{-}\dot{C}F_2 \underset{k_p}{\overset{VDF}{\longrightarrow}} P_n\text{-}CH_2\text{-}CF_2\text{-}CH_2\text{-}\dot{C}F_2 + P_m\text{-}CH_2\text{-}CF_2\text{-}CF_2\text{-}\dot{C}H_2 \quad (4)$$

Chain Transfer to Initiator

$$P_n\text{-}CH_2\text{-}\dot{C}F_2 + R\text{-}X \xrightarrow{k_{1tr}} P_n\text{-}CH_2\text{-}CF_2\text{-}X + R^{\bullet} \quad (5)$$

$$P_m\text{-}CF_2\text{-}\dot{C}H_2 + R\text{-}X \xrightarrow{k_{2tr}} P_m\text{-}CF_2\text{-}CH_2\text{-}X + R^{\bullet} \quad (6)$$

Iodine Degenerative Transfer

$$P_n\text{-}CH_2\text{-}\dot{C}F_2 + P_m\text{-}CH_2\text{-}CF_2\text{-}I \overset{K_{ex}=1}{\rightleftharpoons} P_n\text{-}CH_2\text{-}CF_2\text{-}I + P_m\text{-}CH_2\text{-}\dot{C}F_2 \quad (7)$$

$$P_n\text{-}CH_2\text{-}\dot{C}F_2 + P_m\text{-}CF_2\text{-}CH_2\text{-}I \overset{K_{ex}<<1}{\rightleftharpoons} P_n\text{-}CH_2\text{-}CF_2\text{-}I + P_m\text{-}CF_2\text{-}\dot{C}H_2 \quad (8)$$

$$P_m\text{-}CF_2\text{-}\dot{C}H_2 + P_n\text{-}CF_2\text{-}CH_2\text{-}I \overset{X}{\rightleftharpoons} P_m\text{-}CF_2\text{-}CH_2\text{-}I + P_n\text{-}CF_2\text{-}\dot{C}H_2 \quad (9)$$

Scheme 5.2 Photoinitiated IDT of Vinylidene Fluoride Mediated by Cu (0) as an Iodine trap

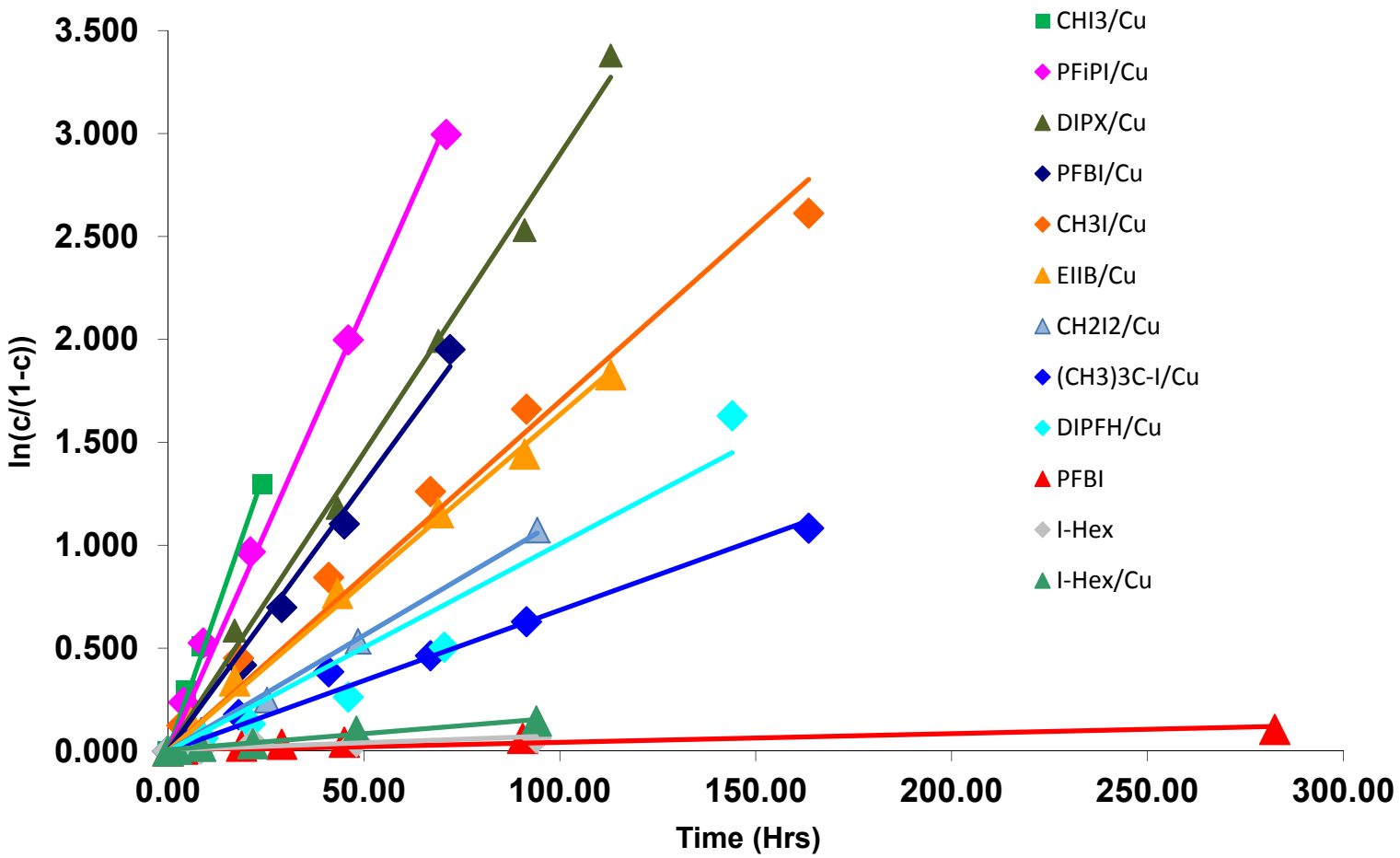

Figure 5.2 Decomposition kinetics of various alkyl and fluoroalkyl iodides demonstrating copper as an iodine trap.

Upon addition of copper wire to the reaction containing only monomer, initiator, and solvent, we were able to generate PVDF-I.(Figure 5.4) The typical PVDF-I sample is shown and addition to acetone (δ = 2.05 ppm),[50] the head-to-tail (HT) -CF_2-[CH_2-CF_2]$_n$-CH_2-, **a** at δ = 2.8-3.1 ppm and noteworthy is the lack of head to head (HH), -CF_2-CH_2-CH_2-CF_2- **a'.**[51,52] Resonance **b** (δ = 3.25 ppm) verifies the R_F-CH_2-CF_2- connectivity with the first polymer unit. The PVDF-CH_2-CF_2-I **c** and PVDF-CF_2-CH_2-I **c'**, iodine chain ends are seen at δ = 3.62 ppm and respectively δ = 3.87 ppm[39]. Amazingly, this system generated the highest total % chain end functionality of any that we have studied, producing ≥99%. Finally to be certain that this still indeed proceeds via IDT-CRP, a kinetic study was performed.(Figure 5.4-5.5) Gratifyingly it exhibits all the typical properties associated with VDF IDT-CRP, indeed confirming our theory correct.

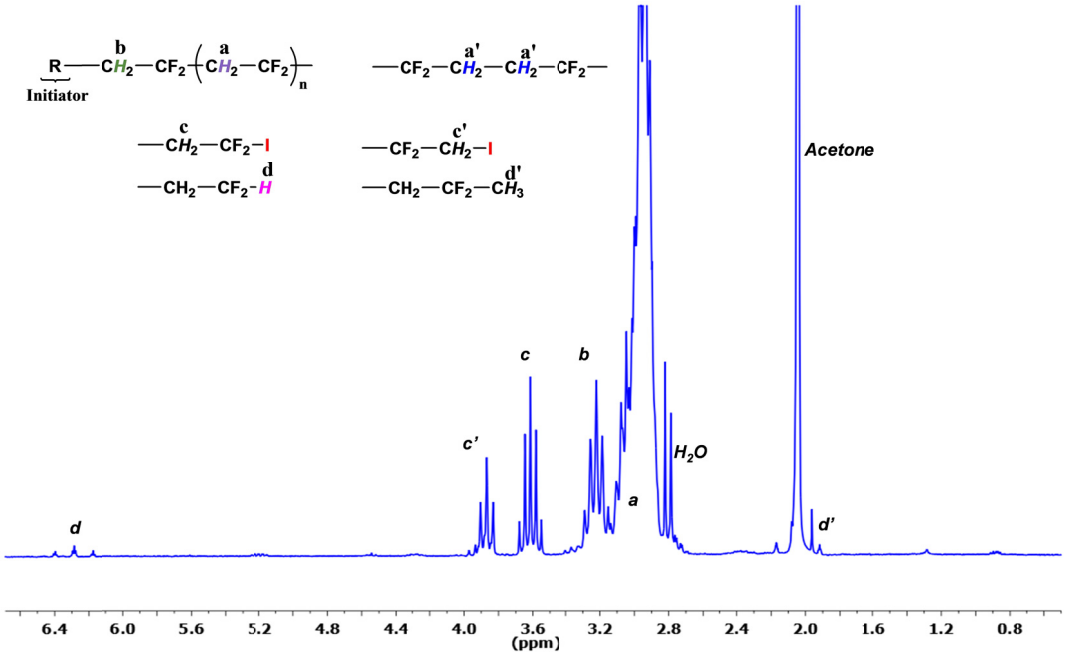

Figure 5.3 PVDF-I sample initiated via photolysis of PBFI in the presence of Cu(0) a 40°C

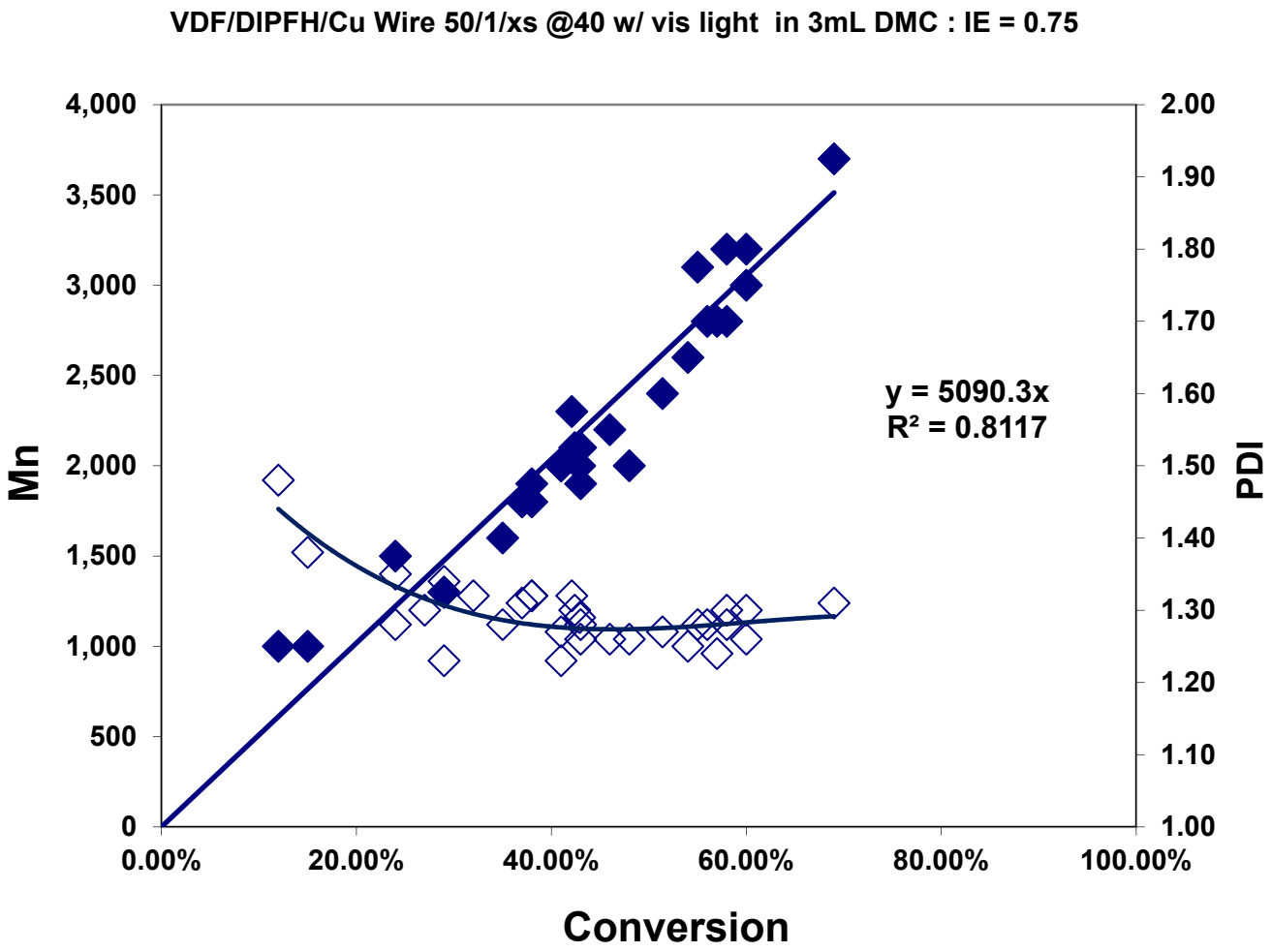

Figure 5.4 Dependence of M_n and M_w/M_n on conversion of the VDF polymerization initiated from DIPFH with Cu(0)

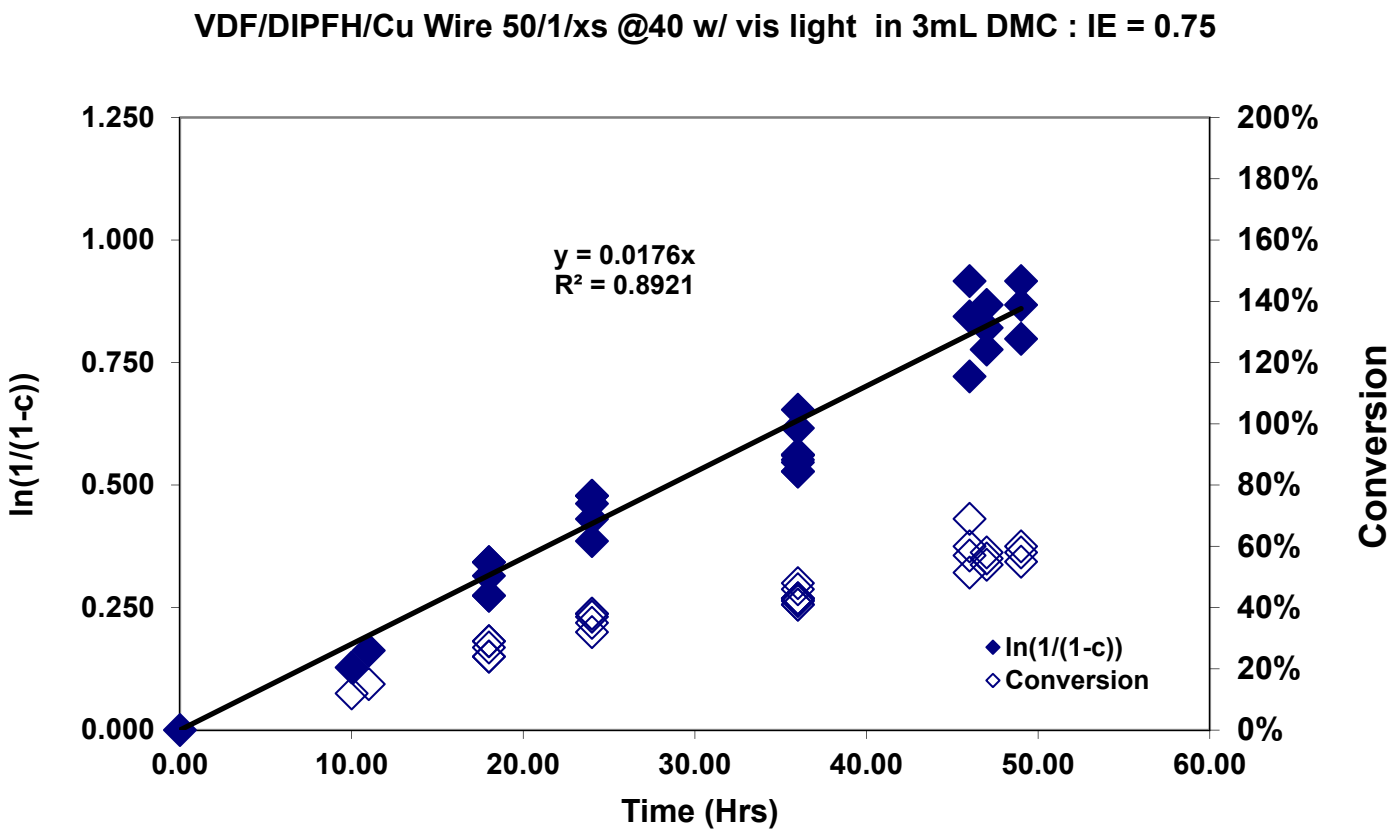

Figure 5.5 Dependence of ln(1/1-c) vs. Time of the VDF polymerization initiated from DIPFH with Cu(0)

5.4 Conclusions

A series of alkyl, perfluoro alkyl and sulfonyl halides, well known to initiate the polymerization of conventional monomers such as styrene and acrylates, were tested as potential initiators for the copper mediated radical polymerization of vinylidene fluoride (VDF) at room temperature (rt) under a variety of conditions (solvents, ligands, reagent ratios, irradiation etc). However, regardless of the reaction conditions, no polymer was obtained. This is most likely the outcome of a series of factors including low rate of initiator or halide chain end activation by Cu at rt, lower reactivity of the potential initiating radicals by comparison with the propagating chain, as well as chain transfer to the solvent, catalyst or ligand.

Finally, we were able to develop a unique methodology utilizing a photo-IDT system, and thus enabled PVDF-I synthesis. This new methodology makes use of perfluoroalkyl iodides as photo-iniferters in conjunction with Cu(0) as a iodine "sink" there to inhibit the persistent radical effect that would otherwise normally prevent these materials from initiating polymerizations. Under irradiation it was demonstrated that in the absence of an iodine "sink" such as copper these alkyl iodides had extremely low decomposition rates (<10% decomposition in 300 hours for PFBI). However, in the presence of Cu(0) this same material was completely decomposed in <72 hours (~65 times faster) at 40°C, and the decomposition kinetics of a set of various alkyl and fluoroalkyl iodides was examined. With iodoform and perfluoroisopropyl iodide having the fastest decomposition rate with iodohexane exhibiting the slowest. Interestingly, while most commercially available alkyl iodide compounds come shipped with copper pellets or turnings as a "stabilizer", this is wrong. Copper is acting as a "sponge" for free iodine that due to dissociations, and preventing self-inhibition via the iodine persistent radical effect. Copper wire was easily able to prevent a build-up of I_2 in solution and thus the PRE and this system was utilized to produce I-PVDF-I. These preliminary experiments showed typical CRP

properties, having a linear dependence of molecular weight on conversion, and most importantly generated the highest total %-functionality of any system previously studied, yielding $\geq$ 99% iodine on the polymer chain ends. This was by far the simplest system, which show extremely promising results. This system can surely be envisioned as applicable and tailored to use with other monomers and various polymerizations and being CRP process is very tolerant of functional groups and solvent, even allowing for the use of emulsion polymerizations.

5.5 References

1 *Handbook of Radical Polymerization*; Matyjaszewski, K., Davis, T. P., Eds.; Wiley-Interscience: New York, **2002**, pp 361-462.
2 Di Lena, F.; Matyjaszewski, K. *Prog. Polym. Sci*. **2010**, *35*, 959–1021.
3 Ameduri, B. *Macromolecules*, **2010**, *43*, 10163–10184.
4 Spencer, R. P.; Schwartz, J. *Tetrahedron*, **2000**, *56*, 2103-2112.
5 Green, M. H.; Lucas, C. R. *J. Chem. Soc. Dalton Trans.* **1972**, *8*, 1000.
6 Barden, M. C.; Schwartz, J. *J. Am. Chem. Soc.* **1996**, *118*, 5484.
7 Rajanbabu, T. V.; Nugent, W. *J. Am. Chem. Soc.* **1994**, *116*, 986.
8 (a) Asandei, A. D.; Moran, I. W.; Chen, Y.; Saha, G. *J. Organomet. Chem.* **2007**, *692*, 3174-3182. (b) Asandei, A. D.; Moran, I. W.; Saha, G.; Chen, Y. *ACS Symp. Ser.* **2006**, *944*, 125. (c) Asandei, A. D.; Moran, I. W.; Saha, G.; Chen. Y. *J. Polym. Sci.: Part A: Polym. Chem.* **2006**, *44*, 2156. (d) Asandei, A. D.; Moran, I. W.; Saha, G.; Chen. Y. *J. Polym. Sci.: Part A: Polym. Chem.* **2006**, *44*, 2015. (e) Asandei, A. D.; Moran, I. W. *J. Polym. Sci.: Part A: Polym. Chem.* **2006**, *44*, 1060. (f) Asandei, A. D.; Moran, I. W. *J. Polym. Sci.: Part A: Polym. Chem.* **2005**, *43*, 6039. (g) Asandei, A. D.; Moran, I. W. *J. Polym. Sci.: Part A: Polym. Chem.* **2005**, *43*, 6028. (h) Asandei, A. D.; Moran I. W. *J. Am. Chem. Soc.* **2004**, *126*, 15932. (i) Asandei; A.D.; Moran; I.W.; Castro, M.A. *Polym. Prepr.* **2003**, *44(1)*, 829. (j) Asandei, A. D.; Chen, Y.; Saha, G.; Moran, I. W.; *Tetrahedron*, **2008**, *64,* 11831.
9 Asandei; A. D; Chen, Y. *Macromolecules* **2006**, *39*, 7549.
10 (a) Asandei, A. D.; Chen, Y. *Polym. Mater.: Sci. Eng.* **2007**, *97*, 450. (b) Asandei, A. D.; Saha, G. *Polym. Prepr.* **2007**, *48*, 272.
11 Asandei, A. D.; Saha, G. *J. Polym. Sci.: Part A: Polym. Chem.* **2006**, *44*, 1106.
12 Asandei, A. D.; Simpson, C. P.; Yu, H. S.; Adebolu, O. I.; Saha, G.; Chen, Y. *ACS Symposium Series,* **2009**, *1024*, 149-166.
13 (a) Asandei, A. D.; Saha, G. *Polym. Prepr*. **2005**, *46(2)*, 474 (b) Asandei, A.D.; Simpson C. *Polym. Prepr*. **2008**, s*49(1)*, 452. (c) Asandei, A. D.; Simpson, C. P.; Yu, H. S. *Polym. Prepr.* **2008**, *49(2)*, 73. (d) Asandei, A. D.; Adebolu, O.; Yu, H. S; Simpson, C. P.; Gilbert, M. *Polym. Prepr.* **2009**, *50(1)*, 177. (e) Asandei, A. D.; Simpson, C. P. *Polym. Prepr.* **2008**, *49(2)*, 75. (f) Asandei, A. D.; Yu, H. S; Adebolu, O.; Simpson, C. P.; Duong, O. *Polym. Mater.: Sci. Eng.* **2009**, *100*, 366. (g) Asandei, A. D.; Yu, H. S*; Polym. Prepr*. **2009**, *50(2)*, 601-602. (h) Asandei, A. D.; Yu, H. S; Adebolu, A. *Polym. Mater.: Sci. Eng.* **2009**, *101*, 1377-1378. (i) Asandei, A. D.; Yu, H. S; Simpson, C. P. *Polym. Mater.: Sci. Eng.* **2009**, *101*, 1379-1380.
14 (a) Asandei, A. D.; Yu, H. S.; Simpson, C. P. *Polym. Prepr.* **2010**, *51(1)*, 545-546. (b) Asandei, A. D.; Yu, H. S.; Simpson, C. P. *Polym. Mater.: Sci. Eng.* **2010**, *103*, 511-512. (c) Asandei, A. D.; Yu, H. S.; Simpson, C. P. *Polym. Prepr.* **2010**, *51(2)*, 584-585. (d) Asandei, A. D.; Yu, H. S.; Simpson, C. P. *Polym. Prepr.* **2010**, *51(2)*, 586-587. (e) (e) Asandei, A. D.; Simpson, C. P.; Olumide, A.; Yu, H. S. *Polym. Mater.: Sci. Eng.* **2010**, *102*, 425-426. (f) Asandei, A. D.; Yu, H. S.; Simpson, C. P. *Polym. Mater.: Sci. Eng.* **2010**, *102*, 68-69. (g) Asandei, A. D.; Yu, H. S. *Polym. Prepr.* **2011**, *52(1)*, 415-416. (h) Asandei, A. D.; Yu, H. S. *Polym. Prepr.* **2011**, *52(1)*, 413-414. (i) Asandei, A. D.; Yu, H. S. *Polym. Mater.: Sci. Eng.* **2011**, *104*, 619-620. (j) Asandei, A. D.; Yu, H. S. *Polym. Mater.: Sci. Eng.* **2011**, *104*, 627-628. (k) Asandei, A. D.; Simpson, C. P.; Olumide, A.; Yu, H. S. *Polym. Prepr.* **2010**, *51(1)*, 553-554. (l) Asandei, A. D.; Simpson, C. P.; Olumide, A.; Yu, H. S. *Polym. Prepr.* **2010**, *51(1)*, 498-499.
15 Asandei, A. D.; Saha, G. *Macromolecules* **2006**, *39,* 8999.

16 (a) Asandei, A. D.; Saha, G. *Macromol. Rapid Commun*. **2005**, 26, 626. (b) Asandei, A. D.; Chen, Y.; Adebolu, O. I.; Simpson, C. P. *J. Polym. Sci.: Part A: Polym. Chem.* **2008**, *46*, 2869. (c) Asandei, A. D.; Chen, Y.; Adebolu, O. I.; Simpson, C. P. *Polym. Prepr.* **2008**, *49(2)*, 740.
17 Ameduri, B. *Chem. Rev.* **2009**, *109*, 6632–6686.
18 Hansen, N.; Jankova, K.; Hvilsted, S. *Eur. Polym. J.* **2007**, *43*, 255.
19 Zhang, Z. C.; Chung, T. C. *Macromolecules*. **2006**, *39*, 5187-5189.
20 (a) Asandei, A. D.; Chen, Y.; *Polym. Mater.: Sci. Eng.* **2008**, *98*, 346-347. (b) Asandei, A. D.; Chen, Y. *Polym. Prepr.* **2007**, *48(2)*, 452-453. (c) Asandei, A. D.; Chen, Y. *Polym. Mater.: Sci. Eng.* **2007**, *97*, 270-271. (d) Asandei, A. D.; Chen, Y. *Polym. Prepr.* **2005**, *46(2)*, 633.
21 Balague, J.; Ameduri, B.; Boutevin, B.; Caporiccio, G. *J. Fluorine Chem.* **1995**, *70*, 215-223.
22 (a) Nguyen, B. V.; Yang, Z. Y.; Burton, D. J. *J. Org. Chem.* **1998**, *63*, 2887-2891. (b) Igumnov, S. M.; Don, V. L.; Vyazkov, V. A.; Narinyan, K. E. *Mendeleev Commun.* **2006**, *16(3)*, 189–190. (c) Chen, Q. Y.; Yang, Z. Y. *J. Fluorine Chem*. **1985**, *28(4)*, 399-411. (d). Ponomarenko, M. V.; Serguchev, Y. A.; Ponomarenko, B. V.; Roschenthaler, G. V.; Fokin, A. A. *J. Fluorine Chem*. **2006**, *127*, 842–849.
23 Li, A. R.; Chen, Q. Y. *J. Fluorine Chem.* **1997**, *81(2)*, 99-101.
24 Chen, M. Y.; Yang, Z. Y.; Zhao, C. X.; Qiu, Z. M. *J. Chem. Soc. Perkin Trans. I*. **1988**, 3, 563-567. (b). Ren, Y.; Hillmyer, M. A.; Lodge, T. P. *Polym. Prepr.* **2000**, *41(2)*, 1596.
25 (a) Metzerg, J. O.; Linker, U. *Liebigs Ann. Chem.* **1992**, *3*, 209-16. (b) Ishihara, T.; Kuroboshi, M. *Synth. Commun.* **1989**, *19(9&10)*, 1611-1617.
26 Hu, C. M.; Qiu, Y. L. *J. Chem. Soc. Perkin Trans. 1.* **1992**, *13*, 1569-1572.
27 (a) Huang, W. Y.; Zhang H. Z. Lu, L. *J. Fluorine Chem*. **1990**, *50(1)*, 133-140 (b) Lumbierres, M.; Moreno-Manas, M; Vallribera, A. *Tetrahedron* **2002**, *58*, 4061-4065.
28 (a) Leung, L.; Linclau, B. *J. Fluorine* Chem. **2008**, *129*, 986–990. (b) Szlávik, Z.; Tárkányi, G.; Gömöry, A.; Rábai, J. *Org. Lett*. **2000**, *2(15)*, 2347-2349.
29 Fang, X.; Yang, X.; Yang, X.; Mao, S.; Wang, Z.; Chena, G.; Wua, F. *Tetrahedron*. **2007**, *63*, 10684–10692.
30 Hu, C. M.; Qing, F. L. *J. Org. Chem.* **1991**, *56*, 6348-6351.
31 Yang, Z. Y.; Burton, D. J. *J. Org. Chem.* **1991**, *56*, 1037-1041.
32 Tsunoi, S.; Ryu, I.; Fukushima, H.; Tanaka, M; Komatsu, M.; Noburu, S. *Synlett*. **1999**, *5*, 1249-1252.
33 Benefice-Malouet, S.; Blancou, H.; Commeyras, A. *J. Fluorine Chem.* **1993**, *63(3)*, 217-226.
34 (a) Fischer, H. *Chem. Rev.* **2001,** *101,* 3581-3610. (b) Fisher, H. *J. Polym. Sci. Part A: Polym. Chem.* **1999**, *37*, 1885-1901.(c) Focsaneanu, K. S., Scaiano, J. C. *Helvetica Chimica Acta* **2006**, *89*, 2473-2482
35 Yamago, S.; Ukai, Y.; Matsumoto, A.; Nakamura, Y. *J. Am. Chem. Soc.* **2009**, *62*, 2100−2101.
36 (a) *Kinetics of Living Radical Polymerization*. Fukuda, T.; Goto, A.; Tsujii, Y. in *Handbook of Radical Polymerization*. Matyjaszewski, K.; Davis, T. P. Eds. Wiley, New York, **2002**, pp. 407-462. *(b) Controlled Radical Polymerization by Degenerative Transfer: Effect of the Structure of the Transfer Agent*. Gaynor, S. G.; Wang, J. S.; Matyjaszewski, K. *Macromolecules*. **1995**, *28*, 8051-8056.
37 *Use of Iodocompounds in Radical Polymerization*. David, G.; Boyer, C.; Tonnar, J.; Ameduri, B.; Lacroix-Desmazes, P.; Boutevin, B. *Chem. Rev.* **2006**, *106*, 3936–3962.
38 (a) *Vinylidene fluoride-hexafluoropropylene copolymer having terminal iodines*. Oka, M.; Tatemoto, M.; in *Contemporary Topics in Polymer Science.* Bailey, W. J.; Tsuruta, T.; Eds. Plenun Press, New-York, **1984**, *4*, pp.763-781. (b) *Fluorinated Thermoplastic Elastomers* Tatemoto, M. *Int. Poly. Sc. Tech*. **1985**, *12*, 85-98. (c) Tatemoto, M. in *Polymeric Materials*

Encyclopedia. Salamone, J. C. Ed., CRC Boca Raton, FL, **1996**, *5*, pp. 3847-3862. (d) *Thermoplastic Elastomers*. Tatemoto, M.; Shimizu, T.; in *Modern Fluoropolymers*. Scheirs, J.; Ed, Wiley, New-York, **1997**, pp. 565-576. (e) *Segmented Polymers Containing Fluorine and Iodine and their Production*. Tatemoto, M.; Nakagawa, T.; U.S. Patent 4,158,678, **1979**.

39 (a) *Mild-Temperature Mn2(CO)10-Photomediated Controlled Radical Polymerization of Vinylidene Fluoride and Synthesis of Well-Defined Poly(vinylidene fluoride) Block Copolymers*. Asandei, A. D.; Olumide, O. I.; Simpson, C. P. *J. Am. Chem. Soc*. **2012**, *134*, 6080-6083. (b) *Visible Light Hypervalent Iodide Carboxylate Photo-Iodo(Trifluoro)Methylations and Controlled Radical Polymerization of Fluorinated Alkenes*. Asandei, A. D.; Adebolu, O. I.; Simpson, C. P.; Kim, J. S. *Angew. Chem. Int. Ed.* **2013**, *52*, 10027-10030. (c) *Towards Metal Mediated Radical Polymerization of Vinylidene Fluoride* Asandei, A. D.; Simpson, C. P.; Adebolu, O. I.; Chen, Y. *Advances in Fluorine-Containing Polymers.* **2012**, *1106*, 47-63.

40 *First MALDI-TOF Mass Spectrometry of Vinylidene Fluoride Telomers Endowed with Low Defect Chaining*. Ameduri, B.; Ladavière, C.; Delolme, F.; Boutevin, B.; *Macromolecules*. **2004**, *37*, 7602-7612.—can cut

41 *Iodine Transfer Polymerization (ITP) of Vinylidene Fluoride (VDF). Influence of the Defect of VDF Chaining on the Control of ITP*. Boyer, C.; Valade, D.; Sauguet, L.; Ameduri, B.; Boutevin, B. *Macromolecules*. **2005**, *38*, 10353-10362.

42 *Kinetics of the Iodine Transfer Polymerization of Vinylidene Fluoride*. Boyer, C.; David, V.; Lacroix-Desmazes, P.; Ameduri, B.; Boutevin, B. *J. Polym. Sci.: Part A: Polym. Chem*. **2006**, *44*, 5763–5777.

43 *Poly(vinylidenefluoride)-b-poly(styrene) Block Copolymers by Iodine Transfer Polymerization (ITP): Synthesis, Characterization, and Kinetics of ITP*. Valade, D.; Boyer, C.; Ameduri, B.; Boutevin, B. *Macromolecules*. **2006**, *39*, 8639-8651.

44 (a) Hauptschein, M.; Fainberg, A. H.; Braid, M. *J. Org. Chem.*, **1958**, *23* (2), 322–322. (b) Pickard, J. M.;Rodgers, A. S. *J. Am. Chem. Soc*., **1977**, *99(3)*, 691–694

45 (a) Schuler, R. H.; Kuntz, R. R. *J. Phys. Chem.* **1963**, *67*, 1004-1011. (b) Foldiak, G.; Schuler, R. H. *J. Phys. Chem.* **1978**, *82*, 2756-2757. (c) Kryger, R. G.; Lorand, J. P.; Stevens, N. R.; Herron, N. R. *J.Am. Chem. Soc.* **1977**, *99*, 7589-7600. (d) LaVerne, J. A.; Wojnarovits, L. *J. Phys. Chem.* **1994**, *98*, 12635.

46 Hauptschein, M.; Oesterling, R. E; Braid, M.; Tyczkowski, E. A.; Gardner, D. M. *J. Org. Chem.* **1963**, *28*, 1281-83

47 Percec,V.; Barboiu, B.; Kim, H. J. *J. Am. Chem. Soc*.**1998** *120*, 305-316.

48 Hester, J. F.; Banerjee, P.; Won, Y.Y.; Akthakul, A.; Acar, H. M.; Mayes. A. M. *Macromolecules* **2002,** *35,* 7652-7661

49 (a) *Mild-Temperature Mn2(CO)10-Photomediated Controlled Radical Polymerization of Vinylidene Fluoride and Synthesis of Well-Defined Poly(vinylidene fluoride) Block Copolymers*. Asandei, A. D.; Olumide, O. I.; Simpson, C. P. *J. Am. Chem. Soc*. **2012**, *134*, 6080-6083. (b) *Visible Light Hypervalent Iodide Carboxylate Photo-Iodo(Trifluoro)Methylations and Controlled Radical Polymerization of Fluorinated Alkenes*. Asandei, A. D.; Adebolu, O. I.; Simpson, C. P.; Kim, J. S. *Angew. Chem. Int. Ed.* **2013**, *52*, 10027-10030. http://dx.doi.org/10.1002/anie.201303826 (c) *Towards Metal Mediated Radical Polymerization of Vinylidene Fluoride* Asandei, A. D.; Simpson, C. P.; Adebolu, O. I.; Chen, Y. *Advances in Fluorine-Containing Polymers.* **2012**, *1106*, 47-63.

[50] *NMR Chemical Shifts of Trace Impurities: Common Laboratory Solvents, Organics, and Gases in Deuterated Solvents Relevant to the Organometallic Chemist*. Fulmer, G. R.; Miller, A. J.

M.; Sherden, N. H.; Gottlieb, H. E.; Nudelman, A.; Stoltz, B. M.; Bercaw, J. E.; Goldberg, K. I. *Organometallics* **2010**, *29*, 2176–2179.

[51] (a) *Controlled step-wise telomerization of vinylidene fluoride, hexafuoropropene and trifuoroethylene with iodofluorinated transfer agents*. Balague, J.; Ameduri, B.; Boutevin, B.; Caporiccio, G. *J. Fluorine Chem.* **2000**, *102*, 253-268. (b) *Use of Telechelic Fuorinated Diiodides to Obtain Well-Defined Fuoropolymers*. Ameduri, B.; Boutevin, B. *J. Fluorine. Chem*. **1999**, *100*, 97-116. (c) *Synthesis of fluorinated telomers.1. Telomerization of vinylidene fluoride with Perfluoroalkyl Iodides*. Balague, J.; Ameduri, B.; Boutevin, B.; Caporiccio, G. *J. Fluorine Chem.* **1995**, *70*, 215-223.

[52] (a) *Effect of molecular weight and chain end groups on crystal forms of poly(vinylidenefluoride) oligomers*. Herman; Uno, T.; Kubono, A.; Umemoto, S.; Kikutani, T.; Okui, N. *Polymer*. **1997**, *38(7)*, 1677-1683. (b) *High Resolution Nuclear Magnetic Resonance of Fluoro Polymers. 2. Fluorine-19 Spectra and Chain Structure of Poly(vinylidene fluoride)*. Ferguson, R. C.; Brame, E. G. *J. Phys. Chem*.**1979**, *83(11)*, 1397-1401. (c) *Radical Homopolymerization of Vinylidene Fluoride Initiated by tert-Butyl Peroxypivalate. Investigation of the Microstructure by 19F and 1H-NMR Spectroscopies and Mechanisms*. Guiot, J.; B. Ameduri, B.; B. Boutevin, B. *Macromolecules* **2002,** *35,* 8694-8707. (d) *End groups in Fluoropolymers*. Pianca, M.; Barchiesi, E.; Esposto, G.; Radice, S. *J. Fluorine Chem*. **1999**, *95*, 71-84. (e) Wormald, P.; Ameduri, B.; Harris, R. K.; Hazendonk, P. *Polymer* **2008**, *49*, 3629–3638.

Chapter 6. Conclusions

The first examples of transition metal mediated controlled radical polymerizations of isoprene were demonstrated using the epoxide/Cp_2TiCl initiator/catalyst system. The initiation was supported by NMR investigations, which indicated the presence of epoxide fragments on the chain end and the stereoselectivity of a conventional radical polymerization. The effect of the reaction variables was studied over a wide range of conditions ([Cp_2TiCl_2]/[epoxide] = 1/1-1/6, ([Cp_2TiCl_2]/[Zn] = 1/0.5-1/8 , [Iso]/[epoxide] = 20/1-1000/1, T = 70-130 °C in THF and dioxane) to reveal a linear dependence of molecular weight on conversion, linear kinetics as well as moderate polydispersities up to high conversions. The initiator efficiency (IE) and the rate increase, while polydispersity decreases with increasing the [Cp_2TiCl_2]/[epoxide] ratios, with an optimum at [epoxide]/[Cp_2TiCl_2]/[Zn] = 1/3/6-1/4/8 at 90 - 110 °C. While IE is independent of temperature, lower polydispersities (1.3-1.4) were obtained at lower temperatures ~ 90 °C. Furthermore, random and block copolymers with styrene could also be obtained.

The Cp_2TiCl_2/epoxide methodology uses off-the-shelf reagents, and mediates isoprene LRP at lower temperatures (70-110 °C vs. 120-130 °C) than the more expensive nitroxide and dithioester LRP methods, to which it offers a convenient and inexpensive alternative. Moreover, refinement of the ligand systems using examples already available in Ti-coordination polymerization is likely to optimize the polymerization further.

This methodology was applied to CRP of butadiene, and dimethyl butadiene, each of which was demonstrated for all three classes of initiators. A controlled radical polymerization was observed for all cases with DMBD below 130C. At higher temperatures, it was noted that the polymerizations was free radical, most likely attributed to the allylic nature of the monomer and polymer allowing for more significant chain transfer at elevated temperatures. Butadiene exhibited some control over molecular weight, but was the worst among the three monomers

examined. Likely this system needs to be individually optimized to obtain better polymerization control.

Then examined was a set of typical free radical initiators such AIBN, BPO, TBPB, TBPO, DCPO, DLPO, and H_2O_2 were evaluated in the thermal or UV-mediated VDF polymerization in TFT, Py, NMP, DMAC, dioxane, THF, DMSO, BN, DMF, and toluene. Better polymerization results were obtained with initiators which generate the most reactive radicals (TBPO) in solvents that minimize chain transfer (ACN), which however, are not necessarily good PVDF solvent as well.

To determine the viability of Cp_2TiCl_2, chemistry for the polymerization of vinylidene fluoride a series of epoxides, aldehydes, halides and peroxides, known to initiate both styrene and diene polymerizations were tested as potential rt VDF initiators. However, regardless of reaction conditions, no polymer was obtained. This is most likely the combined outcome of a series of factors including lower reactivity of the initiating radicals by comparison with the propagating chain, transfer to the solvent or catalyst, low reaction temperature and of several possible organometallic side reactions. The key reason for the failure of these polymerizations is most likely the solvent effect, *i.e.* the incompatibility of solvents appropriate for Cp_2TiCl_2 reductions with those conducive of VDF polymerizations. Thus, the polar solvents that promote a fast and efficient reduction of Cp_2TiCl_2 are strong chain transfer agents towards VDF (dioxane, THF, diglyme, acetone), while solvents that limit chain transfer to PVDF$^{\bullet}$, will react with $Cp_2TiCl^{\bullet}$.

Once it was realized that the metalloradical from Cp_2TiCl_2 was incompatible with the fluorinated monomer systems, a new source of easily in-situ generated, metalloradical was sought. Thus, we were able to demonstrated that the photoinduced initiation of polymerization can easily be obtained using vinylidene fluoride, at relatively mild temperatures, directly from alkyl or perfluoroalkyl halides ($CH_3(CH_2)_5Br$, $CH_3(CH_2)_5I$, CH_3I, CCl_4, CCl_3Br, $CF_3(CF_2)_3I$ $Cl(CF_2)_8Cl$, $Br(CF_2)_6Br$, and $I(CF_2)_6I$) using low power visible light irradiation ($\leq$30W) in conjunction with the

transition metal carbonyl complexes ($Re_2(CO)_{10}$, $Mn_2(CO)_{10}$, $Cp_2W_2(CO)_6$, $Cp_2Mo_2(CO)_6$). The perfluoroalkyl iodides $CF_3(CF_2)_3I$ and especially $I(CF_2)_6I$) with $Mn_2(CO)_{10}$ or $Re_2(CO)_{10}$ mediated the VDF controlled radical polymerization (CRP) via iodine degenerative transfer (IDT) mechanism, while all other combinations yielded either FRP, telomerization, or no reaction at all. The effect of various [VDF]/[PFBI]/[$Mn_2(CO)_{10}$] ratios demonstrated again that poor or no control was obtained with PBFI in either ACN or DMC, with only the higher [VDF]/[PFBI] and lower [PFBI]/[$Mn_2(CO)_{10}$] ratios beginning to show slight IDT-CRP character, confirming DMC as the superior solvent. The effect of [PFBI]/[$Mn_2(CO)_{10}$] revealed a lower limit of [1]/[0.05] below which no polymerization occurs, and an upper limit of [1]/[0.5] above which no further increases in k_p^{app} were observed. The [VDF]/[solvent] ratio had little effect on the polymerization rate *i.e.* maintaining a constant amount of VDF while increasing the solvent twelve-fold yielded similar k_p^{app}. While, maintaining a constant [VDF]/[solvent] ratio with increasing amounts of VDF, brought forth a significant increase in k_p^{app}. This was attributed to the monomer being gaseous, therefore the only effective means of increasing (decreasing) the concentration of the monomer in solution is to increase (decrease) the internal pressure of the reaction vessel. (*i.e.* the addition of larger(smaller) quantities of monomer). Subsequently, a selection of the metal carbonyl complexes were evaluated in the PVDF-CH_2-CF_2-I and PVDF-CF_2-CH_2-I activation, where $Re_2(CO)_{10}$, $Mn_2(CO)_{10}$, $Cp_2W_2(CO)_6$, $Cp_2Mo_2(CO)_6$, and $Cp_2Fe_2(CO)_4$ provided complete activation of both halide polymer chain ends, while $Fe(CO)_5$ and $Cp^*_2Cr_2(CO)_4$ generated β-elimination products following the oxidative insertion into PVDF-CH_2-CF_2-I and PVDF-CF_2-CH_2-I. Finally, $Re_2(CO)_{10}$, $Mn_2(CO)_{10}$, $Cp_2W_2(CO)_6$, $Cp_2Mo_2(CO)_6$, and $Cp_2Fe_2(CO)_4$ provided the synthesis of well-defined block copolymers with vinyl acetate, t-butyl acrylate, methyl methacrylate, isoprene, styrene, and acrylonitrile.

An effort was made to expand the controlled radical polymerizations of fluorinated monomers to use with ATRP. A series of alkyl, perfluoro alkyl and sulfonyl halides, well known to initiate the polymerization of conventional monomers such as styrene and acrylates, were tested as potential initiators for the copper mediated radical polymerization of vinylidene fluoride (VDF) at room temperature (rt) under a variety of conditions (solvents, ligands, reagent ratios, irradiation etc). However, regardless of the reaction conditions, no polymer was obtained. This is most likely the consequence of a series of factors including low rate of initiator or halide polymer chain end activation by Cu at rt. Lower reactivity of the potential initiating radicals by comparison with the propagating chain, inability of copper to activate perfluoroalkyl halides, side reactions of perfluoroalkyl iodides with amine ligands, as well as chain transfer to the solvent, catalyst or ligand. Consequently, do to these incompatibilities it was determined that Cu-mediated VDF CRP was not viable.

Finally, we were able to develop a new and unique methodology for this to succeed with a photo-IDT system, and thus enabled PVDF-I synthesis. This new methodology makes use of perfluoroalkyl iodides as photo-iniferters in conjunction with Cu(0) as a iodine “sink” there to inhibit the persistent radical effect that would otherwise normally prevent these materials from initiating polymerizations. Under irradiation it was demonstrated that in the absence of an iodine “sink” such as copper these alkyl iodides had extremely low decomposition rates (<10% decomposition in 300 hours for PFBI). However, in the presence of Cu(0) this same material was completely decomposed in <72 hours (~65 times faster) at 40°C, and the decomposition kinetics of a set of various alkyl and fluoroalkyl iodides was examined. With iodoform and perfluoroisopropyl iodide having the fastest decomposition rate with iodohexane exhibiting the slowest. Interestingly, while most commercially available alkyl iodide compounds come shipped with copper pellets or turnings as a “stabilizer”, it is very apparent that this incorrect. Copper is

simply acting as a “sponge” for any iodine that may get formed due to dissociations, and preventing the inherent self-inhibition via the iodine persistent radical effect. Once it was apparent that copper wire was easily able to prevent a build-up of I_2 in solution and thus the PRE, this system was utilized to produce I-PVDF-I. These preliminary experiments showed typical CRP properties, having a linear dependence of molecular weight on conversion, and most importantly generated the highest total %-functionality of any system previously studied, yielding $\geq$ 99% iodine on the polymer chain ends. This was by far the simplest system, which show extremely promising results. This system can surely be envisioned as applicable and tailored to use with other monomers and various polymerizations and being CRP process is very tolerant of functional groups and solvent, even allowing for the use of emulsion polymerizations.

Appendix: Granted Permissions / Licenses

Please find on the following pages the permissions/licenses for use of published work in this thesis.

Order Completed

Thank you very much for your order.

This is a License Agreement between Christopher P Simpson ("You") and John Wiley and Sons ("John Wiley and Sons"). The license consists of your order details, the terms and conditions provided by John Wiley and Sons, and the payment terms and conditions.

Get the printable license.

License Number	3226580863476
License date	Sep 12, 2013
Licensed content publisher	John Wiley and Sons
Licensed content publication	Angewandte Chemie International Edition
Licensed content title	Visible-Light Hypervalent Iodide Carboxylate Photo(trifluoro)methylations and Controlled Radical Polymerization of Fluorinated Alkenes
Licensed copyright line	Copyright © 2013 WILEY-VCH Verlag GmbH & Co. KGaA, Weinheim
Licensed content author	Alexandru D. Asandei,Olumide I. Adebolu,Christopher P. Simpson,Joon-Sung Kim
Licensed content date	Aug 12, 2013
Start page	10027
End page	10030
Type of use	Dissertation/Thesis
Requestor type	Author of this Wiley article
Format	Print and electronic
Portion	Full article
Will you be translating?	No
Total	0.00 USD

ORDER MORE... CLOSE WINDOW

Title: Mild-Temperature Mn2(CO)10-Photomediated Controlled Radical Polymerization of Vinylidene Fluoride and Synthesis of Well-Defined Poly(vinylidene fluoride) Block Copolymers

Author: Alexandru D. Asandei, Olumide I. Adebolu, and Christopher P. Simpson

Publication: Journal of the American Chemical Society

Publisher: American Chemical Society

Date: Apr 1, 2012

PERMISSION/LICENSE IS GRANTED FOR YOUR ORDER AT NO CHARGE

This type of permission/license, instead of the standard Terms & Conditions, is sent to you because no fee is being charged for your order. Please note the following:

- Permission is granted for your request in both print and electronic formats, and translations.
- If figures and/or tables were requested, they may be adapted or used in part.
- Please print this page for your records and send a copy of it to your publisher/graduate school.
- Appropriate credit for the requested material should be given as follows: "Reprinted (adapted) with permission from (COMPLETE REFERENCE CITATION). Copyright (YEAR) American Chemical Society." Insert appropriate information in place of the capitalized words.
- One-time permission is granted only for the use specified in your request. No additional uses are granted (such as derivative works or other editions). For any other uses, please submit a new request.

Book: Controlled/Living Radical Polymerization: Progress in RAFT, DT, NMP & OMRP

Chapter: Cp2TiCl-Mediated Controlled Radical Polymerization of Isoprene Initiated by Epoxide Radical Ring Opening

Author: Alexandru D. Asandei, Christopher P. Simpson, Hyun S. Yu et al.

Publisher: American Chemical Society

Date: Aug 13, 2009

PERMISSION/LICENSE IS GRANTED FOR YOUR ORDER AT NO CHARGE

This type of permission/license, instead of the standard Terms & Conditions, is sent to you because no fee is being charged for your order. Please note the following:

- Permission is granted for your request in both print and electronic formats, and translations.
- If figures and/or tables were requested, they may be adapted or used in part.
- Please print this page for your records and send a copy of it to your publisher/graduate school.
- Appropriate credit for the requested material should be given as follows: "Reprinted (adapted) with permission from (COMPLETE REFERENCE CITATION). Copyright (YEAR) American Chemical Society." Insert appropriate information in place of the capitalized words.
- One-time permission is granted only for the use specified in your request. No additional uses are granted (such as derivative works or other editions). For any other uses, please submit a new request.

BACK CLOSE WINDOW

Book: Advances in Fluorine-Containing Polymers

Chapter: Towards Metal Mediated Radical Polymerization of Vinylidene Fluoride

Author: Alexandru D. Asandei, Christopher P. Simpson, Olumide I. Adebolu et al.

Publisher: American Chemical Society

Date: Jan 1, 2012

PERMISSION/LICENSE IS GRANTED FOR YOUR ORDER AT NO CHARGE

This type of permission/license, instead of the standard Terms & Conditions, is sent to you because no fee is being charged for your order. Please note the following:

- Permission is granted for your request in both print and electronic formats, and translations.
- If figures and/or tables were requested, they may be adapted or used in part.
- Please print this page for your records and send a copy of it to your publisher/graduate school.
- Appropriate credit for the requested material should be given as follows: "Reprinted (adapted) with permission from (COMPLETE REFERENCE CITATION). Copyright (YEAR) American Chemical Society." Insert appropriate information in place of the capitalized words.
- One-time permission is granted only for the use specified in your request. No additional uses are granted (such as derivative works or other editions). For any other uses, please submit a new request.